



UNIVERSIDADE ESTADUAL PAULISTA  
"JÚLIO DE MESQUITA FILHO"  
Câmpus de São José do Rio Preto

Paulo Henrique Reis Santana

Planar reversible vector fields, averaging theory and  
polycycles in non-smooth vector fields

São José do Rio Preto  
2021



Paulo Henrique Reis Santana

Planar reversible vector fields, averaging theory and  
polycycles in non-smooth vector fields

Dissertação apresentada como parte dos requisitos para obtenção do título de Mestre em Matemática, junto ao Programa de Pós-Graduação em Matemática, do Instituto de Biociências, Letras e Ciências Exatas da Universidade Estadual Paulista “Júlio de Mesquita Filho”, Câmpus de São José do Rio Preto.

Orientador: Prof. Dr. Claudio Aguinaldo Buzzi

Co-orientador: Prof. Dr. Jaume Llibre

Financiadoras: FAPESP - 2018/23194-9 e 2019/21446-3; CAPES

São José do Rio Preto  
2021

S232p	<p>Santana, Paulo Henrique Reis</p> <p>Planar reversible vector fields, averaging theory and polycycles in non-smooth vector fields / Paulo Henrique Reis Santana. -- São José do Rio Preto, 2021</p> <p>128 p.</p> <p>Dissertação (mestrado) - Universidade Estadual Paulista (Unesp), Instituto de Biociências Letras e Ciências Exatas, São José do Rio Preto</p> <p>Orientador: Claudio Aguinaldo Buzzi</p> <p>Coorientador: Jaume Llibre</p> <p>1. Sistemas dinâmicos. 2. Retratos e fase. 3. Reversibilidade. 4. Teoria da média. 5. Policiclos. I. Título.</p>
-------	---

Sistema de geração automática de fichas catalográficas da Unesp. Biblioteca do Instituto de Biociências Letras e Ciências Exatas, São José do Rio Preto. Dados fornecidos pelo autor(a).

Paulo Henrique Reis Santana

Planar reversible vector fields, averaging theory and  
polycycles in non-smooth vector fields

Dissertação apresentada como parte dos requisitos para obtenção do título de Mestre em Matemática, junto ao Programa de Pós-Graduação em Matemática, do Instituto de Biociências, Letras e Ciências Exatas da Universidade Estadual Paulista “Júlio de Mesquita Filho”, Câmpus de São José do Rio Preto.

Financiadora: FAPESP - 2018/23194-9 e 2019/21446-3; CAPES

Comissão Examinadora

---

Prof. Dr. Claudio Aguinaldo Buzzi  
UNESP - Campus de São José do Rio Preto  
Orientador

---

Profa. Dra. Luci Any Francisco Roberto  
UNESP - Campus de São José do Rio Preto

---

Prof. Dr. João Carlos da Rocha Medrado  
UFG - Universidade Federal de Goiás

São José do Rio Preto  
28 de Junho de 2021



## **AGRADECIMENTOS**

Sozinho eu jamais conseguiria fazer um milésimo do que foi feito aqui. Agradeço ao meu pai Ubaldo por todo o apoio que ele deu e continua dando a seus filhos, matando um leão por dia por nós, sempre provendo para sua família. Agradeço a minha mãe Roseli por todo o apoio que ela deu e continua dando a seus filhos, também matando um leão por dia por nós, sempre cuidando de sua família. É graças ao ambiente amoroso e alegre fornecido pelos dois que eu e minha irmã temos o enorme privilégio de focarmos cem por cento do nosso tempo na corrida pelos nossos sonhos. Agradeço a minha irmã por todo o apoio dado a mim nas horas difíceis. Ter alguém passando pelas mesmas dificuldades acadêmicas que eu, e que portanto também às entende, ajuda muito.

Devo também os mais ternos agradecimentos a minha amada noiva Raquel, mulher de fibra que ocorre atrás de seus sonhos e que me apoia incondicionalmente. Com sua paciência infinita sempre me perdoando pelos incontáveis finais de semanas e feriados que eu tive que passar em meu quarto, estudando, em vez de dar companhia a ela. Por seu amor incontestável ao sempre me apoiar na busca pelo meu sonho.

Sonho este que jamais se realizaria sem o apoio do meu grande orientador Claudio Buzzi, homem de extrema humildade, paciência, competência e generosidade. Sempre abrindo portas para seus alunos, sempre fazendo tudo que está ao alcance dele, e além. Sempre se desdobrando em mil para dar atenção a cada um de nós. Tudo isto sem perder a altíssima qualidade de suas aulas. Agradeço também ao professor Jaime Llibre, um dos maiores pesquisadores da área de sistemas dinâmicos e ainda sim um homem de extrema humildade, paciência, competência e generosidade. Sempre de portas abertas para alunos que não possuem nada além de um sonho. Estes dois grandes professores são um exemplo a ser seguido por todos os alunos ao redor.

Agradeço ao meus Avós Guilherme e Cida, Gerônimo e Wilsa, por sempre terem os sonhos de seus netos como seus próprios sonhos.

Agradeço também aos meus amigos Matheus, João e Fazoli, por todas as risadas e todos os delírios matemáticos que temos juntos no famigerado, e às vezes mal compreendido, grupo “café com CR”. Ter alguém tão desesperado quanto eu com as listas de exercícios era um alívio.

Agradecimentos também ao meu querido amigo Amilton Machado por compartilhar sua sabedoria de vida, obtida a duras penas, para um “bando de muleque” que não sabem nada sobre a vida. Tenho certeza que você olha por nós do céu.

Agradeço também à Fundação de Amparo à Pesquisa do Estado de São Paulo (FAPESP) por me dar a oportunidade única de passar seis meses no exterior, em nome do meu aperfeiçoamento profissional. Fiz e continuarei fazendo o possível e o impossível para honrar o dinheiro público confiado a mim.

O presente trabalho foi realizado com apoio da Fundação de Amparo à Pesquisa do Estado de São Paulo (FAPESP), processos 2018/23194-9 e 2019/21446-3, a qual agradeço.

O presente trabalho foi realizado com apoio da Coordenação de Aperfeiçoamento de Pessoal de Nível Superior - Brasil (CAPES) - Código de Financiamento 001, a qual agradeço.

## RESUMO

Neste trabalho veremos os retratos de fase, no disco de Poincaré, das formas normais locais das singularidades simétricas dos campos reversíveis do tipo  $(2; 0)$  e  $(2; 1)$  de baixa codimensão; uma aplicação da Teoria da Média no campo da Astrofísica, com o objetivo de estudar as órbitas periódicas de um modelo do universo de Friedmann-Robertson-Walker; e algumas generalizações de resultados conhecidos sobre policiclos em campos de vetores suaves para o caso não suave, focando um melhor entendimento de sua estabilidade e da bifurcação de ciclos limite.

Palavras-chave: Sistemas Dinâmicos, Retratos de fase, Reversibilidade, Teoria da Média, Policiclos.



## **ABSTRACT**

*In this work one will see the phase portraits, in the Poincaré disk, of the local normal forms of symmetrical singularities of reversible vector fields of type  $(2; 0)$  and  $(2; 1)$ ; an application of the Averaging Theory at the field of Astrophysics, aiming the study of the periodic orbits in a model of the Friedmann-Robertson-Walker universe; and some generalizations of well established results about the polycycles in smooth vector fields to the non-smooth cases, aiming a better understanding of its stability and the bifurcation of limit cycles.*

*Keywords: Dynamical Systems, Phase portraits, Reversibility, Averaging Theory, Polycycles.*



## LIST OF FIGURES

2.1	Illustration of $l_p$ and $l_q$ . Figure source: made by the author. . . . .	23
2.2	The displacement map $d$ defined near $\mu_0$ . Figure source: made by the author.	28
2.3	The Dulac map near a hyperbolic saddle. Figure source: made by the author.	30
3.1	Phase portraits of $X_1, X_2, X_3, X_4$ and $X_5$ . Figure source: Figure 1 of [13].	35
3.2	Phase portraits of $X_{12}$ . Figure source: Figure 1 of [13]. . . . .	35
3.3	Phase portraits of $X_{34}$ . Figure source: Figures 2 and 3 of [13]. . . . .	35
3.4	Phase portraits of $X_{21}$ and $X_{13}$ . Figure source: Figure 2 of [13]. . . . .	36
3.5	Phase portraits of $X_{43}$ . Figure source: Figure 3 of [13]. . . . .	36
3.6	Phase portraits of $X_{45}$ . Figure source: Figures 3 and 4 of [13]. . . . .	36
3.7	Phase portraits of $X_{24}$ . Figure source: Figures 4 and 5 of [13]. . . . .	36
3.8	Phase portraits of $X_{54}$ . Figure source: Figure 4 of [13]. . . . .	37
3.9	Illustration of $\Gamma$ and $\varphi(\Gamma)$ . Figure source: made by the author. . . . .	37
3.10	Local phase portrait at the origin of chart $U_2$ of $p(X_{34})$ . Figure source: Figure 6 of [13]. . . . .	38
3.11	Local phase portrait of $X_{34}$ at the origin. Figure source: Figure 7 of [13]. .	39
3.12	Heteroclinic orbit between the origin and $p^-$ . Figure source: Figure 8 of [13].	41
3.13	The displacement function $d(\lambda)$ defined for $\lambda$ near $\lambda_0$ . Figure source: Fi- gure 9 of [13]. . . . .	41
3.14	Plot of $H(x, y) = 0$ and $\dot{x} = 0$ at the second quadrant. Figure source: Figure 10 of [13]. . . . .	42
3.15	Unfinished phase portrait of $X_{34}$ for $1 + \sqrt{2} \leq \lambda < 3$ . Figure source: Figure 11 of [13]. . . . .	43
3.16	Illustration of the zeros of $\dot{x} = 0$ and $\dot{y} = 0$ . Figure source: Figure 12 of [13].	43
3.17	Unfinished phase portrait of $X_{34}$ for $\lambda_0 < \lambda < 1 + \sqrt{2}$ . Figure source: Figure 13 of [13]. . . . .	44
3.18	Unfinished phase portrait of $X_{34}$ for $1 < \lambda < \lambda_0$ . Figure source: Figure 14 of [13]. . . . .	45
3.19	Unfinished phase portrait of $X_{34}$ for $0 < \lambda < 1$ . Figure source: Figure 15 of [13]. . . . .	45
3.20	Local phase portrait of $X_{34}$ at $y = \frac{1-\lambda}{2}x$ for $0 < \lambda < 1$ . Figure source: Figure 16 of [13]. . . . .	45
3.21	Local phase portrait of the blow up of the origin of chart $U_2$ . Figure source: Figure 17 of [13]. . . . .	47
4.1	Phase portraits of $X_{01}, X_{02}, X_{11}, X_{12}, X_{13}$ and $X_{14}$ . Figure source: made by the author. . . . .	53
4.2	Phase portrait of $X_{21}$ with $b = 1$ . Figure source: made by the author. . . .	54
4.3	Bifurcation diagram of $X_{21}$ with $b = -1$ . Figure source: made by the author.	54
4.4	Bifurcation diagram of $X_{22a}$ with $a = 1$ . Figure source: made by the author.	55
4.5	Bifurcation diagram of $X_{22a}$ with $a = -1$ . Figure source: made by the author. . . . .	55
4.6	Bifurcation diagram of $X_{24a}$ with $a = 1$ . Figure source: made by the author.	56
4.7	Bifurcation diagram of $X_{25a}$ with $a = 1$ . Figure source: made by the author.	56

4.8	Bifurcation diagram of $X_{25a}$ with $a = -1$ . Figure source: made by the author. . . . .	72
4.9	Bifurcation diagram of $X_{25b}$ with $(a, b, \varepsilon) = (1, 3, 3)$ . Figure source: made by the author. . . . .	72
4.10	Bifurcation diagram of $X_{25b}$ with $(a, b, \varepsilon) = (1, 3, -3)$ . Figure source: made by the author. . . . .	73
4.11	Bifurcation diagram of $X_{25b}$ with $(a, b, \varepsilon) = (3, 1, 3)$ . Figure source: made by the author. . . . .	73
4.12	Bifurcation diagram of $X_{25b}$ with $(a, b, \varepsilon) = (3, 1, -3)$ . Figure source: made by the author. . . . .	74
4.13	Bifurcation diagram of $X_{23}$ with $a = 1$ . We observe that it may be an intersection between 28 and 30. Figure source: made by the author. . . . .	74
4.14	Phase portraits of $X_{23a}$ with $a = 1$ . Figure source: made by the author. . . . .	75
4.15	Possible interception of 28 and 30. Figure source: made by the author. . . . .	76
4.16	Phase portraits of $X_{23a}$ with $a = 1$ . Figure source: made by the author. . . . .	76
4.17	Bifurcation diagram of $X_{23b}$ with $a = -1$ . Figure source: made by the author. . . . .	77
4.18	Phase portraits of $X_{23}$ with $a = -1$ and $(x, y) \mapsto (-x, y)$ . Figure source: made by the author. . . . .	78
4.19	Local phase portrait of $X_{12}$ at the origin where $\lambda = 0$ . Figure source: made by the author. . . . .	78
4.20	Local phase portrait of $X_{12}$ at the regularized infinity. Figure source: made by the author. . . . .	78
4.21	Unfinished local phase portrait of $X_{12}$ at the regularized infinity. Figure source: made by the author. . . . .	79
4.22	Local behavior of the phase portrait of $X_{12}$ for $\lambda < 0$ . Figure source: made by the author. . . . .	79
4.23	Local behavior of the phase portrait of $X_{12}$ for $\lambda = 0$ . Figure source: made by the author. . . . .	79
4.24	Local behavior of the phase portrait of $X_{12}$ for $\lambda > 0$ . Figure source: made by the author. . . . .	79
4.25	Local phase portrait of $X_{21}$ at $p_2 = p_3$ when $D = 0$ . Figure source: made by the author. . . . .	80
4.26	The displacement map $d(\alpha, \beta)$ defined near $(\alpha_0, \beta_0)$ . Figure source: made by the author. . . . .	80
4.27	Illustration of the flow of $X_{22a}$ with $a = 1$ and $\beta < -1$ at the sets $S_x$ and $S_y$ . Figure source: made by the author. . . . .	80
4.28	Unfinished phase portrait of $X_{22a}$ with $a = 1$ , $\beta = 1$ and $\alpha \leq -16$ . Figure source: made by the author. . . . .	80
4.29	Unfinished phase portrait of $X_{22a}$ with $a = -1$ , $\alpha < 0$ and $\beta \geq 1 + 2\sqrt{-\alpha}$ . Figure source: made by the author. . . . .	81
4.30	Illustration of the flow of $X_1$ at the sets $S_{x_1}$ and $S_{y_1}$ . Figure source: made by the author. . . . .	81
4.31	Illustration of the flow of $X_2$ at the sets $S_{x_2}$ and $S_{y_2}$ . Figure source: made by the author. . . . .	81
4.32	Specific local phase portraits of $X_{23}$ at $p$ . Figure source: made by the author. . . . .	82
4.33	Plot of the sets $R(\alpha, \beta) = 0$ and $\alpha + \beta^2 = 0$ . Figure source: made by the author. . . . .	82

4.34	Local phase portrait of $p(X_{23})$ , with $a = 1$ , at the origin of $U_1$ . Figure source: made by the author. . . . .	82
4.35	Unfinished blow up of the origin of chart $U_1$ of $X_{24}$ with $\alpha = 1$ . Figure source: made by the author. . . . .	83
4.36	Local phase portrait of $X_{24}$ the origin of chart $U_1$ with $a = 1$ , $\alpha = 1$ and $\beta \neq 0$ . Figure source: made by the author. . . . .	83
6.1	A polycycle $\Gamma$ composed by a hyperbolic saddle $p_1$ and a tangential singularity $p_2$ . Figure source: made by the author. . . . .	95
6.2	Bifurcation diagram of $\Gamma$ for $r_1 > 1$ . The blue lines represents either a stable polycycle or a hyperbolic and stable limit cycle. The green lines represent a sliding polycycle. Figure source: made by the author. . . . .	96
6.3	Bifurcation diagram of $\Gamma$ for $\frac{1}{2} < r_1 < 1$ . The blue (resp. red) lines represents either a stable (resp. unstable) polycycle or a hyperbolic stable (resp. unstable) limit cycle. The green lines represents either a sliding polycycle or a semi-stable limit cycle. Figure source: made by the author. . . . .	97
6.4	Bifurcation diagram of $\Gamma$ for $r_1 < \frac{1}{2}$ . The blue (resp. red) lines represents either a stable (resp. unstable) polycycle or a hyperbolic stable (resp. unstable) limit cycle. The green lines represents either a sliding polycycle or a semi-stable limit cycle. Figure source: made by the author. . . . .	98
6.5	An example of $\Gamma^3$ with the open ring $A$ contained in the bounded region delimited by $\Gamma^3$ . Figure source: made by the author. . . . .	99
6.6	Examples of a tangential singularity $p$ such that (a) $A_s \neq A_u$ and (b) $A_s = A_u$ . Figure source: made by the author. . . . .	99
6.7	Illustration of the maps $T^u$ and $T^s$ . The choosing between (a) and (c) depends whether the Poincaré map is defined in the bounded or unbounded region delimited by $\Gamma^n$ . Figure source: made by the author. . . . .	101
6.8	Illustration of the maps used in the proof of Theorem 6.4. Figure source: made by the author. . . . .	102
6.9	Illustration of $u_0$ . Figure source: made by the author. . . . .	103
6.10	Illustration of $x_0^s(\mu)$ and $x_0^u(\mu)$ . Figure source: made by the author. . . . .	104
6.11	Illustration of $d(\mu) > 0$ and $d(\mu) < 0$ . Figure source: made by the author. . . . .	105
6.12	Illustration of $\theta_s > 0$ and $\theta_u < 0$ . Figure source: made by the author. . . . .	106
6.13	Illustration of $(s, n)$ along $x_\mu^s(t)$ . Figure source: made by the author. . . . .	107
6.14	Illustration of $R_1, R_2$ and $R_3$ with $d_i(\mu) = 0$ in (a), and $d_i(\mu) < 0$ in (b). Observe that if $d_i(\mu) > 0$ , then the composition may not be well defined. Figure source: made by the author. . . . .	111
6.15	Observe that the arc of orbit between $q_0$ and $P(q_0, \mu)$ together with the perturbation of $\Gamma^3$ creates a positive invariant set in which we can apply the Poincaré-Bendixson theory. Figure source: made by the author. . . . .	112
6.16	An example of the construction of the points $C_i$ and the lines $l_i$ . Figure source: made by the author. . . . .	112
6.17	Illustration of $d_1^* < 0$ for both $r_2 > 1$ and $r_2 < 1$ . Figure source: made by the author. . . . .	113
6.18	Illustration of the sets $G_{i,j}$ . Figure source: made by the author. . . . .	115
6.19	Illustration of the induction process with $R_3 > 1$ and $R_2 < 1$ . Blue (resp. red) means a stable (resp. unstable) polycycle or limite cycle. Figure source: made by the author. . . . .	117

6.20 Illustration of  $\Gamma$  unperturbed (*a*) and perturbed (*b*). Figure source: made by the author. . . . . 118

6.21 Illustration of the maps  $F_i$  and  $G_i$ ,  $i \in \{1, 2\}$ , with  $\beta_1 > 0$  and  $\beta_2 < 0$ . Observe that the point  $p_2$  is equivalent to  $x_2 = 0$ . Figure source: made by the author. . . . . 119

## CONTENTS

1	INTRODUCTION	17
2	PRELIMINARIES	21
2.1	Reversibility . . . . .	21
2.2	Poincaré compactification . . . . .	25
2.3	Blow up technique . . . . .	26
2.4	Markus-Neumann-Peixoto theorem . . . . .	27
2.5	Index of singularities and limit cycles . . . . .	27
2.6	Bifurcation of heteroclinic connections . . . . .	28
2.7	The averaging theory . . . . .	29
2.8	Transition map near a hyperbolic saddle . . . . .	29
2.9	Transition map near a semi-hyperbolic singularity . . . . .	31
2.10	The Cardano-Tartaglia formula . . . . .	31
3	(2;0)-REVERSIBILITY	33
3.1	Statement of the main results . . . . .	33
3.2	Proof of theorem 3.6 . . . . .	37
3.3	Phase portraits . . . . .	38
3.4	Proof of theorem 3.7 . . . . .	49
4	(2;1)-REVERSIBILITY	51
4.1	Statement of the main results . . . . .	51
4.2	Approach method . . . . .	57
4.3	System $X_{21}$ . . . . .	59
4.4	System $X_{22}$ . . . . .	63
4.5	System $X_{23}$ . . . . .	65
4.6	Systems $X_{24}$ and $X_{25}$ . . . . .	70
5	THE FRIEDMANN-ROBERTSON-WALKER SYSTEM	85
5.1	Introduction and statement of the main results . . . . .	85
5.2	Proof of theorem 5.1 . . . . .	86
6	POLYCYCLES IN NON-SMOOTH VECTOR FIELDS	95
6.1	Introduction and description of the results . . . . .	95
6.2	Main results . . . . .	97
6.3	Transition map near a tangential singularity . . . . .	100
6.4	Proofs of theorems 6.4 and 6.7 . . . . .	101
6.5	The displacement map . . . . .	102
6.6	The further displacement map . . . . .	112
6.7	Proof of theorem 6.8 . . . . .	115
6.8	Proof of theorem 6.9 . . . . .	118
7	CONCLUSION	123
	REFERENCES	125



## 1 INTRODUCTION

Let  $P, Q: \mathbb{R}^2 \rightarrow \mathbb{R}$  be two  $C^k$ ,  $k \geq 1$ , functions. A *planar  $C^k$  differential system* is a system of the form

$$\dot{x} = P(x, y), \quad \dot{y} = Q(x, y), \quad (1.1)$$

where the dot in system (1.1) denote the derivative with respect to the independent variable  $t$ . The map  $X = (P, Q)$  is called a *vector field*. If  $P$  and  $Q$  are polynomials such that the maximum of the degrees of  $P$  and  $Q$  is  $n$ , then system (1.1) is a *planar polynomial differential system of degree  $n$* , or just a *polynomial system*. If  $n = 1$ , then system (1.1) is a *planar linear differential system*. This last class of system is already completely understood, see for instance the books [19, 25, 50]. However, if  $n \geq 2$ , then we know very few things. The class of planar polynomial systems with degree  $n \geq 2$ , i.e. the *planar nonlinear polynomial differential systems*, is too wide and thus it is common to study more specific subclasses and to classify them by their topological behavior.

With this in mind, we point out the subclass of the *reversible vector fields*. Given a  $C^k$  planar vector field  $X$  and a  $C^k$  diffeomorphism  $\varphi: \mathbb{R}^2 \rightarrow \mathbb{R}^2$  such that  $\varphi = \varphi^{-1}$  (i.e.  $\varphi$  is an *involution*) we say that  $X$  is a  $\varphi$ -reversible vector field of type  $(2; r)$ ,  $r \in \{0, 1, 2\}$ , if

$$D\varphi(x, y)X(x, y) = -X(\varphi(x, y)), \quad (1.2)$$

for all  $(x, y) \in \mathbb{R}^2$  and  $Fix(\varphi) = \{(x, y) \in \mathbb{R}^2: \varphi(x, y) = (x, y)\}$  is a  $r$ -dimensional manifold. We observe that  $D\varphi(x, y)$  denotes the *Jacobian matrix* of  $\varphi$  applied at the point  $(x, y)$ . In a simple way,  $X$  is  $\varphi$ -reversible if after applying the change of coordinates  $(u, v) = \varphi(x, y)$  one obtains  $-X$ .

Knowing that any planar polynomial vector field  $X$  can be extended analytically to the sphere  $\mathbb{S}^2 = \{(x, y, z) \in \mathbb{R}^3: x^2 + y^2 + z^2 = 1\}$  through the *Poincaré compactification* (see Section 2.2), great advances in the topological classification of the planar nonlinear polynomial differential systems were made by Peixoto [44] and furthermore extended by Sotomayor [54]. From these works we point out the notion of *generic families*. Given a set  $\mathfrak{X}$  we say that  $\xi \in \mathfrak{X}$  is *generic* if  $\xi$  is an element of a collection  $\Sigma \subset \mathfrak{X}$  such that:

- (a)  $\Sigma$  is large with respect to  $\mathfrak{X}$ ;
- (b) its elements are amenable to simple description.

In a more mathematical way, if  $\mathfrak{X}$  is endowed with some interesting topology, then condition (a) can be replaced by

- (a<sub>1</sub>)  $\Sigma$  is open and dense in  $\mathfrak{X}$ .

In [56] Teixeira applied the notion of generic families in the set of one and two-parameters families of germs of reversible vector fields of type  $(2; 1)$ . Moreover, Buzzi [9] also applied this notion in the set of one-parameter families of germs of reversible vector fields of type  $(2; 0)$  with a singularity at the origin. Knowing that the unique germ of reversible vector field of type  $(2; 2)$  is  $X = 0$  we conclude that the works of Teixeira and Buzzi together provide a topological classification of all the symmetrical singularities of germs of planar reversible vector fields of low codimension. In other words, given a

symmetrical singularity of a planar reversible vector field we know all the low codimension bifurcations that can occur on it. Furthermore, Medrado and Teixeira [35, 36] also gave a classification of the symmetrical singularities of the reversible vector fields of type  $(3; 2)$  of codimension zero, one and two. For more works about reversibility see Buzzi, Roberto and Teixeira [14], for a time-reversible system, and Pereira and Pessoa [46, 47], for reversible vector fields over the sphere.

Therefore, based in the works of Buzzi [9] and Teixeira [56], Chapters 3 and 4 of this dissertation concerns with the global phase portrait, in the Poincaré disk, of all the topological normal forms given by [56] and [9]. Since such normal forms are *local*, we observe that their global phase portraits *does not* represent the global phase portrait of all reversible vector fields of type  $(2; 0)$  and  $(2; 1)$  of low codimension. However, for a classification of all the quadratic reversible vector fields of type  $(2; 1)$ , see Llibre and Medrado [30]. Furthermore, see Theorem 3.7 for the phase portraits of the normal forms obtained by Buzzi and Theorem 4.3 for the phase portraits of the normal forms obtained by Teixeira. Given a vector field  $X$ , our approach works as follows.

- (a) First we workout what we call the *local behavior* of the vector field  $X$ , i.e. we
  - 1) study all the possible finite singularities;
  - 2) use the Grobman-Hartman Theorem, The Stable Manifold Theorem and the Blow Up technique to obtain the local phase portrait of  $X$  at each of the finite singularities;
  - 3) look for singularity bifurcations as the saddle-node, the center-focus and the Hopf bifurcation;
  - 4) use tools as the Poincaré-Hopf Theorem and the Bendixson Criterion to understand when and where a limit cycle can appear;
  - 5) study the equator of the compactification  $p(X)$  of  $X$ ;
- (b) Then we look for topological informations which involves more than one singularity as heteroclinic connections and the formation of graphs;
- (c) Finally we look for convenient curves in which the flow of  $X$  crosses it in a convenient way to shrink the possibilities for the  $\alpha$  and  $\omega$ -limit of the separatrices.

We observe that the work contained in both chapters is a co-work with professors Claudio Buzzi and Jaume Llibre, with the work [13] of Chapter 3 already published and the work [11] of Chapter 4 submitted for publication.

Chapter 5 consist in a application of the *Averaging Theory* in the field of Astrophysics, i.e. the application of the Averaging Theory in the four-dimensional Hamiltonian

$$H = \frac{1}{2} (y^2 - x^2 + p_y^2 - p_x^2) + \frac{1}{4} (ax^4 + 2bx^2y^2 + cy^4) - \omega (xp_y - yp_x), \quad (1.3)$$

which models in a simplified way what is called the *Friedmann-Robertson-Walker universe*. We observe that this is a co-work with professors Claudio Buzzi and Jaume Llibre and it was already published. See [12]. Our goal in this work is the description, in an analytical way, of the periodic orbits around the origin of the four-dimensional vector field derived from the Hamiltonian (1.3). See Theorem 5.1. Furthermore, our approach works as follows.

- (a) First we applied the change of coordinates  $(x, y, p_x, p_y) = \sqrt{\varepsilon}(X, Y, p_X, p_Y)$ , obtaining a four-dimensional vector field which is topologically equivalent to the original system, derived from the Hamiltonian (1.3). We observe that this new system has the necessary  $\varepsilon$ -parameter;
- (b) Then we applied a linear change of coordinates  $(X, Y, p_X, p_Y) = (u, v, p_u, p_v)$  such that in these new coordinate the system is in its Jordan coordinates, i.e. its linear part is equal its Jordan Normal form;
- (c) Then we applied the polar change of coordinates

$$(u, v, p_u, p_v) = (r \cos \theta, r \sin \theta, \rho \cos(\theta + \phi), \rho \sin(\theta + \phi)),$$

obtained a never-vanishing  $\dot{\theta}$ ;

- (d) Since  $\dot{\theta}$  never vanishes, we can take  $\theta$  as the independent variable of the polar system and then shrink the dimension of the vector field from four to three;
- (e) In this three-dimensional nonautonomous vector field which has  $\theta$  as its independent variable, we write the variable  $\rho$  as a function of  $(\theta, r, \phi, h)$ , where  $h$  is the fixed-value of the first integral obtained from (1.3) in these new coordinate system. Thus, we obtain a two-dimension vector field which depends on the parameter  $h$ ;
- (f) Hence, we apply the Averaging Theory in this planar nonautonomous vector field obtaining information about its periodic orbits, which translates in to informations about the periodic orbits of the original system.

Chapter 6 concerns with the polycycles of a non smooth vector field (also known as *piecewise* vector fields). More precisely, if  $\Gamma$  is a polycycle of a non-smooth vector field, composed by tangential singularities, hyperbolic saddles and semi-hyperbolic saddles, then in Chapter 6 we prove the following.

- (a) The stability of  $\Gamma$  depends on the stability of its singularities. See Theorem 6.4 and Corollary 6.5;
- (b) If all the singularities of  $\Gamma$  compress the flow (resp. all the singularities repels the flow) around it, then  $\Gamma$  is stable (resp. unstable). Furthermore, if small enough perturbation of  $\Gamma$  has a limit cycle, then it is unique, hyperbolic and stable (resp. unstable). See Theorem 6.7;
- (c) If  $\Gamma$  has  $n$  singularities satisfying some conditions, then there exists a perturbation of  $\Gamma$  such that at least  $n$  limit cycles bifurcate from it. See Theorem 6.8;
- (d) If  $\Gamma$  is composed by a hyperbolic saddle and a quadratic-regular tangential singularity, then the bifurcation diagrams of  $\Gamma$  was completely described in the generic cases. See Theorem 6.9.

Our approach in Chapter 6 relies in the extension of previous results that are already well established in the smooth case, i.e. in polycycles of vector fields of class  $C^\infty$  (see [17, 20, 23, 38, 49]), together with the characterization of the flow of non-smooth vector fields near tangential singularities, obtained by Andrade, Gomide and Novaes [2]. We also observe that this work is a undergoing collaboration with professors Claudio Buzzi and Douglas Novaes.

For the sake of self-containedness, Chapter 2 concerns with some preliminaries necessary for Chapters 3, 4, 5 and 6. Finally, at the end we have a conclusion pointing out the highlights of each chapter.

## 2 PRELIMINARIES

### 2.1 Reversibility

In this subsection we will state some definitions and prove some properties about the planar reversible vector fields. For more details about this class of vector fields, please see the survey [28]. For now on in this subsection  $X$  is always a  $C^k$ ,  $k \geq 1$ ,  $\varphi$ -reversible vector field of type  $(2; r)$ , with  $r \in \{0, 1, 2\}$ .

**Definition 2.1.** If  $p$  is a singularity of  $X$  such that  $p \in \text{Fix}(\varphi)$ , then  $p$  is a *symmetrical singularity* of  $X$ . Moreover, if  $\gamma$  is an orbit of  $X$  such that  $\gamma \cap \text{Fix}(\varphi) \neq \emptyset$ , then  $\gamma$  is a *symmetrical orbit* of  $X$ .

**Property 2.2** (Invariance by change of variables). If  $\Phi: \mathbb{R}^2 \rightarrow \mathbb{R}^2$  is a  $C^k$ ,  $k \geq 1$ , diffeomorphism, then the vector field  $X' = \Phi_*X$  is a  $\psi$ -reversible vector field of type  $(2; r)$ , where  $\psi = \Phi \circ \varphi \circ \Phi^{-1}$ .

*Proof.* Knowing that  $X'(p) = D\Phi(\Phi^{-1}(p))X(\Phi^{-1}(p))$  it follows from the chain rule and from (1.2) that

$$\begin{aligned} D\psi(p)X'(p) &= D\Phi(\varphi(\Phi^{-1}(p)))D\varphi(\Phi^{-1}(p))D\Phi^{-1}(p)D\Phi(\Phi^{-1}(p))X(\Phi^{-1}(p)) \\ &= D\Phi(\varphi(\Phi^{-1}(p)))D\varphi(\Phi^{-1}(p))X(\Phi^{-1}(p)) \\ &= -D\Phi(\varphi(\Phi^{-1}(p)))X(\varphi(\Phi^{-1}(p))), \end{aligned}$$

while,

$$\begin{aligned} -X'(\psi(p)) &= -D\Phi(\Phi^{-1}(\psi(p)))X(\Phi^{-1}(\psi(p))) \\ &= -D\Phi(\varphi(\Phi^{-1}(p)))X(\varphi(\Phi^{-1}(p))). \end{aligned}$$

Hence,  $D\psi(p)X'(p) = -X'(\psi(p))$  for any  $p \in \mathbb{R}^2$ .  $\square$

**Property 2.3** (Relation between the flow  $\Psi$  and  $\varphi$ ). Let  $\Psi$  be the flow of  $X$ . Then

$$\varphi \circ \Psi_t = \Psi_{-t} \circ \varphi.$$

*Proof.* It follows from (1.2) that  $-X = \varphi_*X$ , i.e.  $\varphi$  is a conjugacy between  $X$  and  $-X$  and thus we have the result.  $\square$

**Property 2.4** (Transversality of the flow at  $\text{Fix}(\varphi)$ ). Let  $p \in \text{Fix}(\varphi)$ . Then either  $p$  is a singularity of  $X$  or  $X(p)$  is transversal to  $\text{Fix}(\varphi)$  at  $p$

*Proof.* If the dimension of  $\text{Fix}(\varphi)$  is zero, then  $T_p\text{Fix}(\varphi) = \{(0, 0)\}$  thus the result is immediate. If the dimension of  $\text{Fix}(\varphi)$  is at least one and  $X(p) \in T_p\text{Fix}(\varphi)$ , then there exist  $\alpha: ]-\varepsilon, \varepsilon[ \rightarrow \text{Fix}(\varphi)$  such that  $\alpha(0) = p$  and  $\alpha'(0) = X(p)$ . Knowing that  $\varphi \circ \alpha = \alpha$  it follows that

$$D\varphi(\alpha(t))\alpha'(t) = \alpha'(t)$$

for any  $t \in ]-\varepsilon, \varepsilon[$ . Taking  $t = 0$  we have  $D\varphi(p)X(p) = X(p)$ . Hence, it follows from (1.2) that  $-X(p) = X(p)$  and thus we have the proof.  $\square$

**Remark 2.5.** It follows from Property 2.4 that the unique germ of reversible vector field of type (2; 2) is  $X = 0$ .

**Property 2.6** (Jacobian matrix as an involution). If  $p \in \text{Fix}(\varphi)$ , then  $D\varphi(p)$  is an involution.

*Proof.* Once  $\varphi$  is a diffeomorphism over  $\mathbb{R}^2$  it follows that  $D\varphi(p)$  is also a diffeomorphism over  $\mathbb{R}^2$ . Now, it follows from  $\varphi = \varphi^{-1}$  and  $\varphi(p) = p$  that

$$[D\varphi(p)]^{-1} = D\varphi^{-1}(\varphi(p)) = D\varphi(\varphi(p)) = D\varphi(p).$$

Hence, we have the proof.  $\square$

**Property 2.7** (Relation between  $p$  and  $\varphi(p)$ ). Let  $p$  be a singularity of  $X$  and  $\lambda$  be an eigenvalue of  $DX(p)$  with algebraic dimension  $\alpha$  and geometric dimension  $\beta$ . Then  $\varphi(p)$  is a singularity of  $X$  and  $-\lambda$  is an eigenvalue of  $DX(\varphi(p))$  with algebraic dimension  $\alpha$  and geometric dimension  $\beta$ . Moreover, if  $u$  is an eigenvector of  $DX(p)$  associated with  $\lambda$ , then  $v = D\varphi(p)u$  is an eigenvector of  $DX(\varphi(p))$  associated with  $-\lambda$ .

*Proof.* Derivating (1.2) and then replacing  $(x, y) = p$  one will obtain

$$D\varphi(p)DX(p) = -DX(p)D\varphi(p).$$

Therefore, it follows from Property 2.6 that

$$D\varphi(p)DX(p) [D\varphi(p)]^{-1} = -DX(\varphi(p)),$$

i.e.  $DX(p)$  and  $DX(\varphi(p))$  are similar. The result now follows from the linear algebra.  $\square$

**Property 2.8** (Relations between  $\gamma(t)$  and  $\varphi(\gamma(-t))$ ). The following statements hold.

- (a) If  $\gamma(t)$  is an orbit of  $X$ , then  $\sigma(t) = \varphi(\gamma(-t))$  is also an orbit of  $X$ ;
- (b) If  $\gamma$  intersects  $\text{Fix}(\varphi)$  in two distinct points, then  $\gamma$  is periodic;
- (c) If  $\gamma$  is a periodic orbit of period  $T > 0$ , then  $\sigma$  is also a periodic orbit of period  $T > 0$ .
- (d) If  $\gamma$  is closed and  $\pi_p, \pi_q$  are the Poincaré maps at  $p \in \gamma$  and  $q = \varphi(p) \in \sigma$ , then  $\varphi \circ \pi_p = \pi_q^{-1} \circ \varphi$ .

*Proof.* Let  $\gamma(t)$  be an orbit of  $X$ , i.e.  $\gamma'(t) = X(\gamma(t))$ . It follows from  $\sigma(t) = \varphi(\gamma(-t))$  and from (1.2) that

$$\sigma'(t) = -D\varphi(\gamma(-t))\gamma'(-t) = -D\varphi(\gamma(-t))X(\gamma(-t)) = X(\varphi(\gamma(-t))) = X(\sigma(t)).$$

Therefore,  $\sigma(t)$  is also an orbit of  $X$  and thus we have statement (a).

If  $\gamma(0), \gamma(T) \in \text{Fix}(\varphi)$ , with  $T > 0$ , then  $\gamma(0) = \sigma(0)$  and thus it follows from the Existence and Uniqueness Theorem that  $\gamma(t) = \sigma(t)$ , for every  $t$ . Hence,

$$\gamma(-T) = \sigma(-T) = \varphi(\gamma(T)) = \gamma(T)$$

and thus it follows statement (b).

If  $\gamma(t)$  is a periodic orbit of period  $T > 0$ , i.e.  $T > 0$  is the smallest real number such that  $\gamma(t + T) = \gamma(t)$ , then

$$\sigma(t + T) = \varphi(\gamma(-t - T)) = \varphi(\gamma(-t)) = \sigma(t)$$

and thus  $\sigma$  is also a periodic orbit of period  $T_0 \leq T$ . Knowing that  $\gamma(t) = \varphi(\sigma(-t))$  it follows that  $T_0 = T$  and thus we have statement (c).

Finally, to prove statement (d), let  $l_p$  be a transversal section of  $\gamma$  at  $p$ . If we take  $l_p$  small enough, then  $l_q = \varphi(l_p)$  is also a transversal section of  $\sigma$  at  $q$  and thus  $\pi_p: l_p \rightarrow l_p$ ,  $\pi_q: l_q \rightarrow l_q$  are both well defined. It is well known that there are two maps  $\tau_p: l_p \rightarrow \mathbb{R}^+$ ,  $\tau_q: l_q \rightarrow \mathbb{R}^+$  of the same class of differentiability of  $X$ , such that

$$\pi_p(\xi) = \Psi(\tau_p(\xi), \xi), \quad \pi_q(\xi) = \Psi(\tau_q(\xi), \xi), \quad (2.1)$$

where  $\Psi(t, \xi)$  is the flow of  $X$ . Let  $a \in l_p$ ,  $b = \pi_p(a)$ ,  $\alpha = \varphi(a)$ ,  $\beta = \varphi(b)$  and  $\omega = \pi_q^{-1}(\alpha)$  and observe that  $b \in l_p$  and  $\alpha, \beta, \omega \in l_q$ . See Figure 2.1. Our goal is to prove  $\varphi \circ \pi_p(a) =$

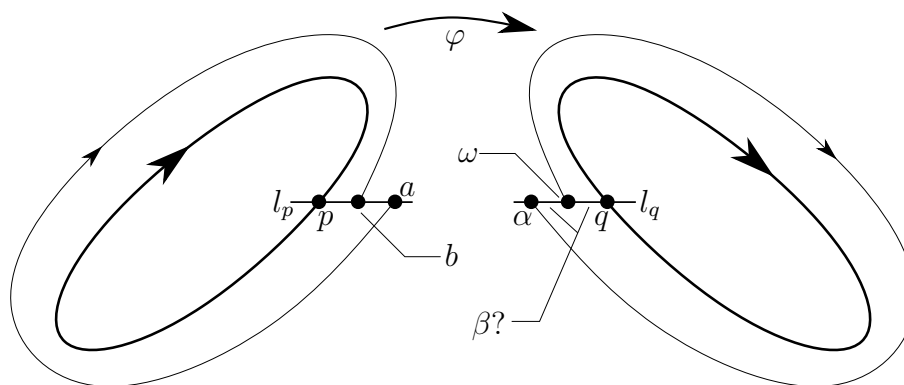


Figure 2.1: Illustration of  $l_p$  and  $l_q$ . Figure source: made by the author.

$\pi_q^{-1} \circ \varphi(a)$  and for it is enough to prove  $\beta = \omega$ . It follows from (2.1) and from Property 2.3 that

$$\begin{aligned} \omega &= \Psi(-\tau_q(\omega), \alpha) = \Psi(-\tau_q(\omega), \varphi(a)) = \varphi(\Psi(\tau_q(\omega), a)), \\ \beta &= \varphi(\pi_p(a)) = \varphi(\Psi(\tau_p(a), a)). \end{aligned} \quad (2.2)$$

Therefore, it is enough to prove that  $\tau_q(\omega) = \tau_p(a)$ . Once  $\omega \in l_q$  it follows from (2.2) that  $\Psi(\tau_q(\omega), a) \in l_p$  and thus  $\tau_q(\omega) \geq \tau_p(a)$ . It follows from (2.2) and from Property 2.3 that

$$\beta = \varphi(\Psi(\tau_p(a), a)) = \Psi(-\tau_p(a), \varphi(a)) = \Psi(-\tau_p(a), \alpha)$$

and thus  $\Psi(-\tau_p(a), \alpha) \in l_q$ . Therefore, we have  $-\tau_p(a) \leq -\tau_q(\omega)$ , i.e.  $\tau_p(a) \geq \tau_q(\omega)$  and hence we have the proof.  $\square$

**Property 2.9** (Relation between the Poincaré maps). Let  $\gamma(t)$  be a periodic orbit of  $X$ ,  $\sigma(t) = \varphi(\gamma(-t))$ ,  $p \in \gamma$  and  $\pi_p, \pi_q$  the Poincaré maps at  $p$  and  $q = \varphi(p) \in \sigma$ . If  $\lambda$  is an eigenvalue of  $D\pi_p(p)$  with algebraic dimension  $\alpha$  and geometric dimension  $\beta$ , then  $\lambda^{-1}$  is an eigenvalue of  $D\pi_q(q)$  with algebraic dimension  $\alpha$  and geometric dimension  $\beta$ . Moreover, if  $u$  is an eigenvector of  $D\pi_p(p)$  associated with  $\lambda$ , then  $v = D\varphi(p)u$  is an eigenvector of  $D\pi_q(q)$  associated with  $\lambda^{-1}$ .

*Proof.* It follows From Property 2.8(d) that  $\varphi \circ \pi_p(\xi) = \pi_q^{-1} \circ \varphi(\xi)$ , for any  $\xi$  in the domain of  $\pi_p$ . Derivating it and then replacing  $\xi = p$  one will obtain

$$D\varphi(p)D\pi_p(p) = D\pi_q^{-1}(q)D\varphi(p).$$

Therefore, we conclude that both  $D\pi_p(p)$  and  $D\pi_q^{-1}(q)$  are similar and thus the result follows from the linear algebra.  $\square$

**Property 2.10** (Relation between the  $\alpha$  and  $\omega$ -limits). Let  $p$  be a singularity of  $X$ ,  $\gamma(t)$  a periodic orbit,  $q = \varphi(p)$  and  $\sigma(t) = \varphi(\gamma(-t))$ . If  $\mu$  is an orbit of  $X$  such that  $p \in \omega(\mu)$ , then  $q \in \alpha(\nu)$ , where  $\nu(t) = \varphi(\mu(-t))$ . Moreover, if  $\gamma \subset \omega(\mu)$ , then  $\sigma \subset \alpha(\nu)$ .

*Proof.* We will prove for the singularity  $p$ . The case of the periodic orbit  $\gamma$  is analogous. Let us assume  $p \in \omega(\mu)$ , i.e there is a sequence  $(t_k)$  of real numbers such that

$$\lim_{k \rightarrow +\infty} t_k = +\infty \text{ and } \lim_{k \rightarrow +\infty} \mu(t_k) = p.$$

It follows from the continuity of  $\varphi$  that  $\varphi(\mu(t_k)) \rightarrow \varphi(p)$  and thus  $(-t_k)$  is a sequence of real numbers such that

$$\lim_{k \rightarrow +\infty} -t_k = -\infty \text{ and } \lim_{k \rightarrow +\infty} \nu(-t_k) = q,$$

i.e.  $q \in \alpha(\nu)$  and thus we have the result.  $\square$

It follows from Properties 2.7, 2.8, 2.9 and 2.10 that given a singularity  $p$  or a periodic orbit  $\gamma(t)$ , a huge amount of information can be carry on to  $q = \varphi(p)$  and  $\sigma(t) = \varphi(\gamma(-t))$ . And even more information can be obtained if  $p$  or  $\gamma$  are symmetrical. Here we point out the following.

- (a)  $p$  (resp.  $\gamma$ ) is hyperbolic if, and only if,  $q$  (resp.  $\sigma$ ) is hyperbolic;
- (b)  $\gamma$  is stable outwards (resp. inwards) if, and only if,  $\sigma$  is unstable outwards (resp. inwards);
- (c)  $p$  is a stable node (resp. stable focus) if, and only if,  $q$  is an unstable node (resp. unstable focus);
- (d)  $p$  is a saddle if, and only if,  $q$  is a saddle;
- (e) If we have a center-focus problem at  $p$  and  $p$  is symmetrical, then  $p$  is a center;
- (f) If  $\gamma$  is a symmetrical periodic orbit, then it is not a limit cycle.

**Property 2.11** (Local linearization of the involution). If  $p \in \text{Fix}(\varphi)$ , then there is a neighborhood of  $p$  such that  $\varphi$  is  $C^k$ -conjugate to one of the following involutions.

- (a)  $\Phi(x_1, x_2) = (-x_1, -x_2)$  if  $X$  is (2; 0)-reversible;
- (b)  $\Phi(x_1, x_2) = (x_1, -x_2)$  if  $X$  is (2; 1)-reversible;
- (c)  $\Phi(x_1, x_2) = (x_1, x_2)$  if  $X$  is (2; 2)-reversible.

*Proof.* Given  $x \in \mathbb{R}^2$ , let  $T(x) = x + p$  and  $\psi(x) = T^{-1} \circ \varphi \circ T$ . Observe that  $\psi(0) = 0$  and  $\psi = \psi^{-1}$ . Therefore,  $\varphi$  is conjugate to another involution  $\psi$  such that  $\psi(0) = 0$  and thus we can now suppose  $p = 0$ . Let  $Q = D\varphi(0)$  and  $\sigma(x) = x + Q\varphi(x)$ . Derivating  $\sigma$  we obtain  $D\sigma(x) = I_2 + QD\varphi(x)$  and thus it follows from Property 2.6 that  $D\sigma(0) = 2I_2$ . Hence, it follows from the Inverse Function Theorem that  $\sigma$  is locally a diffeomorphism at the origin. Observe that  $\sigma(0) = 0$  and  $\sigma$  has the same class of differentiability as  $\varphi$ . Now, observe that

$$\sigma(\varphi(x)) = \varphi(x) + Qx = Q(Q\varphi(x) + x) = Q\sigma(x)$$

and thus  $\sigma$  conjugates  $\varphi$  and  $Q$ . Therefore, it follows from the theory of manifolds that  $\text{Fix}(Q)$  is a  $r$ -dimensional subspace of  $\mathbb{R}^2$  and thus with a change of basis we have the result.  $\square$

## 2.2 Poincaré compactification

Let  $X$  be a planar *polynomial* vector field of degree  $n$ . The *Poincaré compactified vector field*  $p(X)$  is an analytic vector field on  $\mathbb{S}^2$  constructed as follow (for more details see Chapter 5 of [19]).

First we identify  $\mathbb{R}^2$  with the plane  $(x_1, x_2, 1)$  in  $\mathbb{R}^3$  and define the *Poincaré sphere* as  $\mathbb{S}^2 = \{y = (y_1, y_2, y_3) \in \mathbb{R}^3 : y_1^2 + y_2^2 + y_3^2 = 1\}$ . We define the *northern hemisphere*, the *southern hemisphere* and the *equator* respectively by  $H_+ = \{y \in \mathbb{S}^2 : y_3 > 0\}$ ,  $H_- = \{y \in \mathbb{S}^2 : y_3 < 0\}$  and  $\mathbb{S}^1 = \{y \in \mathbb{S}^2 : y_3 = 0\}$ .

Consider the projections  $f_{\pm} : \mathbb{R}^2 \rightarrow H_{\pm}$  given by  $f_{\pm}(x_1, x_2) = \pm\Delta(x_1, x_2)(x_1, x_2, 1)$ , where  $\Delta(x_1, x_2) = (x_1^2 + x_2^2 + 1)^{-\frac{1}{2}}$ . These two maps define two copies of  $X$ , one copy  $X^+$  in  $H_+$  and one copy  $X^-$  in  $H_-$ . Consider the vector field  $X' = X^+ \cup X^-$  defined in  $\mathbb{S}^2 \setminus \mathbb{S}^1$ . Note that the *infinity* of  $\mathbb{R}^2$  is identified with the equator  $\mathbb{S}^1$ . The Poincaré compactified vector field  $p(X)$  is the analytic extension of  $X'$  from  $\mathbb{S}^2 \setminus \mathbb{S}^1$  to  $\mathbb{S}^2$  given by  $y_3^{n-1}X'$ . The *Poincaré disk*  $\mathbb{D}$  is the projection of the closed northern hemisphere to  $y_3 = 0$  under  $(y_1, y_2, y_3) \mapsto (y_1, y_2)$  (the vector field given by this projection will also be denoted by  $p(X)$ ). Note that to know the behavior  $p(X)$  near  $\mathbb{S}^1$  is the same than to know the behavior of  $X$  near the infinity. We define the local charts of  $\mathbb{S}^2$  by  $U_i = \{y \in \mathbb{S}^2 : y_i > 0\}$  and  $V_i = \{y \in \mathbb{S}^2 : y_i < 0\}$  for  $i \in \{1, 2, 3\}$ . In these charts we define  $\phi_i : U_i \rightarrow \mathbb{R}^2$  and  $\psi_i : V_i \rightarrow \mathbb{R}^2$  by  $\phi_i(y_1, y_2, y_3) = -\psi_i(y_1, y_2, y_3) = \left(\frac{y_m}{y_i}, \frac{y_n}{y_i}\right)$ , where  $m \neq i, n \neq i$  and  $m < n$ . Denoting by  $(u, v)$  the image of  $\phi_i$  and  $\psi_i$  in every chart (therefore,  $(u, v)$  will play different roles in each chart) one can see the following expressions for  $p(X)$ :

$$\begin{aligned} &v^n \eta(u, v) \left( Q \left( \frac{1}{v}, \frac{u}{v} \right) - uP \left( \frac{1}{v}, \frac{u}{v} \right), -vP \left( \frac{1}{v}, \frac{u}{v} \right) \right) \text{ in } U_1, \\ &v^n \eta(u, v) \left( P \left( \frac{u}{v}, \frac{1}{v} \right) - uQ \left( \frac{u}{v}, \frac{1}{v} \right), -vQ \left( \frac{u}{v}, \frac{1}{v} \right) \right) \text{ in } U_2, \\ &\eta(u, v)(P(u, v), Q(u, v)) \text{ in } U_3, \end{aligned}$$

where  $\eta(u, v) = (u^2 + v^2 + 1)^{-\frac{1}{2}(n-1)}$ . We can omit the term  $\eta(u, v)$  by a time rescaling of  $p(X)$ . Therefore, we obtain a polynomial expression of  $p(X)$  in each  $U_i$ . The expressions of  $p(X)$  in each  $V_i$  is the same as that for each  $U_i$ , except by a multiplicative factor of  $(-1)^{n-1}$ . In these coordinates for  $i \in \{1, 2\}$ ,  $v = 0$  always represents the points of  $\mathbb{S}^1$  and thus the infinity of  $\mathbb{R}^2$ . Note that  $\mathbb{S}^1$  is invariant under the flow of  $p(X)$ .

### 2.3 Blow up technique

If the origin is an isolated singularity of a *polynomial* planar vector field  $X$ , then we can apply the change of coordinates  $\phi : \mathbb{R}_+ \times \mathbb{S}^1 \rightarrow \mathbb{R}^2$  given by  $\phi(\theta, r) = (r \cos \theta, r \sin \theta) = (x, y)$ , where  $\mathbb{R}_+ = \{r \in \mathbb{R} : r > 0\}$ . Therefore, we can induce a vector field  $X_0$  in  $\mathbb{R}_+ \times \mathbb{S}^1$  by pullback, i.e.  $X_0 = D\phi^{-1}X$ . One can see that if the  $k$ -jet of  $X$  (i.e. the Taylor expansion of order  $k$  of  $X$ , denoted by  $j_k$ ) is zero at the origin, then the  $k$ -jet of  $X_0$  is also zero in every point of  $\{0\} \times \mathbb{S}^1$ . Thus, taking the first  $k \in \mathbb{N}$  satisfying  $j_k(0, 0) = 0$  and  $j_{k+1}(0, 0) \neq 0$  we can define the vector field  $\hat{X} = \frac{1}{r^k}X_0$ . Therefore, to know the behavior of  $\hat{X}$  near  $\mathbb{S}^1$  is the same than to know the behavior of  $X$  near the origin. One can also see that  $\mathbb{S}^1$  is invariant under the flow of  $\hat{X}$ . For a more detailed study of this technique, see Chapter 3 of [19]. One can also see that  $\hat{X}$  is given by

$$\dot{r} = \frac{x\dot{x} + y\dot{y}}{r^{k+1}}, \quad \dot{\theta} = \frac{x\dot{y} - y\dot{x}}{r^{k+2}}.$$

There is a generalization of the Blow Up Technique, known as *Quasihomogeneous Blow Up*. This time we consider the change of coordinates  $\psi(\theta, r) = (r^\alpha \cos \theta, r^\beta \sin \theta) = (x, y)$  for  $(\alpha, \beta) \in \mathbb{N}^2$ . Similarly to the previous technique, we can induce a vector field  $X_0$  in  $\mathbb{R}_+ \times \mathbb{S}^1$ . For some  $k \in \mathbb{N}$  maximal one can define  $X_{\alpha, \beta} = \frac{1}{r^k}X_0$  and see that this vector field is given by

$$\dot{r} = \xi(\theta) \frac{\cos \theta r^\beta \dot{x} + \sin \theta r^\alpha \dot{y}}{r^{\alpha+\beta+k-1}}, \quad \dot{\theta} = \xi(\theta) \frac{\alpha \cos \theta r^\alpha \dot{y} - \beta \sin \theta r^\beta \dot{x}}{r^{\alpha+\beta+k}},$$

where  $\xi(\theta) = (\beta \sin^2 \theta + \alpha \cos^2 \theta)^{-1}$ . Observe that the factor  $\xi(\theta)$  can be cancel out. Similarly to the previous technique, to know the behavior of  $X_{\alpha, \beta}$  near  $\mathbb{S}^1$  (which is invariant) is the same than to know the behavior of  $X$  near the origin. For more details see chapter 3 of [19].

There is another blow up technique, known as *Quasihomogeneous directional Blow Up*. This time we consider the change of coordinates

$$\begin{cases} (x, y) \rightarrow (x_1^\alpha, x_1^\beta y_1) & \text{positive } x\text{-direction} \\ (x, y) \rightarrow (-x_1^\alpha, x_1^\beta y_1) & \text{negative } x\text{-direction} \\ (x, y) \rightarrow (x_1 y_1^\alpha, y_1^\beta) & \text{positive } y\text{-direction} \\ (x, y) \rightarrow (x_1 y_1^\alpha, -y_1^\beta) & \text{negative } y\text{-direction,} \end{cases}$$

where  $(\alpha, \beta) \in \mathbb{N}^2$ . For example, if we do a Quasihomogeneous blow up at the positive  $x$ -direction, leading to a vector field  $X_+^x$ , then to understand the positive  $x$ -direction, i.e.  $x > 0$ , of  $X$  is the same than to understand the positive  $x_1$ -direction of vector field  $X_+^x$ . Similarly to the previous techniques, for some  $k \in \mathbb{N}$  maximal one can divide  $X_+^x$  and  $X_-^x$  by  $x^k$  (and  $X_+^y, X_-^y$  by  $y^k$ ) and study a regularized version of these systems. Moreover,

this vectors fields (not regularized) are given by

$$\begin{aligned} \dot{x}_1 &= \frac{1}{\alpha} x_1^{1-\alpha} \dot{x}, & \dot{y}_1 &= \frac{x_1^\alpha \dot{y} - \frac{\beta}{\alpha} \dot{x} y}{x_1^{\alpha+\beta}} && \text{at the positive } x\text{-direction;} \\ \dot{x}_1 &= -\frac{1}{\alpha} x_1^{1-\alpha} \dot{x}, & \dot{y}_1 &= \frac{x_1^\alpha \dot{y} + \frac{\beta}{\alpha} \dot{x} y}{x_1^{\alpha+\beta}} && \text{at the negative } x\text{-direction;} \\ \dot{x}_1 &= \frac{y_1^\beta \dot{x} - \frac{\alpha}{\beta} \dot{y} x}{y_1^{\alpha+\beta}}, & \dot{y}_1 &= \frac{1}{\beta} y_1^{1-\beta} \dot{y} && \text{at the positive } y\text{-direction;} \\ \dot{x}_1 &= \frac{y_1^\beta \dot{x} + \frac{\alpha}{\beta} \dot{y} x}{y_1^{\alpha+\beta}}, & \dot{y}_1 &= -\frac{1}{\beta} y_1^{1-\beta} \dot{y} && \text{at the negative } y\text{-direction.} \end{aligned}$$

## 2.4 Markus-Neumann-Peixoto theorem

Let  $X$  be a *polynomial* vector field,  $p(X)$  its compactification defined on  $\mathbb{D}$  and  $\phi$  the flow defined by  $p(X)$ . The separatrices of  $p(X)$  are:

- (a) all the orbits contained in  $\mathbb{S}^1$ , i.e. at infinity;
- (b) all the singular points;
- (c) all the separatrices of the hyperbolic sectors of the finite and infinite singular points; and
- (d) all the limit cycles of  $X$ .

Denote by  $\mathcal{S}$  the set of all separatrices. It is known that  $\mathcal{S}$  is closed, see for instance [19]. Each connected component of  $\mathbb{D} \setminus \mathcal{S}$  is called a *canonical region* of the flow  $(\mathbb{D}, \phi)$ . The *separatrix configuration*  $\mathcal{S}_c$  of a flow  $(\mathbb{D}, \phi)$  is the union of all the separatrices  $\mathcal{S}$  of the flow together with one orbit belonging to each canonical region. The separatrix configuration  $\mathcal{S}_c$  of the flow  $(\mathbb{D}, \phi)$  is topologically equivalent to the separatrix configuration  $\mathcal{S}_c^*$  of the flow  $(\mathbb{D}, \phi^*)$  if there exists a homeomorphism from  $\mathbb{D}$  to  $\mathbb{D}$  which transforms orbits of  $\mathcal{S}_c$  into orbits of  $\mathcal{S}_c^*$ , orbits of  $\mathcal{S}$  into orbits of  $\mathcal{S}^*$  and preserves or reverses the orientation of all these orbits.

**Theorem 2.12** (Markus-Neumann-Peixoto). *Let  $p(X)$  and  $p(Y)$  be two Poincaré compactifications in the Poincaré disk  $\mathbb{D}$  of the two polynomial vector fields  $X$  and  $Y$  with finitely many singularities, respectively. Then the phase portraits of  $p(X)$  and  $p(Y)$  are topologically equivalent if and only if their separatrix configurations are topologically equivalent.*

For a proof of this Theorem see [34, 39, 45, 6].

## 2.5 Index of singularities and limit cycles

Let  $p$  be an isolated singularity of a *polynomial* vector field  $X$ . Let  $e$  and  $h$  denote the number of elliptical and hyperbolic sectors of  $p$ , respectively. The *Poincaré index* of

$p$  is given by

$$i_p = \frac{e - h}{2} + 1.$$

It is known that  $i_p \in \mathbb{Z}$ . See for instance chapter 6 of [19].

**Proposition 2.13.** *Let  $\Gamma$  be a limit cycle of a planar polynomial vector field  $X$ . Then there is at least one singularity in the bounded region limited by it. Moreover, if there is a finite number of singularities in the bounded region limited by  $\Gamma$ , then the sum of their Poincaré index is 1.*

**Theorem 2.14** (Poincaré-Hopf Theorem). *Let  $X$  be a planar polynomial vector field and  $p(X)$  its compactification defined on  $\mathbb{S}^2$ . If  $p(X)$  has a finite number of singularities, then the sum of their Poincaré index is 2.*

For a proof of Proposition 2.13 and Theorem 2.14 see chapter 6 of [19].

## 2.6 Bifurcation of heteroclinic connections

Let  $X = X(x, y; \mu)$  be a  $C^k$ ,  $k \geq 1$ , planar vector field depending on a parameter  $\mu \in \mathbb{R}^n$  such that at  $\mu = \mu_0$  there is a *graph*  $G$  of saddles connected by heteroclinic orbits. Moreover, let  $p_u$  and  $p_s$  be two hyperbolic saddles of  $G$  connected by the heteroclinic orbit  $\Gamma_0$ . Following [49] we denote  $\gamma_0(t)$  a parametrization of  $\Gamma_0$  and define  $x_0 = \gamma_0(0)$  and  $l_0$  a transversal section of  $\Gamma_0$  passing through  $x_0$ . We also denote  $\Gamma_u$  and  $\Gamma_s$  the perturbations of  $\Gamma_0$ , for  $\|\mu - \mu_0\|$  small enough, such that  $\alpha(\Gamma_u) = p_u$  and  $\omega(\Gamma_s) = p_s$ . Let  $x_s$  and  $x_u$  be the intersections of  $\Gamma_s$  and  $\Gamma_u$  with  $l_0$ , respectively, and let  $n_s$  and  $n_u$  be its coordinates along the line  $l_0$  in such a way that  $n(x) > 0$  outside the graph,  $n(x_0) = 0$  and  $n(x) < 0$  inside the graph. Now we define the *displacement function*  $d(\mu) = n_u - n_s$ . See Figure 2.2.

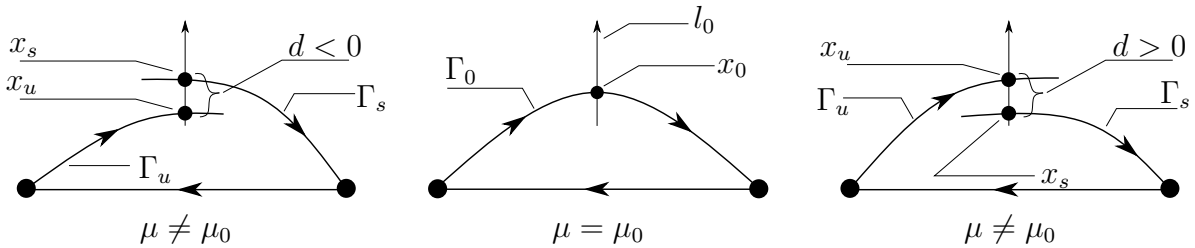


Figure 2.2: The displacement map  $d$  defined near  $\mu_0$ . Figure source: made by the author.

It follows from [49] that  $d$  is well defined and

$$\frac{\partial d}{\partial \mu_i}(\mu_0) = -\frac{\omega_0}{\|X(x_0; \mu_0)\|} \int_{-\infty}^{+\infty} \left( e^{-\int_0^t \text{Div}(X(\gamma_0(s); \mu_0)) ds} \right) X(\gamma_0(t); \mu_0) \wedge \frac{\partial X}{\partial \mu_i}(\gamma_0(t); \mu_0) dt,$$

where  $(x_1, x_2) \wedge (y_1, y_2) = x_1 y_2 - x_2 y_1$ ,  $\mu = (\mu_1, \dots, \mu_n) \in \mathbb{R}^n$  and  $\omega_0 = 1$  if the orientation of  $G$  is positive or  $\omega_0 = -1$  if the orientation of  $G$  is negative. For more details see also [26, 22].

## 2.7 The averaging theory

In this section we recall the averaging theory of first order for finding periodic solutions. The averaging theory up to third order specifically for studying periodic orbit was developed in [8]. The averaging theory of higher order can be found in [31]. Other versions of the averaging theory can also be found in [7] and in Theorems 11.5 and 11.6 of [57]. For a general view on the averaging theory see the book [53].

**Theorem 2.15.** *Consider the differential system*

$$\dot{x}(t) = \varepsilon F(t, x) + \varepsilon^2 R(t, x, \varepsilon), \quad (2.3)$$

where  $F : \mathbb{R} \times D \rightarrow \mathbb{R}^n$ ,  $R : \mathbb{R} \times D \times (-\varepsilon_f, \varepsilon_f) \rightarrow \mathbb{R}^n$  are continuous functions,  $T$ -periodic in the first variable and  $D$  is an open subset of  $\mathbb{R}^n$ . We define  $f : D \rightarrow \mathbb{R}^n$  as

$$f(z) = \frac{1}{T} \int_0^T F(s, z) ds,$$

and assume that

- (i)  $F$  and  $R$  are locally Lipschitz with respect to  $x$ ;
- (ii) for all  $a \in D$  with  $f(a) = 0$ , there exists a neighborhood  $V$  of  $a$  such that  $f(z) \neq 0$  for all  $z \in \bar{V} \setminus \{a\}$  and  $d_B(f, V, 0) \neq 0$  (see its definition later on).

Then for  $|\varepsilon| > 0$  small enough there exists a  $T$ -periodic solution  $\varphi(\cdot, \varepsilon)$  of system (2.3) such that  $\varphi(\cdot, \varepsilon) \rightarrow a$  as  $\varepsilon \rightarrow 0$ .

We denoted by  $d_B(f, V, 0)$  the *Brouwer degree* at the triple  $(f, V, 0)$ . A sufficient condition for showing that the Brouwer degree is non-zero is that the Jacobian of the function  $f$  at  $a$  (when it is defined) is non-zero, for a proof see [32]. For more details about the Brouwer degree see [5].

## 2.8 Transition map near a hyperbolic saddle

Let  $X_\mu$  be a  $C^\infty$  planar vector field depending on a  $C^\infty$ -way on a parameter  $\mu \in \mathbb{R}^r$ ,  $r \geq 1$ , defined in a neighborhood of a hyperbolic saddle  $p_0$  at  $\mu = \mu_0$ . Let  $\Lambda \subset \mathbb{R}^r$  be a small enough neighborhood of  $\mu_0$ ,  $\nu(\mu) < 0 < \lambda(\mu)$  be the eigenvalues of the hyperbolic saddle  $p(\mu)$ ,  $\mu \in \Lambda$ , and  $r(\mu) = \frac{|\nu(\mu)|}{\lambda(\mu)}$  be the *hyperbolicity ratio* of  $p(\mu)$ . Let  $B$  be a small enough neighborhood of  $p_0$  and  $\Phi : B \times \Lambda \rightarrow \mathbb{R}^2$  be a  $C^\infty$ -change of coordinates such that  $\Phi$  sends the hyperbolic saddle  $p(\mu)$  to the origin and its unstable and stable manifolds  $W^u(\mu)$  and  $W^s(\mu)$  to the axis  $Ox$  and  $Oy$ , respectively (see Figure 2.3). Let  $\sigma$  and  $\tau$  be two small enough transversal sections of  $Oy$  and  $Ox$ , respectively. We can suppose that  $\sigma$  and  $\tau$  are parametrized by  $x \in [0, x_0]$  and  $y \in [0, y_0]$ , with  $x = 0$  and  $y = 0$  corresponding to  $Oy \cap \sigma$  and  $Ox \cap \tau$ , respectively. Clearly the flow of  $X_\mu$ , in this new coordinate system, defines a transition map:

$$D : ]0, x_0] \times \Lambda \rightarrow ]0, y_0]$$

called the *Dulac map*, since it was study first by Dulac in [18]. See Figure 2.3. Observe that  $D$  is  $C^\infty$  for  $x \neq 0$  and it can be continuously extend by  $D(0, \mu) = 0$  for all  $\mu \in \Lambda$ .

**Definition 2.16.** Given  $k \geq 0$ , we will denote by  $I_k$  the set of functions  $f : [0, x_0] \times \Lambda_k \rightarrow \mathbb{R}$  with the following properties:

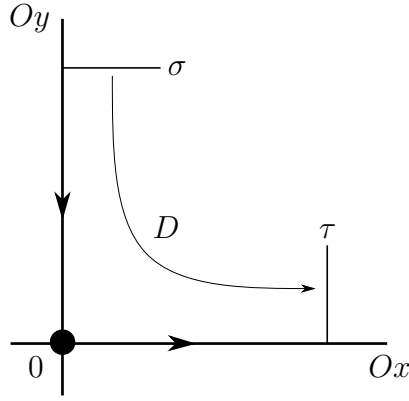


Figure 2.3: The Dulac map near a hyperbolic saddle. Figure source: made by the author.

- (a)  $f$  is  $C^\infty$  on  $]0, x_0] \times \Lambda_k$ ;
- (b) For each  $j \in \{0, \dots, k\}$  we have that  $\varphi_j = x^j \frac{\partial^j f}{\partial x^j}(x, \mu)$  is continuous on  $]0, x_0] \times \Lambda_k$  with  $\varphi_j(x, \mu) \rightarrow 0$  for  $x \rightarrow 0$ , uniformly in  $\mu$ .

Furthermore, we will say that a function  $f : [0, x_0] \times \Lambda \rightarrow \mathbb{R}$  is class  $I$  if  $f$  is  $C^\infty$  on  $]0, x_0] \times \Lambda$  and for every  $k \geq 0$  there exists a neighborhood  $\Lambda_k \subset \Lambda$  of  $\mu_0$  such that  $f$  is of class  $I^k$  on  $]0, x_0] \times \Lambda_k$ .

To put it briefly, condition (a) of Definition 2.16 means that  $f$  works as desired when  $x \neq 0$ , while condition (b) give us some control of  $f$  and its  $x$ -partial derivatives as  $x \rightarrow 0$ , saying that if  $x \rightarrow 0$ , then  $f(x, \mu) \rightarrow 0$  uniformly in  $\mu$  and its  $x$ -partial derivatives may explode, but if it does, then it is on a uniformly way in  $\mu$  and it will not explode infinitely fast.

**Theorem 2.17** (Mourtada). *Let  $X_\mu$ ,  $\sigma$ ,  $\tau$ , and  $D$  be as above. Then*

$$D(x, \mu) = x^{r(\mu)}(A(\mu) + \phi(x, \mu)), \quad (2.4)$$

with  $\phi \in I$  and  $A$  a positive  $C^\infty$  function.

*Proof.* See [38, 20]. □

Following [20] we call *Mourtada's form* the expression (2.4) of the Dulac map and denote by  $\mathfrak{D}$  the class of maps given by (2.4).

**Proposition 2.18.** *Given  $D(x, \mu) = x^{r(\mu)}(A(\mu) + \phi(x, \mu)) \in \mathfrak{D}$  the following statements hold.*

- (a)  $D^{-1}$  is well defined and  $D^{-1}(x, \mu) = x^{\frac{1}{r(\mu)}}(B(\mu) + \psi(x, \mu)) \in \mathfrak{D}$ ;
- (b)  $\frac{\partial D}{\partial x}$  is well defined and

$$\frac{\partial D}{\partial x}(x, \mu) = r(\mu)x^{r(\mu)-1}(A(\mu) + \xi(x, \mu)),$$

with  $\xi \in I$ .

*Proof.* See [38, 20]. □

## 2.9 Transition map near a semi-hyperbolic singularity

Let  $X_\mu$  be a  $C^\infty$  planar vector field depending on a  $C^\infty$ -way on a parameter  $\mu \in \mathbb{R}^r$ ,  $r \geq 1$ , defined, at  $\mu = \mu_0$ , in a neighborhood of a singularity  $p_0$  such that  $p_0$  has a unique non-zero eigenvalue  $\lambda \in \mathbb{R} \setminus \{0\}$  and one of its sectors is hyperbolic, e.g. a saddle-node or a degenerated saddle. Reversing the time if necessary, we can assume  $\lambda < 0$ .

**Theorem 2.19.** *Let  $X_\mu$  and  $p_0 \in \mathbb{R}^2$  be as above. Then, for each  $k \geq 1$ , there exists a  $C^k$ -family of diffeomorphisms of  $\mathbb{R}^2$  such that at this new coordinate system  $X_\mu$  is given by*

$$\dot{x} = g(x, \mu), \quad \dot{y} = -y,$$

except by the multiplication of a  $C^k$ -positive function. Furthermore,

$$g(0, \mu_0) = \frac{\partial g}{\partial x}(0, \mu_0) = 0,$$

and  $g(x, \mu_0) > 0$  for  $0 < x < \varepsilon$  small enough.

*Proof.* See [20]. □

In this new coordinate system given by Theorem 2.19, let  $\sigma(\mu)$  and  $\tau$  be two small transversal sections of the axis  $Oy$  and  $Ox$  (which are, respectively, the stable and the central manifolds of the origin at  $\mu = \mu_0$ ). Let us parametrize  $\sigma(\mu)$  and  $\tau$  by  $x \in [x^*(\mu), x_0]$  and  $y \in [0, y_0]$ , where  $x^*(\mu)$  is the largest zero of  $g(x, \mu) = 0$ . As in Section 2.8, in this new coordinate system the flow of  $X_\mu$  defines a transition map:

$$F: ]x^*(\mu), x_0] \times \Lambda \rightarrow ]0, y_0].$$

**Theorem 2.20.** *Let  $X_\mu$  and  $F$  be as above. Then*

$$F(x, \mu) = ke^{-T(x, \mu)},$$

where  $k > 0$  and  $T: ]x^*(\mu), x_0] \times \Lambda \rightarrow \mathbb{R}^+$  is the time function to go from  $\sigma(\mu)$  to  $\tau$ .

*Proof.* See [20]. □

## 2.10 The Cardano-Tartaglia formula

Given a cubic equation

$$x^3 + px + q = 0, \tag{2.5}$$

if one make the change of variable  $x = u + v$  on (2.5) one will obtain

$$u^3 + v^3 + (3uv + p)(u + v) + q = 0.$$

Assuming that  $3uv + p = 0$  one will obtain  $u^3 + v^3 = -q$ . The combination of the equations

$$u^3 v^3 = -\frac{1}{27}p^3 \text{ and } u^3 + v^3 = -q$$

imply that  $u^3$  and  $v^3$  are the zeros of

$$z^2 + qz - \frac{1}{27}p^3 = 0.$$

Therefore,

$$u^3 = -\frac{q}{2} + \left(\frac{q^2}{4} + \frac{p^3}{27}\right)^{\frac{1}{2}}, \quad v^3 = -\frac{q}{2} - \left(\frac{q^2}{4} + \frac{p^3}{27}\right)^{\frac{1}{2}}.$$

**Remark 2.21.** We observe that  $x^{\frac{1}{n}}$  denotes the standard  $n$ th root of  $x$ , i.e. if  $x = re^{i\theta}$ , then  $x^{\frac{1}{n}} = \sqrt[n]{r}e^{i\frac{\theta}{n}}$ , where  $\sqrt[n]{x}$  denotes the  $n$ th real root (when it exists) of  $x$ . For example,  $8^{\frac{1}{3}} = \sqrt[3]{8} = 2$ , but  $(-8)^{\frac{1}{3}} = 1 + i\sqrt{3}$ , while  $\sqrt[3]{-8} = -2$ . In general both functions coincide when  $x$  is a non-negative real number.

Let  $D = \frac{1}{4}q^2 + \frac{1}{27}p^3$  and observe that if  $D \geq 0$ , then  $u^3$  and  $v^3$  are real numbers and thus we can take

$$u = \sqrt[3]{u^3} \text{ and } v = \sqrt[3]{v^3}.$$

Of course these values satisfy  $u^3 + v^3 = -q$  and  $3uv + p = 0$ , hence

$$x = \sqrt[3]{-\frac{q}{2} + \left(\frac{q^2}{4} + \frac{p^3}{27}\right)^{\frac{1}{2}}} + \sqrt[3]{-\frac{q}{2} - \left(\frac{q^2}{4} + \frac{p^3}{27}\right)^{\frac{1}{2}}}$$

is a (real) solution of (2.5). Let  $\xi = e^{i\frac{\pi}{3}}$  be a unity root and observe that the three solutions of (2.5), when  $D \geq 0$ , are given by

$$x_k = \xi^k \sqrt[3]{-\frac{q}{2} + \left(\frac{q^2}{4} + \frac{p^3}{27}\right)^{\frac{1}{2}}} + \xi^{2k} \sqrt[3]{-\frac{q}{2} - \left(\frac{q^2}{4} + \frac{p^3}{27}\right)^{\frac{1}{2}}},$$

where  $k \in \{0, 1, 2\}$ . If  $D < 0$  we cannot take any third root of  $u^3$  and  $v^3$  because not every choosing of roots satisfy  $uv = -\frac{1}{27}p^3$ . To satisfy this it is enough that  $u$  be the conjugate of  $v$ . Therefore, we can take

$$u = (u^3)^{\frac{1}{3}} \text{ and } v = (v^3)^{\frac{1}{3}}.$$

Hence, the solutions of (2.5), when  $D < 0$ , are given by

$$x_k = \xi^k \left(-\frac{q}{2} + \left(\frac{q^2}{4} + \frac{p^3}{27}\right)^{\frac{1}{2}}\right)^{\frac{1}{3}} + \xi^{2k} \left(-\frac{q}{2} - \left(\frac{q^2}{4} + \frac{p^3}{27}\right)^{\frac{1}{2}}\right)^{\frac{1}{3}},$$

where  $k \in \{0, 1, 2\}$ . Observe that if we take these roots when  $D \geq 0$ , then  $u$  will not necessarily be the conjugate of  $v$  (for example if both  $u^3$  and  $v^3$  are negative real numbers) and thus we would not have a solution of (2.5). At the other hand, we cannot always apply the  $\sqrt[3]{\cdot}$  when  $D < 0$  because not every complex number has a third real root.

If one let  $S$  and  $T$  denotes the *convenient root* of  $u^3$  and  $v^3$  (i.e. denotes the root according to the logic of this section), respectively, then the solutions of (2.5) are given by

$$\begin{cases} x_1 = S + T; \\ x_2 = -\frac{1}{2}(S + T) + \frac{1}{2}\sqrt{3}(S - T)i; \\ x_3 = -\frac{1}{2}(S + T) - \frac{1}{2}\sqrt{3}(S - T)i. \end{cases}$$

One can see that if  $D < 0$ , then all solutions are real and simple. If  $D = 0$  and  $q \neq 0$ , then  $x_1$  is a real simple solution and  $x_2 = x_3$  is a double real solution. If  $D = q = 0$ , then  $x_1 = x_2 = x_3$  is a real triple solution. Finally, if  $D > 0$ , then  $x_1$  is a real simple solution and  $x_2, x_3$  are two complex conjugates solutions.

### 3 (2;0)-REVERSIBILITY

#### 3.1 Statement of the main results

We recall that this is a co-work with professors Claudio Buzzi and Jaume Llibre and it was already published, see [13]. In the space of planar  $C^\infty$  reversible vector fields we consider the following equivalence relation:  $X \sim Y$  if there is a neighborhood  $U$  of  $(0, 0)$  such that  $X$  and  $Y$  coincide in  $U$ . The equivalence class of  $X$  is called the *germ* of  $X$ . We will denote the germ of  $X$  also by  $X$ . In this chapter we study the space of germs of  $C^\infty$  reversible vector fields of type  $(2; 0)$  with a singularity at the origin. This class of vector fields, endowed with the  $C^\infty$  topology, will be denoted by  $\mathfrak{X}$ . From now on any vector field will be a  $C^\infty$  vector field, unless we say other thing. In what follows we will state some necessary definitions.

**Definition 3.1.** Two germs of vector fields  $X, Y \in \mathfrak{X}$  are *topologically equivalent* if there are two neighborhoods  $U, V$  of the origin and a homeomorphism  $h : U \rightarrow V$  which sends orbits of  $X$  to orbits of  $Y$  preserving or reversing the orientation of all orbits. The homeomorphism  $h$  is a topological equivalence between  $X$  and  $Y$ .

**Definition 3.2.** A germ of vector field  $X \in \mathfrak{X}$  is *structural stable* if there is a neighborhood  $N$  of  $X$  such that  $X$  is topologically equivalent to every  $Y \in N$ . The set of the structural stable germs will be denoted by  $\Sigma_0$ . We will also consider the set  $\mathfrak{X}_1 = \mathfrak{X} \setminus \Sigma_0$ , i.e. the bifurcation set of  $\mathfrak{X}$ .

**Definition 3.3.** Let  $J = [-\varepsilon, \varepsilon]$  be a closed interval. Denote by  $\Theta$  the space of  $C^1$  mappings  $\xi : J \rightarrow \mathfrak{X}$  endowed with the  $C^1$  topology. Its elements will be called *one-parameter families of germs of vector fields* of  $\mathfrak{X}$ .  $\xi$  is generic if

1.  $\xi(-\varepsilon), \xi(\varepsilon) \in \Sigma_0$ ;
2. there is at most one  $\varepsilon_0 \in J$  such that  $\xi(\varepsilon_0) \in \mathfrak{X}_1$  and in this case  $\xi(\varepsilon_0)$  is structural stable in  $\mathfrak{X}_1$ ;
3. it is transversal to  $\mathfrak{X}_1$ .

**Definition 3.4.** Two one-parameter families  $\xi, \eta \in \Theta$  are *topologically equivalent* if there is a reparametrization  $h : J \rightarrow J$  and a family of homeomorphisms  $H : J \rightarrow \text{Hom}(U, V)$ , not necessarily continuous, such that for every  $\lambda \in J$  we have that  $H(\lambda)$  is a topological equivalence between  $\xi(\lambda)$  and  $\eta(h(\lambda))$ .

For more details about generic one-parameter families and bifurcation sets, see [44, 54]. Buzzi proved in [9] the following theorem about  $\mathfrak{X}$ .

**Theorem 3.5.** *The following statements hold.*

(a) *Every structural stable germ of a vector field in  $\mathfrak{X}$  is topologically equivalent to one of the following germs:*

1.  $X_1 = (x^2 - y^2, 2xy)$ ;
2.  $X_2 = (-x^2 - 2y^2, xy)$ ;

3.  $X_3 = (2x^2 - y^2, xy)$ ;
4.  $X_4 = (-x^2 - y^2, -2xy)$ ;
5.  $X_5 = (x^2 - 2y^2, -xy)$ .

(b) For  $\lambda$  small enough every generic one-parameter family of germs of vector fields of  $\mathfrak{X}$  is topologically equivalent to one of the following families:

1. Every germ given in (a);
2.  $(X_{12})_\lambda = (-\lambda x^2 - y^2 + x^4, (1 - \lambda)xy)$ ;
3.  $(X_{21})_\lambda = (\lambda x^2 - y^2 - x^4, (1 + \lambda)xy)$ ;
4.  $(X_{34})_\lambda = (\lambda x^2 + 2xy - y^2 - x^4, (\lambda - 1)xy + 2y^2)$ ;
5.  $(X_{43})_\lambda = (-\lambda x^2 + 2xy - y^2 + x^4, -(\lambda + 1)xy + 2y^2)$ ;
6.  $(X_{45})_\lambda = (\lambda x^2 - y^2 - x^4, (\lambda - 1)xy)$ ;
7.  $(X_{54})_\lambda = (-\lambda x^2 - y^2 + x^4, -(\lambda + 1)xy)$ ;
8.  $(X_{13})_\lambda = ((2 + \lambda)x^2 - y^2 + x^4, -\lambda x^2 + 2xy + y^2)$ ;
9.  $(X_{24})_\lambda = ((\lambda - 1)x^2 - xy - y^2 + x^4, -\lambda x^2 - xy)$ .

We note that all the germs of vector fields which appear in the statement of the previous theorem are polynomial. Theorem 3.5 motivated us to classify the phase portrait of the differential vector fields which appear in its statement and thus to extend the results of [9]. Our first result provides a tool for studying periodic orbits of those vector fields.

**Theorem 3.6.** *If  $X$  is a  $C^1$   $\varphi$ -reversible vector field of type (2;0) satisfying  $\text{Fix}(\varphi) = \{p\}$ , then there is no periodic orbit surrounding  $p$ .*

The main result of this chapter is the phase portraits, in the Poincaré disk, of the vector fields in the statements of Theorem 3.5. See Subsection 2.2 for more details of the Poincaré compactification.

**Theorem 3.7.** *The phase portraits in the Poincaré disk of the vector fields in Theorem 3.5 are given in Figures 3.1-3.8.*

**Remark 3.8.** We observe that the phase portraits given in Figures 3.1-3.8 *does not* represent the global phase portraits of all reversible vector fields of type (2;0) of low codimension. In fact, unless we are given a maximum degree, a reversible vector field of type (2;0) may have as many singularities as we want. Therefore, there is infinitely many of such phase portraits. However, it follows from Theorem 3.5 that a symmetrical singularity of codimension zero or one, of a reversible vector field of type (2;0), is topologically equivalent *at the origin*, for  $\lambda \approx 0$ , to one of the phase portraits given in Figures 3.1-3.8.

**Remark 3.9.** Figures 3.1-3.8 work as follow. The thicker lines represent the separatrices of the phase portrait and the thin lines represent generic orbits of the canonical regions (see Subsection 2.4 for more details). The biggest dots represent isolated singularities. The dot line at  $X_{12}$  and  $X_{45}$  for  $\lambda = 1$  and at  $X_{54}$  for  $\lambda = -1$  represents a line of singularities.

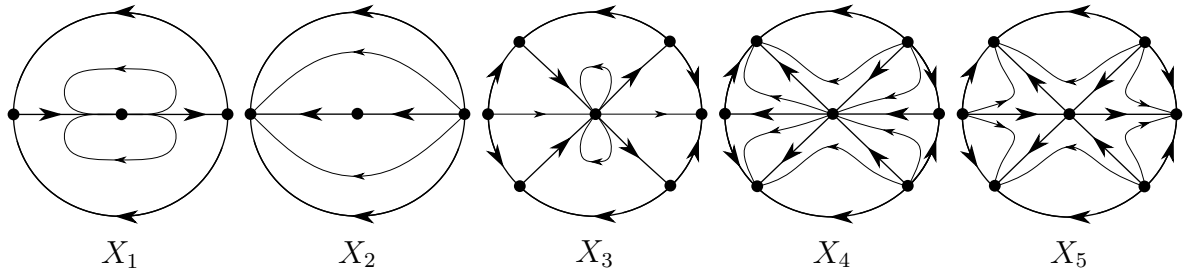


Figure 3.1: Phase portraits of  $X_1, X_2, X_3, X_4$  and  $X_5$ . Figure source: Figure 1 of [13].

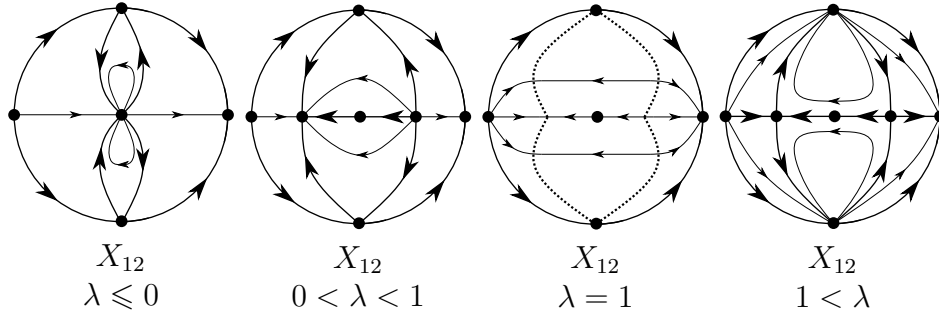


Figure 3.2: Phase portraits of  $X_{12}$ . Figure source: Figure 1 of [13].

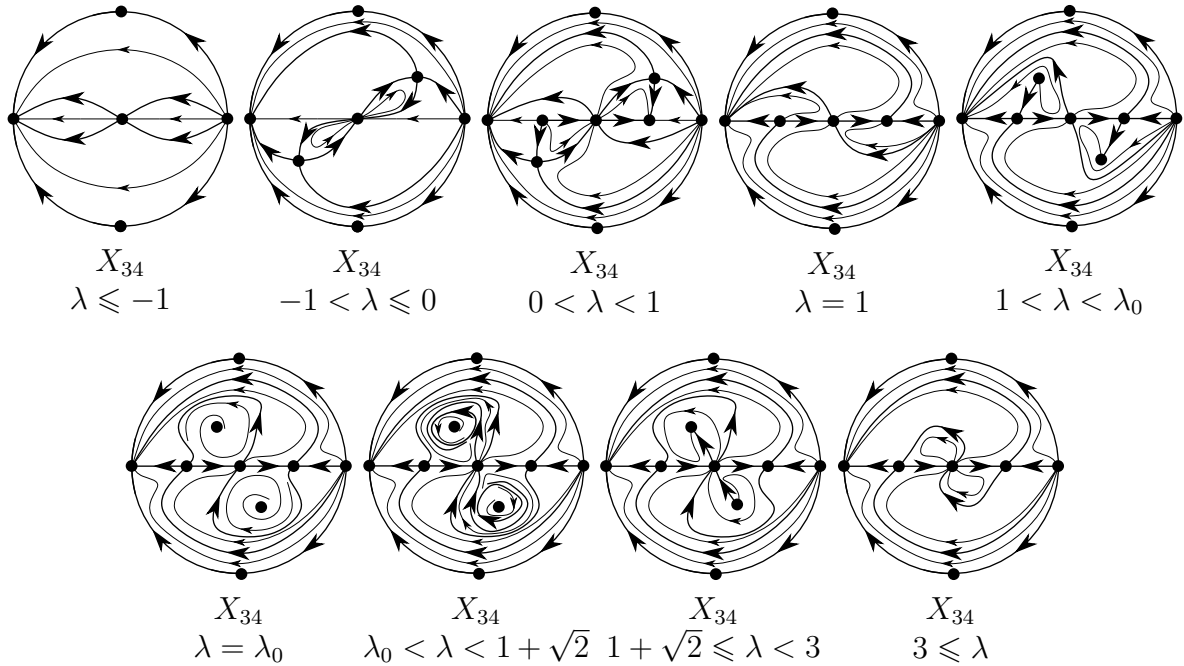


Figure 3.3: Phase portraits of  $X_{34}$ . Figure source: Figures 2 and 3 of [13].

**Remark 3.10.** Although we struggled to give as many analytical proofs as possible, one shall see in Proposition 3.13 that dealing analytically with limit cycles is a very difficult task and therefore we point out that numerical calculations about the number of limit cycles of system  $X_{34}$  were used for  $\lambda \in (1, 3)$ .

This section is organized as follows. Theorem 3.6 is proved in Section 3.2. In Sec-

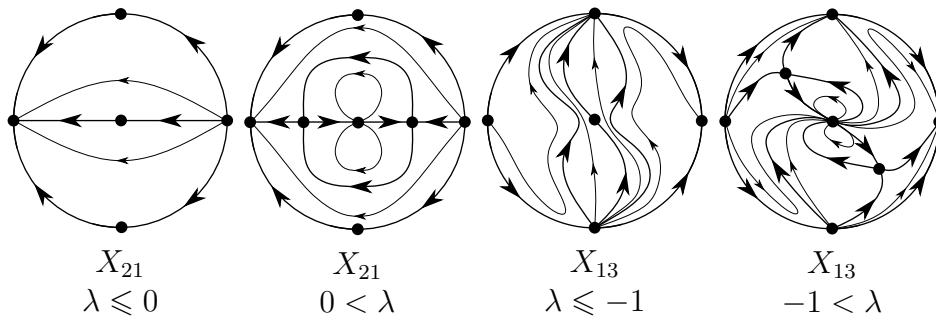


Figure 3.4: Phase portraits of  $X_{21}$  and  $X_{13}$ . Figure source: Figure 2 of [13].

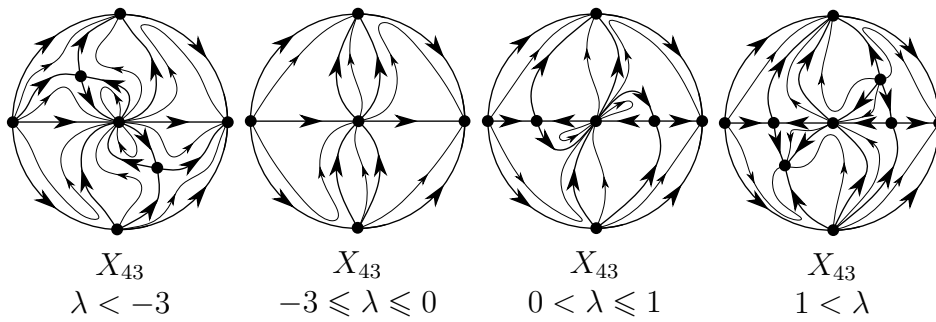


Figure 3.5: Phase portraits of  $X_{43}$ . Figure source: Figure 3 of [13].

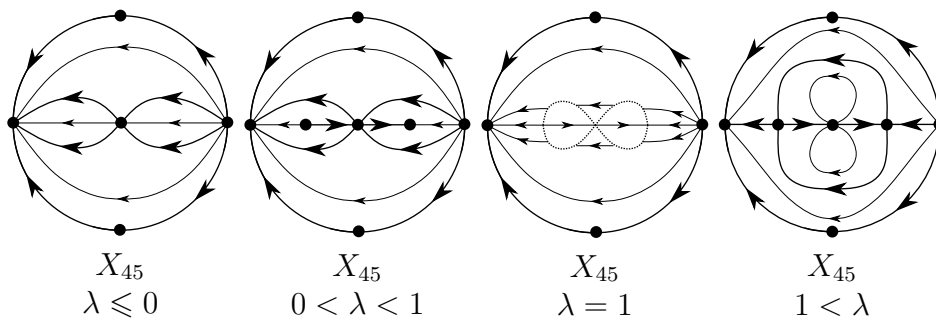


Figure 3.6: Phase portraits of  $X_{45}$ . Figure source: Figures 3 and 4 of [13].

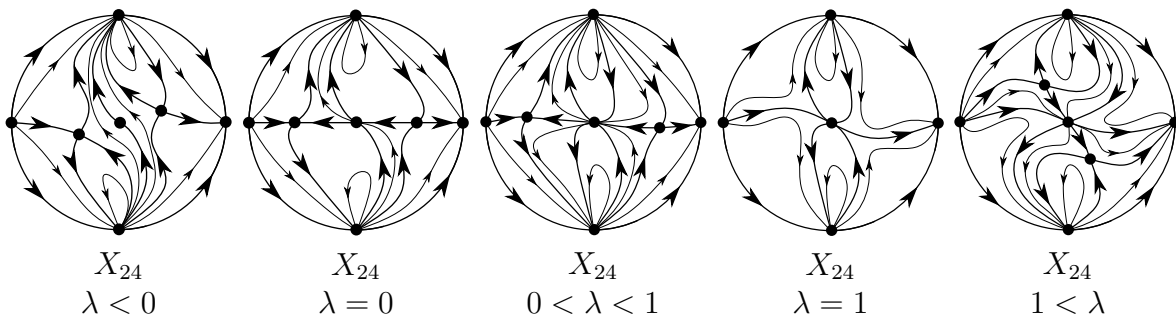


Figure 3.7: Phase portraits of  $X_{24}$ . Figure source: Figures 4 and 5 of [13].

tion 3.3 we study the phase portraits. Theorem 3.7 is proved in Section 3.4 .

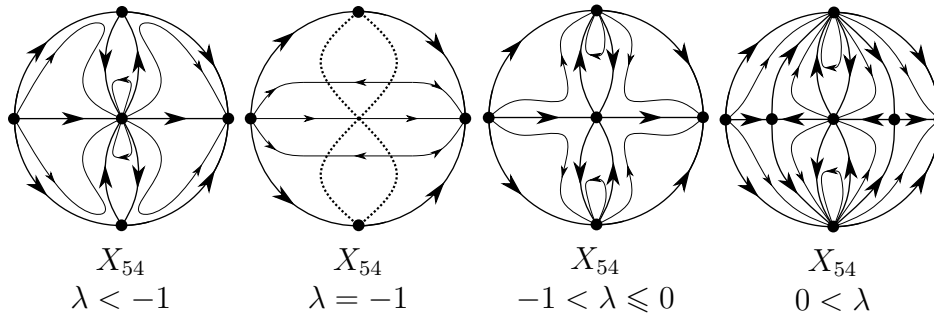


Figure 3.8: Phase portraits of  $X_{54}$ . Figure source: Figure 4 of [13].

### 3.2 Proof of theorem 3.6

*Proof.* The proof is by contradiction. Without loss of generality we can suppose  $p = (0, 0)$ . Let  $\gamma = \gamma(t)$  be a periodic orbit of period  $T > 0$  surrounding  $p$ . There are two options: either the sets  $\Gamma = \gamma([0, T])$  and  $\varphi(\Gamma)$  are disjoint or not.

If  $\Gamma$  intersects  $\varphi(\Gamma)$ , then there are  $t_1, t_2 \in \mathbb{R}$  satisfying  $\gamma(t_1) = \varphi(\gamma(t_2))$ . Define  $t_3 = (t_1 + t_2)/2$ ,  $t_4 = (t_1 - t_2)/2$ ,  $\xi(t) = \gamma(t + t_3)$  and  $\nu(t) = \varphi(\xi(-t))$ . It is clear that  $\xi$  and  $\nu$  are both solutions of  $X$  and that  $\xi(t_4) = \nu(t_4)$ . Therefore, by the Existence and Uniqueness Theorem we have  $\xi(t) = \nu(t)$  for all  $t \in \mathbb{R}$ . Hence,  $\xi(0) = \nu(0)$ , i.e.  $\gamma(t_3) = \varphi(\gamma(t_3))$  and therefore  $\gamma(t_3) = p$ , contradicting the fact that  $\gamma$  surrounds  $p$ .

If  $\Gamma$  does not intersect  $\varphi(\Gamma)$ , then denote by  $A$  the ring delimited by  $\Gamma$  and by  $\varphi(\Gamma)$ . Denote by  $U$  the interior of the region delimited by  $\Gamma$ . Once  $p \in U$  it follows that  $p \in \varphi(U)$ . Without loss of generality we can suppose that  $\Gamma$  delimit the *inner boundary* of  $A$ , i.e.  $\Gamma \subset \varphi(U)$ . Let  $r$  be any straight line through  $p$  and  $\tau : \mathbb{R} \rightarrow \mathbb{R}^2$  a parametrization of  $r$  with  $\tau(0) = p$ . Let  $\eta_1 < 0$  be the greatest and  $\eta_2 > 0$  the smallest real numbers satisfying  $q_i = \tau(\eta_i) \in \Gamma$ , for  $i \in \{1, 2\}$ . Observe that  $\tau([\eta_1, \eta_2])$  does not intersect  $\varphi(\Gamma)$ . Define  $\mu = \varphi \circ \tau$  and note that  $\mu$  is continuous,  $\mu(\eta_i) = \varphi(q_i)$  for  $i \in \{1, 2\}$  and  $\mu(0) = p$ . See Figure 3.9. It follows from the continuity that  $\mu([\eta_1, \eta_2])$  must intersect  $\Gamma$

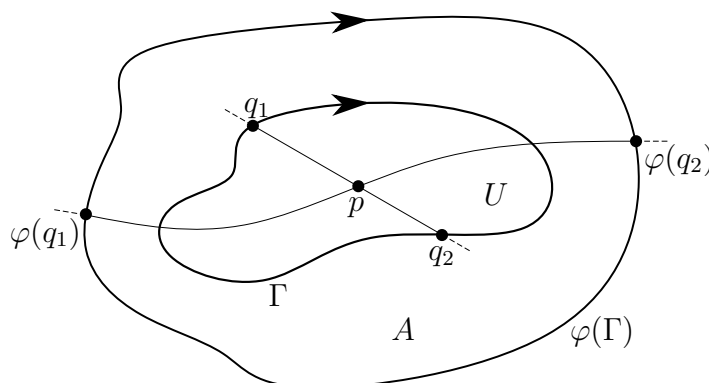


Figure 3.9: Illustration of  $\Gamma$  and  $\varphi(\Gamma)$ . Figure source: made by the author.

and therefore  $\tau([\eta_1, \eta_2])$  must intersect  $\varphi(\Gamma)$ . But this contradicts the fact that  $\tau([\eta_1, \eta_2])$  does not intersect  $\varphi(\Gamma)$ .  $\square$

### 3.3 Phase portraits

We will show how to obtain the phase portraits of the vector field  $X_{34}$  and give a sketch of how to obtain the phase portraits of the other families. First we remember that  $X_{34}$  is given by

$$\dot{x} = \lambda x^2 + 2xy - y^2 - x^4, \quad \dot{y} = (\lambda - 1)xy + 2y^2.$$

Note that  $\{(x, y) \in \mathbb{R}^2 : \dot{y} = 0\}$  is the union of the straight lines  $y = 0$  and  $y = \frac{1-\lambda}{2}x$ . Therefore, one can see that all the possible finite singularities are given by the origin and the points

$$p^\pm = \pm (\sqrt{\lambda}, 0), \quad q^\pm = \pm \left( \frac{1}{2}\sqrt{f(\lambda)}, \frac{1}{4}(1-\lambda)\sqrt{f(\lambda)} \right),$$

where  $f(\lambda) = -(\lambda+1)(\lambda-3)$ . By *possible* singularities we mean that  $p^\pm$  are well defined only for  $\lambda \geq 0$  and  $q^\pm$  are well defined only for  $-1 \leq \lambda \leq 3$ . In the following three propositions we study the *local behavior* of  $X_{34}$ , i.e. we study the local phase portrait of  $X_{34}$  at each finite and infinite singularity and the existence of limit cycles for every  $\lambda \in \mathbb{R}$ .

**Proposition 3.11.** *For every  $\lambda \in \mathbb{R}$  the following statements hold.*

- (a) *The origin is the only singularity of the chart  $U_1$  and it is an unstable node.*
- (b) *The origin is the only singularity of the chart  $U_2$  and its local phase portrait is given by Figure 3.10.*

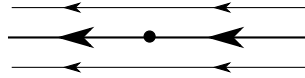


Figure 3.10: Local phase portrait at the origin of chart  $U_2$  of  $p(X_{34})$ . Figure source: Figure 6 of [13].

*Proof.* The first statement follows from the fact that  $p(X_{34})$  is given in the chart  $U_1$  by

$$\dot{u} = u - uv^2 + u^3v^2, \quad \dot{v} = v - \lambda v^3 - 2uv^3 + u^2v^3.$$

To prove the second statement we will do a quasihomogeneous blow up at the origin of the chart  $U_2$ . Following the algorithm of section 3.3 of [19] we choose  $(\alpha, \beta) = (1, 2)$  to apply the technique. Doing that one will obtain the vector field  $X_0 = X_0(r, \theta)$  given by

$$\dot{r} = rR_1(r, \theta), \quad \dot{\theta} = f(\theta) \sin \theta + rR_2(r, \theta),$$

where  $f(\theta) \neq 0$  for all  $\theta \in \mathbb{S}^1$ . The linear part of  $X_0$  at  $(0, 0)$  and at  $(0, \pi)$  are given by

$$DX_0(0, 0) = -DX_0(0, \pi) = \begin{pmatrix} -1 & 0 \\ 0 & 2 \end{pmatrix}.$$

Therefore, all the singularities of  $\mathbb{S}^1$  are hyperbolic and thus one can conclude Figure 3.10.  $\square$

**Proposition 3.12.** *The following statements hold.*

- (a) Singularity  $p^+$  (resp.  $p^-$ ) is a stable (resp. unstable) node for  $0 < \lambda < 1$ . For  $1 < \lambda$  both singularities  $p^\pm$  are saddles.
- (b) Singularities  $q^\pm$  are both saddles for  $-1 < \lambda < 1$ . For  $1 < \lambda < 1.4314..$  singularity  $q^+$  (resp.  $q^-$ ) is a stable (resp. unstable) node. For  $1.4314.. \leq \lambda < 1 + \sqrt{2}$  singularity  $q^+$  (resp.  $q^-$ ) is a stable (resp. unstable) focus. For  $1 + \sqrt{2} \leq \lambda \leq 2.8549..$  singularity  $q^+$  (resp.  $q^-$ ) is a unstable (resp. stable) focus. For  $2.8549.. < \lambda < 3$  singularity  $q^+$  (resp.  $q^-$ ) is a unstable (resp. stable) node.
- (c) For  $\lambda = 1$  we have  $q^\pm = p^\pm$  and they are both saddle-nodes.
- (d) The local phase portrait of  $X_{34}$  at the origin and its Poincaré index  $i$  are given by Figure 3.11.
- (e) It occurs a Hopf bifurcation at  $q^+$  (resp.  $q^-$ ) when  $\lambda = 1 + \sqrt{2}$ . Moreover, there is a hyperbolic stable (resp. unstable) limit cycle surrounding  $q^+$  (resp.  $q^-$ ) for  $1 + \sqrt{2} - \varepsilon < \lambda < 1 + \sqrt{2}$ .

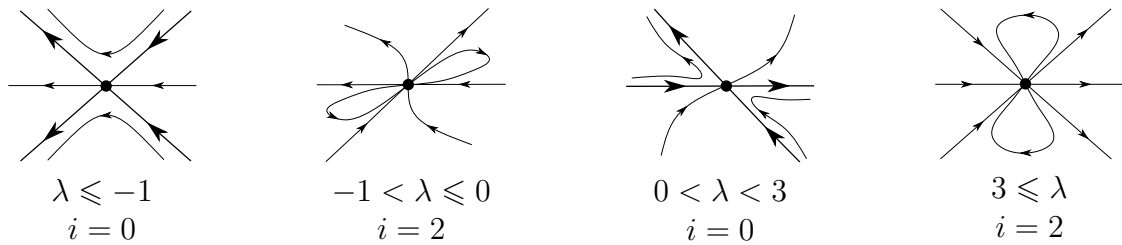


Figure 3.11: Local phase portrait of  $X_{34}$  at the origin. Figure source: Figure 7 of [13].

*Proof.* The first statement follows from

$$DX_{34}(p^+) = \begin{pmatrix} -2\lambda^{\frac{3}{2}} & 2\sqrt{\lambda} \\ 0 & (\lambda - 1)\sqrt{\lambda} \end{pmatrix}.$$

Using the Theorem of Hartman-Grobman, the *Trace-Determinant Theory* (see Section 4.1 of [25]) and knowing that the determinant and the trace of  $DX_{34}(q^+)$  are given, respectively, by

$$\begin{aligned} \text{Det}(\lambda) &= \frac{1}{8}(\lambda + 1)^2(\lambda - 1)(\lambda - 3)^2, \\ \text{Tr}(\lambda) &= \frac{1}{2} \left[ \lambda - (1 - \sqrt{2}) \right] \left[ \lambda - (1 + \sqrt{2}) \right] \sqrt{f(\lambda)}, \end{aligned}$$

one can prove the second statement.

Doing the change of coordinates  $(u, v) = (x - 1, y)$  and then applying the blow up technique at the origin of the vector field  $Y = Y(u, v)$  we obtain the vector field  $Y_0 = Y_0(r, \theta)$  given by

$$\dot{r} = rR_1(r, \theta), \quad \dot{\theta} = 2 \sin \theta (\cos \theta - \sin \theta) + rR_2(r, \theta).$$

Therefore, the singularities of  $\mathbb{S}^1$  are given by  $(r, \theta) = (0, \theta_0)$ , where  $\theta_0 \in \{0, \frac{\pi}{4}, \pi, \frac{5\pi}{4}\}$ . Observe that

$$DY_0(0, 0) = DY_0(0, \pi) = \begin{pmatrix} -2 & 0 \\ 0 & 2 \end{pmatrix},$$

$$DY_0\left(0, \frac{\pi}{4}\right) = -DY_0\left(0, \frac{5\pi}{4}\right) = \begin{pmatrix} 0 & 0 \\ * & -2 \end{pmatrix}.$$

Applying the *Center Manifold Theorem* (see Section 2.7 of [50]) at the non-hyperbolic points and knowing that  $\dot{v} > 0$  for every point outside the  $u$ -axis we can conclude that  $(0, \frac{\pi}{4})$  is a saddle and  $(0, \frac{5\pi}{4})$  is a stable node for  $Y_0$  and thus prove the third statement.

To prove the fourth statement note that the origin is a degenerated singularity, i.e.  $DX_{34}(0, 0) = 0$ . Doing a blow up at the origin one will obtain a vector field  $X_0 = X_0(r, \theta)$  given by

$$\dot{r} = rR_1(r, \theta), \quad \dot{\theta} = \sin\theta(\sin^2\theta - \cos^2\theta) + rR_2(r, \theta).$$

Therefore, the singularities of  $\mathbb{S}^1$  are given by  $(r, \theta) = (0, \theta_0)$ , where  $\theta_0 \in \{0, \frac{\pi}{4}, \frac{3\pi}{4}, \pi, \frac{5\pi}{4}, \frac{7\pi}{4}\}$ . Observe that

$$\begin{aligned} DX_0(0, 0) &= -DX_0(0, \pi) = \begin{pmatrix} \lambda & 0 \\ 0 & -1 \end{pmatrix}, \\ DX_0\left(0, \frac{\pi}{4}\right) &= -DX_0\left(0, \frac{5\pi}{4}\right) = \begin{pmatrix} f_1(\lambda) & 0 \\ 0 & \sqrt{2} \end{pmatrix}, \\ DX_0\left(0, \frac{3\pi}{4}\right) &= -DX_0\left(0, \frac{7\pi}{4}\right) = \begin{pmatrix} f_2(\lambda) & 0 \\ 0 & -\sqrt{2} \end{pmatrix}, \end{aligned}$$

where  $f_1(\lambda) = \frac{1}{2}\sqrt{2}(\lambda+1)$  and  $f_2(\lambda) = -\frac{1}{2}\sqrt{2}(\lambda-3)$ . Therefore, all the six singularities are hyperbolic for  $\lambda \notin \{-1, 0, 3\}$  and thus one can conclude the local phase portrait. When  $\lambda \in \{-1, 0, 3\}$  we have a saddle-node bifurcation at  $\{(0, \frac{1}{4}\pi), (0, \frac{5}{4}\pi)\}$ ,  $\{(0, 0), (0, \pi)\}$  and  $\{(0, \frac{3}{4}\pi), (0, \frac{7}{4}\pi)\}$ , respectively.

The fifth statement follows from general results on the Hopf bifurcation. See for instance sections 3.4 and 3.5 of [27].  $\square$

**Proposition 3.13.** *The vector field  $X_{34}$  may admit the existence of some limit cycle only if  $\lambda \in (1, 3)$ . Moreover, there is a unique  $\lambda_0 \in (1, 3)$  in which occurs the formation of a polycycle between the origin and  $p^-$  (and  $p^+$ ).*

*Proof.* It follows from Proposition 2.13 that there is at least one singularity in the interior of the bounded region limited by a limit cycle. From Theorem 3.6 we know that this singularity cannot be the origin. Also it cannot be singularities  $p^\pm$  because the  $x$ -axis is invariant. For  $-1 < \lambda < 1$  singularities  $q^\pm$  are both saddles and therefore cannot have a limit cycle surrounding them because the topological index of a saddle is  $-1$  (otherwise it must have another singularity in the bounded region limited by the limit cycle, which is impossible). Therefore, if there is a limit cycle, then it surrounds one (and only one) of the singularities  $q^\pm$  and  $1 < \lambda < 3$ . From now on we will focus on the  $q^-$  singularity at the second quadrant. The dynamics at  $q^+$  follows from the symmetry of the system.

At  $\lambda = 1$  we have a saddle-node bifurcation between singularities  $p^-$  and  $q^-$ . At  $\lambda = 3$  we have another saddle-node bifurcation, but now between a hyperbolic saddle at the blow up of the origin and  $q^-$ . Therefore, from the continuity of the vector field we conclude that there is a bifurcation of a heteroclinic orbit  $\Gamma_0$  between the hyperbolic saddles  $p_0$  and  $p^-$  for some value of the parameter  $\lambda = \lambda_0$ , see Figure 3.12. Let  $x_0 \in \Gamma_0$  and  $l_0$  be a transversal section of  $\Gamma_0$  passing through  $x_0$ . Following Section 2.6 we define  $n$  to be the coordinate along the normal line  $l_0$  such that  $n > 0$  outside the graph and  $n < 0$  inside the graph. We also denote by  $\Gamma_\lambda^s$  and  $\Gamma_\lambda^u$  the perturbations of  $\Gamma_0$ , for  $|\lambda - \lambda_0|$  small enough, such that  $\omega(\Gamma_\lambda^s) = p^-$  and  $\alpha(\Gamma_\lambda^u) = (0, 0)$ . Let  $x_\lambda^s$  and  $x_\lambda^u$  be the intersection of  $\Gamma_\lambda^s$  and  $\Gamma_\lambda^u$  with  $l_0$  and  $n^s(\lambda)$ ,  $n^u(\lambda)$  its coordinates along  $l_0$ , respectively. We define the displacement

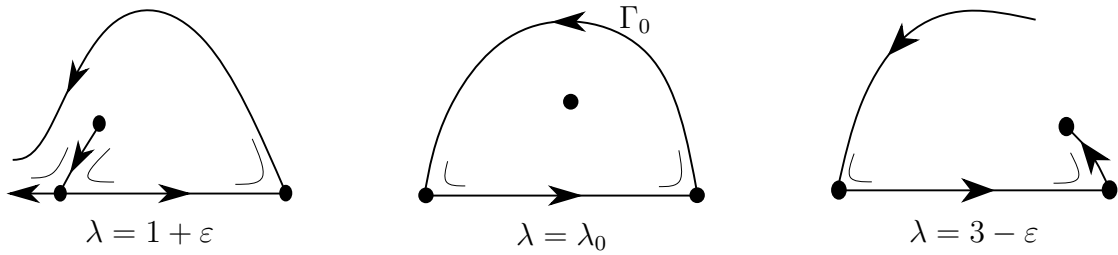


Figure 3.12: Heteroclinic orbit between the origin and  $p^-$ . Figure source: Figure 8 of [13].

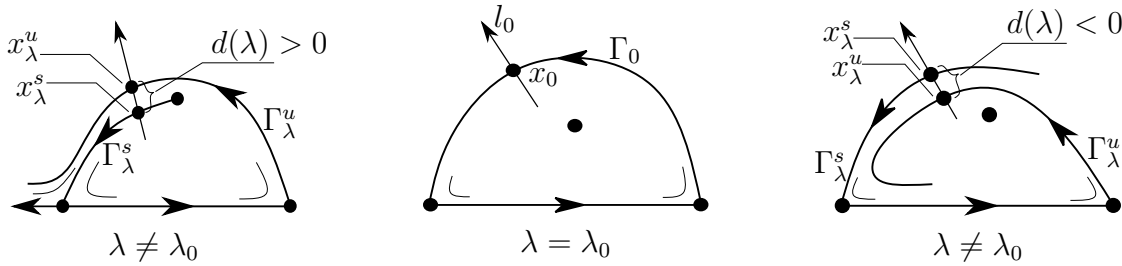


Figure 3.13: The displacement function  $d(\lambda)$  defined for  $\lambda$  near  $\lambda_0$ . Figure source: Figure 9 of [13].

function  $d(\lambda) = n^u(\lambda) - n^s(\lambda)$ . See Figure 3.13. Let  $\gamma_0(t)$  be a parametrization of  $\Gamma_0$ , with  $\gamma_0(0) = x_0$ . It follows from [49] that

$$d'(\lambda_0) = -\frac{1}{\|X_{34}(x_0; \lambda_0)\|} \int_{-\infty}^{+\infty} \left[ e^{-\int_0^t \text{Div}(X_{34}(\gamma_0(s); \lambda_0)) ds} \right] X_{34}(\gamma_0(t); \lambda_0) \wedge \frac{\partial X_{34}}{\partial \lambda}(\gamma_0(t); \lambda_0) dt,$$

where  $(x_1, x_2) \wedge (y_1, y_2) = x_1 y_2 - x_2 y_1$ . One can see that

$$X_{34}(x, y; \lambda) \wedge \frac{\partial X_{34}}{\partial \lambda}(x, y; \lambda) = x^3 y - x y^3 - x^5 y = H(x, y).$$

Therefore, the set  $\{(x, y) \in \mathbb{R}^2 : H(x, y) = 0\}$  is given by the union of the graphs of  $y = 0$  and  $y = \pm \sqrt{x^2 - x^4}$ . We denote  $y_1(x) = \sqrt{x^2 - x^4}$  when  $-1 \leq x \leq 0$ . The graph of  $y_1$  is given by the solid line of Figure 3.14. The dashed line denotes the points which satisfy  $\dot{x} = 0$ , given explicitly by  $y = x(1 - \sqrt{\lambda + 1 - x^2})$  when  $-\sqrt{\lambda} \leq x \leq 0$ . One can see that the flow of  $X_{34}$  is transversal to the graph of  $y_1$ , except at  $q^- = (q_1, q_2)$ , for every  $1 < \lambda < 3$ . Moreover it points outwards for  $x > q_1$  and inwards for  $x < q_1$ . One can also see that  $H$ , inside the second quadrant, is positive at the unbounded region delimited by the graph of  $y_1$  and negative at the bounded region. The Taylor series of  $y_1$  at  $x = 0$  is given by

$$y_1(x) = -x + 3x^3 + O(x^5).$$

On the other hand the separatrix  $\Gamma_0$  is given, for  $|x|$  small, by

$$y_2(x) = -x + \frac{1}{8 - 2\lambda} x^3 + O(x^5).$$

Therefore, for  $x < 0$  small enough we have

$$y_2(x) - y_1(x) = \left( \frac{1}{8 - 2\lambda} - 3 \right) x^3 + O(x^5).$$

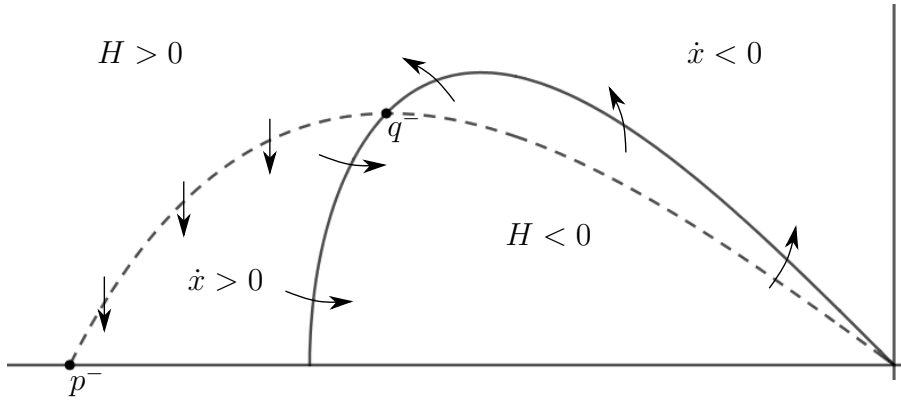


Figure 3.14: Plot of  $H(x, y) = 0$  and  $\dot{x} = 0$  at the second quadrant. Figure source: Figure 10 of [13].

Hence, the heteroclinic orbit  $\Gamma_0$  is above the graph of  $y_1$  and therefore we conclude that

$$f(t; \lambda_0) \wedge \frac{\partial f}{\partial \lambda}(t; \lambda_0) > 0$$

for every  $t \in \mathbb{R}$ , independently of the exactly value of  $\lambda_0$ . Hence,  $d'(\lambda_0) < 0$ . Thus, we conclude that if a heteroclinic orbit  $\Gamma_0$  exists at  $\lambda = \lambda_0$ , then for  $|\lambda - \lambda_0|$  small enough the displacement function is well defined and is given by

$$d(\lambda) = a_1(\lambda - \lambda_0) + O((\lambda - \lambda_0)^2),$$

with  $a_1 < 0$ . Therefore, we have  $d(\lambda) > 0$  if  $\lambda < \lambda_0$  and  $d(\lambda) < 0$  if  $\lambda > 0$ . See Figure 3.13. And this happens independently of the value of  $\lambda_0$ . Hence, there is a unique  $\lambda_0 \in (1, 3)$  for which  $\Gamma_0$  exists.  $\square$

If  $\Gamma_n$  is a graph with  $n$  hyperbolic saddles such that  $\mu_i < 0 < \nu_i$  are its eigenvalues, then we say that  $\Gamma_n$  is simple if

$$H(\Gamma_n) = \prod_{i=1}^n \frac{|\mu_i|}{\nu_i} \neq 1.$$

Moreover  $\Gamma_n$  is stable if  $H(\Gamma_n) > 1$  and unstable if  $H(\Gamma_n) < 1$ . See for instance [16, 55, 18]. The graph  $\Gamma$  that bifurcate at  $\lambda = \lambda_0$  is formed by  $p^-$  and from two hyperbolic saddles from the blow up of the origin. Hence, one can calculate that

$$H(\Gamma_0) = \frac{\lambda - 1}{3 - \lambda}.$$

To precise in an analytical way how many limit cycles exists in a given interval in general is a very difficult task. But numerical computations (see chapters 9 and 10 of [19]) points that  $\lambda_0 = 2.3761..$  and thus  $\Gamma$  is stable. Moreover the numerical computations also indicates that there is no limit cycles for  $\lambda \in (1, \lambda_0) \cup (1 + \sqrt{2}, 3)$  and that there is a unique limit cycle for  $\lambda \in (\lambda_0, 1 + \sqrt{2})$ . So to provide an analytic proof of these two facts is an open problem. Knowing this, it follows from [48] that the limit cycle which ends at the Hopf bifurcation belongs to an open maximal family of limit cycles which born at the polycycle for  $\lambda = \lambda_0$ .

In what follows we will study some cases of  $X_{34}$ . The other cases can be obtained similarly.

**Remark 3.14.** To simplify the writing from now on we will call the origin of the charts  $U_2$ ,  $V_2$ ,  $U_1$  and  $V_1$  of the Poincaré compactification (see Section 2.2) as *north pole*, *south pole*, *east pole* (right) and *west pole* (left), respectively.

**Proposition 3.15.** *The phase portrait of  $X_{34}$  for  $1 + \sqrt{2} \leq \lambda < 3$  is the one in Figure 3.3.*

*Proof.* From Propositions 3.11, 3.12, 3.13 and from the invariance of the  $x$ -axis we can conclude Figure 3.15. We claim that separatrix 1 must have the west pole as its  $\omega$ -limit.

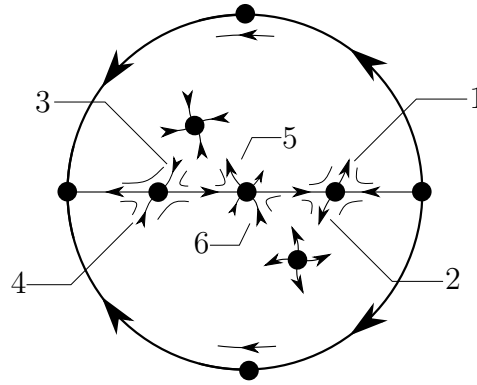


Figure 3.15: Unfinished phase portrait of  $X_{34}$  for  $1 + \sqrt{2} \leq \lambda < 3$ . Figure source: Figure 11 of [13].

To prove this consider Figure 3.16. Denote  $S = \{(x, y) \in \mathbb{R}^2 : \dot{x} = 0\}$  and observe that it

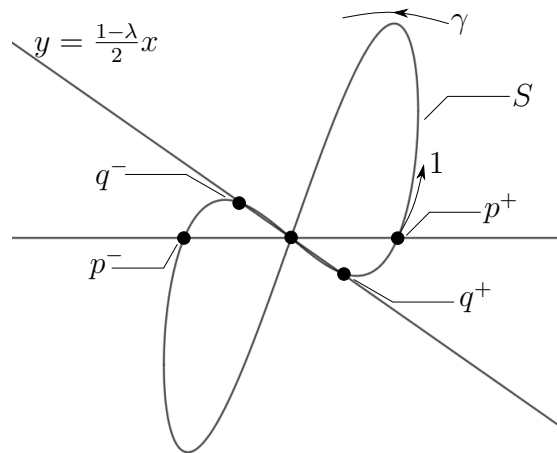


Figure 3.16: Illustration of the zeros of  $\dot{x} = 0$  and  $\dot{y} = 0$ . Figure source: Figure 12 of [13].

is given explicitly by

$$y = x \pm \sqrt{x^2(\lambda + 1) - x^4}.$$

Observe that separatrix 1 must cross the  $y$ -axis because all its options for  $\omega$ -limit are at the second quadrant. At the bounded region limited by  $S$  we have  $\dot{x} > 0$ , therefore separatrix 1 must pass above  $S$ , at least somewhere near  $\gamma$ . Observe that this does not depend if separatrix 1 is tangential or not with  $S$ . One can prove using the *Lagrange Multipliers* that the maximum value of  $y$  at  $S$  is given by

$$y_0 = \frac{\sqrt{2}}{8} \left( 2\sqrt{3 + 4\lambda + \sqrt{9 + 8\lambda}} + \sqrt{3 + 12\lambda + 8\lambda^2 + \sqrt{9 + 8\lambda}} \right).$$

At the region limited by  $y > 0$  and  $y > \frac{1-\lambda}{2}x$  we have  $\dot{y} > 0$  and therefore separatrix 1 will cross the straight line given by  $y = \frac{1-\lambda}{2}x$  at a point  $(x_1, y_1)$  such that  $y_1 > y_0$ . This is enough to ensure that separatrix 1 cannot end at separatrix 3 nor at the stable node because  $\dot{x} < 0$  at the unbounded region delimited by  $S$ . Therefore, separatrix 1 ends at the west pole and  $q^-$  is in the bounded region limited by it. Separatrix 3 has no other option than born at the origin. Once the stable node (i.e. the singularity  $q^-$ ) came from a saddle-node bifurcation at the origin at  $\lambda = 3$  we conclude that separatrix 5 end at this node. The symmetry of the system is now enough to finish the phase portrait.  $\square$

**Proposition 3.16.** *The phase portrait of  $X_{34}$  for  $\lambda_0 < \lambda < 1 + \sqrt{2}$  is the one given by Figure 3.3.*

*Proof.* Similarly to Proposition 3.15, here we conclude Figure 3.17 and the fact that separatrix 1 also end at the west pole with the limit cycle in the bounded region delimited by it. Follows from Proposition 3.15 and the continuity of  $X_{34}$  with respect to  $\lambda$  that

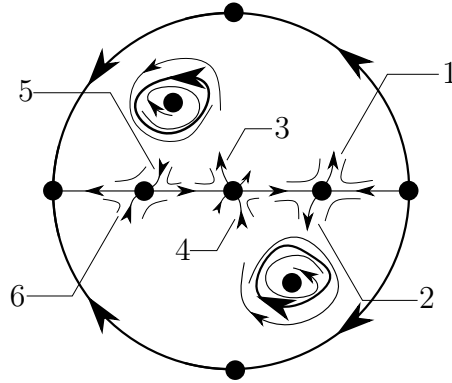


Figure 3.17: Unfinished phase portrait of  $X_{34}$  for  $\lambda_0 < \lambda < 1 + \sqrt{2}$ . Figure source: Figure 13 of [13].

separatrix 3 must end at the limit cycle. Separatrix 5 has no other option than born at the origin. Symmetry is now enough to finish the phase portrait.  $\square$

**Proposition 3.17.** *The phase portrait of  $X_{34}$  for  $1 < \lambda < \lambda_0$  is the one given by Figure 3.3.*

*Proof.* Similarly to Propositions 3.15 and 3.16, here we conclude Figure 3.18 and the fact that separatrix 1 also end at the west pole with the unstable node (i.e. the singularity  $q^-$ ) in the bounded region delimited by it. Once we have a generic saddle-node bifurcation at  $\lambda = 1$  we conclude that separatrix 5 born at the unstable node. Separatrix 3 has no other option than end at the west pole. Symmetry is now enough to finish the phase portrait.  $\square$

**Proposition 3.18.** *The phase portrait of  $X_{34}$  for  $0 < \lambda < 1$  is the one given by Figure 3.3.*

*Proof.* Similarly to Propositions 3.15, 3.16 and 3.17 in this case we have Figure 3.19. Observe that  $\dot{x} = -y^2$  if  $x = 0$ , therefore no orbit can cross the  $y$ -axis from left to right. Remember that  $y = \frac{1-\lambda}{2}x$  imply  $\dot{y} = 0$  and thus we conclude Figure 3.20. Observe that separatrix 2 cannot end at separatrix 1 nor at separatrix 3, otherwise it would have a singularity in the bounded region limited by it. If separatrix 2 ends at stable node,

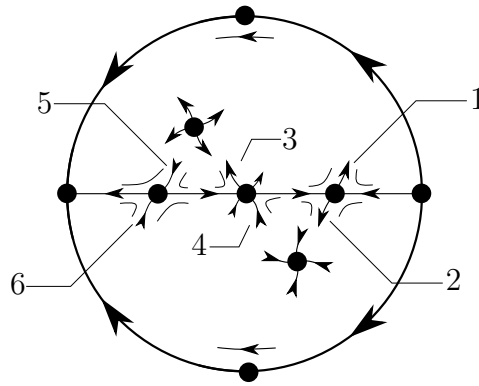


Figure 3.18: Unfinished phase portrait of  $X_{34}$  for  $1 < \lambda < \lambda_0$ . Figure source: Figure 14 of [13].

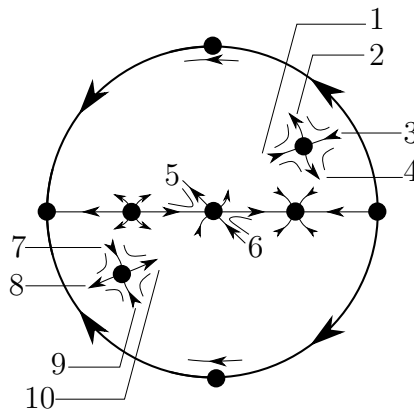


Figure 3.19: Unfinished phase portrait of  $X_{34}$  for  $0 < \lambda < 1$ . Figure source: Figure 15 of [13].

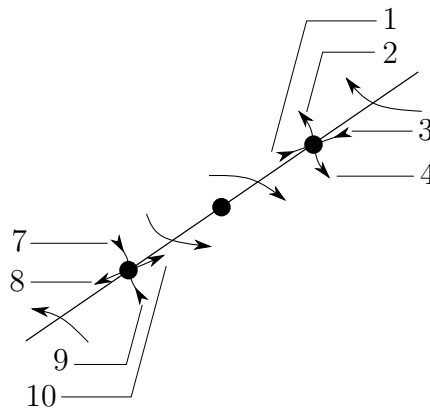


Figure 3.20: Local phase portrait of  $X_{34}$  at  $y = \frac{1-\lambda}{2}x$  for  $0 < \lambda < 1$ . Figure source: Figure 16 of [13].

then by Figure 3.20 separatrix 1 could not born anywhere. Therefore, the only option to separatrix 2 is to end at the west pole. Separatrix 4 must end at the stable node because we have a generic saddle-node bifurcation. There is no other option for separatrix 3 other than born at the east pole. The fact that no orbit can cross the  $y$ -axis from left to right give to separatrix 1 no other option than born at the origin (not at separatrix 5).

Separatrix 5 cannot cross the  $y$ -axis, therefore it must end at the west pole. Symmetry is now enough to finish the phase portrait.  $\square$

**Remark 3.19.** The proofs for  $\lambda \leq 0$  and  $3 \leq \lambda$  are similarly as Propositions 3.15, 3.16, 3.17 and 3.18.

**Remark 3.20.** Theorem 3.6 in addition with observations as the invariance of the  $x$ -axis, the fact that the index of a saddle is  $-1$  and the Bendixson criterion proves the nonexistence of any limit cycles at the others families of vector fields.

**Proposition 3.21.** *The phase portrait of  $X_{12}$  for  $\lambda \in \mathbb{R}$  are those given by Figure 3.2.*

*Proof.* Once  $\dot{y} = 0$  if, and only if  $x = 0$  or  $y = 0$  or  $\lambda = 1$  one can see that the only possible finite singularities are the origin and the points  $p^\pm = \pm(\sqrt{\lambda}, 0)$  if  $\lambda \neq 1$ , and the algebraic curve  $-x^2 - y^2 + x^4 = 0$  if  $\lambda = 1$ . Doing a blow up at the origin and knowing that

$$DX_{12}(p^+) = \begin{pmatrix} 2\lambda^{\frac{3}{2}} & 0 \\ 0 & (1-\lambda)\sqrt{\lambda} \end{pmatrix},$$

one can understand the *local behavior* of  $X_{12}$ , similarly as we did with  $X_{34}$ . At the infinite one will see that the only singularities are the origins of each chart. The origin of the chart  $U_1$  (the east pole) is a stable node for every  $\lambda \in \mathbb{R}$ . The origin of the chart  $U_2$  requires a blow up. First note that the field  $p(X_{12})$  at this chart is given by

$$\dot{u} = -v^2 + u^4 - u^2v^2, \quad \dot{v} = (\lambda - 1)uv^3.$$

Assume  $\lambda \neq 1$ . Doing a quasihomogeneous blow up with  $(\alpha, \beta) = (1, 2)$  one will see that the only singularities of our interest (i.e. those with  $r = 0$ ) are given by the zeros of

$$\sin \theta (\cos^4 \theta - \sin^2 \theta) = 0,$$

for  $0 \leq \theta < 2\pi$ . There are six singularities, given by  $\theta = 0$ ,  $\theta = \pi$  and  $\theta = \theta_i$ ,  $i \in \{1, 2, 3, 4\}$ , where  $\theta_i$  is the solution of  $\cos^4 \theta = \sin^2 \theta$  at the  $i$ -th quadrant of  $\mathbb{S}^1$ . The linear part of the vector field  $X_0 = X_0(r, \theta)$  in each of these singularities are given by

$$\begin{aligned} DX_0(0, 0) &= \begin{pmatrix} 1 & 0 \\ 0 & -2 \end{pmatrix}, & DX_0(0, \theta_1) &= \begin{pmatrix} 0 & 0 \\ 0 & \eta \end{pmatrix}, \\ DX_0(0, \theta_2) &= \begin{pmatrix} 0 & 0 \\ 0 & -\eta \end{pmatrix}, & DX_0(0, \pi) &= \begin{pmatrix} -1 & 0 \\ 0 & 2 \end{pmatrix}, \\ DX_0(0, \theta_3) &= \begin{pmatrix} 0 & 0 \\ 0 & -\eta \end{pmatrix}, & DX_0(0, \theta_4) &= \begin{pmatrix} 0 & 0 \\ 0 & \eta \end{pmatrix}, \end{aligned}$$

where  $\eta = 4\sqrt{\sqrt{5} - 2}$ . Using the *Hartman-Grobman Theorem* at  $(0, 0)$  and  $(0, \pi)$  and the *Center Manifold Theorem* at  $(0, \theta_i)$ , for  $i \in \{1, 2, 3, 4\}$  one can obtain Figure 3.21(a). Remember that  $\dot{v} = (\lambda - 1)uv^3$  and therefore

$$\text{sign}(\dot{v}) = \text{sign}(\lambda - 1)\text{sign}(u)\text{sign}(v),$$

where  $\text{sign}(x)$  denotes the *signal* of  $x$ , i.e.  $\text{sign}(x) = -1$  if  $x < 0$ ,  $\text{sign}(x) = 0$  if  $x = 0$  and  $\text{sign}(x) = 1$  if  $x > 0$ . Therefore, we can complete Figure 3.21(a), obtaining Figure 3.21(b) for  $\lambda < 1$  and Figure 3.21(c) for  $\lambda > 1$ . Observe that  $\dot{x} \leq 0$  if  $y = 0$ . The invariance of

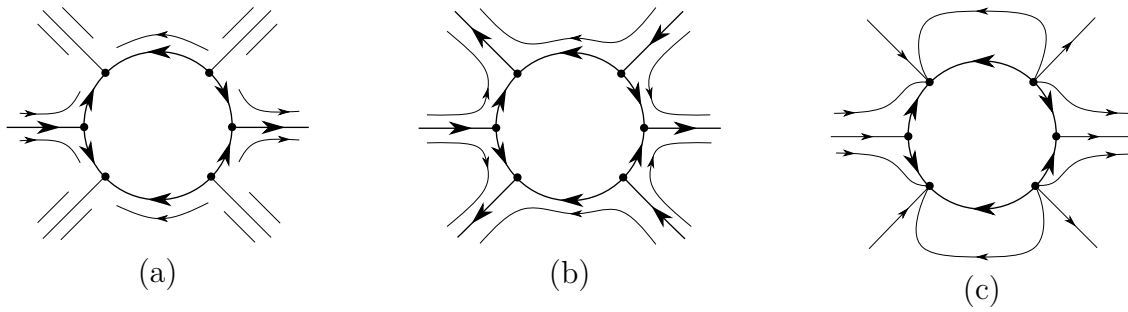


Figure 3.21: Local phase portrait of the blow up of the origin of chart  $U_2$ . Figure source: Figure 17 of [13].

the  $x$ -axis does not permit any limit cycle here. With this information one can obtain the phase portrait of  $X_{12}$  similarly as we did with  $X_{34}$ . When  $\lambda = 1$  the equation of the vector field  $X_{12}$  becomes

$$\dot{x} = -x^2 - y^2 + x^4, \quad \dot{y} = 0.$$

So all the straight lines  $y = \text{constant}$  are invariant and the algebraic curve  $-x^2 - y^2 + x^4 = 0$  is filled up with singularities.  $\square$

**Proposition 3.22.** *The phase portrait of  $X_{21}$  for  $\lambda \in \mathbb{R}$  are those given by Figure 3.4.*

*Proof.* First assume  $\lambda \neq -1$ . Observe that the only possible singularities are the origin and the points  $p^\pm = \pm(\sqrt{\lambda}, 0)$ . With a blow up at the origin and an analysis of  $DX_{21}(p^\pm)$  one can conclude the *local behavior* of  $X_{21}$ . At the infinity only the origins of the charts are singularities. The origin of  $U_1$  is an unstable node and a quasihomogeneous blow up with  $(\alpha, \beta) = (1, 2)$  at the origin of  $U_2$  is necessary. But in this case the analysis of this blow up is much more simple than the last one. Finally, observe that  $X_{21}$  is also reversible with  $\varphi(x, y) = (-x, y)$ , i.e. it is reversible in respect to the  $y$ -axis and that no limit cycle can exist due to the invariance of the  $x$ -axis. Also observe that  $\dot{x} < 0$  if  $x = 0$ . When  $\lambda = -1$  the equation of the vector field  $X_{21}$  becomes

$$\dot{x} = -x^2 - y^2 - x^4, \quad \dot{y} = 0,$$

so all the straight lines  $y = \text{constant}$  are invariant. Note that the only finite singularity is the origin because the algebraic curve  $-x^2 - y^2 - x^4 = 0$  is degenerated.  $\square$

**Proposition 3.23.** *The phase portrait of  $X_{43}$  for  $\lambda \in \mathbb{R}$  are those given by Figure 3.5.*

*Proof.* Note that the zeros of  $\dot{y} = 0$  are given by  $y = 0$  and  $y = \frac{1+\lambda}{2}x$ . The finite singularities are the origin and the points

$$p^\pm = (\pm\sqrt{\lambda}, 0), \quad q^\pm = \pm \left( \frac{1}{2}\sqrt{f(\lambda)}, \frac{1}{4}(1+\lambda)\sqrt{f(\lambda)} \right),$$

where  $f(\lambda) = (\lambda+3)(\lambda-1)$ . An analysis of  $DX_{43}$  at  $p^\pm$  and  $q^\pm$  and a blow up at the origin is enough to obtain the *local behavior* of  $X_{43}$ . The origin of the chart  $U_1$  is a stable node and the origin of  $U_2$  requires an analysis similar to the vector field  $X_{12}$ . The nonexistence of limit cycles can be proved similarly as we did in Proposition 3.13. Finally, note that  $\dot{x} < 0$  if  $x = 0$  and an analysis (as we did in Proposition 3.18) of the flow on the straight line  $y = \frac{1+\lambda}{2}x$  is necessary to complete the phase portrait.  $\square$

**Proposition 3.24.** *The phase portrait of  $X_{45}$  for  $\lambda \in \mathbb{R}$  are those given by Figure 3.6.*

*Proof.* The only finite singularities are the origin and the points  $p^\pm = \pm(\sqrt{\lambda}, 0)$ . A blow up at the origin and an analysis of  $DX_{45}(p^\pm)$  is enough to know the *local behavior* of  $X_{45}$ . The origin of the chart  $U_1$  is an unstable node for every  $\lambda \in \mathbb{R}$  and the origin of the chart  $U_2$  requires a quasihomogeneous blow up with  $(\alpha, \beta) = (1, 2)$ . The analysis of this blow up is simple and there is no other infinite singularity for this vector field. The invariance of the  $x$ -axis does not permit any limit cycle here. Finally, note that  $X_{45}$  is also invariant with  $\phi(x, y) = (-x, y)$  and that  $\dot{x} < 0$  if  $x = 0$ .  $\square$

**Proposition 3.25.** *The phase portrait of  $X_{54}$  for  $\lambda \in \mathbb{R}$  are those given by Figure 3.8.*

*Proof.* The only finite singularities are the origin and the points  $p^\pm = \pm(\sqrt{\lambda}, 0)$ . As before, a blow up at the origin and an analysis of  $DX_{54}$  is enough to describe the *local behavior* of  $X_{54}$ . The origins of the charts are only infinite singularities. The origin of  $U_1$  is a stable node and the origin of  $U_2$  requires a quasihomogeneous blow up, with  $(\alpha, \beta) = (1, 2)$ , and an analysis similarly as we did with  $X_{12}$ . The invariance of the  $x$ -axis does not let any limit cycle to exist. Finally, observe that  $\dot{x} < 0$  if  $x = 0$  and that  $X_{54}$  is invariant with  $\varphi(x, y) = (-x, y)$ .  $\square$

**Proposition 3.26.** *The phase portrait of  $X_{13}$  for  $\lambda \in \mathbb{R}$  are those given by Figure 3.4.*

*Proof.* First observe that

$$\dot{y} = \left[ y + (1 + \sqrt{\lambda + 1})x \right] \left[ y + (1 - \sqrt{\lambda + 1})x \right].$$

Knowing this one can see that the only finite singularities are the origin and the points

$$p^\pm = \pm \left( \sqrt{2}\sqrt[4]{\lambda + 1}, - (1 + \sqrt{\lambda + 1}) \sqrt{2}\sqrt[4]{\lambda + 1} \right).$$

An analysis of the determinant of  $DX_{13}(p^\pm)$  is enough to describe the local phase portrait of  $X_{13}$  at these singularities. A blow up at the origin is necessary. At this case the singularities of the blow up are given by the zeros of

$$-\lambda \cos^3 \theta - \lambda \cos^2 \theta \sin \theta + \cos \theta \sin^2 \theta + \sin^3 \theta = 0,$$

which are given by

$$\frac{3\pi}{4}, \frac{7\pi}{4}, \pm \arctan \sqrt{\lambda} \quad \text{and} \quad \pi \pm \arctan \sqrt{\lambda}.$$

Therefore, a non usual number of bifurcations will occur at the origin. But they are all very simple and almost never changes the phase portrait. The infinite singularities are given by the origins of the charts. The origin of  $U_1$  is a stable node. As we did in  $X_{12}$ , a quasihomogeneous blow up with  $(\alpha, \beta) = (1, 2)$  is required for the origin of  $U_2$ . The nonexistence of limit cycles can be prove similarly as we did in Proposition 3.13. Observe that  $\dot{x} < 0$  if  $x = 0$ . Finally, an analysis of the flow on the straight line  $y = -(1 + \sqrt{\lambda + 1})x$  is necessary to complete the phase portraits.  $\square$

**Proposition 3.27.** *The phase portrait of  $X_{24}$  for  $\lambda \in \mathbb{R}$  are those given by Figure 3.7.*

*Proof.* First note that the zeros of  $\dot{y} = 0$  are the union of the straight lines  $x = 0$  and  $y = -\lambda x$ . Therefore, the only finite singularities are the origin and the points

$$p^\pm = \pm(\lambda - 1, -\lambda(\lambda - 1)).$$

An analysis of the determinant of  $DX_{24}(p^\pm)$  is enough to describe the local behavior of the singularities  $p^\pm$ . A blow up at the origin is necessary. Similarly to  $X_{13}$  the singularities are given by

$$\frac{3\pi}{4}, \frac{7\pi}{4}, \pm \arctan \sqrt{\lambda} \text{ and } \pi \pm \arctan \sqrt{\lambda}.$$

Once more the infinite singularities are the origins of the charts. The origin of  $U_1$  is a stable node. A quasihomogeneous blow up, with  $(\alpha, \beta) = (1, 2)$ , is necessary at the origin of  $U_2$  and the analysis is similarly to  $X_{12}$ . An analysis of the straight line  $y = -\lambda x$ , as we did at Proposition 3.18, is necessary at every case. Finally, follows from the blow up at the origin that for  $0 < \lambda < 1$  and for  $1 < \lambda$  that the separatrix at the fourth quadrant of the hyperbolic sector of the origin is always tangent to the line  $y = -x$ , which is, respectively, *bellow* and *above* the straight line given by  $y = -\sqrt{\lambda}x$ , for  $x > 0$ . Therefore, the flow at this last straight line must be analyzed to complete the phase portrait.  $\square$

**Proposition 3.28.** *The phase portrait of  $X_1, X_2, X_3, X_4$  and  $X_5$  are those given by Figure 3.1.*

*Proof.* No bifurcations occurs at any of this five vector fields. The origin is always the unique finite singularity. A blow up is enough to describe their local phase portrait at the origin. The nonexistence of limit cycles follows from Theorem 3.6. Every infinite singularity is hyperbolic. Finally, note that the straight lines  $y = \pm x$  are invariant by  $X_3, X_4$  and  $X_5$ .  $\square$

### 3.4 Proof of theorem 3.7

*Proof.* It follows from Theorem 3.5 that to prove Theorem 3.7 it is enough to describe the global phase portrait of each one of those normal forms given at Theorem 3.5. Hence, the proof follows from Section 3.3.  $\square$



## 4 (2;1)-REVERSIBILITY

### 4.1 Statement of the main results

We recall that this is a co-work with professors Claudio Buzzi and Jaume Llibre and it was submitted for publication, see [11]. Following the notation of Teixeira in [56] we denote by  $\Omega$  the space of germs of  $C^k$ ,  $k \geq 3$ ,  $\varphi$ -reversible vector fields of type (2; 1). It follows from Property 2.11 that we can choose the coordinate system in  $\mathbb{R}^2, 0$  in such a way that  $\varphi(x, y) = (x, -y)$ . From now on in this chapter any vector field will be a  $C^k$ ,  $k \geq 3$ , vector field, unless we say other thing.

Let  $M = \{(u, v) \in \mathbb{R}^2 : \|(u, v)\| < \varepsilon, v \geq 0\}$ ,  $S$  the boundary of  $M$  and  $\mathfrak{X}$  the space of all germs defined in  $M$ . A point  $p \in S$  is a *S-singularity* of  $F \in \mathfrak{X}$  if  $F(p)$  is tangent to  $S$  at  $p$ . Two germs of vector fields  $F, G \in \mathfrak{X}$  are *topologically equivalent* if there if there is a homeomorphism  $h : M \rightarrow M$  which sends orbits of  $F$  to orbits of  $G$  preserving or reversing the orientation of all orbits such that  $h(S) = S$ .  $F$  is *structural stable* in  $\mathfrak{X}$  if there is a neighborhood  $N \subset \mathfrak{X}$  of  $F$  such that  $F$  is topologically equivalent to every  $G \in N$ .

We denote *set of the structural stable germs* of  $\Omega$  by  $\omega_0$ . We will also consider the set  $\Omega_1 = \Omega \setminus \omega_0$  and denote by  $\omega_1$  the set of the structural stable germs, relative to  $\Omega_1$ , of  $\Omega_1$ . Finally we define  $\Omega_2 = \Omega_1 \setminus \omega_1$  and denote by  $\omega_2$  the set of the structural stable germs, relative to  $\Omega_2$ , of  $\Omega_2$ . In a similar way we denote *set of the structural stable germs* of  $\mathfrak{X}$  by  $\Sigma_0$ . We will also consider the set  $\mathfrak{X}_1 = \mathfrak{X} \setminus \Sigma_0$  and denote by  $\Sigma_1$  the set of the structural stable germs, relative to  $\mathfrak{X}_1$ , of  $\mathfrak{X}_1$ . Finally we define  $\mathfrak{X}_2 = \mathfrak{X}_1 \setminus \Sigma_1$  and denote by  $\Sigma_2$  the set of the structural stable germs, relative to  $\mathfrak{X}_2$ , of  $\mathfrak{X}_2$ .

Given  $X \in \Omega$  it is clear that  $X = \left(yf(x, y^2), \frac{1}{2}g(x, y^2)\right)$ , for some  $f$  and  $g$ . In the half-plane  $y > 0$  one can consider the change of variables  $(x, y) \mapsto (u, \sqrt{v})$  and thus obtain system  $X_1(u, v) = (\sqrt{v}f(u, v), \sqrt{v}g(u, v))$ . Following [56] we define  $F = (f(u, v), g(u, v))$  and observe that  $F = F(X)$  and  $X$  are topologically equivalent at  $y > 0$ . Let  $\nu_i = \{X \in \Omega : F(X) \in \Sigma_i\}$ ,  $i \in \{0, 1, 2\}$ . Teixeira proved in [56] that  $\nu_0 = \omega_0$ ,  $\nu_1 = \omega_1$  and  $\nu_2 \subset \omega_2$ . Moreover Teixeira also proved that  $\nu_i$  is open and dense at  $\Omega_i$ ,  $i \in \{1, 2\}$ .

**Definition 4.1.** Let  $J \subset \mathbb{R}^i$  be an open set,  $i \in \{1, 2\}$ . Denote by  $\Theta_i$  the space of  $C^1$  mappings  $\xi : J \rightarrow \Omega$  endowed with the  $C^1$  topology. Its elements will be called  $i$ -parameter families of germs of vector fields of  $\Omega$ . We say that  $\xi$  is *generic* if

1. there is at most one  $\mu_0 \in J$  such that  $\xi(\mu_0) \in \Omega_i$  and in this case  $\xi(\mu_0) \in \nu_i$ ;
2. it is transversal to  $\nu_i$ .

The following theorem proved by Teixeira [56] states the basis of our main result of this chapter.

**Theorem 4.2.** *The following statements hold.*

- (a) *(Codimension zero classification) The  $C^0$ -normal forms of the structurally stable vector fields in  $\Omega$  are:*

1.  $X_{01} = \left(0, \frac{1}{2}\right)$ ;

2.  $X_{02} = (y, \varepsilon x)$ ,  $\varepsilon = \pm 1$ ;

(b) (Codimension one classification) In the space of the one-parameter families of vector fields in  $\Omega$ , an everywhere dense set is formed by generic families such that their ( $C^0$ -) normal forms are:

1. the normal forms of  $C^0$ -structurally stable vector fields in  $\Omega$ ;

2.  $X_{11} = \left(y, \frac{1}{2}(\lambda + x^2)\right)$ ;

3.  $X_{12} = \left(\varepsilon xy, \frac{1}{2}(2\varepsilon y^2 + x + \lambda)\right)$ ,  $\varepsilon = \pm 1$ ;

4.  $X_{13} = \left(xy, \frac{1}{2}(-y^2 + x + \lambda)\right)$ ;

5.  $X_{14} = \left(xy + y^3, \frac{1}{2}(-x + y^2 + \lambda)\right)$ .

(c) (Codimension two classification) In the space of the two-parameter families of vector fields in  $\Omega$ , an everywhere dense set is formed by generic families such that their ( $C^0$ -) normal forms are:

1. All the normal forms listed in statement (b);

2.  $X_{21} = \left(y, \frac{1}{2}(bx^3 + \beta x + \alpha)\right)$ ,  $b = \pm 1$ ;

3. i)  $X_{22a} = \left(ay(x - y^2) + \beta y(x + y^2), \frac{1}{2}(\alpha + (x + y^2)^2)\right)$ ,  $a = \pm 1$ ;

ii)  $X_{22b} = \left(y(x - y^2) + \beta y(x + y^2), \frac{1}{2}(\alpha + a(x + y^2)^2)\right)$ ,  $a = \pm 1$ ;

4.  $X_{23} = \left(-y^3 + axy(\alpha + x^2 + y^4), \frac{1}{2}(ax - y^2(\alpha + x^2 + y^4) + \beta)\right)$ ,  $a = \pm 1$ ;

5.  $X_{24} = \left(axy + \alpha y^3, \frac{1}{2}(x + ay^2 + \beta)\right)$ ,  $a = \pm 1$ ;

6. i)  $X_{25a} = \left(xy, \frac{1}{2}(\alpha x - y^2 + ax^2 + \beta)\right)$ ,  $a = \pm 1$ ;

ii)  $X_{25b} = \left(axy, \frac{1}{2}(\alpha x + by^2 + \varepsilon x^2 + \beta)\right)$ ,  $ab > 0$ ,  $\varepsilon = \pm 3$   
and  $\{(a = \pm 1 \text{ and } b = \pm 3) \text{ or } (a = \pm 3 \text{ and } b = \pm 1)\}$ .

As in Chapter 3, we note that all the germs of vector fields which appear in the statement of the previous theorem are polynomial. Theorem 4.2 motivated us to classify the phase portrait of the differential vector fields which appear in its statement and thus to extend the results of [56]. The next theorem summarize our results in this chapter.

**Theorem 4.3.** *The phase portraits in the Poincaré disk of the vector fields in Theorem 4.2 are given in Figures 4.1-4.18.*

**Remark 4.4.** As in Chapter 3, we observe that the phase portraits given in Figures 4.1-4.18 does not represent the global phase portraits of all reversible vector fields of type (2; 1) of low codimension. As stated in Remark 3.8, unless we are given a maximum degree, there is infinitely many of such phase portraits. However, it follows from Theorem 4.2 that a symmetrical singularity of codimension zero, one or two, of a reversible vector field of type (2; 1), is topologically equivalent *at the origin*, for  $\lambda \approx 0$  or  $(\alpha, \beta) \approx (0, 0)$ , to one of the phase portraits given in Figures 4.1-4.18. Furthermore, as stated in the introduction, we remember that Llibre and Medrado [30] already classified all the phase portraits of the quadratic reversible vector fields of type (2; 1).

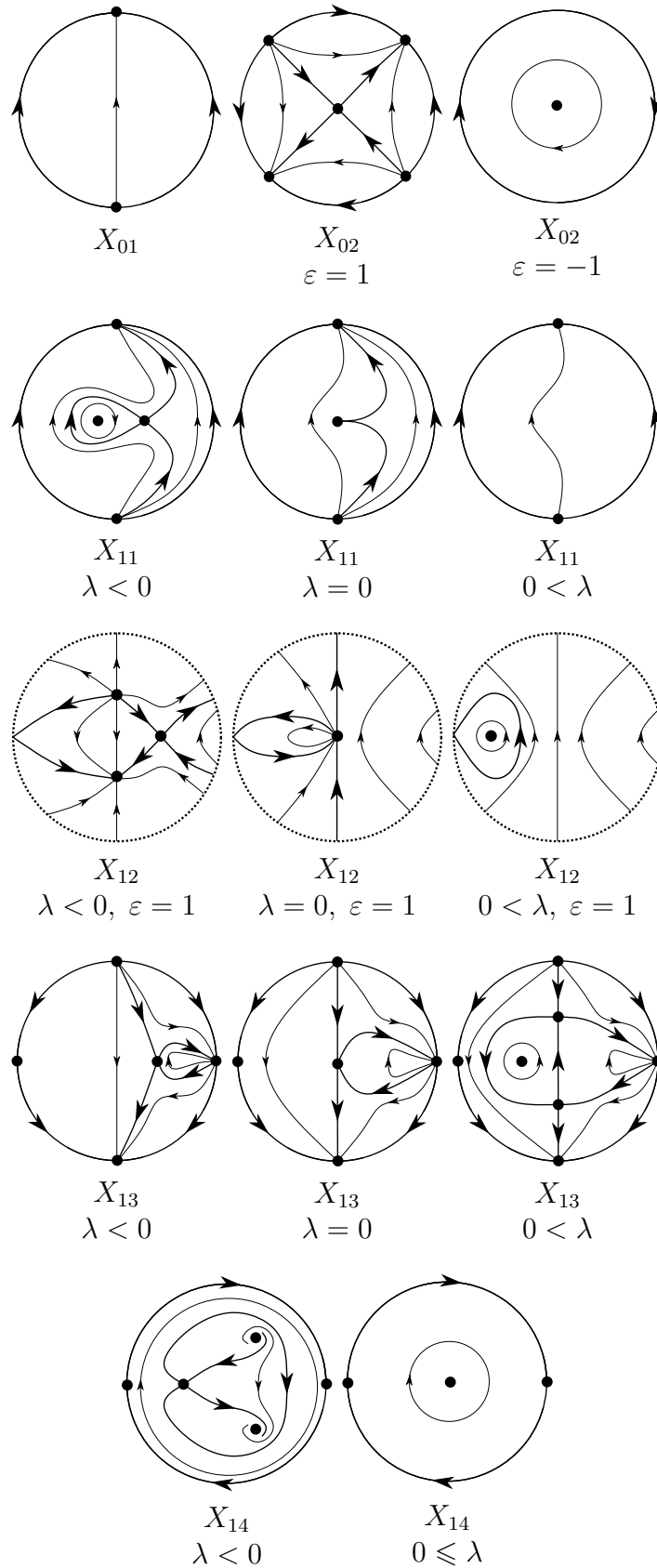


Figure 4.1: Phase portraits of  $X_{01}$ ,  $X_{02}$ ,  $X_{11}$ ,  $X_{12}$ ,  $X_{13}$  and  $X_{14}$ . Figure source: made by the author.

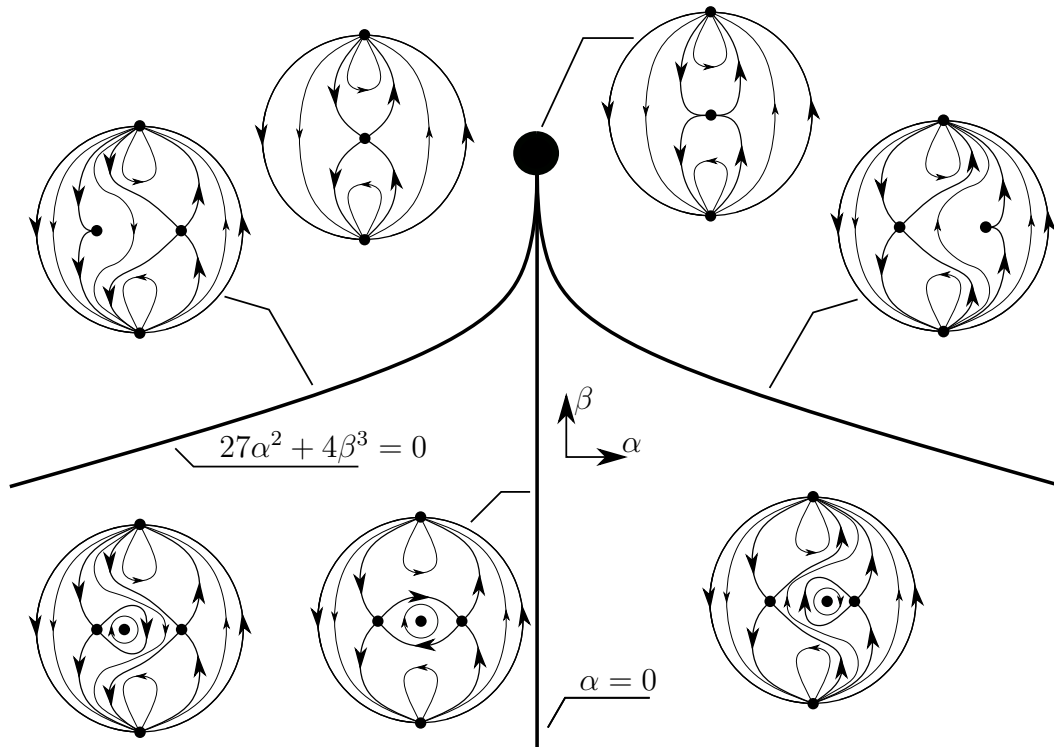


Figure 4.2: Phase portrait of  $X_{21}$  with  $b = 1$ . Figure source: made by the author.

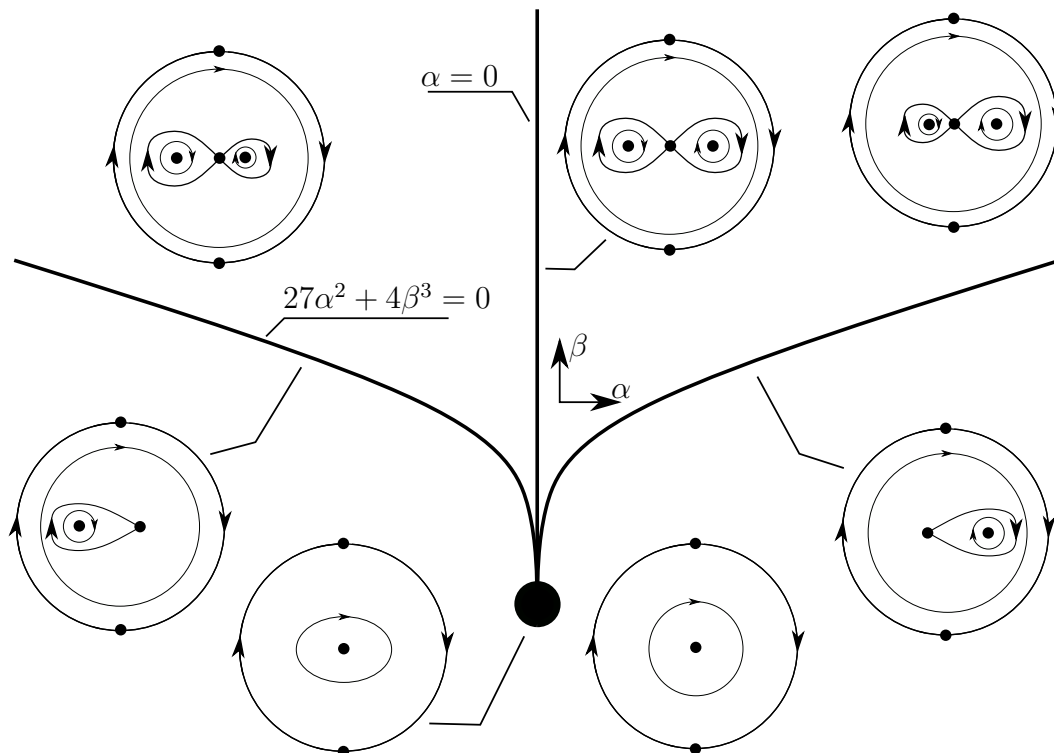


Figure 4.3: Bifurcation diagram of  $X_{21}$  with  $b = -1$ . Figure source: made by the author.

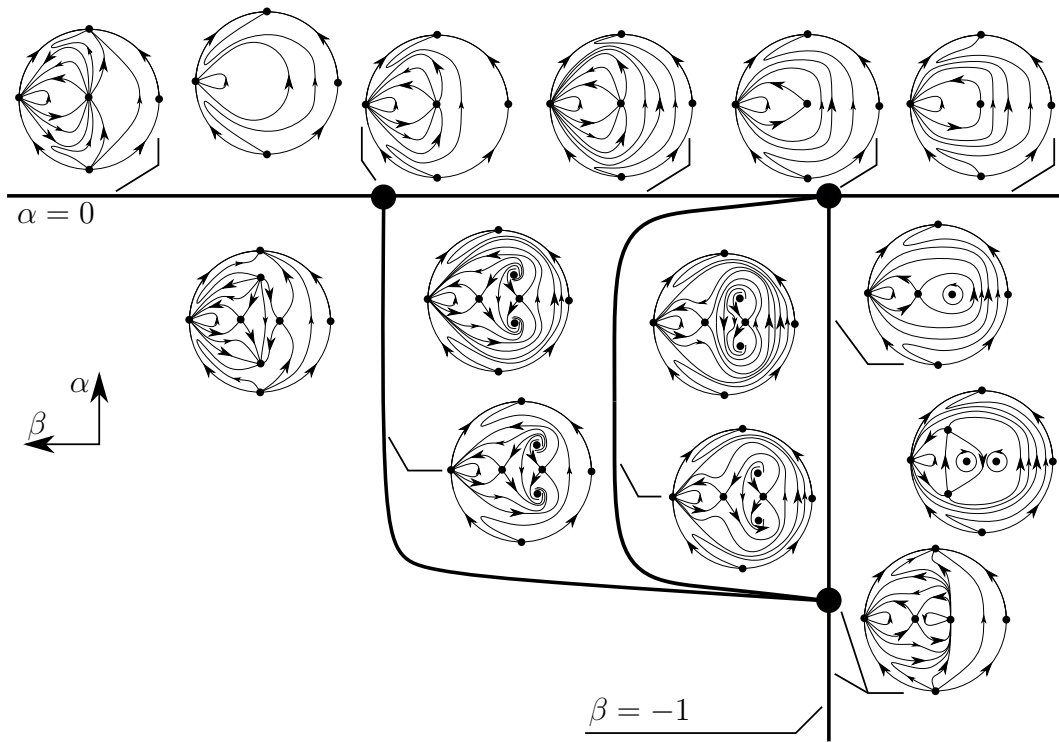


Figure 4.4: Bifurcation diagram of  $X_{22a}$  with  $a = 1$ . Figure source: made by the author.

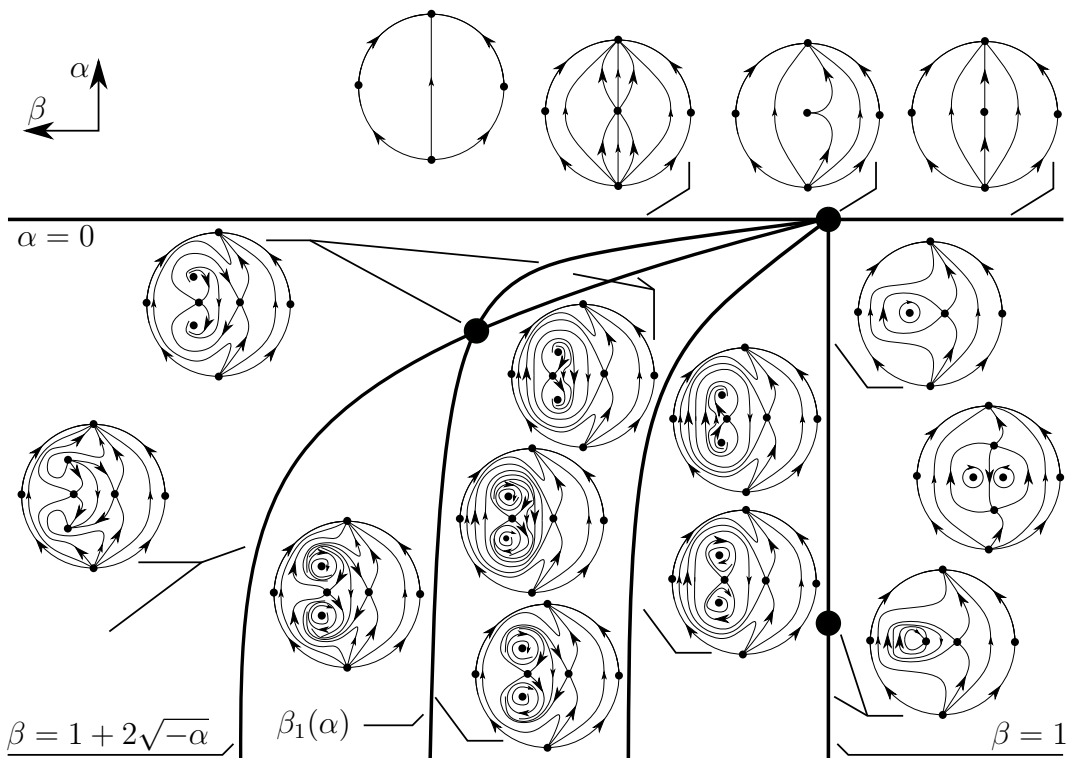


Figure 4.5: Bifurcation diagram of  $X_{22a}$  with  $a = -1$ . Figure source: made by the author.

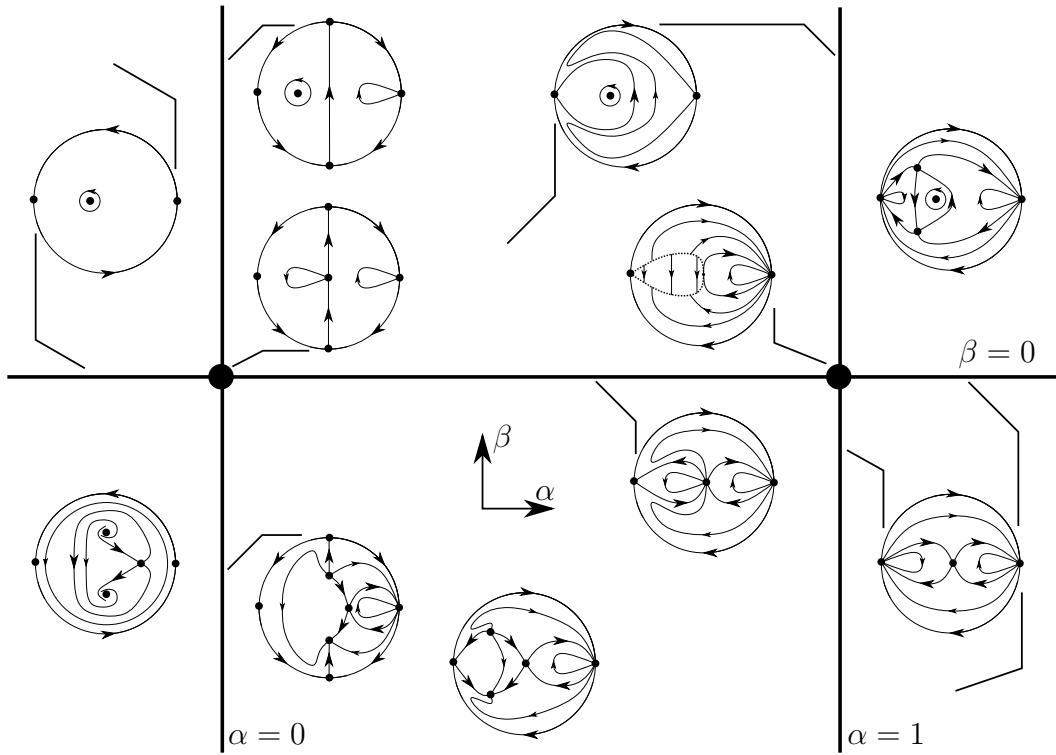


Figure 4.6: Bifurcation diagram of  $X_{24a}$  with  $a = 1$ . Figure source: made by the author.

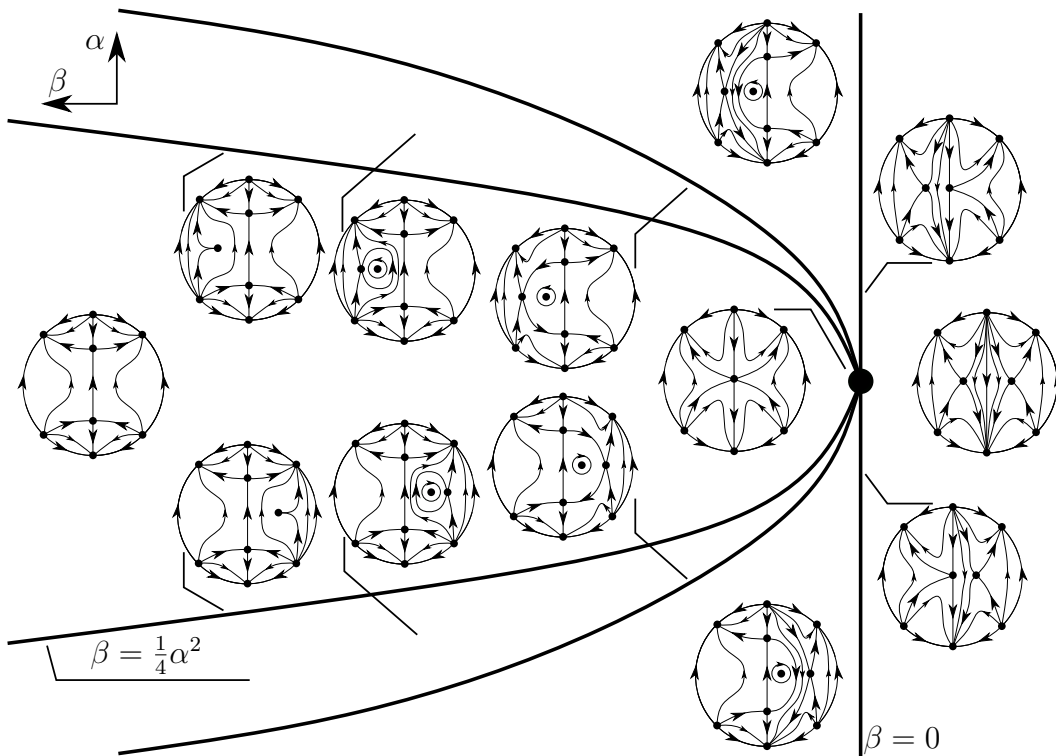


Figure 4.7: Bifurcation diagram of  $X_{25a}$  with  $a = 1$ . Figure source: made by the author.

It follows from Theorem 4.2 that it is enough to give the complete global phase portrait of each of those families, for any  $\lambda \in \mathbb{R}$  and  $(\alpha, \beta) \in \mathbb{R}^2$ . Once we already presented our approach method in Chapter 3 we will in this chapter point out only some specific argumentations to solve some problems that we faced, mainly in the two-parameters families.

## 4.2 Approach method

As in Chapter 3, the backbone of our approach is first to study all the local phase portrait at every finite singularity and at the infinity, to discover when it may exist some limit cycle and when it may happen some bifurcation as the saddle-node, the center-focus or the Hopf bifurcation. After this we study where a given separatrix must end or start. To do this we use a large amount of convenient straight lines and curves to see at which direction the flow crosses it.

Let us take system  $X_{12}$  as an example. We remember that system  $X_{12}$  is given by

$$\dot{x} = \varepsilon xy, \quad \dot{y} = \frac{1}{2} (2\varepsilon y^2 + x + \lambda),$$

where  $\varepsilon \in \{-1, 1\}$ . First we observe that if  $\varepsilon = -1$ , then with the change of variables (and parameter)  $(x, y; \lambda) \mapsto (-x_1, -y_1; -\lambda_1)$  we go back to the case  $\varepsilon = 1$  and thus both cases are equivalent. Therefore, we can assume  $\varepsilon = 1$ . Now we will only point out its behavior near the infinity due the fact that it is the only system such that the infinity is filled up of singularities.

**Proposition 4.5.** *The following statements hold.*

- (a)  $p$  is a hyperbolic saddle if  $\lambda < 0$  and a center if  $\lambda > 0$ ;
- (b)  $q^+$  (resp.  $q^-$ ) is a unstable node (resp. stable node) if  $\lambda < 0$ ;
- (c) The origin is the unique finite singularity if  $\lambda = 0$  and its phase portrait is given by Figure 4.19;
- (d)  $X_{12}$  does not have any limit cycle.

*Proof.* Knowing that a symmetric singularity cannot be a focus, statements (a) and (b) follows from the linear parts of  $X_{12}$  at the singularities  $p$  and  $q^\pm$ :

$$DX_{12}(p) = \begin{pmatrix} 0 & -\lambda \\ \frac{1}{2} & 0 \end{pmatrix}, \quad DX_{12}(q^\pm) = \pm \begin{pmatrix} \frac{1}{\sqrt{2}}\sqrt{-\lambda} & 0 \\ \star & \sqrt{2}\sqrt{-\lambda} \end{pmatrix}.$$

Doing a quasihomogeneous blow up at the origin when  $\lambda = 0$ , with weights  $(\alpha, \beta) = (2, 1)$ , one will obtain the vector field  $X_0 = X_0(r, \theta)$  or its differential system

$$\dot{r} = rR_1(r, \theta), \quad \dot{\theta} = \cos \theta (\cos \theta + \sin^2 \theta) + rR_2(r, \theta).$$

Therefore, the singularities of  $X_0$  such that  $r = 0$  are given by  $\theta \in \{\pm\frac{1}{2}\pi, \theta^\pm\}$ , where  $\theta^\pm = \pm \arccos\left(\frac{1}{2}(1 - \sqrt{5})\right)$ . Hence, statement (c) follows from

$$DX_0\left(0, \pm\frac{\pi}{2}\right) = \pm \begin{pmatrix} 1 & 0 \\ 0 & -1 \end{pmatrix},$$

$$DX_0(0, \theta^\pm) = \pm \begin{pmatrix} \frac{1}{2}\sqrt{5(\sqrt{5}-2)} & 0 \\ 0 & \sqrt{5(\sqrt{5}-2)} \end{pmatrix}.$$

Statement (d) follows from the invariance of the  $y$ -axis and the fact that a limit cycle cannot surround only a unique saddle.  $\square$

**Proposition 4.6.** *The infinity of  $X_{12}$  is filled up of singularities and its local phase portrait is given by Figure 4.20.*

*Proof.* At chart  $U_1$  of the Poincaré compactification system  $X_{12}$  becomes

$$\dot{u} = \frac{1}{2}v + \frac{\lambda}{2}v^2, \quad \dot{v} = -uv.$$

And at the chart  $U_2$  we have

$$\dot{u} = -\frac{1}{2}u^2v - \frac{\lambda}{2}uv^2, \quad \dot{v} = -v - \frac{1}{2}uv^2 - \frac{\lambda}{2}v^3.$$

Therefore, we conclude that the infinity is filled up of singularities. Doing a regularization in  $v$ , i.e. dividing both systems by  $v$ , one can see that the flow of the regularized system at  $v = 0$  is given by Figure 4.21. Let  $X = X(u, v)$  be the regularized version of system  $X_{12}$  at the chart  $U_1$ , i.e.  $X$  is given by

$$\dot{u} = \frac{1}{2} + \frac{\lambda}{2}v, \quad \dot{v} = -u.$$

Let  $h(u, v) = v$ ,  $Xh(p) = \langle X(p), \nabla h(p) \rangle$  and  $X^n h(p) = \langle X(p), \nabla X^{n-1} h(p) \rangle$ , where  $\langle \cdot, \cdot \rangle$  denotes the standard inner product of  $\mathbb{R}^2$ . One can easily conclude that  $h(0, 0) = Xh(0, 0) = 0$ ,  $X^2 h(0, 0) = -\frac{1}{2}$  and thus we conclude Figure 4.21.  $\square$

Now we have the *Local Behavior* of  $X_{12}$  in all its singularities, finite and infinite, and thus we can start working on its separatrices.

**Proposition 4.7.** *The phase portrait of  $X_{12}$  for  $\lambda < 0$  is the one given in Figure 4.1.*

*Proof.* From Propositions 4.5 and 4.6 we conclude Figure 4.22. First we observe that the flow crosses the  $x$ -axis downwards if  $x < -\lambda$  and upwards if  $x > -\lambda$ . Therefore, separatrix 4 cannot cross the  $x$ -axis, otherwise separatrix 2 would have no  $\alpha$ -limit. Hence, separatrix 4 has no other option than ending at the stable node. By symmetry separatrix 3 borns at the unstable node. Now separatrix 1 has no other option than ending at some singularity of the first quadrant of the infinity and thus separatrix 2 borns at the symmetrical singularity at the forth quadrant. Clearly separatrix 6 has no option than ending at the stable node and therefore separatrix 5 borns at the unstable node.  $\square$

**Proposition 4.8.** *The phase portrait of  $X_{12}$  for  $\lambda = 0$  is the one given in Figure 4.1.*

*Proof.* From Propositions 4.5 and 4.6 we conclude Figure 4.23. We know that the flow crosses the  $x$ -axis downwards if  $x < 0$ , therefore separatrix 4 has no other option than glue up to separatrix 2 and thus by symmetry separatrix 1 glues up to separatrix 3.  $\square$

**Proposition 4.9.** *The phase portrait of  $X_{12}$  for  $\lambda > 0$  is the one given in Figure 4.1.*

*Proof.* From Propositions 4.5 and 4.6 we conclude Figure 4.24. Here we just need to observe that separatrix 1 must cross the  $x$ -axis and thus by symmetry it will glue to separatrix 2.  $\square$

With this same approach, one can also conclude the phase portraits of  $X_{01}$ ,  $X_{02}$ ,  $X_{11}$ ,  $X_{13}$  and  $X_{14}$ .

Before we study the systems of codimension 2 we must know when they are topologically equivalent, at some finite singularity, to the origin of  $X_{11}$ ,  $X_{12}$ ,  $X_{13}$  or  $X_{14}$ , for  $\lambda \approx 0$ .

**Definition 4.10.** Let  $p$  be a  $S$ -singularity of  $F \in \mathfrak{X}$ . We say that  $p$  is a

- (a) cusp  $S$ -singularity if  $h(p) = Fh(p) = F^2h(p) = 0$  and  $F^3h(p) \neq 0$ ;
- (b) nodal  $S$ -singularity if  $F(p) = 0$ , the eigenvalues of  $DF(p)$  ( $\lambda_1$  and  $\lambda_2$ ) are real, distinct,  $\lambda_1\lambda_2 > 0$  and the eigenspaces are transverse to  $S$  at  $p$ ;
- (c) saddle  $S$ -singularity if  $F(p) = 0$ , the eigenvalues of  $DF(p)$  ( $\lambda_1$  and  $\lambda_2$ ) are real, distinct,  $\lambda_1\lambda_2 < 0$  and the eigenspaces are transverse to  $S$  at  $p$ ;
- (d) focal  $S$ -singularity if  $p$  is a hyperbolic critical point of  $F$  and the eigenvalues of  $DF(p)$  are  $\lambda = a + ib$  with  $b \neq 0$ .

It follows from Lemma 4.2 of [56] that if  $p$  is a cusp, nodal, saddle or focal  $S$ -singularity, then  $X$  is locally topologically equivalent at  $p$  to the origin of  $X_{11}$ ,  $X_{12}$ ,  $X_{13}$  or  $X_{14}$ , respectively, for  $\lambda \approx 0$ .

### 4.3 System $X_{21}$

Let us remember that system  $X_{21}$  is given by

$$\dot{x} = y, \quad \dot{y} = \frac{1}{2} (bx^3 + \beta x + \alpha),$$

where  $b \in \{-1, 1\}$ . From now on we will assume  $b = 1$ . Clearly the finite singularities of  $X_{21}$  are given by  $(x_0, 0)$ , where  $x_0$  is a real root of the polynomial  $p(x) = x^3 + \beta x + \alpha$ . Following the Cardano-Tartaglia formula (see Section 2.10) we define  $D = \frac{1}{27}\beta^3 + \frac{1}{4}\alpha^2$  and observe that  $D = 0$  if, and only if,  $\beta = \beta(\alpha)$  where  $\beta(\alpha) = -\frac{3}{\sqrt[3]{4}}\sqrt[3]{\alpha^2}$ . Therefore,

- (a) if  $\beta > \beta(\alpha)$  we have a unique finite singularity;
- (b) if  $\beta < \beta(\alpha)$  we have three finite singularities;
- (c) if  $\beta = \beta(\alpha)$  and  $\alpha \neq 0$  we have two finite singularities;
- (d) if  $\beta = \beta(\alpha)$  and  $\alpha = 0$ , then the origin is the unique finite singularity.

Moreover, denoting by  $x^{\frac{1}{3}}$  the standard third root of  $x$  and by  $\sqrt[3]{x}$  the real third root of  $x$  (when it exists) we can denote the zeros of  $p(x) = 0$  by

$$x_1 = S + T, \quad x_2 = -\frac{1}{2}(S + T) + \frac{1}{2}\sqrt{3}(S - T)i, \quad x_3 = -\frac{1}{2}(S + T) - \frac{1}{2}\sqrt{3}(S - T)i,$$

where

$$S = f\left(-\frac{\alpha}{2} + D^{\frac{1}{2}}\right), \quad T = f\left(-\frac{\alpha}{2} - D^{\frac{1}{2}}\right), \quad f(x) = \begin{cases} \sqrt[3]{x}, & \text{if } D \geq 0 \\ x^{\frac{1}{3}}, & \text{if } D < 0. \end{cases}$$

**Proposition 4.11.** *The disposal of the real solutions of  $p$  is the following.*

- (a) *If  $D < 0$ , then  $x_2 < x_3 < x_1$ ;*
- (b) *If  $D = 0$  and  $\alpha < 0$ , then  $x_2 = x_3 < x_1$ ;*
- (c) *If  $D = 0$  and  $\alpha > 0$ , then  $x_1 < x_2 = x_3$ ;*
- (d) *Otherwise  $x_1$  is the unique real solution.*

*Proof.* We start with statement (a), which will be separated in three parts. If  $D < 0$  and  $\alpha < 0$ , then  $S = (a + ib)^{\frac{1}{3}}$ , where  $a = -\frac{1}{2}\alpha > 0$  and  $b = \sqrt{-D} > 0$ . Therefore, if we denote  $r = \sqrt{a^2 + b^2}$  and  $\theta = \frac{1}{3} \arctan\left(\frac{b}{a}\right)$  we obtain  $S = \sqrt{-\frac{\beta}{3}}(\cos \theta + i \sin \theta)$ . In a similar way one can see that  $T = \sqrt{-\frac{\beta}{3}}(\cos \theta - i \sin \theta)$ . Hence,

$$\begin{aligned} x_1 &= 2\sqrt{-\frac{\beta}{3}} \cos \theta, \\ x_2 &= -\sqrt{-\frac{\beta}{3}}(\cos \theta + \sqrt{3} \sin \theta), \\ x_3 &= -\sqrt{-\frac{\beta}{3}}(\cos \theta - \sqrt{3} \sin \theta). \end{aligned}$$

Observe that

$$\frac{b}{a} = \frac{\sqrt{-D}}{-\frac{1}{2}\alpha} = -\frac{2}{\alpha} \sqrt{-\frac{\beta^3}{27} - \frac{\alpha^2}{4}} = \frac{2}{|\alpha|} \sqrt{-\frac{\beta^3}{27} - \frac{\alpha^2}{4}} = \sqrt{\frac{4}{27} \frac{(-\beta)^3}{\alpha^2} - 1}.$$

Given  $\beta_0 < 0$  fixed we know that  $\alpha \in (\alpha(\beta_0), 0)$ , where  $\alpha(\beta) = -\sqrt{-\frac{4}{27}\beta^3}$ . Similarly, given  $\alpha_0 < 0$  fixed we know that  $\beta \in (-\infty, \beta(\alpha))$ . Therefore, it is not hard to see that  $\theta = \theta(\alpha, \beta) \in \left(0, \frac{1}{6}\pi\right)$  and

$$\lim_{D \rightarrow 0} \theta(\alpha, \beta) = 0 \text{ and } \lim_{\beta \rightarrow -\infty} \theta(\alpha_0, \beta) = \lim_{\alpha \rightarrow 0} \theta(\alpha, \beta_0) = \frac{\pi}{6}.$$

Therefore, we conclude that in this case we have  $x_2 < x_3 < 0 < x_1$ ,

$$\lim_{D \rightarrow 0} |x_2 - x_3| = 0 \text{ and } \lim_{\beta \rightarrow -\infty} x_3(\alpha_0, \beta) = \lim_{\alpha \rightarrow 0} x_3(\alpha, \beta_0) = 0.$$

If  $D < 0$  and  $\alpha > 0$  we have

$$\begin{aligned} x_1 &= 2\sqrt{-\frac{\beta}{3}} \cos \theta, \\ x_2 &= -\sqrt{-\frac{\beta}{3}}(\cos \theta + \sqrt{3} \sin \theta), \\ x_3 &= -\sqrt{-\frac{\beta}{3}}(\cos \theta - \sqrt{3} \sin \theta), \end{aligned}$$

where  $\theta = \frac{1}{3} \arctan\left(-\frac{2}{\alpha}\sqrt{-D}\right) + \frac{1}{3}\pi$ . Once we have  $\alpha > 0$  it follows that

$$-\frac{2}{\alpha}\sqrt{-D} = -\sqrt{\frac{4}{27} \frac{(-\beta)^3}{\alpha^2} - 1}.$$

Given  $\beta_0 < 0$  fixed we know that  $\alpha \in (0, \alpha(\beta_0))$ , where  $\alpha(\beta) = \sqrt{-\frac{4}{27}\beta^3}$ . Similarly, given  $\alpha_0 > 0$  fixed we know that  $\beta \in (-\infty, \beta(\alpha))$ . It is not hard to see that  $\theta = \theta(\alpha, \beta) \in \left(\frac{1}{6}\pi, \frac{1}{3}\pi\right)$  and

$$\lim_{D \rightarrow 0} \theta(\alpha, \beta) = \frac{\pi}{3} \text{ and } \lim_{\beta \rightarrow -\infty} \theta(\alpha_0, \beta) = \lim_{\alpha \rightarrow 0} \theta(\alpha, \beta_0) = \frac{\pi}{6}.$$

Therefore, in this case we have  $x_2 < 0 < x_3 < x_1$ ,

$$\lim_{D \rightarrow 0} |x_1 - x_3| = 0 \text{ and } \lim_{\beta \rightarrow -\infty} x_3(\alpha_0, \beta) = \lim_{\alpha \rightarrow 0} x_3(\alpha, \beta_0) = 0.$$

If  $D < 0$  and  $\alpha = 0$ , then

$$S = \frac{1}{2}\sqrt{-\frac{\beta}{3}}(\sqrt{3} + i), \quad T = \frac{1}{2}\sqrt{-\frac{\beta}{3}}(\sqrt{3} - i),$$

and thus

$$x_1 = \sqrt{-\beta}, \quad x_2 = -\sqrt{-\beta}, \quad x_3 = 0.$$

Moreover, observe that in this case we have

$$\lim_{D \rightarrow 0} x_1(\alpha, \beta) = \lim_{D \rightarrow 0} x_2(\alpha, \beta) = 0,$$

and one can conclude statement (a).

If  $D = 0$ , then  $S = T = \sqrt[3]{-\frac{1}{2}\alpha}$  and thus

$$x_1 = 2\sqrt[3]{-\frac{1}{2}\alpha}, \quad x_2 = x_3 = \sqrt[3]{\frac{1}{2}\alpha}. \quad (4.1)$$

Statements (b) and (c) follows from (4.1) if one replace  $\alpha \neq 0$ . Replacing  $\alpha = 0$  one obtain  $x_1 = x_2 = x_3$  as in statement (d).

Finally, if  $D > 0$ , then the unique real zero is given by

$$x_1 = \sqrt[3]{-\frac{\alpha}{2} + \sqrt{D}} + \sqrt[3]{-\frac{\alpha}{2} - \sqrt{D}},$$

as in statement (d). □

**Remark 4.12.** We observe that inside each case if we look at its boundary case (for example if we look at the limit  $D \rightarrow 0$  when  $D < 0$ ), then a permutation of the index of the solutions may happen.

**Proposition 4.13.** *Let  $p_i = (x_i, 0)$ ,  $i \in \{1, 2, 3\}$  be the singularities of  $X_{21}$ . The local phase portraits of  $X_{21}$  at these singularities are the following.*

- (a) *If  $D > 0$ , then  $p_1$  is a saddle;*
- (b) *If  $D < 0$ , then  $p_1$  and  $p_2$  are saddles and  $p_3$  is a center;*
- (c) *If  $D = 0$  and  $\alpha \neq 0$ , then  $p_1$  is a saddle and  $p_2 = p_3$  is a cusp, as in Figure 4.25;*
- (d) *If  $D = \alpha = 0$ , then  $p_1$  is a non-hyperbolic saddle.*

*Proof.* One can easily see that the Jacobian matrix at a singularity  $p_i$  is given by

$$DX_{21}(p_i) = \begin{pmatrix} 0 & 1 \\ \frac{1}{2}\beta + \frac{3}{2}x_i^2 & 0 \end{pmatrix}.$$

Let us first work statement (a). In this case  $p_1$  is the unique finite singularity. Clearly it is a saddle if  $\beta \geq 0$ . If  $\beta < 0$ , then

$$\frac{1}{2}\beta + \frac{3}{2}x_1^2 = \frac{3}{2}(S^2 + T^2) - \frac{1}{2}\beta > 0.$$

Therefore, if  $D > 0$ , then the unique finite singularity is always a hyperbolic saddle.

Let us now work statement (b) assuming  $D < 0$ . Using the expressions of this case one can see that

$$\frac{1}{2}\beta + \frac{3}{2}x_1^2 = -\beta \left( 2 \cos^2 \theta - \frac{1}{2} \right) > 0,$$

because  $\beta < 0$  and  $\theta \in \left(0, \frac{1}{3}\pi\right)$ . Therefore,  $p_1$  is a hyperbolic saddle. Observe now that

$$\frac{1}{2}\beta + \frac{3}{2}x_2^2 = -\beta \sin \theta (\sin \theta + \sqrt{3} \cos \theta) > 0,$$

because  $\beta < 0$  and  $\theta \in \left(0, \frac{1}{3}\pi\right)$ . Therefore,  $p_2$  is also a hyperbolic saddle. Finally,

$$\frac{1}{2}\beta + \frac{3}{2}x_3^2 = -\beta \sin \theta (\sin \theta - \sqrt{3} \cos \theta) < 0,$$

because  $\beta < 0$  and  $\theta \in \left(0, \frac{1}{3}\pi\right)$ . This, in addition with the fact that  $p_3$  is a symmetric singularity ensures that it is a center.

Let us now work statement (c). Observe that

$$\frac{1}{2}\beta + \frac{3}{2}x_1^2 = \frac{9}{2}\sqrt[3]{\frac{\alpha^2}{4}} > 0, \quad \frac{1}{2}\beta + \frac{3}{2}x_2^2 = 0,$$

because  $\beta = -3\sqrt[3]{\frac{\alpha^2}{4}}$ . Therefore,  $(x_1, 0)$  is a hyperbolic saddle and  $(x_2, 0)$  is degenerated. Translating  $(x_2, 0)$  to the origin and then doing a quasihomogenous blow up with  $(\alpha, \beta) = (2, 3)$  one will obtain Figure 4.25.

Finally, assuming the hypothesis of statement (d) one will obtain  $\alpha = \beta = 0$  and then the origin is the unique finite singularity and it is clearly a non-hyperbolic saddle.  $\square$

**Proposition 4.14.** *The phase portrait of  $X_{21}$  with  $b = 1$  is the one given by Figure 4.2.*

*Proof.* First we observe that  $X_{21}$  cannot hold any limit cycle because every finite singularity is symmetric. Using the same approach of Section 4.2 one can conclude the phase portraits of  $X_{21}$  when  $D \geq 0$ . Knowing that  $X_{21}$  is  $\varphi$ -reversible with  $\varphi(x, y) = (-x, y)$  when  $\alpha = 0$  one can conclude its phase portrait when  $D < 0$  and  $\alpha = 0$ . Knowing that singularity  $p_2 = p_3$  is a *cusplike* singularity of  $F(X_{21})$  when  $D = 0$  and  $\alpha \neq 0$  one can also conclude the phase portrait for  $D < 0$ , but near the boundary  $D = 0$ . Now we must prove that this last phase portrait holds for any  $(\alpha, \beta)$  such that  $D < 0$  and  $\alpha \neq 0$ .

If  $D < 0$  we know that we have three finite singularities, a center  $p_3$  in the middle and a hyperbolic saddle  $p_2$  on its left side and another hyperbolic saddle  $p_1$  on its right side. Let  $\mu_0 = (\alpha_0, \beta_0) \in \mathbb{R}^2$  be such that there is a heteroclinic orbit  $\Gamma_0$  connecting both hyperbolic saddles,  $x_0 \in \mathbb{R}^2$  the intersection of  $\Gamma_0$  with the  $y$ -axis and  $l_0$  a transversal section of  $\Gamma_0$  passing through  $x_0$ . Following Section 2.6 we define  $n$  to be the coordinate along the normal line  $l_0$  such that  $n > 0$  outside the polycycle (observe that there is another heteroclinic connection due the symmetry) and  $n < 0$  inside the polycycle. We also denote  $\Gamma_s$  and  $\Gamma_u$  the perturbations of  $\Gamma_0$ , for  $|(\alpha - \alpha_0, \beta - \beta_0)|$  small enough, such that  $\omega(\Gamma_s) = p_1$  and  $\alpha(\Gamma_u) = p_2$ . Let  $x_s$  and  $x_u$  be the intersections of  $\Gamma_s$  and  $\Gamma_u$  with  $l_0$ , respectively, and let  $n_s$  and  $n_u$  be its coordinates along the line  $l_0$ . We now define the displacement map  $d(\alpha, \beta) = n_u - n_s$ . See Figure 4.26. Let  $\gamma_0(t)$  be a parametrization of  $\Gamma_0$  with  $\gamma_0(0) = x_0$ . It follows from [49] that

$$\frac{\partial d}{\partial \alpha}(\mu_0) = \frac{1}{\|X_{21}(x_0; \mu_0)\|} \int_{-\infty}^{+\infty} \left( e^{-\int_0^t \text{Div}(X_{21}(\gamma_0(s); \mu_0)) ds} \right) X_{21}(\gamma_0(t); \mu_0) \wedge \frac{\partial X_{21}}{\partial \alpha}(\gamma_0(t); \mu_0) dt,$$

where  $(x_1, x_2) \wedge (y_1, y_2) = x_1y_2 - x_2y_1$ . Knowing that

$$X_{21}(x, y; \alpha, \beta) \wedge \frac{\partial X_{21}}{\partial \alpha}(x, y; \alpha, \beta) = \frac{1}{2}y,$$

one can see that  $\frac{\partial d}{\partial \alpha}(\mu_0) > 0$  whenever  $d$  is defined. Hence, given  $\beta = \beta_0 < 0$  fixed and  $\alpha_0 = \alpha_0(\beta_0)$  such that  $d(\alpha_0, \beta_0) = 0$  we conclude that  $d(\cdot, \beta_0)$  increases for  $\alpha \approx \alpha_0$  and thus  $\alpha_0$  if  $\alpha_0$  exists it is unique. But we already know that  $d(0, \beta) = 0$  for every  $\beta < 0$  and thus given  $\beta = \beta_0 < 0$  fixed it follows that  $\alpha = 0$  is the unique value that satisfy  $d(\alpha_0, \beta_0) = 0$ .  $\square$

In a similar way one can prove that the phase portrait of  $X_{21}$  with  $b = -1$  is the one given by Figure 4.3.

#### 4.4 System $X_{22}$

Let us remember that system  $X_{22a}$  is given by

$$\dot{x} = (\beta + a)xy + (\beta - a)y^3, \quad \dot{y} = \frac{\alpha}{2} + \frac{1}{2}x^2 + xy^2 + \frac{1}{2}y^4,$$

where  $a \in \{-1, 1\}$ . On the other hand, system  $X_{22b}$  is given by

$$\dot{x} = (\beta + 1)xy + (\beta - 1)y^3, \quad \dot{y} = \frac{\alpha}{2} + \frac{a}{2}x^2 + axy^2 + \frac{a}{2}y^4,$$

where  $a \in \{-1, 1\}$ . Observe that they are both equal if we replace  $a = 1$ . Moreover, if one replace  $a = -1$  on  $X_{22b}$  and then apply the change of variables and parameters

$$(x, y; \alpha, \beta) \mapsto (x_1, -y_1; -\alpha_1, -\beta_1)$$

one will obtain system  $X_{22a}$  with  $a = -1$ . Hence, both systems are equivalent and we will focus on  $X_{22a}$ .

Let us define  $S_x = \{(x, y) \in \mathbb{R}^2 : \dot{x}(x, y) = 0\}$  and  $S_y = \{(x, y) \in \mathbb{R}^2 : \dot{y}(x, y) = 0\}$ . In this case it is easy to see that

$$S_x = \{(x, y) \in \mathbb{R}^2 : y = 0 \text{ or } x = \frac{a-\beta}{a+\beta}y^2\},$$

$$S_y = \{(x, y) \in \mathbb{R}^2 : x = -y^2 \pm \sqrt{-\alpha}\}.$$

**Proposition 4.15.** *The phase portrait of  $X_{22a}$  with  $a = 1$  is the one given by Figure 4.4.*

*Proof.* Approaching system  $X_{22a}$  as in Section 4.2 (which include the study of  $F(X_{22a})$ ) and knowing that the *Bendixson Criterion* (see Section 3.9 of [50]) prevents any limit cycles in this case, one can work a lot of the separatrices. But here one must look also at the flows at sets  $S_x$  and  $S_y$ . Take for example Figure 4.27. One will obtain this with an analysis of the flow on the sets  $S_x$  and  $S_y$  together with an analysis at the eigenvectors of the hyperbolic saddles. Now one can conclude that separatrix 1 must cross the  $x$ -axis and thus it will glue with separatrix 8 due to symmetry. At other hand, separatrix 3 is trapped between the  $x$ -axis and  $S_y$  and thus it will end at infinity. Finally, separatrix 7 has no other option than either ending at infinity (precisely at the west pole) or crossing the  $x$ -axis. Let  $q = q(\alpha, \beta)$  be the hyperbolic saddle inside the half-plane  $y < 0$  and  $\lambda^- < 0 < \lambda^+$ ,  $\lambda^\pm = \lambda^\pm(\alpha, \beta)$ , the eigenvalues of  $DX_{22a}(q)$ . Let  $v = v(\alpha, \beta)$  be an

eigenvector of  $DX_{22a}(q)$  with respect to  $\lambda^+$ ,  $l(t) = q + tv$  and  $t_0 = t_0(\alpha, \beta)$  such that  $l(t_0)$  is the intersection of  $l$  and the  $x$ -axis. Calculations shows that separatrix 7 is above  $l$  and if  $t$  is between 0 and  $t_0$ , then the flow of  $X_{22a}$  is transversal to  $l$  and it points upwards. Therefore, separatrix 7 cannot cross  $l$  and thus it must cross the  $x$ -axis and hence it glues up with separatrix 4 due to the symmetry.

The unique special analysis lies in the case of Figure 4.28. To prove that separatrix 2, which borns at the singularity  $p = (\sqrt{-\alpha}, 0)$ , ends at the north pole we calculate the flow at the parabola  $x = -\frac{1}{2}y^2 + \sqrt{-\alpha}$  and observe that it points upwards if  $y \neq 0$ . We also calculate that separatrix 2 near  $p$  is given by  $(f(y), y)$ , where

$$f(y) = -\frac{\sqrt{-4\sqrt{-\alpha} - \alpha} + \alpha}{2\alpha}y^2 + O(y^4).$$

Knowing that

$$-\frac{1}{2} \leq -\frac{\sqrt{-4\sqrt{-\alpha} - \alpha} + \alpha}{2\alpha},$$

with the right hand side equals  $-\frac{1}{2}$  if and only if  $\alpha = -16$ , one can concludes that if  $\alpha < -16$ , then separatrix 2 ends at the north pole. Moreover, if  $\alpha = -16$ , then

$$f(y) = -\frac{1}{2}y^2 + \frac{1}{32}y^4 + O(y^6)$$

and thus separatrix 2 goes to the north pole in this case too.  $\square$

**Proposition 4.16.** *The phase portrait of  $X_{22a}$  with  $a = -1$  is the one given by Figure 4.5.*

*Proof.* Here we point out two things. First we assume  $\alpha < 0$  and  $\beta \geq 1 + 2\sqrt{-\alpha}$ . In this case one can see that the *local behavior* is given by Figure 4.29. We want to prove that for  $\beta$  big enough separatrix 6 will end at the north pole. Doing the change of coordinates  $(x, y) = (x_1, \sqrt{y_1})$  for  $y > 0$  one will get system  $X_1 = X_1(x_1, y_1)$  given by

$$\dot{x}_1 = \sqrt{y_1}[(\beta - 1)x_1 + (\beta + 1)y_1], \quad \dot{y}_1 = \sqrt{y_1}[\alpha + x_1^2 + 2x_1y_1 + y_1^2].$$

The fact that separatrix 6 at system  $X_{22a}$  crosses the set  $S_x$  above the unstable node implies, at system  $X_1$ , that separatrix 6 also crosses the set  $S_{x_1}$  above the unstable node  $q^+$ . See Figure 4.30. Taking  $\beta \geq 1 + 2\sqrt{-\alpha} + 4\sqrt[4]{-\alpha}$  and defining the line

$$l = q^+ + t \left( 1, \frac{\alpha}{(-\alpha)^{\frac{3}{4}} - \alpha} \right)$$

one can conclude that the flows crosses  $l$  upwards and thus separatrix 6 must cross the line of  $S_{y_1}$  which contains  $p^+$ . But at the right side of this line we have  $\dot{y}_1 > 0$  and thus separatrix 6 cannot end at  $p^+$  and hence it must end at the north pole.

Second, we must prove the relative position of the curves  $\beta_1(\alpha)$  and  $\beta_h(\alpha) = 1 + 2\sqrt{-\alpha}$  as in Figure 4.5, i.e. we must prove  $\beta_1 < \beta_h$  for  $\alpha < 0$  large enough and  $\beta_h < \beta_1$  for  $\alpha < 0$  small enough. We remember that  $\beta_1$  represents the moment when it exists a heteroclinic connection between both saddles. From now on we will assume  $(\alpha, \beta) = (\lambda, 1 + 2\sqrt{-\lambda})$ ,  $\lambda \leq 0$ , and we will prove that for  $\alpha < 0$  large enough the connection already broke and thus  $\beta_1 < \beta_h$ . Translating the saddle on the left to the origin and then doing a simple blow up at the  $y$  direction one will obtain system  $X_2 = X_2(x_2, y_2)$  given by

$$\begin{aligned} \dot{x}_2 &= 2\lambda + \sqrt{-\lambda}x_2^2 + 3\sqrt{-\lambda}x_2y_2 + 2(1 + \sqrt{-\lambda})y_2^2 - \frac{1}{2}x_2^3y_2 - x_2^2y_2^2 - \frac{1}{2}x_2y_2^3, \\ \dot{y}_2 &= -\sqrt{-\lambda}x_2y_2 - \sqrt{-\lambda}y_2^2 + \frac{1}{2}x_2^2y_2^2 + x_2y_2^3 + \frac{1}{2}y_2^4. \end{aligned}$$

In this coordinates set  $S_{x_2}$  has a closed component. Let  $p_1 = (x_0, y_0)$  be the higher point in this closed component. Calculations shows that  $p_1$  lies on the left of the straight line  $r$  given by  $x_2 + y_2 = -\sqrt{-\lambda}$ . Let  $p_2 = (-y_0, y_0)$  be the projection of  $p_1$  on  $r$  and observe that  $p_2$  is above the focus  $p_3$ , which lies in the same line. See Figure 4.31. Follows from an analysis at set  $S_{x_2}$  that separatrix  $s$  must cross  $r$  above point  $p_2$ . Let  $l$  be the segment given by  $p_2 + t\left(1, -\frac{1}{2}\right)$  such that it ends at the other component  $r_1$  of  $S_{y_2}$ . For  $\alpha < 0$  large enough calculations shows that the flow at  $l$  points upwards and thus separatrix  $s$  must cross  $r_1$ . But at the right side of  $r_1$  we have  $\dot{y}_1 > 0$  and thus  $s$  must end at the north pole. Therefore, for  $\alpha < 0$  large enough we have  $\beta_1 < \beta_h$ . Once we cannot give  $\beta_1$  explicitly and that there is nothing that prevents either  $\beta_1 < \beta_h$  or  $\beta_h < \beta_1$  it turns out to be a very difficult task to understand completely and in a analytical way the relative position of  $\beta_h$  and  $\beta_1$ . But numerical computations (see chapters 9 and 10 of [19]) shows that  $\lambda_0 \approx -\frac{2}{3}$  is the unique intersection of  $\beta_1$  and  $\beta_h$ . Moreover it also shows that  $\beta_h < \beta_1$  if  $\lambda \in (\lambda_0, 0)$  and  $\beta_1 < \beta_h$  if  $\lambda \in (-\infty, \lambda_0)$ . So to provide an analytic proof of these facts is an open problem.  $\square$

#### 4.5 System $X_{23}$

Let us remember that system  $X_{23}$  is given by

$$\dot{x} = a\alpha xy - y^3 + ax^3y + axy^5, \quad \dot{y} = \frac{\beta}{2} + \frac{a}{2}x - \frac{\alpha}{2}y^2 - \frac{1}{2}x^2y^2 - \frac{1}{2}y^6,$$

where  $a \in \{-1, 1\}$ .

Once this system has a particular higher degree than the previous one it is not practical to find analytic expressions for the finite singularities as we did with the previous systems. Therefore, we will change our approach. First we do the change of variables given by  $(x, y) = (x_1, \sqrt{y_1})$ , obtaining, with  $a = 1$ , the vector field

$$\dot{x}_1 = \sqrt{y_1}(-y_1 + x_1(x_1^2 + y_1^2 + \alpha)), \quad \dot{y}_1 = \sqrt{y_1}(x_1 - y_1(x_1^2 + y_1^2 + \alpha) + \beta).$$

Dividing both equations by  $\sqrt{y_1}$  we obtain the vector field  $Y = (\dot{x}_2, \dot{y}_2)$ , given by

$$\dot{x}_2 = -y_2 + x_2(x_2^2 + y_2^2 + \alpha), \quad \dot{y}_2 = x_2 - y_2(x_2^2 + y_2^2 + \alpha) + \beta.$$

Observe that  $X_{23}$  and  $Y$  are topologically equivalent for  $y > 0$  (which is equivalent to  $y_2 > 0$ ) and  $Y$  has degree 3 while  $X_{23}$  has degree 6. Therefore, the approach is the following. We will study  $Y$  at  $y_2 > 0$  and then draw conclusions for  $X_{23}$  for  $y > 0$  (and thus for  $y < 0$  too due to its symmetry) and study locally the unique singularity  $p = (-a\beta, 0)$  of  $X_{23}$  at the  $x$ -axis.

**Proposition 4.17.** *The following statement holds.*

- (a)  $p$  is hyperbolic saddle if  $\beta(\alpha + \beta^2) < 0$  and a center if  $\beta(\alpha + \beta^2) > 0$ ;
- (b)  $p$  is a center if  $\{\beta = 0 \text{ and } -1 \leq \alpha < 1\}$  or  $\{\alpha + \beta^2 = 0 \text{ and } |\beta| < 1\}$ ;
- (c) Otherwise the local phase portrait of  $X_{23}$  at  $p$  is given by Figure 4.32.

*Proof.* Statement (a) follows from

$$DX_{23}(p) = \begin{pmatrix} 0 & -\beta(\alpha + \beta^2) \\ \frac{1}{2} & 0 \end{pmatrix}$$

and the fact that  $p$  is a symmetric singularity. Statements (b) and (c) follows from a quasihomogeneous blow up with  $(\alpha, \beta) = (2, 1)$ .  $\square$

Let us define the following functions.

$$\begin{aligned} p_1(x_2) &= 2x_2^2 + \beta x_2 + \alpha; \\ p_2(x_2) &= 4x_2^5 + 5\beta x_2^4 + (4\alpha + \beta^2)x_2^3 + 2\alpha\beta x_2^2 + (\alpha^2 - 1)x_2 - \beta; \\ f(x_2) &= \sqrt{x_2(x_2 + \beta)}; \\ R(\alpha, \beta) &= -256(\alpha^2 - 1)^3 - 192\alpha(\alpha^4 + 7\alpha^2 + 28)\beta^2 \\ &\quad + 60(\alpha^4 - 28\alpha^2 - 72)\beta^4 - 4\alpha(\alpha^2 - 108)\beta^6 - 27\beta^8. \end{aligned} \tag{4.2}$$

In what follows we will list some analytic properties of the finite singularities of  $Y$  at  $y_2 > 0$ .

**Proposition 4.18.** *Let  $q = (x_0, y_0) \in \mathbb{R}^2$  such that  $y_0 > 0$ . The following statements holds.*

(a)  $q$  is a finite singularity of  $Y$  if, and only if,

$$y_0 = \frac{x_0 + \beta}{p_1(x_0)} = x_0 p_1(x_0) = f(x_0);$$

(b) If  $q$  is a finite singularity of  $Y$ , then  $p_2(x_0) = 0$  and  $x_0 p_1(x_0) > 0$ ;

(c) If  $q_0 = (x_0, f(x_0))$  is such that  $p_2(x_0) = 0$  and  $x_0 p_1(x_0) > 0$ , then  $q_0$  is a finite singularity of  $Y$ ;

(d) If  $q$  is a non-hyperbolic finite singularity of  $Y$ , then either  $\beta = 0$  or  $R(\alpha, \beta) = 0$ .

*Proof.* Isolating  $u = x_2^2 + y_2^2 + \alpha$  at  $\dot{x}_2 = 0$  and  $\dot{y}_2 = 0$  we see that a necessary condition for a point  $(x_0, y_0)$  be a singularity of  $Y$  is that it satisfies

$$\frac{y_0}{x_0} = \frac{x_0 + \beta}{y_0}.$$

Knowing that  $y_0 > 0$  we obtain  $y_0 = f(x_0)$ . Statement (a) now follows from  $Y(x_0, f(x_0)) = (0, 0)$ .

From statement (a) one concludes that if  $q$  is a finite singularity of  $Y$ , then  $x_0 p_1^2(x_0) - (x_0 + \beta) = 0$  and  $x_0 p_1(x_0) = f(x_0) \geq 0$ . Statement (b) now follows from the fact that  $x_0 \neq 0$  and  $p_2(x_0) = x_0 p_1^2(x_0) - (x_0 + \beta)$ .

To prove statement (c) first observe that  $p_2(x_0) = 0$  implies  $x_0 p_1(x_0)^2 = x_0 + \beta$  and thus

$$x_0 p_1(x_0)^2 = x_0 + \beta = \frac{f(x_0)^2}{x_0}.$$

Hence,  $x_0^2 p_1(x_0)^2 = f(x_0)^2$ . Squaring both sides and knowing that  $x_0 p_1(x_0) > 0$  we obtain statement (c).

Now observe that the Jacobian matrix of  $Y$  is given by

$$DY(x_2, y_2) = \begin{pmatrix} 3x_2^2 + y_2^2 + \alpha & 2x_2y_2 - 1 \\ 1 - 2x_2y_2 & -(x_2^2 + 3y_2^2 + \alpha) \end{pmatrix}.$$

Replacing  $y_0 = f(x_0)$  and calculating the trace and the determinant and then replacing  $f(x_0) = x_0p_1(x_0)$  we obtain

$$\text{Tr}(x_0) = -2x_0\beta, \quad \text{Det}(x_0) = -p_2'(x_0).$$

It follows from the *Trace-Determinant Theory* (see Section 4.1 of [25]) that a singularity  $q$  is non-hyperbolic if  $\text{Tr}(x_0) = 0$ ,  $\text{Det}(x_0) = 0$  or both. Statement (d) now follows from the fact that it is impossible that  $x_0 = 0$  and that  $R(\alpha, \beta)$  is the *resultant* (except by a constant) in  $x_2$  between  $p_2$  and  $p_2'$ .  $\square$

In what follows we will list some properties of  $R(\alpha, \beta)$  and the parabola  $\alpha + \beta^2 = 0$ .

**Proposition 4.19.** *The following statement holds.*

- (a)  $R(\alpha, \beta) = 0$  has four branches (two positives and two negatives) if  $\alpha \leq -1$ , two branches (one positive and one negative) if  $-1 < \alpha \leq 1$  and no branch at all if  $\alpha > 1$ ;
- (b) Let  $\beta_+$  be the negative branch that borns at  $\alpha = 1$  and  $\beta_-$  the negative branch that borns at  $\alpha = -1$ . Then  $\mu_1 \approx (-3.398\dots, -1.849\dots)$  is the unique intersection between  $\beta_+$  and  $\beta_-$ ;
- (c)  $\mu_2 \approx (-3.389\dots, -1.841\dots)$  is the unique intersection between the parabola  $\alpha + \beta^2 = 0$  and  $R(\alpha, \beta) = 0$  at  $\beta < 0$ . Moreover it occurs at  $\beta_-$ . See Figure 4.33.

*Proof.* Fortunately  $R(\alpha, \beta)$  is biquadratic at  $\beta$  and thus we can do the change of variables  $\beta \mapsto \pm\sqrt{b}$  (both will give the same result) and obtain the quartic polynomial in  $b$

$$\begin{aligned} R_1(\alpha, b) = & -256(\alpha^2 - 1)^3 - 192\alpha(\alpha^4 + 7\alpha^2 + 28)b \\ & + 60(\alpha^4 - 28\alpha^2 - 72)b^2 - 4\alpha(\alpha^2 - 108)b^3 - 27b^4. \end{aligned}$$

Given  $\alpha_0 \in \mathbb{R}$  fixed we want to know how many positive roots the polynomial  $R_1(\alpha_0, b)$  has. The discriminant in  $b$  of  $R_1$  is given, except by a constant, by

$$\begin{aligned} D(\alpha) = & -1\,871\,773\,696 - 10\,034\,479\,104\,\alpha^2 - 19\,980\,402\,688\,\alpha^4 \\ & - 17\,398\,321\,152\,\alpha^6 - 5\,393\,464\,832\,\alpha^8 + 250\,599\,680\,\alpha^{10} \\ & + 64\,492\,352\,\alpha^{12} + 870\,480\,\alpha^{14} - 190\,633\,\alpha^{16} - 9\,567\,\alpha^{18} \\ & - 167\,\alpha^{20} - \alpha^{22}. \end{aligned}$$

Computations shows that  $D(\alpha) \leq 0$  with the equality happening only if  $\alpha = \pm 3.398\dots$ . It is well known that if  $D < 0$ , then  $R_1$  has two distinct real roots and two complex conjugate roots. If  $\{b_1, b_2, b_3, b_4\}$  are the four roots in  $b$  of  $R_1$ , then

$$R_1(\alpha, \beta) = -27(b - b_1)(b - b_2)(b - b_3)(b - b_4)$$

and thus  $27b_1b_2b_3b_4 = 256(\alpha^2 - 1)^3$ . Supposing that  $b_1, b_2$  are the real solutions and  $b_3, b_4$  the complex solutions we conclude that  $\text{sign}(b_1b_2) = \text{sign}(\alpha^2 - 1)$ . Hence, there is a unique positive solution at  $-1 < \alpha < 1$ . Moreover  $b_1$  and  $b_2$  can change signal only if  $\alpha = \pm 1$ . Choosing arbitrarily  $\alpha = \pm 2$  we see that there is no positive solutions for  $\alpha = 2$  and there is two positive real solutions for  $\alpha = -2$ . Hence, we conclude that there is no branch of positive real solutions of  $R_1$  if  $\alpha > 1$ ; one branch if  $-1 < \alpha \leq 1$  and two branches if  $\alpha \leq -1$ . Squaring those branches and then reflecting it at the  $x$ -axis one can conclude statement (a). For more details about the nature of the roots of a polynomial of degree four see [52].

If the two branches  $\beta_{\pm}$  intersect each other, then we have a double positive real solution of  $R_1$  which requires  $D(\alpha) = 0$  and thus  $\alpha = -3.398\dots$ . Replacing this at  $R_1$  one can see that there is two complex conjugate solutions and a double positive real root and thus we have statement (b).

Knowing that  $R(\alpha, -\sqrt{-\alpha}) = 256 + 288\alpha^2 - 27\alpha^4$  one can calculate its roots and see that the unique root  $\alpha_0 \leq -1$  is given by  $\alpha_0 = -\frac{4}{3}\sqrt{3 + 2\sqrt{3}}$  and thus  $\mu_2 = (\alpha_0, -\sqrt{-\alpha_0})$  is the unique intersection between the sets  $\alpha + \beta^2 = 0$  and  $R(\alpha, \beta) = 0$ . The relative position of  $\mu_1, \mu_2$  and the parabola  $\alpha + \beta^2 = 0$  and the fact that  $\beta_{\pm}$  are the graphs of some continuous function implies that  $\mu_2 \in \beta_-$  and thus we have statement (c).  $\square$

Numerical computations shows that the branches  $-\beta_{\pm}$  of  $R(\alpha, \beta) = 0$  perturb the double roots  $x_0$  of  $p_2$  which do not satisfy  $x_0p_1(x_0) > 0$  and thus perturb the roots that are not related to the finite singularities of  $Y$  and thus can be ignored. Moreover, the negative branches  $\beta_{\pm}$  perturb the double roots  $x_0$  of  $p_2$  which do satisfy  $x_0p_1(x_0) > 0$  and thus perturb the roots that are related to the finite singularities. One can now draw the backbone of the bifurcation diagram of  $X_{23}$ , with  $a = 1$ , and thus obtain the solid lines of Figure 4.13.

**Proposition 4.20.** *Let  $(\alpha_0, \beta_0) \in \mathbb{R}^2$  such that  $\beta_0 = \beta_{\pm}(\alpha_0)$  (i.e. be a point in one of the branches  $\beta_{\pm}$ ), with  $\beta_0 < 0$ , and  $\gamma(t) = (t + \alpha_0, \beta_0)$ ,  $|t| < \varepsilon$ , be a transversal segment through  $\beta_{\pm}$ . Then a saddle-node bifurcation happens at  $\gamma(0)$  in such way that it vanishes as  $t$  increases.*

*Proof.* We know that at  $t = 0$  we have a double real root  $x_0$  of  $p_2$  which do satisfy  $x_0p_1(x_0) > 0$ . Therefore, it follows from statement (c) of Proposition 4.18 that  $q_0 = (x_0, f(x_0))$  is a non-hyperbolic finite singularity of  $X_{23}$ . Since  $\beta_0 < 0$  we know that the trace of  $DX_{23}(q_0)$  is not zero and thus  $DX_{23}(q_0)$  has only one eigenvalue equal zero. Hence,  $q_0$  is a non-hyperbolic saddle, a non-hyperbolic node or a saddle-node.

Computations shows that if  $t < 0$ , then the double root  $x_0$  splits in two simple real roots  $x_-, x_+$  satisfying  $x_{\pm}p_1(x_{\pm}) > 0$ . Hence, it follows from Proposition 4.18 that  $q_{\pm} = (x_{\pm}, f(x_{\pm}))$  are both hyperbolic finite singularities of  $X_{23}$ . The proof now follows from the fact that if  $t > 0$ , then the double real root  $x_0$  goes to the complex realm and thus the finite singularity  $q_0$  vanishes.  $\square$

Calculating the infinity of  $X_{23}$ , with  $a = 1$ , one will see that the only singularities are the origins of the charts  $U_1$  and  $U_2$ . While the origin of  $U_2$  is an unstable node, the local phase portrait at the origin of  $U_1$  is given by Figure 4.34. To prove this last claim, one must do a quasihomogeneous directional blow up at the direction  $x^+$  with  $(\alpha, \beta) = (3, 2)$  and then a quasihomogenous blow up with  $(\alpha, \beta) = (1, 4)$  at the unique singularity that will appear. Therefore, it follows from Theorem 2.14 that *the sum of the Poincaré indexes of all the finite singularities must always be equal to  $-1$ .*

Studying the system  $F = F(X_{23})$  one can conclude that  $X_{23}$  with  $a = 1$  is topologically equivalent at  $p = (-\lambda, 0)$  to the origin of

- (a)  $X_{12}$  when  $\alpha_0 + \beta_0^2 = 0$ ,  $|\beta_0| \geq 1$  and  $|\beta - \beta_0| < \varepsilon$ ;
- (b)  $X_{13}$  when  $\beta_0 = 0$ ,  $|\alpha_0| > 1$  and  $|\beta| < \varepsilon$ ;
- (c)  $X_{14}$  when  $\alpha_0 + \beta_0^2 = 0$ ,  $0 < |\beta_0| < 1$  and  $|\beta - \beta_0| < \varepsilon$ .

Although we have the local equivalence between  $p$  at  $X_{23}$  and the origin of  $X_{12}$ ,  $X_{13}$  or  $X_{14}$  we do not have the direction of the bifurcation, i.e. as  $\beta$  increases do  $\lambda$  increase or decrease? The following proposition set this up.

**Proposition 4.21.** *Let  $\lambda$  be the parameter of  $X_{12}$ ,  $X_{13}$  and  $X_{14}$  and  $(\alpha_0, \beta_0) \in \mathbb{R}^2$  fixed. The following statement holds.*

- (a) *If  $\alpha_0 + \beta_0^2 = 0$ ,  $|\beta_0| \geq 1$  and  $|\beta - \beta_0| < \varepsilon$ , then as  $|\beta|$  increases  $\lambda$  also increases;*
- (b) *If  $\beta_0 = 0$ ,  $|\alpha_0| > 1$  and  $|\beta| < \varepsilon$ , then as  $\beta$  increases  $\lambda$  increases if  $\alpha_0 > 1$  and decreases if  $\alpha_0 < -1$ ;*
- (c) *If  $\alpha_0 + \beta_0^2 = 0$ ,  $0 < |\beta_0| < 1$  and  $|\beta - \beta_0| < \varepsilon$ , then as  $\beta$  increases  $\lambda$  also increases.*

*Proof.* All statements follows from statement (a) of Proposition 4.17 and the fact that if  $\lambda > 0$ , then  $X_{12}$ ,  $X_{13}$  and  $X_{14}$  has a lonely center while if  $\lambda < 0$  it has a hyperbolic saddle.  $\square$

Finally we point out that at  $\beta = 0$  and  $\alpha < -1$  we have a center-focus problem at the singularity  $p_0 = \frac{1}{\sqrt{2}}(-\sqrt{-1-\alpha}, \sqrt{-1-\alpha})$  of  $Y$ . Translating this singularity to the origin one will obtain system  $Y_1$  given by

$$\begin{aligned} \dot{x} &= -(2 + \alpha)x + \alpha y - \frac{3}{\sqrt{2}}\sqrt{-1-\alpha}x^2 + \sqrt{2}\sqrt{-1-\alpha}xy - \frac{\sqrt{-1-\alpha}}{\sqrt{2}}y^2 \\ &\quad + x^3 + xy^2 \\ \dot{y} &= -\alpha x + (2 + \alpha)y - \frac{\sqrt{-1-\alpha}}{\sqrt{2}}x^2 + \sqrt{2}\sqrt{-1-\alpha}xy - \frac{3}{\sqrt{2}}\sqrt{-1-\alpha}y^2 \\ &\quad - x^2y - y^3. \end{aligned}$$

Knowing that system  $Y_1$  is  $\varphi$ -reversible with  $\varphi(x, y) = (-y, -x)$  we conclude that  $p_0$  is a center.

**Proposition 4.22.** *The bifurcation diagram of  $X_{23}$  with  $a = 1$  is the one given by Figures 4.13, 4.14 and 4.16.*

*Proof.* With an analysis of  $f(x_2)$  and  $x_2p_1(x_2)$  (see the functions defined at (4.2)) one can see that at region 1 of Figure 4.13 there is only one pair of singularities aside  $p = (-\lambda, 0)$  and at region 23 there is no other singularity other than  $p$ .

Using the same techniques as in the previous systems, and the information that we already have, one can conclude phase portraits 1, 2, 3, 4, 5, 13, 23, 31 and 32. Looking at 13 and 23 and knowing that at 22 we have the ‘‘closing’’ of the saddle-node bifurcation one can obtain 22. Again if we ‘‘close’’ the saddle-node of 5 we will obtain phase portrait

14. As we get down at  $\beta_-$  this saddle-node get away from  $p$  and phase portraits 15 and 16 rise and with them 6 and 7, respectively.

At the intersection of  $\beta_+$  and  $\beta = 0$  if get down at  $\beta_+$ , then a saddle-node will born at  $p$ . Calculations shows that near  $\beta = 0$  the direction of the unstable manifold of this saddle-node is very near the direction of the straight line  $y = x$  and thus we obtain 24. As we follow  $\beta_+$  the direction of the unstable manifolds approach the direction of  $y = 0$  and then we can see 25 and 26. Looking at 26 and 22 we can see 21. At 20 we know that the saddle-node at the right will open and then we obtain its phase portrait and thus we also obtain 11. From 20 and 32 and knowing the bifurcation that happens at  $p$  at  $\alpha + \beta^2 = 0$  we can conclude 19. Now we can conclude 17 and 18 if we look at 16 and 19. From it one can obtain 8, 9 and 10. From 11 and 13 we have 12. From 24 we obtain 27. From 26 we obtain 29. From 27 and 29 we obtain 28. Finally, from 29 and 31 we obtain 30.

We observe that it follows from the continuity that it is impossible that the curves defined by 8 and 6 intercept each other. On the other hand it is possible that the curves defined by 28 and 30 intercept each other, rising Figure 4.15, and thus region defined by 29 will be disconnected.  $\square$

Let  $X_{23a} = (P, Q)$  be  $X_{23}$  with  $a = 1$  and  $X_{23b}$  be  $X_{23}$  with  $a = -1$ . Observe that if we do the change of coordinates  $(x, y) \mapsto (-x, y)$  at  $X_{23b}$ , then we will obtain  $X_{23b} = (-P, Q)$ . Hence, a huge amount of information of  $X_{23a}$  can be carry on to  $X_{23b}$ . The most important ones are the following.

1. The relative position of the finite singularities are the same. Hence, the solid lines of Figure 4.13 are carried on to the bifurcation diagram of  $X_{23b}$ ;
2. The determinant of the Jacobian matrices at the finite singularities are the same except by a factor of  $-1$ . Therefore, if  $q$  is a saddle (focus/node) of  $X_{23a}$ , then it is a focus/node (saddle) of  $X_{23b}$ ;
3. If  $\beta(\alpha + \beta^2) \neq 0$ , then  $p = (-\beta, 0)$  is center (saddle) at  $X_{23a}$  if, and only if, it is a saddle (center) at  $X_{23b}$ .

With the same approach as the previous cases, mainly  $X_{23a}$ , one can conclude the following proposition.

**Proposition 4.23.** *The phase portrait of  $X_{23}$  with  $a = -1$  is the one given by Figures 4.17 and 4.18.*

#### 4.6 Systems $X_{24}$ and $X_{25}$

Let us remember that  $X_{24}$  is given by

$$\dot{x} = axy + \alpha y^3, \quad \dot{y} = \frac{\beta}{2} + \frac{1}{2}x + \frac{a}{2}y^2,$$

where  $a \in \{-1, 1\}$ . First we observe that if we replace  $a = -1$  and then do the change of variables

$$(x, y, \alpha, \beta) = (-x_1, -y_1, \alpha_1, -\beta_1),$$

then we will get the same system with  $a = 1$ . Therefore, from now on we will assume  $a = 1$ . In this system we point out that it is the unique system which the maximum degree depends on the parameters. Observe that the maximum degree is three if  $\alpha \neq 0$

and two if  $\alpha = 0$ . Therefore, one must do an analysis at each case. Here we only point out some information about the local phase portrait at the origin of chart  $U_1$  for  $\alpha = 1$  and  $\beta \neq 0$ . In this case the local phase portrait of the blow up is incomplete due the existence of two singularities with a unique eigenvalue (the radial one) equal zero. See Figure 4.35. Calculations shows that in this case a center manifold of the origin of chart  $U_1$  such that  $v < 0$ ,  $|v| < \varepsilon$ , is given by the graph of

$$v(u) = -u^2 - \frac{\beta}{2}u^4 + O(u^6).$$

This in addition with the fact that

$$\dot{v}|_{\alpha=1} = -uv(u^2 + v)$$

is enough to calculate the direction of the flow on the center manifold and thus to complete the blow up when  $\beta \neq 0$ . See Figure 4.36.

Let us remember that system  $X_{25b}$  is given by

$$\dot{x} = axy, \quad \dot{y} = \frac{\beta}{2} + \frac{\alpha}{2}x + \frac{\varepsilon}{2}x^2 + \frac{b}{2}y^2,$$

where  $ab > 0$ ,  $\varepsilon \in \{-3, 3\}$  and

$$\{(a \in \{-1, 1\} \text{ and } b \in \{-3, 3\}) \text{ or } (a \in \{-3, 3\} \text{ and } b \in \{-1, 1\})\}.$$

Here we observe that with the change of variables

$$(x, y, \alpha, \beta) \rightarrow (x_1, -y_1, -\alpha_1, -\beta_1)$$

it is enough to study only the four cases given by

- (a)  $a = 1$ ,  $b = 3$  and  $\varepsilon = 3$ ;
- (b)  $a = 1$ ,  $b = 3$  and  $\varepsilon = -3$ ;
- (c)  $a = 3$ ,  $b = 1$  and  $\varepsilon = 3$ ;
- (d)  $a = 3$ ,  $b = 1$  and  $\varepsilon = -3$ .

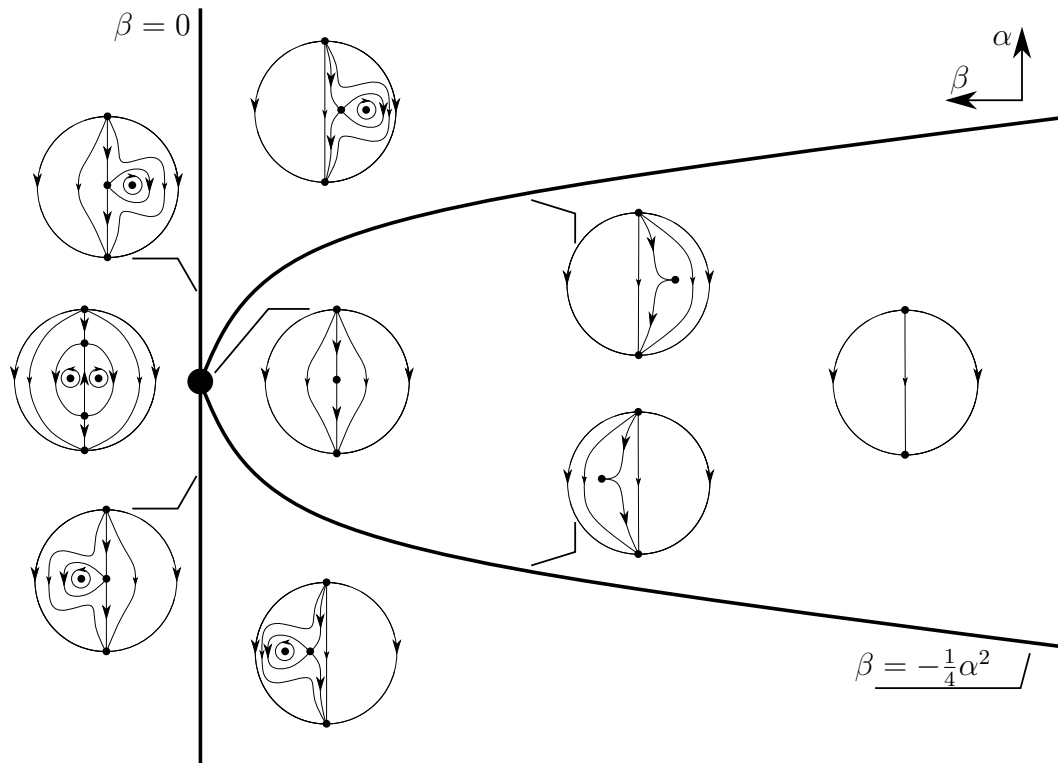


Figure 4.8: Bifurcation diagram of  $X_{25a}$  with  $a = -1$ . Figure source: made by the author.

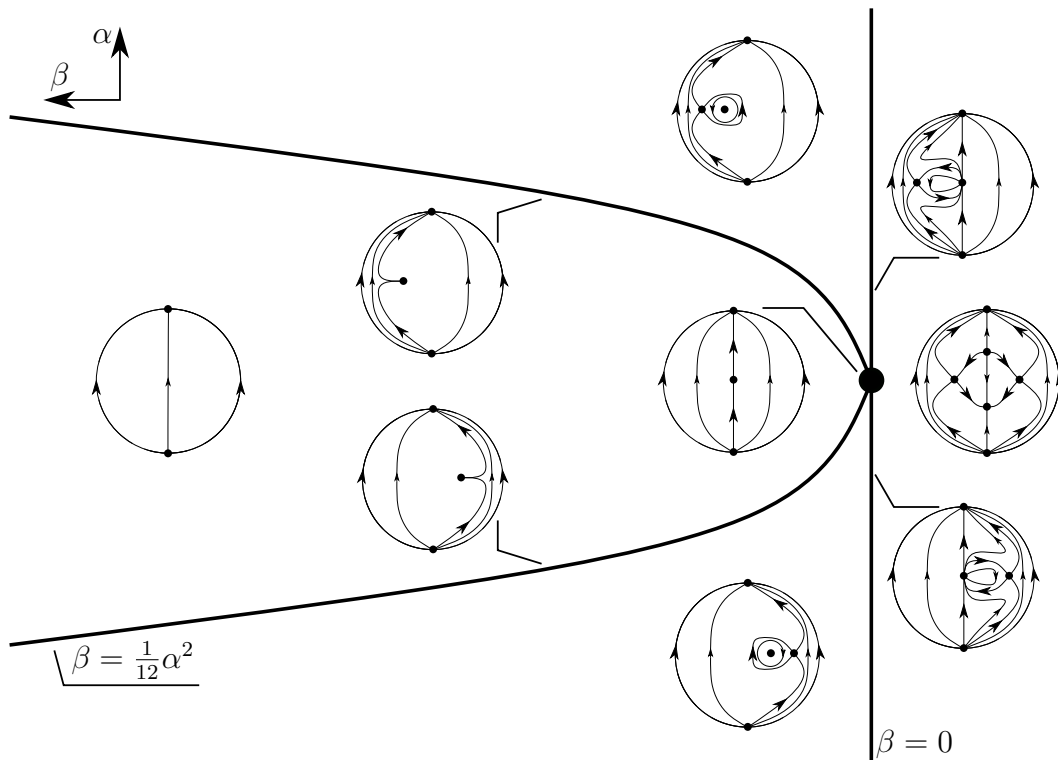


Figure 4.9: Bifurcation diagram of  $X_{25b}$  with  $(a, b, \varepsilon) = (1, 3, 3)$ . Figure source: made by the author.

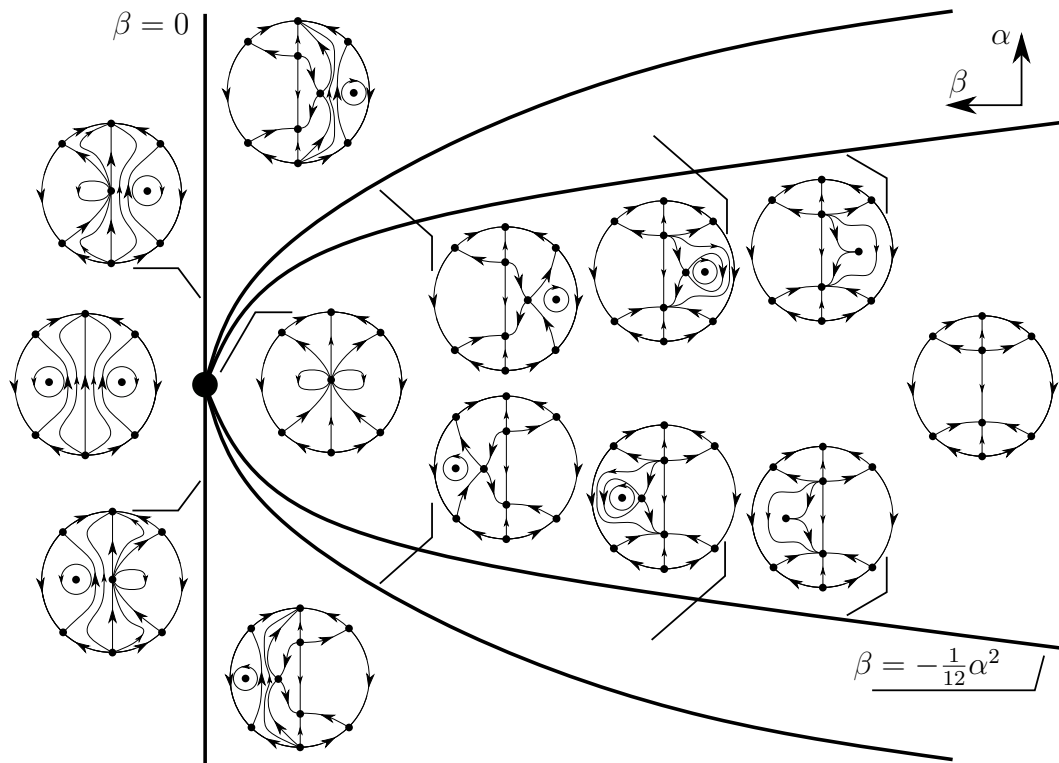


Figure 4.10: Bifurcation diagram of  $X_{25b}$  with  $(a, b, \varepsilon) = (1, 3, -3)$ . Figure source: made by the author.

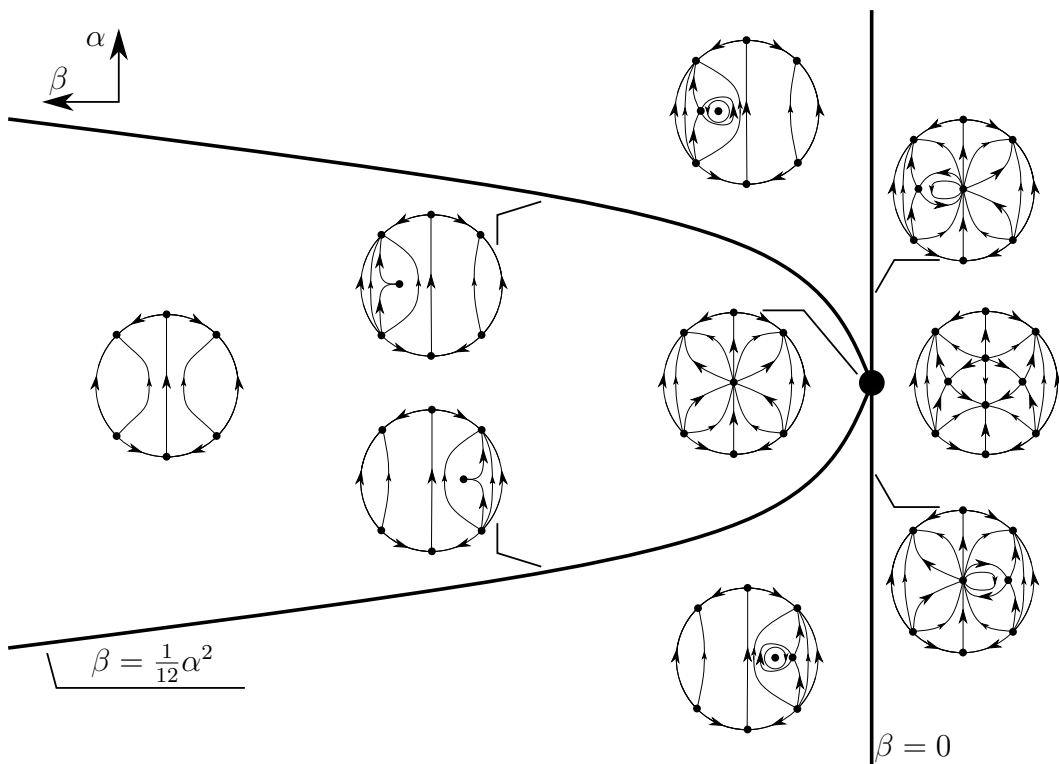


Figure 4.11: Bifurcation diagram of  $X_{25b}$  with  $(a, b, \varepsilon) = (3, 1, 3)$ . Figure source: made by the author.

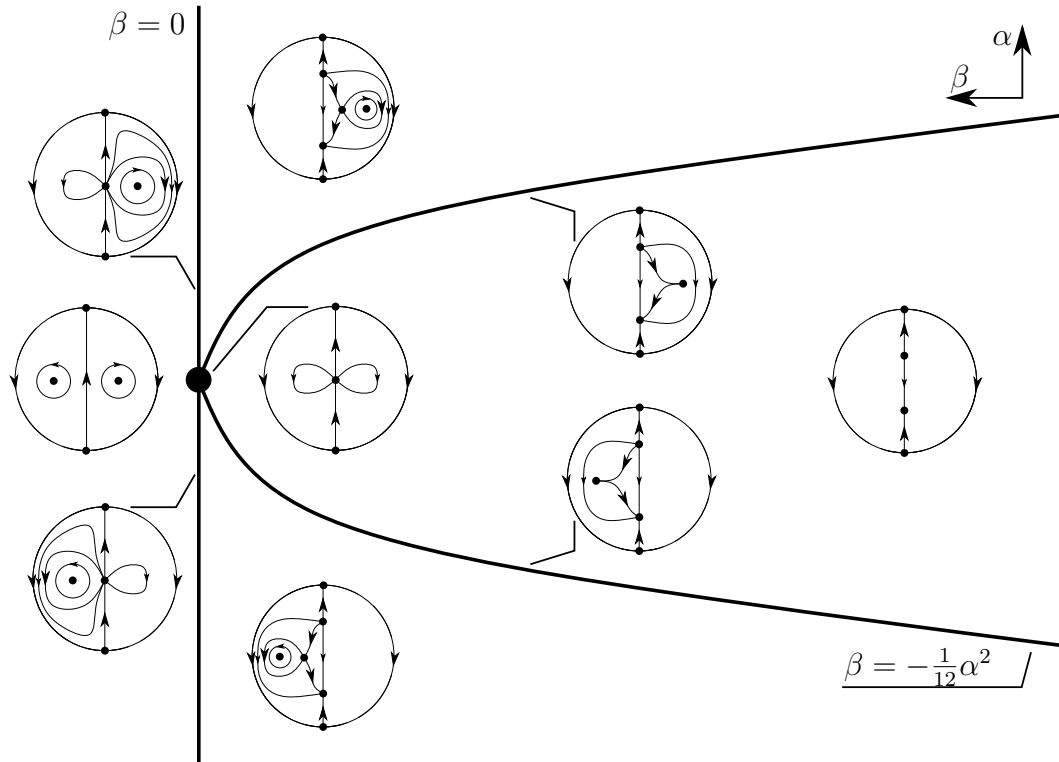


Figure 4.12: Bifurcation diagram of  $X_{25b}$  with  $(a, b, \varepsilon) = (3, 1, -3)$ . Figure source: made by the author.

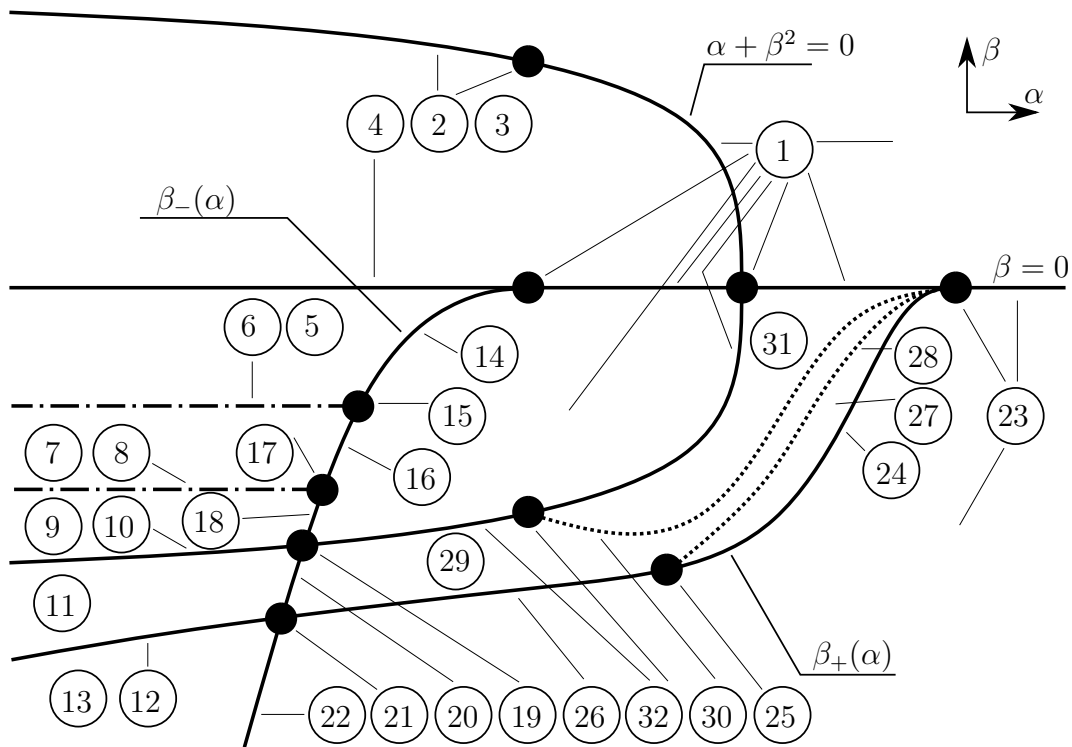


Figure 4.13: Bifurcation diagram of  $X_{23}$  with  $a = 1$ . We observe that it may be an intersection between 28 and 30. Figure source: made by the author.

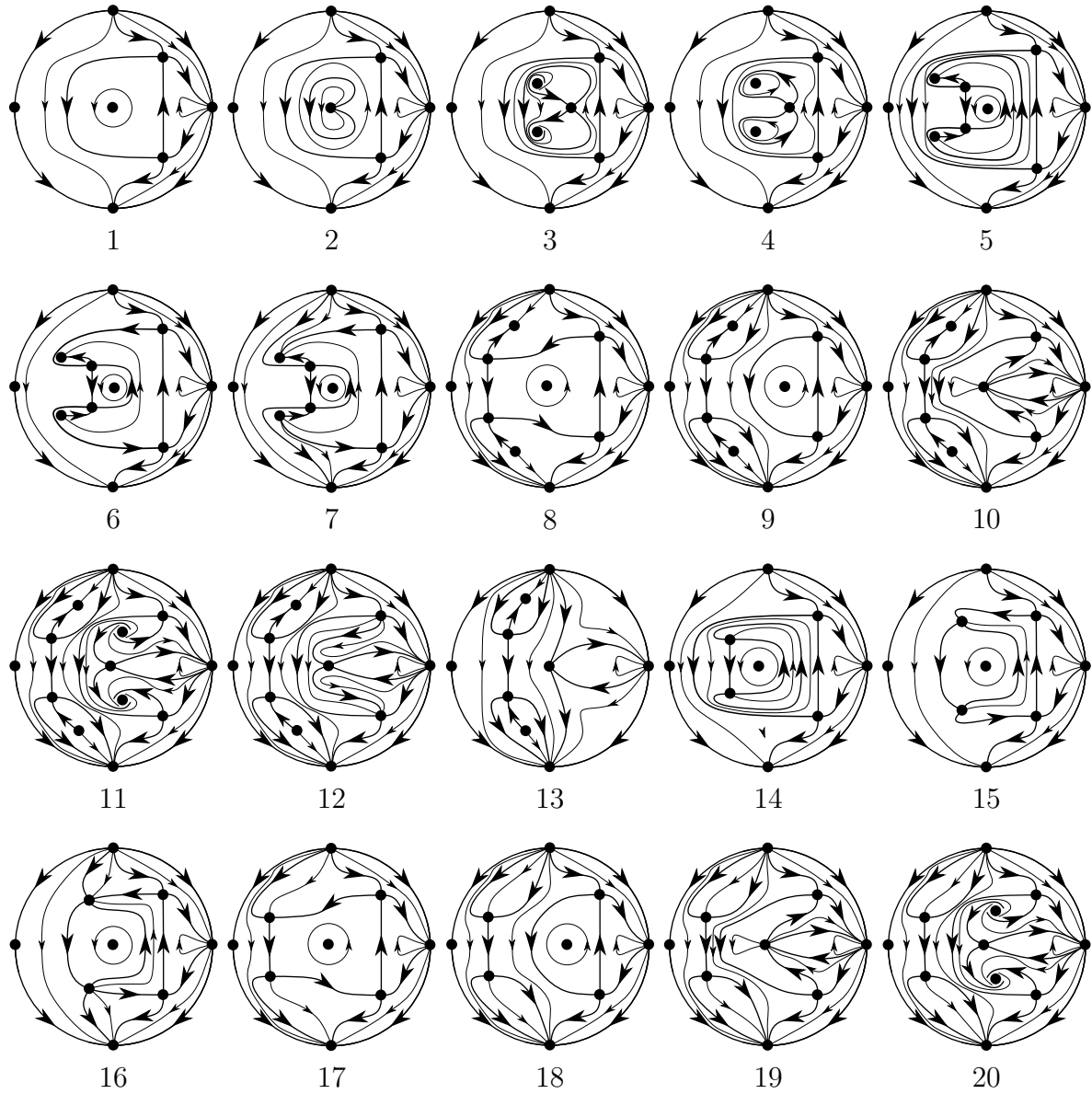


Figure 4.14: Phase portraits of  $X_{23a}$  with  $a = 1$ . Figure source: made by the author.

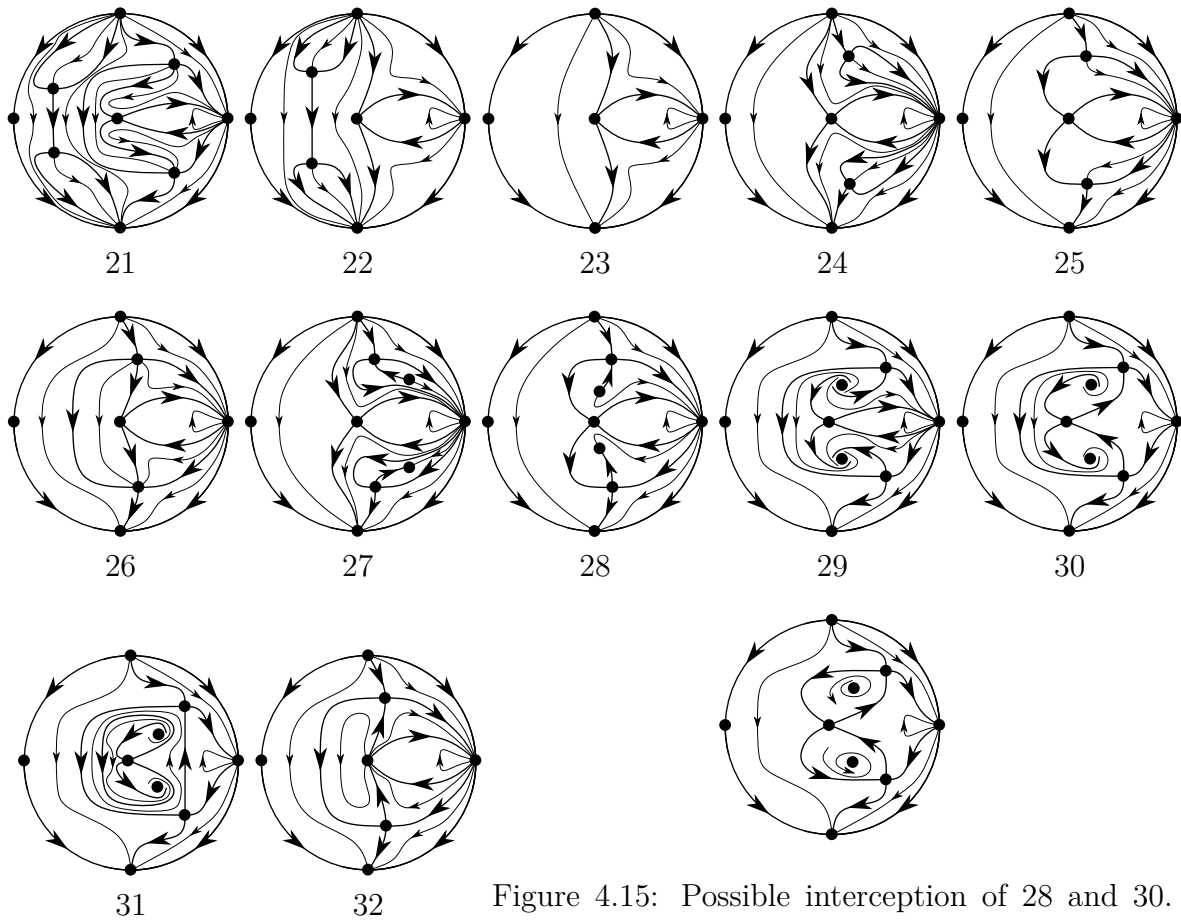


Figure 4.16: Phase portraits of  $X_{23a}$  with  $a = 1$ . Figure source: made by the author.

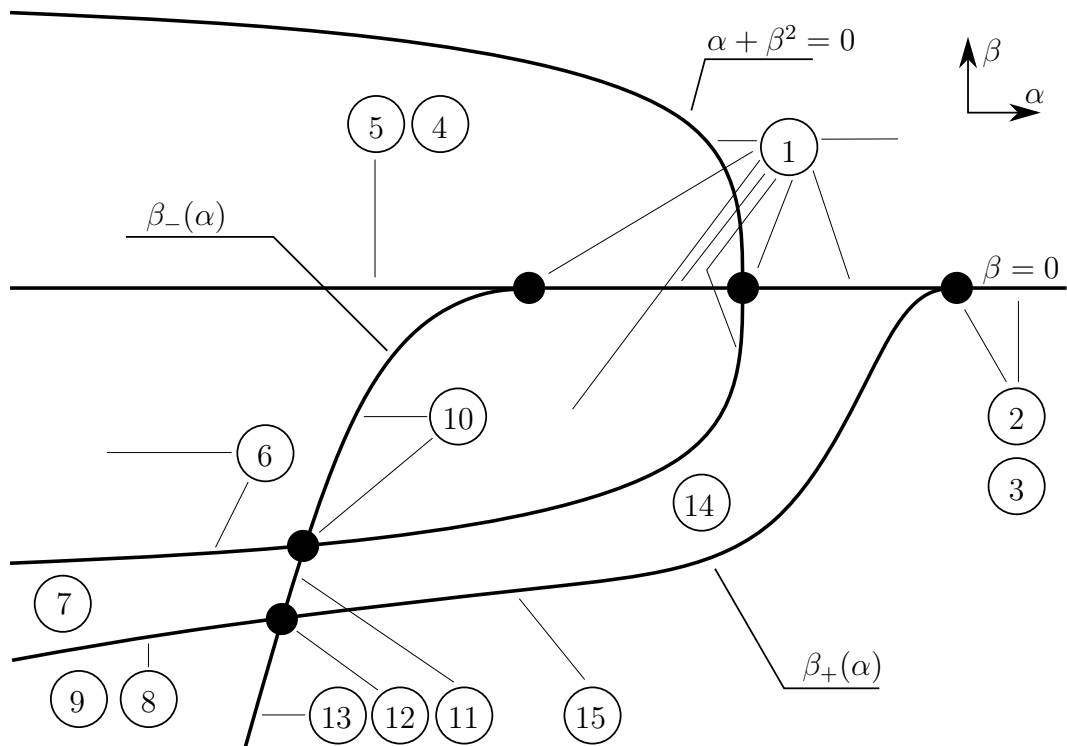


Figure 4.17: Bifurcation diagram of  $X_{23b}$  with  $a = -1$ . Figure source: made by the author.

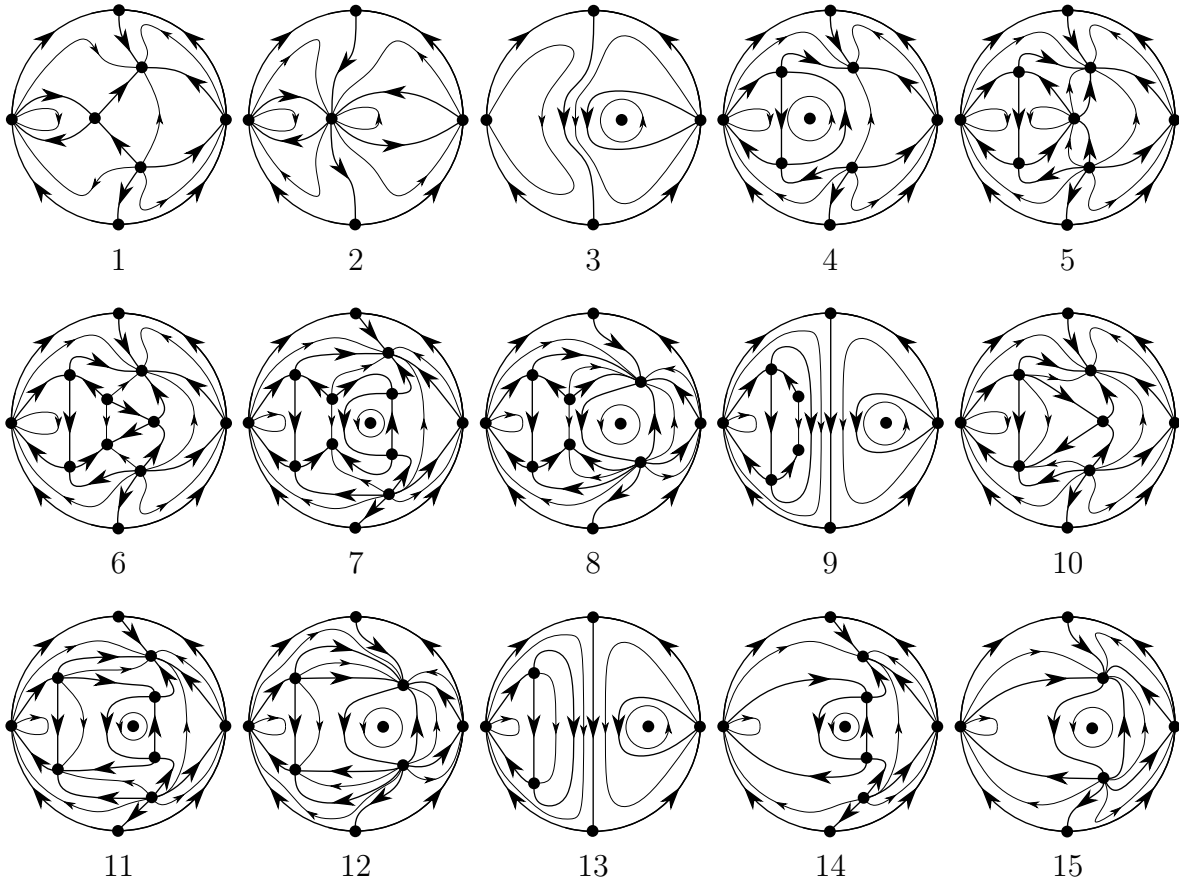


Figure 4.18: Phase portraits of  $X_{23}$  with  $a = -1$  and  $(x, y) \mapsto (-x, y)$ . Figure source: made by the author.

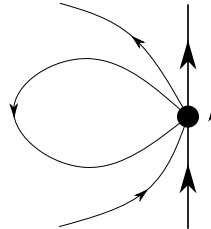


Figure 4.19: Local phase portrait of  $X_{12}$  at the origin where  $\lambda = 0$ . Figure source: made by the author.

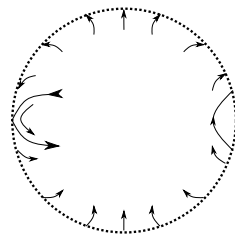


Figure 4.20: Local phase portrait of  $X_{12}$  at the regularized infinity. Figure source: made by the author.

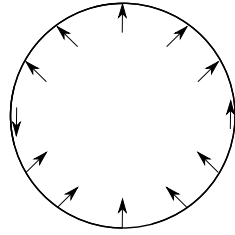


Figure 4.21: Unfinished local phase portrait of  $X_{12}$  at the regularized infinity. Figure source: made by the author.

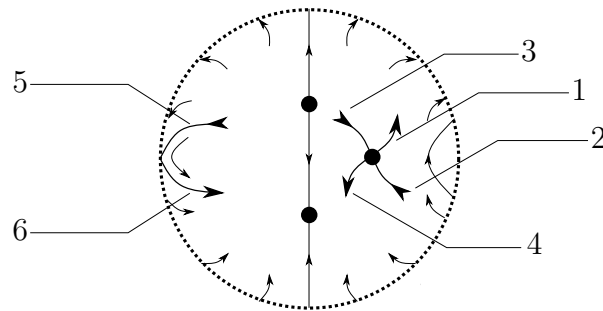


Figure 4.22: Local behavior of the phase portrait of  $X_{12}$  for  $\lambda < 0$ . Figure source: made by the author.

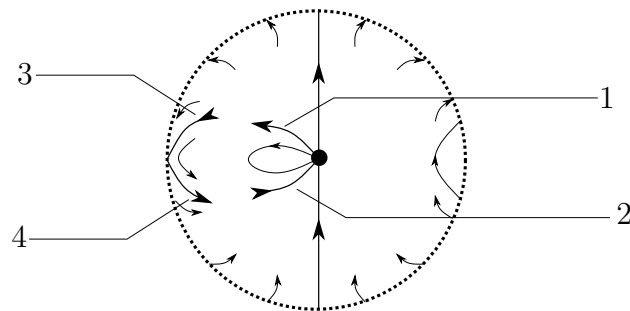


Figure 4.23: Local behavior of the phase portrait of  $X_{12}$  for  $\lambda = 0$ . Figure source: made by the author.

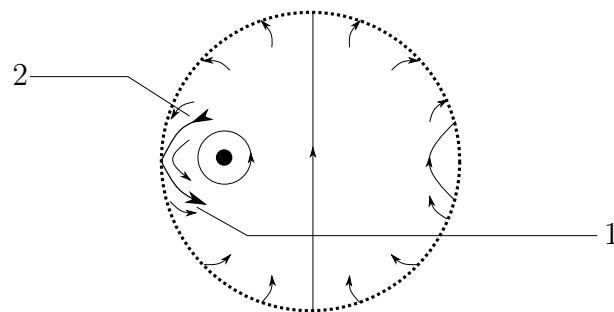


Figure 4.24: Local behavior of the phase portrait of  $X_{12}$  for  $\lambda > 0$ . Figure source: made by the author.



Figure 4.25: Local phase portrait of  $X_{21}$  at  $p_2 = p_3$  when  $D = 0$ . Figure source: made by the author.

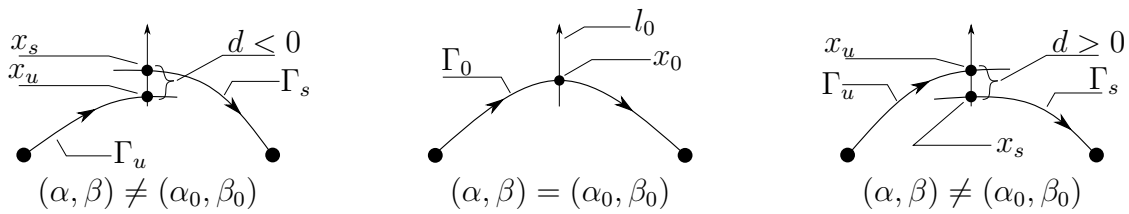


Figure 4.26: The displacement map  $d(\alpha, \beta)$  defined near  $(\alpha_0, \beta_0)$ . Figure source: made by the author.

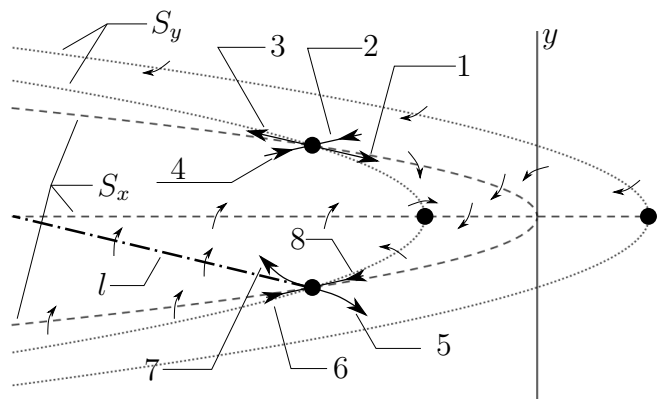


Figure 4.27: Illustration of the flow of  $X_{22a}$  with  $a = 1$  and  $\beta < -1$  at the sets  $S_x$  and  $S_y$ . Figure source: made by the author.

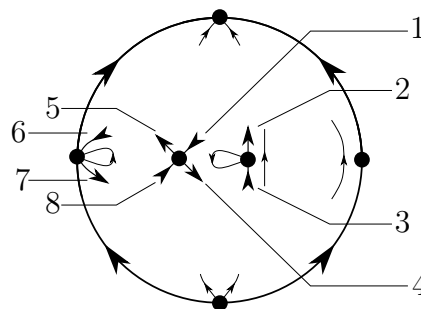


Figure 4.28: Unfinished phase portrait of  $X_{22a}$  with  $a = 1$ ,  $\beta = -1$  and  $\alpha \leq -16$ . Figure source: made by the author.

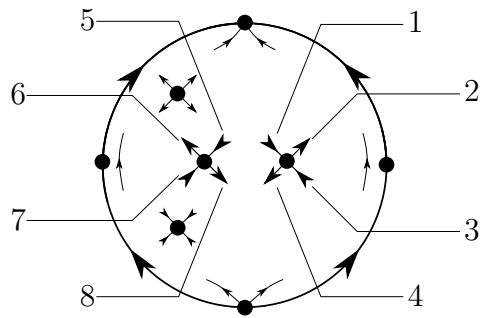


Figure 4.29: Unfinished phase portrait of  $X_{22a}$  with  $a = -1$ ,  $\alpha < 0$  and  $\beta \geq 1 + 2\sqrt{-\alpha}$ . Figure source: made by the author.

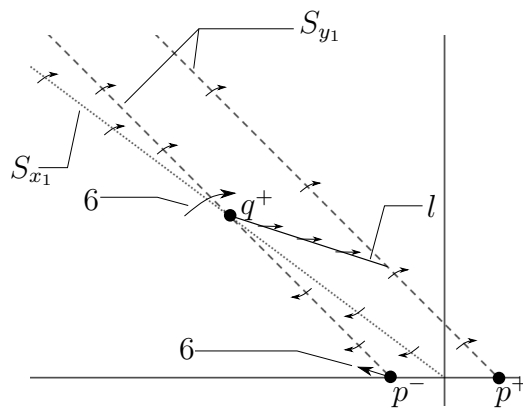


Figure 4.30: Illustration of the flow of  $X_1$  at the sets  $S_{x_1}$  and  $S_{y_1}$ . Figure source: made by the author.

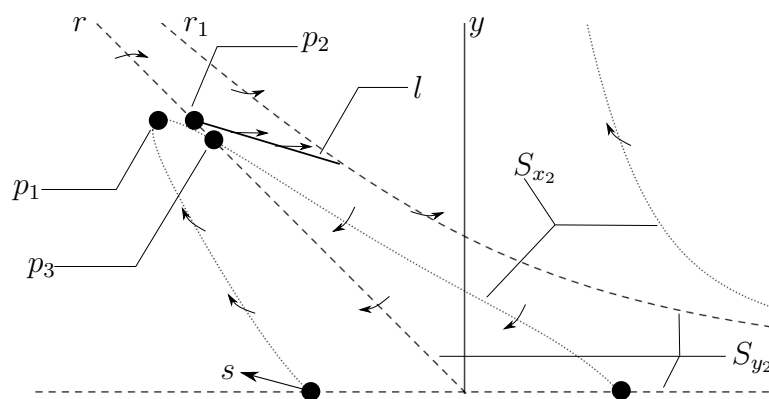


Figure 4.31: Illustration of the flow of  $X_2$  at the sets  $S_{x_2}$  and  $S_{y_2}$ . Figure source: made by the author.

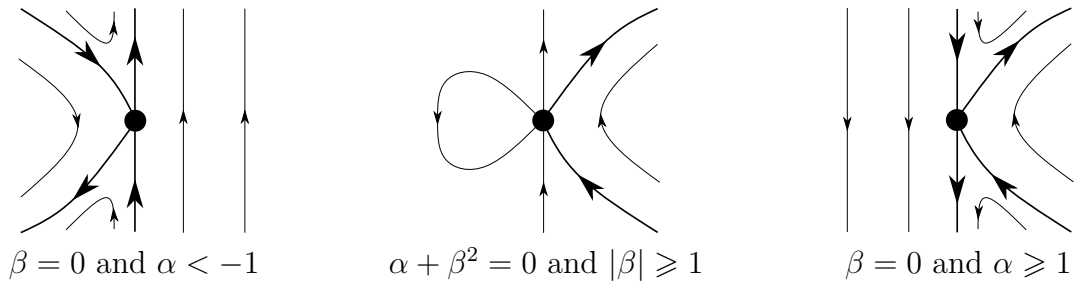


Figure 4.32: Specific local phase portraits of  $X_{23}$  at  $p$ . Figure source: made by the author.

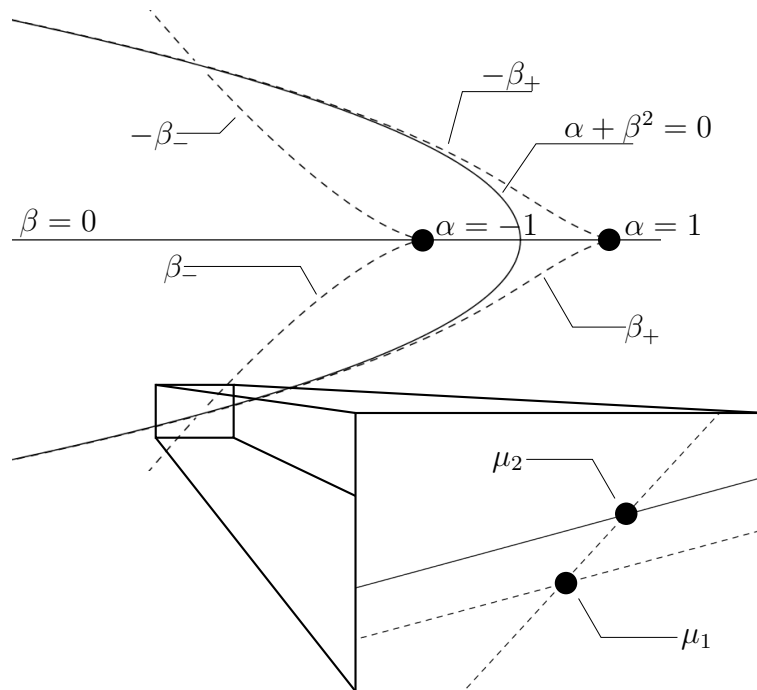


Figure 4.33: Plot of the sets  $R(\alpha, \beta) = 0$  and  $\alpha + \beta^2 = 0$ . Figure source: made by the author.

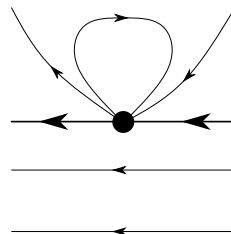


Figure 4.34: Local phase portrait of  $p(X_{23})$ , with  $a = 1$ , at the origin of  $U_1$ . Figure source: made by the author.

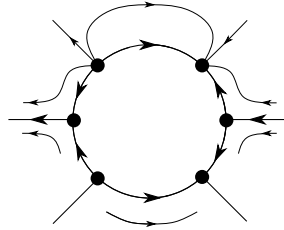


Figure 4.35: Unfinished blow up of the origin of chart  $U_1$  of  $X_{24}$  with  $\alpha = 1$ . Figure source: made by the author.



Figure 4.36: Local phase portrait of  $X_{24}$  the origin of chart  $U_1$  with  $a = 1$ ,  $\alpha = 1$  and  $\beta \neq 0$ . Figure source: made by the author.



## 5 THE FRIEDMANN-ROBERTSON-WALKER SYSTEM

### 5.1 Introduction and statement of the main results

We recall that this is a co-work with professors Claudio Buzzi and Jaume Llibre and it was already published, see [12]. In astrophysics the study of the dynamics of the universe is an area where the application of the techniques of the dynamical systems provide good results, mainly in galactic dynamics, see the articles [4, 37, 42, 43, 58] and the references cited therein.

Recently chaotic motion has been detected in the following simplified version of the Friedmann-Robertson-Walker Hamiltonian

$$H = \frac{1}{2}(p_Y^2 - p_X^2) + \frac{1}{2}(Y^2 - X^2) + \frac{b}{2}X^2Y^2, \quad (5.1)$$

introduced by Calzeta and Hasi in [15]. In fact this model is too simplified in order to be considered realistic, but it is interesting due to its simplicity and for showing the existence of chaos in cosmology, look for more details in [15]. Hawking [24] and Page [41] used analogous models to analyze the relation between the thermodynamic arrow of time and the cosmology.

A large number of potentials in galactic dynamics are of the form  $V(x^2, y^2)$ , see the article [51] and the previous mentioned articles on galactic dynamics. These potentials show a reflection symmetry with respect to both axes. Then in [29] was studied the following generalized version of the Calzeta–Hasi’s model

$$H = \frac{1}{2}(p_Y^2 - p_X^2) + \frac{1}{2}(Y^2 - X^2) + \frac{a}{4}X^4 + \frac{b}{2}X^2Y^2 + \frac{c}{4}Y^4. \quad (5.2)$$

Following the classical restricted circular three-body problem in which its dynamics is better understand in a rotating frame than in a sidereal frame of coordinates, our objective is to study the dynamics of the generalized version of the Calzeta–Hasi’s model (5.2) in rotating coordinates. More precisely, we consider the following generalized version of the Calzeta–Hasi’s model in rotating coordinates that itself is a simplified version of the Friedmann-Robertson-Walker Hamiltonian

$$H = \frac{1}{2}(y^2 - x^2 + p_y^2 - p_x^2) + \frac{1}{4}(ax^4 + 2bx^2y^2 + cy^4) - \omega(xp_y - yp_x), \quad (5.3)$$

where  $a, b, c, \omega \in \mathbb{R}$  and  $\omega > 0$ . Therefore, the corresponding Hamiltonian system is

$$\begin{aligned} \dot{x} &= \omega y - p_x, \\ \dot{y} &= -\omega x + p_y, \\ \dot{p}_x &= x + \omega p_y - ax^3 - bxy^2, \\ \dot{p}_y &= -y - \omega p_x - bx^2y - cy^3. \end{aligned} \quad (5.4)$$

In the qualitative theory of differential equations any orbit or trajectory is homeomorphic either to a straight line, or to a circle, or to a point. The equilibrium points are the orbits homeomorphic to a point and the periodic orbits are the ones homeomorphic to a circle. These two types of orbits are relevant in the study of the dynamics of a differential system, and usually their study is simpler than the study of the orbits homeomorphic to

straight lines, that in general exhibit more complicate dynamics. Therefore, in order to understand the dynamics of a differential system we must start analyzing its equilibrium points and its periodic solutions.

The objective of this chapter is to study analytically the periodic orbits of the Hamiltonian system (5.4) in each Hamiltonian level  $H = h$  varying  $h \in \mathbb{R}$ . For obtaining the results we shall use the averaging theory for computing periodic solutions. We shall give sufficient conditions on the parameters of the Hamiltonian system (5.4) implying the existence of continuous families of periodic orbits parameterized by  $h$ , and the expression of these families are provided explicitly up to first order in a small parameter.

Our main result is the following one.

**Theorem 5.1.** *In section 5.2 we provide sufficient conditions for the existence of twelve families of periodic orbits of the Hamiltonian system (5.4) parametrized by the values of the Hamiltonian (5.3). Six of these families only exist for positive values of the Hamiltonian, two only exist for negative values of the Hamiltonian, and the remaining four families can exist either for positive or negative values of the Hamiltonian depending on the values of the parameters  $a$ ,  $b$  and  $c$ . All these twelve families are born at the equilibrium point localized at the origin of coordinates of the Hamiltonian system (5.4).*

## 5.2 Proof of theorem 5.1

To prove Theorem 5.1 we apply the Averaging Theorem (see Section 2.7) to the Hamiltonian system (5.4). Generically the periodic orbits of a Hamiltonian system with more than one degree of freedom are on cylinders fulfilled of periodic orbits, see [1]. Therefore, we cannot apply Averaging Theorem directly to system (5.4), because the Jacobian will always be zero. Then we must apply Averaging Theorem at each Hamiltonian fixed level where the periodic orbits generically are isolated.

In order to apply Averaging Theorem we need a small parameter  $\varepsilon > 0$ . So in the Hamiltonian system (5.4) we scaling the variables as follows

$$(x, y, p_x, p_y) = \sqrt{\varepsilon}(X, Y, p_X, p_Y). \quad (5.5)$$

In these new variables system (5.4) becomes

$$\begin{aligned} \dot{X} &= \omega Y - p_X, \\ \dot{Y} &= -\omega X + p_Y, \\ \dot{p}_X &= X + \omega p_Y - \varepsilon(aX^3 + bXY^2), \\ \dot{p}_Y &= -Y - \omega p_X - \varepsilon(bX^2Y + cY^3). \end{aligned} \quad (5.6)$$

This system is again Hamiltonian with Hamiltonian

$$\frac{Y^2 - X^2 + p_Y^2 - p_X^2}{2} + \frac{\varepsilon(aX^4 + 2bX^2Y^2 + cY^4)}{4} - \omega(Xp_Y - Yp_X). \quad (5.7)$$

Therefore, for all  $\varepsilon \neq 0$  the original and the transformed systems (5.4) and (5.6) have essentially the same phase portrait. The linear part of system (5.6) at the origin of coordinates is

$$L = \begin{pmatrix} 0 & \omega & -1 & 0 \\ -\omega & 0 & 0 & 1 \\ 1 & 0 & 0 & \omega \\ 0 & -1 & -\omega & 0 \end{pmatrix}.$$

One can see that  $L$  has two eigenvalues of multiplicity two, given by  $\pm i\sqrt{1+\omega^2}$ . Therefore, we can apply a linear change of variables  $(X, Y, p_X, p_Y)$  to  $(u, v, p_u, p_v)$  such that the new system has the linear part

$$J = \begin{pmatrix} 0 & \sqrt{1+\omega^2} & 0 & 0 \\ -\sqrt{1+\omega^2} & 0 & 0 & 0 \\ 0 & 0 & 0 & \sqrt{1+\omega^2} \\ 0 & 0 & -\sqrt{1+\omega^2} & 0 \end{pmatrix}$$

at the origin of coordinates in the real Jordan normal form. A linear change of variables doing this is

$$X = u, \quad Y = \frac{p_u + \sqrt{1+\omega^2}v}{\omega}, \quad p_X = p_u, \quad p_Y = \frac{\sqrt{1+\omega^2}p_v - u}{\omega}.$$

Therefore, the new system becomes

$$\begin{aligned} \dot{u} &= \sqrt{1+\omega^2}v, \\ \dot{v} &= -\sqrt{1+\omega^2}u + \varepsilon \frac{a\omega^2u^3 + bu(p_u^2 + 2\sqrt{1+\omega^2}p_uv + (1+\omega^2)v^2)}{\omega^2\sqrt{1+\omega^2}}, \\ \dot{p}_u &= \sqrt{1+\omega^2}p_v - \varepsilon \left( au^3 + \frac{bu(p_u + \sqrt{1+\omega^2}v)^2}{\omega^2} \right), \\ \dot{p}_v &= -\sqrt{1+\omega^2}p_u - \varepsilon \frac{(p_u + \sqrt{1+\omega^2}v)(b\omega^2u^2 + c(p_u + \sqrt{1+\omega^2}v)^2)}{\omega^2\sqrt{1+\omega^2}}, \end{aligned} \tag{5.8}$$

and the old Hamiltonian becomes the first integral

$$\begin{aligned} &\frac{1+\omega^2}{2\omega^2} (u^2 + v^2 + p_u^2 + p_v^2 + 2\sqrt{1+\omega^2}(vp_u - up_v)) \\ &+ \varepsilon \frac{1}{4} \left( au^4 + \frac{2bu^2(p_u + \sqrt{1+\omega^2}v)^2}{\omega^2} + \frac{c(p_u + \sqrt{1+\omega^2}v)^4}{\omega^4} \right). \end{aligned} \tag{5.9}$$

Now we apply a generalized polar change of coordinates given by

$$u = r \cos \theta, \quad v = r \sin \theta, \quad p_u = \rho \cos(\theta + \phi), \quad p_v = \rho \sin(\theta + \phi).$$

We recall that this is a change of variables when  $r > 0$  and  $\rho > 0$ . Moreover, doing this change of variables, the angular variables  $\theta$  and  $\phi$  appear in the system. Later on the variable  $\theta$  will be used for obtaining the periodicity necessary for applying the averaging theory. After this change of variables the first integral writes

$$H_0 = \frac{1+\omega^2}{2\omega^2} (r^2 + \rho^2 - 2r\rho\sqrt{1+\omega^2}\sin \phi) + \varepsilon W_1, \tag{5.10}$$

where

$$\begin{aligned} W_1 &= \frac{1}{4} \left( ar^4 \cos^4 \theta + \frac{2b}{\omega^2} r^2 \cos^2 \theta W_2^2 + \frac{c}{\omega^4} W_2^4 \right), \\ W_2 &= \rho \cos(\theta + \phi) + r\sqrt{1+\omega^2} \sin \theta. \end{aligned}$$

In the new variables system (5.8) writes

$$\begin{aligned}
\dot{r} &= \varepsilon \frac{r \cos \theta \sin \theta}{\omega^2 \sqrt{1 + \omega^2}} W_3, \\
\dot{\theta} &= -\sqrt{1 + \omega^2} + \varepsilon \frac{\cos^2 \theta}{\omega^2 \sqrt{1 + \omega^2}} W_3, \\
\dot{\rho} &= -\varepsilon \left( r \cos \theta \cos(\theta + \phi) W_5 + \frac{1}{\sqrt{1 + \omega^2}} W_6 \right), \\
\dot{\phi} &= \varepsilon \left( \frac{r \cos \theta}{\rho} W_7 - \frac{\cos^2 \theta}{\omega^2 \sqrt{1 + \omega^2}} W_3 - \frac{\cos(\theta + \phi)}{\rho \sqrt{1 + \omega^2}} W_8 \right),
\end{aligned} \tag{5.11}$$

where

$$\begin{aligned}
W_3 &= b\rho^2 \cos^2(\theta + \phi) + a\omega^2 r^2 \cos^2 \theta + b r \sin \theta W_4, \\
W_4 &= 2\rho \sqrt{1 + \omega^2} \cos(\theta + \phi) + r(1 + \omega^2) \sin \theta, \\
W_5 &= ar^2 \cos^2 \theta + \frac{b}{\omega^2} W_2^2, \\
W_6 &= W_2 \left( br^2 \cos^2 \theta + \frac{c}{\omega^2} W_2^2 \right) \sin(\theta + \phi), \\
W_7 &= \left( ar^2 \cos^2 \theta + \frac{b}{\omega^2} W_2^2 \right) \sin(\theta + \phi), \\
W_8 &= W_2 \left( br^2 \cos^2 \theta + \frac{c}{\omega^2} W_2^2 \right).
\end{aligned}$$

In order to apply the averaging theory we take  $\theta$  as the new independent variable, and denote by a prime the derivative with respect to  $\theta$ . With this change of independent variable system (5.11) goes over to

$$\begin{aligned}
r' &= -\varepsilon \frac{r \cos \theta \sin \theta}{\omega^2(1 + \omega^2)} W_3 + O(\varepsilon^2), \\
\rho' &= \frac{\varepsilon}{\sqrt{1 + \omega^2}} \left( r \cos \theta \cos(\theta + \phi) W_5 + \frac{1}{\sqrt{1 + \omega^2}} W_6 \right) + O(\varepsilon^2), \\
\phi' &= \frac{-\varepsilon}{\sqrt{1 + \omega^2}} \left( \frac{r \cos \theta}{\rho} W_7 - \frac{\cos^2 \theta}{\omega^2 \sqrt{1 + \omega^2}} W_3 - \frac{\cos(\theta + \phi)}{\rho \sqrt{1 + \omega^2}} W_8 \right) + O(\varepsilon^2).
\end{aligned} \tag{5.12}$$

This system has only three equations because we do not need the  $\dot{\theta}$  equation of (5.11). Observe that system (5.12) is  $2\pi$ -periodic in the variable  $\theta$ . To apply Averaging Theorem we must fix the value of the first integral at  $h \in \mathbb{R}$ . By solving equation (5.10) in  $\rho$  we obtain

$$\rho = r\sqrt{1 + \omega^2} \sin \phi + \sqrt{\frac{2h\omega^2 - r^2(1 + \omega^2) + r^2(1 + \omega^2)^2 \sin^2 \phi}{1 + \omega^2}} + O(\varepsilon).$$

Substituting  $\rho$  into equations (5.12) we obtain the two differential equations

$$\begin{aligned}
r' &= -\varepsilon \frac{r \cos \theta \sin \theta}{\omega^2(1 + \omega^2)} \overline{W}_3 + O(\varepsilon^2), \\
\phi' &= \frac{-\varepsilon}{\sqrt{1 + \omega^2}} \left( \frac{r \cos \theta}{\rho} \overline{W}_7 - \frac{\cos^2 \theta}{\omega^2 \sqrt{1 + \omega^2}} \overline{W}_3 - \frac{\cos(\theta + \phi)}{\rho \sqrt{1 + \omega^2}} \overline{W}_8 \right) + O(\varepsilon^2),
\end{aligned} \tag{5.13}$$

where  $\overline{W}_i = W_i(\theta, r, \rho(r, \phi), \phi)$  with

$$\rho(r, \phi) = r\sqrt{1 + \omega^2} \sin \phi + \sqrt{\frac{2h\omega^2 - r^2(1 + \omega^2) + r^2(1 + \omega^2)^2 \sin^2 \phi}{1 + \omega^2}}. \quad (5.14)$$

We observe that in order to apply the first order averaging theory it is not necessary to have information about the terms in  $O(\varepsilon^2)$ .

One can now see that system (5.13) satisfies the assumptions of Averaging Theorem, and it has the form (2.3) with  $T = \pi$  and  $F = (F_1, F_2)$  analytic where

$$F_1 = -\frac{r \cos \theta \sin \theta}{\omega^2(1 + \omega^2)} \overline{W}_3,$$

$$F_2 = -\frac{1}{\sqrt{1 + \omega^2}} \left( \frac{r \cos \theta}{\rho} \overline{W}_7 - \frac{\cos^2 \theta}{\omega^2 \sqrt{1 + \omega^2}} \overline{W}_3 - \frac{\cos(\theta + \phi)}{\rho \sqrt{1 + \omega^2}} \overline{W}_8 \right).$$

The averaging function of first order is

$$f(r, \phi) = (f_1(r, \phi), f_2(r, \phi)) = \frac{1}{\pi} \int_0^\pi (F_1(\theta, r, \phi), F_2(\theta, r, \phi)) d\theta,$$

becomes

$$f_1(r, \phi) = \frac{br \cos \phi \rho(r, \phi) (\sin \phi \rho(r, \phi) - r\sqrt{1 + \omega^2})}{4\omega^2(1 + \omega^2)},$$

$$f_2(r, \phi) = -\frac{Ar^3 \sin \phi + Br^2 \rho(r, \phi) + Cr \sin \phi \rho(r, \phi)^2 + D\rho(r, \phi)^3}{8\omega^2 \sqrt{1 + \omega^2} \rho(r, \phi)}, \quad (5.15)$$

where

$$A = (1 + \omega^2) (b + 2b\omega^2 + 3(c + (a + c)\omega^2)),$$

$$B = -\sqrt{1 + \omega^2} (b + 6c + 3(a + b + 2c)\omega^2 - (2b + 3c + (b + 3c)\omega^2) \cos(2\phi)),$$

$$C = 3(1 + \omega^2)(b + 3c),$$

$$D = -\sqrt{1 + \omega^2} (2b + 3c + b \cos(2\phi)).$$

According with Averaging Theorem we must find the zeros  $(r_0, \phi_0)$  of the function  $f = (f_1, f_2)$  and check that the Jacobian determinant of  $f$  at these points is not zero.

From  $f_1(r, \phi) = 0$  we obtain  $r = r(\phi)$ , and in order that  $\rho(r(\phi), \phi) \neq 0$  (otherwise  $f_2(r, \phi)$  is not defined), we get that

$$r(\phi) = \begin{cases} R_0 & \text{with } h > 0, \\ R_1 & \text{with } h > 0 \text{ and } \sin \phi > 0, \\ R_2(\phi) & \text{with } h(1 + \omega^2 - (1 + 2\omega^2) \sin^2 \phi) > 0, \end{cases}$$

where

$$R_0 = 0, \quad R_1 = \sqrt{\frac{2h\omega^2}{1 + \omega^2}}, \quad R_2(\phi) = \sqrt{\frac{2h\omega^2}{(1 + \omega^2)(1 + \omega^2 - (1 + 2\omega^2) \sin^2 \phi)}} \sin \phi.$$

Substituting  $r = R_0$  into  $f_2(r, \phi) = 0$ , and solving with respect to  $\phi$  we obtain the following two zeros of the averaged function  $f(r, \phi)$

$$(r_1, \phi_1) = \left( 0, \arccos \sqrt{-\frac{b+3c}{2b}} \right),$$

$$(r_2, \phi_2) = \left( 0, -\arccos \sqrt{-\frac{b+3c}{2b}} \right).$$

Since the value of

$$\rho(r_i, \phi_i) = \frac{\omega \sqrt{2h(\omega^2 + 1)}}{1 + \omega^2} \quad \text{for } i = 1, 2,$$

and the determinant of the Jacobian matrix of  $f$  at these two zeros is

$$\frac{3h^2(b+c)(b+3c)}{8(1+\omega^2)^4},$$

it follows from the Averaging Theorem that if

$$h > 0, \quad 0 < -\frac{b+3c}{2b} \leq 1, \quad \text{and } (b+c)(b+3c) \neq 0,$$

then the zeros  $(r_i, \phi_i)$  provide two periodic solutions of the differential system (5.13), and consequently of the Hamiltonian system (5.4) in every level  $H = h > 0$ .

Substituting  $r = R_1$  into  $f_2(r, \phi) = 0$ , and solving with respect to  $\phi$  we obtain the following six zeros of the averaged function  $f(r, \phi)$

$$(r_3, \phi_3) = \left( \sqrt{\frac{2h\omega^2}{1+\omega^2}}, \pi \right),$$

$$(r_4, \phi_4) = \left( \sqrt{\frac{2h\omega^2}{1+\omega^2}}, 0 \right),$$

$$(r_5, \phi_5) = \left( \sqrt{\frac{2h\omega^2}{1+\omega^2}}, -\arccos \sqrt{\frac{b(4\omega^2+3) - \sqrt{b(12(\omega^2+1)(\omega^2(a+c)+c)+b(24\omega^4+36\omega^2+13))}}{8b(1+\omega^2)}} \right),$$

$$(r_6, \phi_6) = \left( \sqrt{\frac{2h\omega^2}{1+\omega^2}}, \arccos \sqrt{\frac{b(4\omega^2+3) - \sqrt{b(12(\omega^2+1)(\omega^2(a+c)+c)+b(24\omega^4+36\omega^2+13))}}{8b(1+\omega^2)}} \right),$$

$$(r_7, \phi_7) = \left( \sqrt{\frac{2h\omega^2}{1+\omega^2}}, -\arccos \sqrt{\frac{b(4\omega^2+3) + \sqrt{b(12(\omega^2+1)(\omega^2(a+c)+c)+b(24\omega^4+36\omega^2+13))}}{8b(1+\omega^2)}} \right),$$

$$(r_8, \phi_8) = \left( \sqrt{\frac{2h\omega^2}{1+\omega^2}}, \arccos \sqrt{\frac{b(4\omega^2+3) + \sqrt{b(12(\omega^2+1)(\omega^2(a+c)+c)+b(24\omega^4+36\omega^2+13))}}{8b(1+\omega^2)}} \right).$$

Since the value of

$$\rho(r_3, \phi_3) = \rho(r_4, \phi_4) = 0,$$

$$\rho(r_5, \phi_5) = \rho(r_6, \phi_6) = \omega \sqrt{\frac{h(b(4\omega^2+5) + \sqrt{b(12(\omega^2+1)(\omega^2(a+c)+c)+b(24\omega^4+36\omega^2+13))}}{b(1+\omega^2)}},$$

$$\rho(r_7, \phi_7) = \rho(r_8, \phi_8) = \omega \sqrt{\frac{h(b(4\omega^2+5) - \sqrt{b(12(\omega^2+1)(\omega^2(a+c)+c)+b(24\omega^4+36\omega^2+13))}}{b(1+\omega^2)}}.$$

Since  $\rho(r_i, \phi_i)$  cannot be zero, otherwise  $f_2$  is not defined, for the zeros  $\rho(r_i, \phi_i)$  with  $i = 3, 4$  the averaging theory does not provide any information about if these zeros produce or not periodic solutions of the differential system (5.13).

The determinant  $D(r, \phi)$  of the Jacobian matrix of  $f$  at the other four zeros is

$$D(r_5, \phi_5) = D(r_6, \phi_6) = \frac{h^{7/2}\omega^7(\omega^2+1)^6 \sin(2\phi)(bF+eD)(2A\sqrt{h}\omega(\omega^2+1)-\sqrt{2}BC)}{8b^2},$$

$$D(r_7, \phi_7) = D(r_8, \phi_8) = \frac{h^{7/2}\omega^7(\omega^2+1)^6 \sin(2\phi)(bF-eD)(2A\sqrt{h}\omega(\omega^2+1)-\sqrt{2}BC)}{8b^2},$$

where

$$A = \sqrt{\frac{-2\omega^4(3a+2b+3c) - 2\omega^2(3a+b+6c) + b - 6c - D}{b(\omega^2+1)^2}},$$

$$B = \sqrt{\frac{h\omega^2(1+\omega^2)(4b\omega^2+5b+D)}{b}},$$

$$C = \sqrt{\frac{b(4\omega^2+3) - D}{b(1+\omega^2)}},$$

$$D = \sqrt{b(12(\omega^2+1)(\omega^2(a+c)+c) + b(24\omega^4+36\omega^2+13))},$$

$$E = 3\omega^4(15ab - 9ac + 34b^2 - 15bc - 9c^2) + \omega^2(42ab - 27ac + 145b^2 - 66bc - 54c^2) + 9(b-c)(5b+3c),$$

$$F = 18\omega^6(3a+14b-9c)(a+2b+c) + \omega^4(54a^2+579ab-225ac+1082b^2 - 147bc - 495c^2) + 3\omega^2(72ab-39ac+247b^2-24bc-168c^2) + 3(b-c)(55b+57c).$$

From Averaging Theorem if for  $i = 5, 6$  we have that

$$0 \leq \frac{b(4\omega^2+3) - \sqrt{b(12(\omega^2+1)(\omega^2(a+c)+c) + b(24\omega^4+36\omega^2+13))}}{b(1+\omega^2)} \leq 1,$$

$$\frac{b(4\omega^2+5) + \sqrt{b(12(\omega^2+1)(\omega^2(a+c)+c) + b(24\omega^4+36\omega^2+13))}}{b(1+\omega^2)} \geq 0,$$

$$h > 0, \quad \sin \phi_i > 0, \quad \rho(r_i, \phi_i) > 0 \quad \text{and} \quad D(r_i, \phi_i) \neq 0,$$

then these two zeros  $(r_i, \phi_i)$  provide two periodic solutions of the differential system (5.13), and consequently of the Hamiltonian system (5.4) in every level  $H = h > 0$ .

From Averaging Theorem if for  $i = 7, 8$  we have that

$$0 \leq \frac{b(4\omega^2+3) + \sqrt{b(12(\omega^2+1)(\omega^2(a+c)+c) + b(24\omega^4+36\omega^2+13))}}{b(1+\omega^2)} \leq 1,$$

$$\frac{b(4\omega^2+5) - \sqrt{b(12(\omega^2+1)(\omega^2(a+c)+c) + b(24\omega^4+36\omega^2+13))}}{b(1+\omega^2)} \geq 0,$$

$$h > 0, \quad \sin \phi_i > 0, \quad \rho(r_i, \phi_i) > 0 \quad \text{and} \quad D(r_i, \phi_i) \neq 0,$$

then these two zeros  $(r_i, \phi_i)$  provide two periodic solutions of the differential system (5.13), and consequently of the Hamiltonian system (5.4) in every level  $H = h > 0$ .

Substituting  $r = R_2$  into  $f_2(r, \phi) = 0$ , and solving with respect to  $\phi$  we obtain the following

$$\phi = \pm \arccos \left( \sqrt{\frac{-(a+b)\omega^2}{b+c+(c-a)\omega^2}} \right).$$

Substituting these values of  $\phi$  into  $R_2$  we get the following two zeros of the averaged function  $f(r, \phi)$

$$(r_9, \phi_9) = \left( \sqrt{\frac{-2(b+c)h}{(a+2b+c)(1+\omega^2)}}, -\arccos \sqrt{\frac{-(a+b)\omega^2}{b+c+(c-a)\omega^2}} \right),$$

$$(r_{10}, \phi_{10}) = \left( \sqrt{\frac{-2(b+c)h}{(a+2b+c)(1+\omega^2)}}, \arccos \sqrt{\frac{-(a+b)\omega^2}{b+c+(c-a)\omega^2}} \right).$$

We cannot guarantee that these last two solutions are all the solutions for  $r = R_2$ , these are the ones that we can obtain explicitly.

Since the value of

$$\rho(r_i, \phi_i) = \left( \omega^2|a+b| + (1+\omega^2)(b+c) \right) \sqrt{\frac{-2h}{(1+\omega^2)(a+2b+c)(b+c+(c-a)\omega^2)}},$$

for  $i = 9, 10$ , and we denote the determinant of the Jacobian matrix of  $f$  at these two zeros by  $D(r_i, \phi_i)$ , we do not give its huge expression here.

It follows from the Averaging Theorem that if

$$0 \leq \frac{-(a+b)\omega^2}{b+c+(c-a)\omega^2} \leq 1, \quad \frac{-2(b+c)h}{a+2b+c} > 0, \quad \rho(r_i, \phi_i) > 0, \quad \text{and} \quad D(r_i, \phi_i) \neq 0,$$

then the zeros  $(r_i, \phi_i)$  for  $i = 9, 10$  provide two periodic solutions of the differential system (5.13), and consequently of the Hamiltonian system (5.4) in every level  $H = h$ .

From  $f_1(r, \phi) = 0$  we obtain  $\phi = \phi(r)$ , and in order that  $\rho(r(\phi), \phi) \neq 0$  (otherwise  $f_2(r, \phi)$  is not defined), we get that

$$\phi(r) = \begin{cases} \Phi_1 & \text{with } h < 0, \\ \Phi_2(\phi) & \text{with } \frac{(b+3c)h}{(3a+2b+3c)} < 0, \end{cases}$$

where

$$\Phi_1 = \pm \frac{\pi}{2}, \quad \Phi_2 = \pm \arcsin \left( \frac{r(1+\omega^2)}{\sqrt{r^2(1+3\omega^2+2\omega^4)+2h\omega^2}} \right).$$

Substituting  $\phi = \Phi_1$  into  $f_2(r, \phi) = 0$ , and solving with respect to  $r$  we obtain the following four zeros of the averaged function  $f(r, \phi)$

$$(r_{11}, \phi_{11}) = \left( \sqrt{-\frac{2h}{1+\omega^2}}, -\frac{\pi}{2} \right),$$

$$(r_{12}, \phi_{12}) = \left( \sqrt{-\frac{2h}{1+\omega^2}}, \frac{\pi}{2} \right),$$

$$(r_{13}, \phi_{13}) = \left( \sqrt{-\frac{2(b+3c)h}{(3a+2b+3c)(1+\omega^2)}}, -\frac{\pi}{2} \right),$$

$$(r_{14}, \phi_{14}) = \left( \sqrt{-\frac{2(b+3c)h}{(3a+2b+3c)(1+\omega^2)}}, \frac{\pi}{2} \right).$$

Since the value of

$$\begin{aligned}\rho(r_i, \phi_i) &= \sqrt{-2h} \quad \text{for } i = 11, 12, \\ \rho(r_{13}, \phi_{13}) &= \sqrt{\frac{2h(3a+b)\omega^2}{(1+\omega^2)(3a+2b+3c)}} + \sqrt{-\frac{2h(b+3c)}{3a+2b+3c}}, \\ \rho(r_{14}, \phi_{14}) &= \sqrt{\frac{2h(3a+b)\omega^2}{(1+\omega^2)(3a+2b+3c)}} - \sqrt{-\frac{2h(b+3c)}{3a+2b+3c}}.\end{aligned}$$

and the determinant of the Jacobian matrix of  $f$  at these four zeros is

$$\begin{aligned}D(r_i, \phi_i) &= \frac{bh^2(3a+b)}{8(1+\omega^2)^4} \quad \text{for } i = 11, 12, \\ D(r_i, \phi_i) &= -\frac{bh^2(3a+b)(b+3c)}{4(1+\omega^2)^4(3a+2b+3c)} \quad \text{for } i = 13, 14.\end{aligned}$$

Again, from Averaging Theorem we obtain that

$$h < 0, \quad \text{and} \quad D(r_i, \phi_i) \neq 0,$$

then the two zeros  $(r_i, \phi_i)$  for  $i = 11, 12$  provide two periodic solutions of the differential system (5.13), and consequently of the Hamiltonian system (5.4) in every level  $H = h < 0$ .

Also from Averaging Theorem we get that

$$r_i > 0, \quad \rho_i > 0, \quad D(r_i, \phi_i) \neq 0,$$

then the two zeros  $(r_i, \phi_i)$  for  $i = 13, 14$  provide two periodic solutions of the differential system (5.13), and consequently of the Hamiltonian system (5.4) in every level  $H = h$ .

Substituting  $\phi = \Phi_2$  into  $f_2(r, \phi) = 0$ , and solving with respect to  $r$  we obtain again the solutions  $(r_i, \phi_i)$  for  $i = 9, 10, 11, 12$ . Again we cannot guarantee that these last four solutions are all the solutions for  $\phi = \Phi_2$ , because these four solutions are the ones that we can obtain explicitly.

For  $i = 1, 2, 5, 6, 7, 8, 9, 10, 11, 12, 13, 14$  and according with Theorem 2.15 the zero  $(r_i, \phi_i)$  provides a periodic solution  $(\bar{r}_i(\theta, \varepsilon), \bar{\phi}_i(\theta, \varepsilon))$  of the differential system (5.13) such that

$$(\bar{r}_i(0, \varepsilon), \bar{\phi}_i(0, \varepsilon)) \rightarrow (r_i, \phi_i) \quad \text{when } \varepsilon \rightarrow 0.$$

Going back to the differential system (5.12) we obtain for this system a periodic solution  $(\bar{r}_i(\theta, \varepsilon), \bar{\rho}_i(\theta, \varepsilon), \bar{\phi}_i(\theta, \varepsilon))$  such that

$$(\bar{r}_i(0, \varepsilon), \bar{\rho}_i(0, \varepsilon), \bar{\phi}_i(0, \varepsilon)) \rightarrow (r_i, \rho_i, \phi_i) \quad \text{when } \varepsilon \rightarrow 0,$$

where  $\rho_i = \rho(r_i, \phi_i)$ . Now going back to the differential system (5.11) we get for this system a periodic solution  $(\bar{r}_i(t, \varepsilon), \bar{\theta}(t, \varepsilon), \bar{\rho}_i(t, \varepsilon), \bar{\phi}_i(t, \varepsilon))$  such that

$$(\bar{r}_i(0, \varepsilon), \bar{\theta}(0, \varepsilon), \bar{\rho}_i(0, \varepsilon), \bar{\phi}_i(0, \varepsilon)) \rightarrow (r_i, 0, \rho_i, \phi_i) \quad \text{when } \varepsilon \rightarrow 0.$$

Again going back to the differential system (5.8) we have for this system a periodic solution  $(\bar{u}(t, \varepsilon), \bar{v}(t, \varepsilon), \bar{p}_u(t, \varepsilon), \bar{p}_v(t, \varepsilon))$  such that

$$(\bar{u}(0, \varepsilon), \bar{v}(0, \varepsilon), \bar{p}_u(0, \varepsilon), \bar{p}_v(0, \varepsilon)) \rightarrow (r_i, 0, \rho_i \cos \phi_i, \rho_i \sin \phi_i) \quad \text{when } \varepsilon \rightarrow 0.$$

Going back to the Hamiltonian system (5.6) we have for this system a periodic solution  $(\bar{X}(t, \varepsilon), \bar{Y}(t, \varepsilon), \bar{p}_X(t, \varepsilon), \bar{p}_Y(t, \varepsilon))$  such that

$$(\bar{X}(0, \varepsilon), \bar{Y}(0, \varepsilon), \bar{p}_X(0, \varepsilon), \bar{p}_Y(0, \varepsilon)) \rightarrow \left( r_i, \frac{\rho_i \cos \phi_i}{\omega}, \rho_i \cos \phi_i, \frac{\sqrt{1 + \omega^2} \rho_i \sin \phi_i - r_i}{\omega} \right)$$

when  $\varepsilon \rightarrow 0$ . Finally going back to the Hamiltonian system (5.4) we have for this system a periodic solution  $(\bar{x}(t, \varepsilon), \bar{y}(t, \varepsilon), \bar{p}_x(t, \varepsilon), \bar{p}_y(t, \varepsilon))$  such that

$$\begin{aligned} (\bar{x}(0, \varepsilon), \bar{y}(0, \varepsilon), \bar{p}_x(0, \varepsilon), \bar{p}_y(0, \varepsilon)) &\rightarrow \sqrt{\varepsilon} \left( r_i, \frac{\rho_i \cos \phi_i}{\omega}, \rho_i \cos \phi_i, \frac{\sqrt{1 + \omega^2} \rho_i \sin \phi_i - r_i}{\omega} \right) \\ &\rightarrow (0, 0, 0, 0), \end{aligned}$$

when  $\varepsilon \rightarrow 0$ . In summary, these 12 families of periodic orbits of the Hamiltonian system (5.4) born at the equilibrium localized at the origin of coordinates. This completes the proof of Theorem 5.1.

## 6 POLYCYCLES IN NON-SMOOTH VECTOR FIELDS

### 6.1 Introduction and description of the results

The field of Dynamic Systems had developed and now have many branches, being one of them the field of *non-smooth vector fields*, a common frontier between mathematics, physics and engineering. See [3, 21] for the pioneering works in this area. A polycycle is a simple closed curve composed by a collection of singularities and regular orbits, inducing a first return map. There are many works in the literature about polycycles in smooth vector fields, take for example some works about its stability [16, 18, 55], the number of limit cycles which bifurcates from it [38, 20, 23], the displacement maps [49, 26, 22, 17] and some bifurcation diagrams [20]. As far as we know, there are not many works in the literature about the extension of well established results of smooth vector fields to the non-smooth realm. Take for example the relatively new extension of the Poincaré-Bendixson theory to non-smooth vector fields [10].

Therefore, the main goal of this paper is to extend to non-smooth vector fields some of the results established about polycycles in smooth vector fields. To do this, we lay, as in the smooth case, mainly in the idea of obtaining global properties of a polycycle from local properties of its singularities. Based on the works [38, 20], of Mourtarda, and the work [2], of Andrade, Gomide and Novaes, we established some results about the stability of a polycycle and the number of limit cycles which bifurcates from it. Take for example the polycycle  $\Gamma$  given by Figure 6.1. Let  $2k$  be the contact of the non-smooth vector field

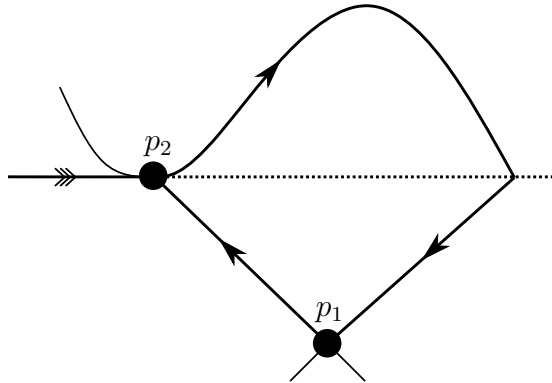


Figure 6.1: A polycycle  $\Gamma$  composed by a hyperbolic saddle  $p_1$  and a tangential singularity  $p_2$ . Figure source: made by the author.

at  $p_2$ ,  $\nu < 0 < \lambda$  be the two eigenvalues of the hyperbolic saddle  $p_1$  and  $r_1 = \frac{|\nu|}{\lambda}$  the *hyperbolicity ratio* of  $p_1$ . Knowing that  $p_1$  contracts the flow if  $r_1 > 1$ , and repels it if  $r_1 < 1$ , and that  $p_2$ , in the orientation given by  $\Gamma$ , contract the flow with strength of order  $2k$ , it was possible to prove that  $\Gamma$  attract the flow in the bounded component delimit by it if

$$2kr_1 > 1,$$

and repels it if the above constant is less than one. See Theorem 6.4. Thus, to overwhelm  $p_2$  and force the whole polycycle to repel the flow,  $p_1$  needs not only to repel the flow

itself, but to do it with strength greater than  $2k$ . But, if  $p_1$  and  $p_2$  help themselves and they both contract the flow, then it follows from Theorem 6.8 that at most one limit cycle can bifurcate from  $\Gamma$  and, if it does, then the limit cycle is hyperbolic and it also contract the flow. Furthermore, if  $p_1$  and  $p_2$  disturb themselves, i.e. one contract the flow while the other one repels it, then it follows from Theorem 6.9 that there exists an arbitrarily small perturbation of  $\Gamma$  such that at least two limit cycles bifurcates from it. In fact, if we have a polycycle with  $n$  hyperbolic singularities and  $m$  tangential singularities such that the singularities perturb themselves in a particular way, then at least  $n + m$  limit cycles will bifurcate from it. On the other hand, if every singularity contracts (resp. repels) the flow, then at most one limit cycle can bifurcate and if it does, it is hyperbolic and also contract (resp. repels) the flow.

Moreover, in Theorem 6.9 we give the unfolding of the polycycle  $\Gamma$  with  $k = 1$  and  $r_1 \in \mathbb{R}^+ \setminus \{\frac{1}{2}, 1\}$ . See Figures 6.2, 6.3 and 6.4. See also [2, 40] for the bifurcation diagrams of others polycycles.

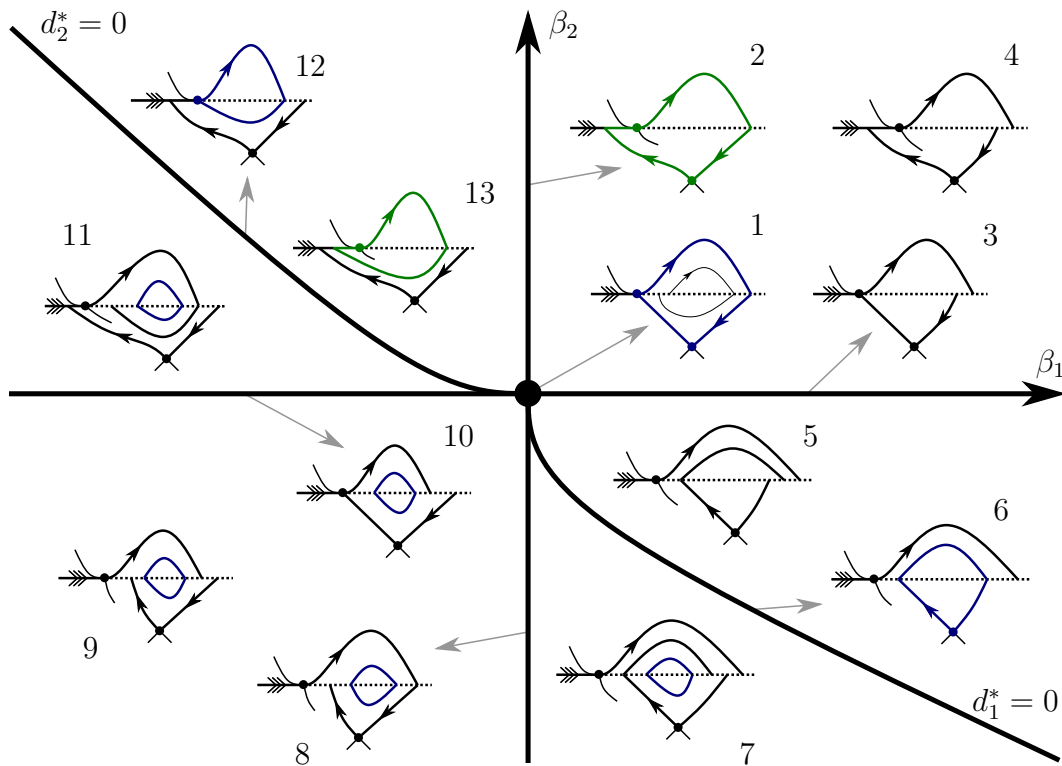


Figure 6.2: Bifurcation diagram of  $\Gamma$  for  $r_1 > 1$ . The blue lines represents either a stable polycycle or a hyperbolic and stable limit cycle. The green lines represent a sliding polycycle. Figure source: made by the author.

The chapter is organized as follows. In Section 6.2 we establish the main theorems. Theorems 6.4 and 6.7 are proved in Section 6.4. In Sections 6.5 and 6.6 we prove some minors results about the displacement maps  $d$  and  $d^*$  and their partial derivatives. Theorem 6.8 is proved in Section 6.7 and Theorem 6.9 is proved in Section 6.8.

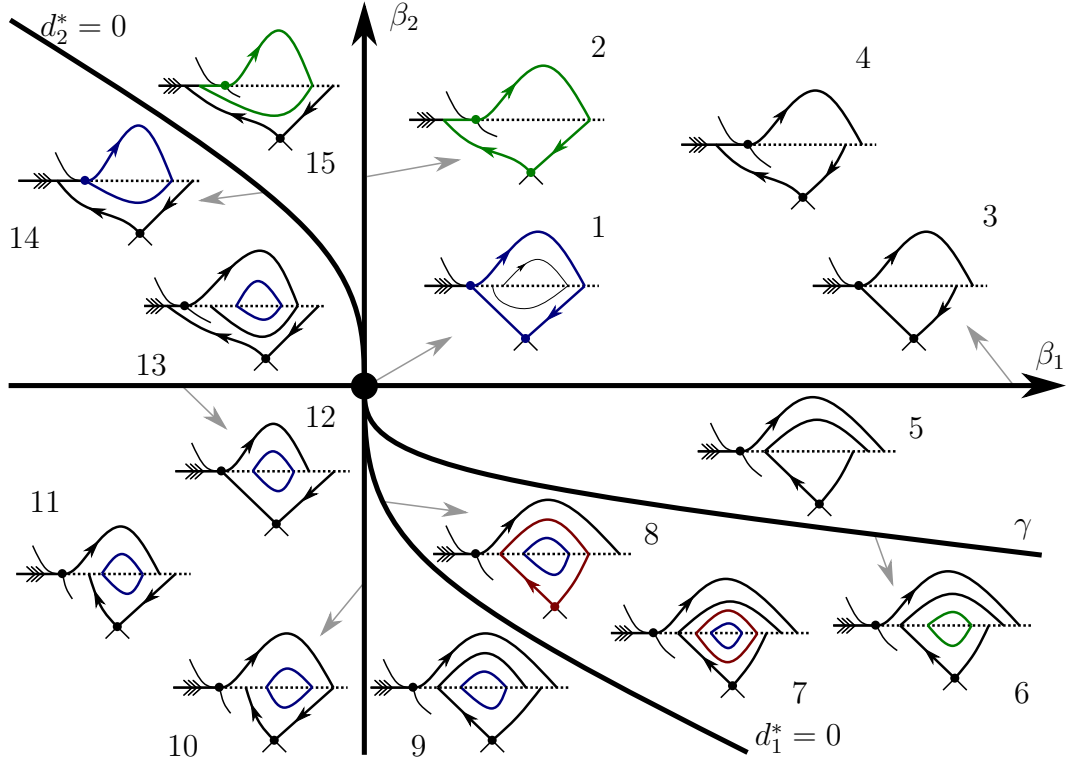


Figure 6.3: Bifurcation diagram of  $\Gamma$  for  $\frac{1}{2} < r_1 < 1$ . The blue (resp. red) lines represents either a stable (resp. unstable) polycycle or a hyperbolic stable (resp. unstable) limit cycle. The green lines represents either a sliding polycycle or a semi-stable limit cycle. Figure source: made by the author.

## 6.2 Main results

Let  $Z = (X_1, \dots, X_M)$ ,  $M \geq 2$ , be a planar non-smooth vector field depending on a parameter  $\mu \in \mathbb{R}^r$  with  $N \geq 1$  discontinuities  $\Sigma_1, \dots, \Sigma_N$ ,  $\Sigma = \cup_{i=1}^N \Sigma_i$ , given by  $h_1(x) = 0, \dots, h_N(x) = 0$ ,  $x \in \mathbb{R}^2$ , with each  $X_i = X_i(x, \mu)$  of class  $C^\infty$  in  $(x, \mu) \in \mathbb{R}^2 \times \mathbb{R}^r$ ,  $h_j = h_j(x)$  of class  $C^\infty$  in  $x \in \mathbb{R}^2$  and 0 a regular value of  $h_1, \dots, h_N$ , i.e.,  $\nabla h_j(x) \neq 0$  for all  $x \in h_j^{-1}(0)$ ,  $j \in \{1, \dots, N\}$ . Let  $A_1, \dots, A_M$  be the open connected components of  $\mathbb{R}^2 \setminus \Sigma$  with each  $X_i$  defined over  $\overline{A_i}$ ,  $i \in \{1, \dots, M\}$ .

Let  $p \in \Sigma_i \subset \Sigma$ , with  $p \notin \Sigma_j \cap \Sigma_k$  for any  $j \neq k$ , and let  $X$  be one of the two components of  $Z$  defined at  $p$ . The *Lie derivative* of  $h_i$  in the direction of the vector field  $X$  at  $p$  is defined as

$$Xh_i(p) = \langle X(p), \nabla h_i(p) \rangle,$$

where  $\langle \cdot, \cdot \rangle$  is the standard inner product of  $\mathbb{R}^2$ .

**Definition 6.1.** We say that a point  $p \in \Sigma_i \subset \Sigma$  is a tangential singularity if

- (a)  $p \notin \Sigma_j \cap \Sigma_k$  for any  $j \neq k$ ;
- (b)  $X_a h_i(p) X_b h_i(p) = 0$  and  $X_a(p), X_b(p) \neq 0$ , where  $X_a$  and  $X_b$  are the two components of  $Z$  defined at  $p$ .

We also suppose that at  $\mu = \mu_0$  we have a polycycle  $\Gamma^n$  composed by  $n$  singularities  $p_1, \dots, p_n \in \mathbb{R}^2$  such that each  $p_i$  is either a hyperbolic saddle or a tangential singularity.

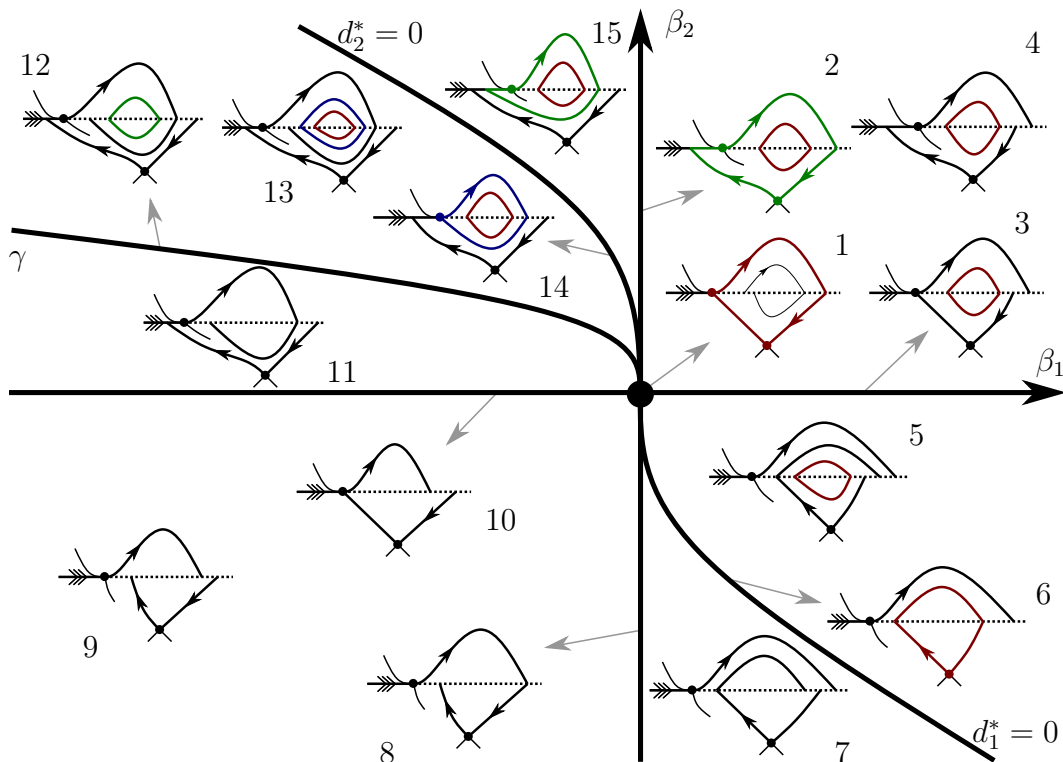


Figure 6.4: Bifurcation diagram of  $\Gamma$  for  $r_1 < \frac{1}{2}$ . The blue (resp. red) lines represents either a stable (resp. unstable) polycycle or a hyperbolic stable (resp. unstable) limit cycle. The green lines represents either a sliding polycycle or a semi-stable limit cycle. Figure source: made by the author.

Let  $L_1, \dots, L_n$  denote the heteroclinic connections of  $\Gamma^n$  such that  $\omega(L_i) = p_i$  and  $\alpha(L_i) = p_{i+1}$ , with  $\alpha(L_n) = p_1$ . Let us also assume that if  $L_i$  intersects  $\Sigma \setminus \{p_1, \dots, p_n\}$ , then it does at most in a finite number of points  $\{x_{i,0}, x_{i,1}, \dots, x_{i,n(i)}\}$  and  $x_{i,j} \notin \Sigma_r \cap \Sigma_s$ , for any  $r \neq s$ ,  $j \in \{0, \dots, n(i)\}$ . In this case let  $\gamma_i(t)$  be a parametrization of  $L_i$  such that  $\gamma_i(t_{i,j}) = x_{i,j}$ ,  $0 = t_{i,0} > t_{i,1} > \dots > t_{i,n(i)}$ . Let us also assume that around each  $x_{i,j}$  there is a neighborhood  $N_{i,j}$  of  $x_{i,j}$  such that  $\Sigma \cap N_{i,j}$  is a crossing region of  $\Sigma$ , i.e. if  $x_{i,j} \in \Sigma_r$  and  $X_s, X_u$  are the two components of  $Z$  defined at  $x_{i,j}$ , then  $X_s h_r(x_{i,j}) X_u h_r(x_{i,j}) > 0$ . If  $L_i$  does not intersect  $\Sigma$ , then take any point  $x_{i,0} \in L_i$  and a parametrization  $\gamma_i(t)$  of  $L_i$  such that  $\gamma_i(0) = x_{i,0}$ . Let us also assume that  $\Gamma^n$  is a connected component of the boundary of some open ring  $A \subset \mathbb{R}^2$ . See Figure 6.5. Furthermore, we say that the *cyclicity* of  $\Gamma^n$  is  $k$  if at most  $k$  limit cycles can bifurcate from a arbitrarily small perturbation of  $\Gamma^n$ .

**Definition 6.2.** Let  $p \in \Sigma_i \subset \Sigma$  be a tangential singularity,  $X$  one of the components of  $Z$  defined at  $p$  and let  $X^k h_i(p) = \langle X(p), \nabla X^{k-1} h_i(p) \rangle$ ,  $k \geq 2$ . We say that  $X$  has  $m$ -order contact with  $\Sigma$  at  $p$ ,  $m \geq 1$ , if  $m$  is the first positive integer such that  $X^m h_i(p) \neq 0$ .

**Definition 6.3.** Let  $p \in \Sigma_i \subset \Sigma$  be a tangential singularity of  $\Gamma^n$ ,  $L_s$  and  $L_u$  the heteroclinic connections of  $\Gamma^n$  such that  $\omega(L_s) = p$  and  $\alpha(L_u) = p$ . Let  $X_a$  and  $X_b$  be the two components of  $Z$  defined at  $p$  and let  $A_a, A_b$  be the respective connected components of  $\mathbb{R}^2 \setminus \Sigma$  such that  $X_a$  and  $X_b$  is defined over  $\overline{A_a}$  and  $\overline{A_b}$ . Let  $A_s, A_u \in \{A_a, A_b\}$  be such that  $A_s \cap L_s \neq \emptyset$  and  $A_u \cap L_u \neq \emptyset$ . Let  $X_s, X_u \in \{X_a, X_b\}$  denote the components of  $Z$  defined at  $A_s$  and  $A_u$ . Observe that we may have  $A_s = A_u$  and thus  $X_s = X_u$ . See Figure 6.6. We define the unstable and stable contact order of  $p$  as the contact order  $n_s$

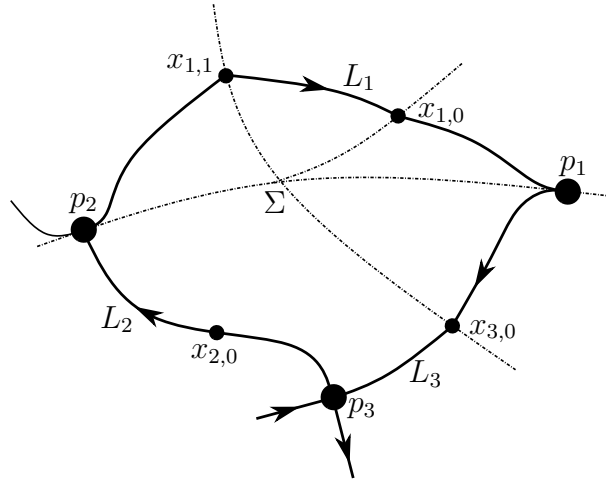


Figure 6.5: An example of  $\Gamma^3$  with the open ring  $A$  contained in the bounded region delimited by  $\Gamma^3$ . Figure source: made by the author.

and  $n_u$  of  $X_s$  and  $X_u$  with  $\Sigma$  at  $p$ , respectively. Furthermore we also say that  $X_s$  and  $X_u$  are the stable and unstable components of  $Z$  defined at  $p$ , respectively.

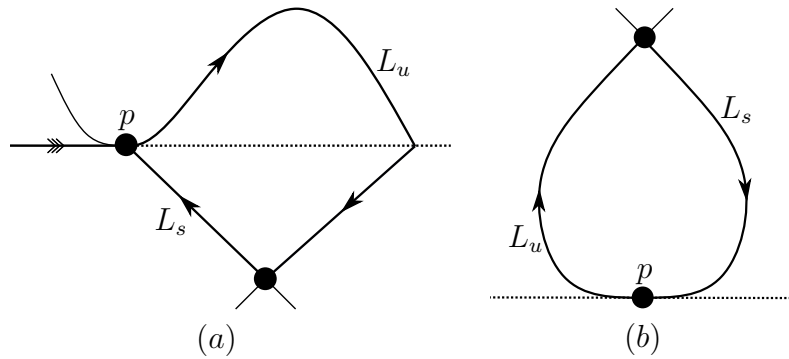


Figure 6.6: Examples of a tangential singularity  $p$  such that (a)  $A_s \neq A_u$  and (b)  $A_s = A_u$ . Figure source: made by the author.

**Theorem 6.4.** *Let  $Z$  and  $\Gamma^n$  be as above. Let  $n_{i,s}$  and  $n_{i,u}$  be the stable and unstable contact orders of the tangential singularities  $p_i$  of  $\Gamma^n$ ,  $\nu_i < 0 < \lambda_i$  be the eigenvalues of the hyperbolic saddles  $p_i$  of  $\Gamma^n$  and in either case define  $r_i = \frac{n_{i,u}}{n_{i,s}}$  or  $r_i = \frac{|\nu_i|}{\lambda_i}$ , respectively. Finally, let*

$$p(\Gamma^n) = \prod_{i=1}^n r_i. \quad (6.1)$$

*If  $p(\Gamma^n) > 1$  (resp.  $p(\Gamma^n) < 1$ ), then there is a neighborhood  $N_0$  of  $\Gamma^n$  such that the orbit of  $Z$  through any point  $p \in N_0 \cap A$  has  $\Gamma^n$  as  $\omega$ -limit (resp.  $\alpha$ -limit).*

Let  $\Gamma^{n,l}$  denote a polycycle composed by  $n$  singularities  $p_1, \dots, p_n \in \mathbb{R}^2$  such that each  $p_i$  is either a hyperbolic saddle or a tangential singularity, and by  $l$  semi-hyperbolic singularities  $q_1, \dots, q_l \in \mathbb{R}^2 \setminus \Sigma$ , i.e. each  $q_i$  has a unique non-zero eigenvalue. Let us also suppose that the heteroclinic connections  $L_{s,i}$  and  $L_{u,i}$  of  $\Gamma^{n,l}$  such that  $\omega(L_{s,i}) = q_i$ ,

$\alpha(L_{u,i}) = q_i$  are the boundaries of a hyperbolic sector of  $q_i$  contained in the open ring  $A$ , e.g. a saddle-node or a degenerated saddle. Assume that  $\Gamma^{n,l}$  satisfies the established hypothesis for  $\Gamma^n$ . With little adaptations in the proof of Theorem 6.4, one can use Subsection 2.9 to prove the following result.

**Corollary 6.5.** *Let  $Z$  and  $\Gamma^{n,l}$ ,  $l \geq 1$ , be as above. Let  $\lambda_i \in \mathbb{R} \setminus \{0\}$  denote the non-zero eigenvalue of the semi-hyperbolic singularity  $q_i$ . If every  $\lambda_i < 0$  (resp. every  $\lambda_i > 0$ ), then there is a neighborhood  $N_0$  of  $\Gamma^{n,l}$  such that the orbit of  $Z$  through any point  $p \in N_0 \cap A$  has  $\Gamma^{n,l}$  as  $\omega$ -limit (resp.  $\alpha$ -limit).*

**Definition 6.6.** Given a hyperbolic saddle  $p_i$  of a polycycle  $\Gamma^{n,l}$  let  $r_i \in \mathbb{R}_+$  be as in Theorem 6.4. We say that  $p_i$  is a *stable singular point* (resp. *unstable singular point*) of  $\Gamma^{n,l}$  if  $r_i > 1$  (resp.  $r_i < 1$ ). Given a tangential singularity  $p_i$  of  $\Gamma^{n,l}$  we say that  $p_i$  is a *stable singular point* (resp. *unstable singular point*) if  $n_s = 1$  (resp.  $n_u = 1$ ). Furthermore, if  $q_i$  is a semi-hyperbolic singularity of  $\Gamma^{n,l}$  with its unique non-zero eigenvalue given by  $\lambda_i \in \mathbb{R} \setminus \{0\}$ , then  $q_i$  is a *stable singular point* (resp. *unstable singular point*) of  $\Gamma^{n,l}$  if  $\lambda_i < 0$  (resp.  $\lambda_i > 0$ ).

**Theorem 6.7.** *Let  $Z$  and  $\Gamma^{n,l}$ ,  $n + l \geq 1$ , be as above. Suppose that each singularity  $p_i$  and  $q_j$  is a stable (resp. unstable) singular point of  $\Gamma^{n,l}$ . If a small perturbation of  $\Gamma^{n,l}$  has a limit cycle, then it is unique, hyperbolic and stable (resp. unstable). Furthermore, the cyclicity of  $\Gamma^{n,l}$  is one.*

**Theorem 6.8.** *Let  $Z_0$  and  $\Gamma^n$  be as in Section 6.2 and define  $R_i = r_1 \dots r_i$ ,  $i \in \{1, \dots, n\}$ . Suppose  $R_n \neq 0$  and, if  $n \geq 2$ , suppose  $(R_i - 1)(R_{i+1} - 1) < 0$  for  $i \in \{1, \dots, n-1\}$ . Then, there exists a  $C^\infty$  map  $g(x, \mu) = O(\|\mu\|)$ ,  $\mu \in \mathbb{R}^n$ , such that the vector field  $Z = Z_0 + g$  has at least  $n$  limit cycles in a neighborhood of  $\Gamma^n$  for some  $\mu$  arbitrarily near the origin. Therefore, the cyclicity of  $\Gamma^n$  is at least  $n$ .*

**Theorem 6.9.** *Let  $\Gamma$  be polycycle composed by a hyperbolic saddle  $p_1$  and a quadratic-regular tangential singularity. Then the bifurcation diagrams of  $\Gamma$  for  $r_1 > 1$ ,  $\frac{1}{2} < r_1 < 1$  and  $r < \frac{1}{2}$  are those given by Figures 6.2, 6.3 and 6.4, respectively.*

### 6.3 Transition map near a tangential singularity

Let  $p$  be a tangential singularity of  $\Gamma^n$  and  $X_s, X_u$  be the stable and unstable components of  $Z$  defined at  $p_0$  with  $\mu = \mu_0$ . Let  $B$  be a small enough neighborhood of  $p_0$  and  $\Phi : B \times \Lambda \rightarrow \mathbb{R}^2$  be a  $C^\infty$  change of coordinates such that  $\Phi(p_0, \mu_0) = (0, 0)$  and  $\Phi(B \cap \Sigma) = Ox$ . Let  $l_s = \Phi(B \cap L_s)$ ,  $l_u = \Phi(B \cap L_u)$  and  $\tau_s, \tau_u$  two small enough transversal sections of  $l_s$  and  $l_u$ , respectively. Furthermore, let  $\sigma = [0, \varepsilon[\times\{0\}, \sigma = ]-\varepsilon, 0] \times \{0\}$  or  $\sigma = \{0\} \times [0, \varepsilon[$ , depending on  $\Gamma^n$ . It follows from [2]  $\Phi$  can be choose such that the transition maps  $T^{s,u} : \sigma \times \Lambda \rightarrow \tau_{s,u}$  given by the flow of  $X_{s,u}$  in this new coordinate system are well defined and given by

$$T^u(h_\mu(x), \mu) = \sum_{i=0}^{n_u-2} \lambda_i^u(\mu)x_i + k_u(\mu)x^{n_u} + O(x^{n_u+1}),$$

$$T^s(h_\mu(x), \mu) = \sum_{i=0}^{n_s-2} \lambda_i^s(\mu)x_i + k_s(\mu)x^{n_s} + O(x^{n_s+1}),$$

with  $\lambda_i^{s,u}(\mu_0) = 0$ ,  $k_{s,u}(\mu_0) \neq 0$ ,  $h_\mu : \mathbb{R} \rightarrow \mathbb{R}$  a diffeomorphism, and with  $h_\mu$  and  $\lambda_i^{s,u}$  depending continuously on  $\mu$ . See Figure 6.7.

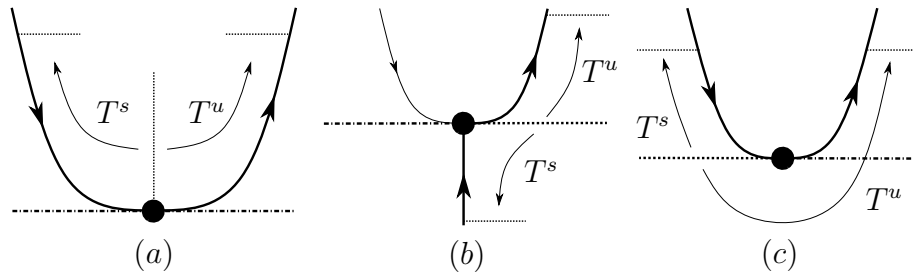


Figure 6.7: Illustration of the maps  $T^u$  and  $T^s$ . The choosing between (a) and (c) depends whether the Poincaré map is defined in the bounded or unbounded region delimited by  $\Gamma^n$ . Figure source: made by the author.

#### 6.4 Proofs of theorems 6.4 and 6.7

*Proof of Theorem 6.4.* For simplicity let us assume that  $\Sigma = h^{-1}(0)$  with 0 a regular value of  $h$ , and  $Z = (X_1, X_2)$ . Let also  $\Gamma = \Gamma^3$  be composed by two tangential singularities  $p_1, p_2$  and by a hyperbolic saddle  $p_3$ . See Figure 6.8. Following [55], let  $B_i$  be a small enough neighborhood of  $p_i$  and let  $\Phi_i: B_i \times \{\mu_0\} \rightarrow \mathbb{R}^2$  be chosen as in Section 6.3,  $i \in \{1, 2\}$ . Let also  $B_3$  be a neighborhood of  $p_3$  and  $\Phi_3: B_3 \times \{\mu_0\} \rightarrow \mathbb{R}^2$  be chosen as in Section 2.8. Knowing that  $T_i^{s,u}: \sigma_i \times \{\mu_0\} \rightarrow \tau_i^{s,u}$  and  $D: \sigma \times \{\mu_0\} \rightarrow \tau$ , let

$$\bar{\sigma}_i = \Phi_i^{-1}(\sigma_i) \quad \bar{\tau}_i^s = \Phi_i^{-1}(\tau_i^s), \quad \bar{\tau}_i^u = \Phi_i^{-1}(\tau_i^u)$$

$$J_s = \Phi_3^{-1}(\sigma), \quad J_u = \Phi_3^{-1}(\tau),$$

with  $i \in \{1, 2\}$ . Let also

$$\bar{\rho}_1: \tau_1^u \rightarrow \tau_2^s, \quad \bar{\rho}_2: \tau_2^u \rightarrow J_s, \quad \bar{\rho}_3: J_u \rightarrow \tau_1^s$$

be defined by the flow of  $X_1$  and  $X_2$ . See Figure 6.8. Finally let

$$\rho_1 = \Phi_2 \circ \bar{\rho}_1 \circ \Phi_1^{-1}, \quad \rho_2 = \Phi_3 \circ \bar{\rho}_2 \circ \Phi_2^{-1}, \quad \rho_3 = \Phi_1 \circ \bar{\rho}_3 \circ \Phi_3^{-1},$$

and

$$\bar{T}_i^s = \Phi_i^{-1} \circ T_i^s \circ \Phi_i, \quad \bar{T}_i^u = \Phi_i^{-1} \circ T_i^u \circ \Phi_i, \quad \bar{D} = \Phi_3^{-1} \circ D \circ \Phi_3$$

with  $i \in \{1, 2\}$ . See Figure 6.8. Let  $\nu < 0 < \lambda$  be the eigenvalues of  $p_3$  and denote  $r = \frac{|\nu|}{\lambda}$ . Let also  $n_{i,s}$  and  $n_{i,u}$  denote the stable and unstable order of  $q_i$ ,  $i \in \{1, 2\}$ . Therefore, it follows from Sections 2.8 and 6.3 that

$$T_i^s(x) = k_{i,s}x^{n_{i,s}} + O(x^{n_{i,s}+1}), \quad T_i^u(x) = k_{i,u}x^{n_{i,u}} + O(x^{n_{i,u}+1}),$$

$$D(x) = ax^r + O(x^{r+1}), \quad \rho_j(x) = a_jx + O(x^2),$$

with  $k_{i,s}, k_{i,u}, a_j, a \neq 0$ ,  $i \in \{1, 2\}$  and  $j \in \{1, 2, 3\}$ . Therefore, if we define

$$\pi = \rho_2 \circ T_2^u \circ (T_2^s)^{-1} \circ \rho_1 \circ T_1^u \circ (T_1^s)^{-1} \circ \rho_3 \circ D,$$

then one can conclude that

$$\pi(x) = Kx^{n_0} + O(x^{n_0+1}),$$

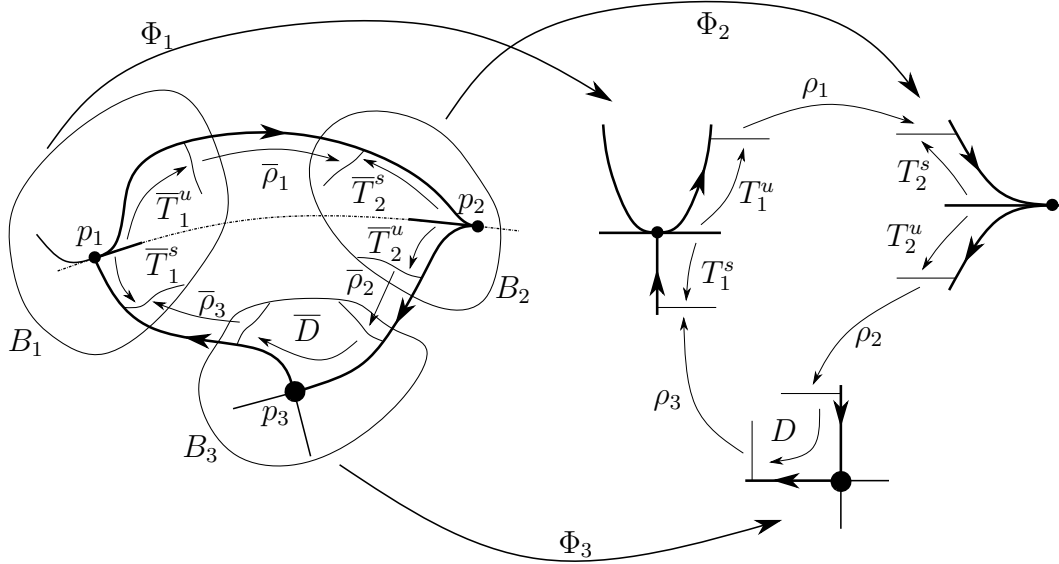


Figure 6.8: Illustration of the maps used in the proof of Theorem 6.4. Figure source: made by the author.

with  $K \neq 0$  and  $n_0 = p(\Gamma)$ , as in (6.1). Hence, if  $x$  is small enough we conclude that  $\pi(x) < x$  if  $n_0 > 1$  and  $\pi(x) > x$  if  $n_0 < 1$ . The result now follows from the fact that the Poincaré map

$$P = \bar{\rho}_2 \circ \bar{T}_2^u \circ (\bar{T}_2^s)^{-1} \circ \bar{\rho}_1 \circ \bar{T}_1^u \circ (\bar{T}_1^s)^{-1} \circ \bar{\rho}_3 \circ \bar{D}$$

satisfies  $P = \Phi_3^{-1} \circ \pi \circ \Phi_3$ . □

*Proof of Theorem 6.7.* Let us suppose that every singular point of  $\Gamma^{n,l}$  is attracting. Following [20] and the proof of Theorem 6.4, we observe that the Poincaré map, when well defined, can be written as a composition

$$P_\mu = G_k \circ F_k \circ \dots \circ G_1 \circ F_1,$$

where each  $F_i$  is the transition map near a hyperbolic saddle, a semi-hyperbolic singularity, or a tangential singularity, and each  $G_i$  is the composition of a finite number of regular transitions, i.e. a  $C^\infty$  diffeomorphism in  $x$ . We call  $y_1 = F_1(x_1)$ ,  $x_2 = G_1(y_1)$ , ...,  $y_k = F_k(x_k)$ ,  $x_{k+1} = G_k(y_k)$ . Thus,

$$P'_\mu(x_1) = G'_k(y_k)F'_k(x_k) \dots G'_1(y_1)F'_1(x_1).$$

Therefore, it follows from Sections 2.8 and 2.9 that for all  $\varepsilon > 0$  there exists a neighborhood  $\Lambda$  of  $\mu = \mu_0$  and neighborhoods  $W_i$  of  $x_i = 0$ ,  $i \in \{1, \dots, k + 1\}$  such that if  $x_1 \in W_1$ , then  $x_i \in W_i$  and  $|F'_i(x_i)| < \varepsilon$  for all  $i \in \{1, \dots, k + 1\}$  and  $\mu \in \Lambda$ . Also, if  $\Lambda$  and each  $W_i$  are small enough, then each  $G'_i(y_i)$  is bounded, and bounded away from zero. Hence, for  $\varepsilon > 0$  small enough it follows that  $P'_\mu(x_1) < 1$  for  $(x_1, \mu) \in W_1 \times \Lambda$  and thus a unique limit cycle exists and it is hyperbolic and attracting. The repelling case follows by time reversing. □

### 6.5 The displacement map

Let  $Z$  and  $\Gamma^n$  be as in Section 6.2. For simplicity let  $p_1 \in A_1$  and  $p_2 \in A_2$  be two hyperbolic saddles of  $\Gamma^n$  with the heteroclinic connection  $L_0$  such that  $\omega(L_0) =$

$p_1$ ,  $\alpha(L_0) = p_2$  and  $L_0 \cap \Sigma = \{x_0\}$ ,  $\Sigma = h^{-1}(0)$ . Let  $\gamma_0(t)$  be a parametrization of  $L_0$  such that  $\gamma_0(0) = x_0$  and  $u_0$  be an unitarian vector orthogonal to  $T_{x_0}\Sigma$  such that  $\text{sign}(\langle u_0, \nabla h(x_0) \rangle) = \text{sign}(X_1 h(x_0)) = \text{sign}(X_2 h(x_0))$ . See Figure 6.9. Let us define

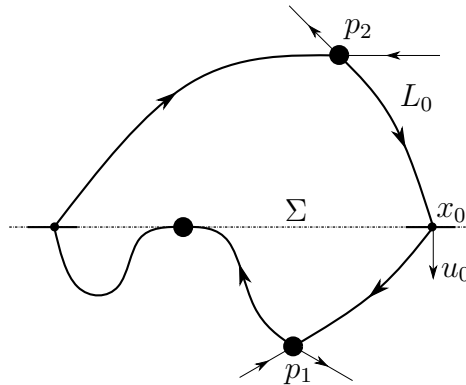


Figure 6.9: Illustration of  $u_0$ . Figure source: made by the author.

$\omega_0 \in \{-1, 1\}$  such that  $\omega_0 = 1$  if the orientation of  $\Gamma^n$  is counterclockwise and  $\omega_0 = -1$  if the orientation of  $\Gamma^n$  is clockwise. We denote by  $DX(p, \mu^*)$  the Jacobian matrix of  $X|_{\mu=\mu^*}$  at  $p$ , i.e. if  $X = (P, Q)$ , then

$$DX(p, \mu^*) = \begin{pmatrix} \frac{\partial P}{\partial x_1}(p, \mu^*) & \frac{\partial P}{\partial x_2}(p, \mu^*) \\ \frac{\partial Q}{\partial x_1}(p, \mu^*) & \frac{\partial Q}{\partial x_2}(p, \mu^*) \end{pmatrix}.$$

Following [49], we know from the Implicit Function Theorem that if  $\mu \in \Lambda$ , then  $p_i(\mu) \in A_i$  is a hyperbolic saddle of  $X_i$  and  $p_i(\mu) \rightarrow p_i$  as  $\mu \rightarrow \mu^*$ , with  $p_i(\mu)$  of class  $C^\infty$ ,  $i \in \{1, 2\}$ . Let  $(y_{i,1}, y_{i,2}) = (y_{i,1}(\mu), y_{i,2}(\mu))$  be a coordinate system with its origin at  $p_i(\mu)$  and such that the  $y_{i,1}$ -axis and the  $y_{i,2}$ -axis are the one-dimensional stable and unstable spaces  $E_i^s(\mu)$  and  $E_i^u(\mu)$  of the linearization of  $X_i(\cdot, \mu)$  at  $p_i(\mu)$ ,  $i \in \{1, 2\}$ . It follows from the Stable Manifold Theorem that the stable and unstable manifolds  $S_i^\mu$  and  $U_i^\mu$  of  $X_i(\cdot, \mu)$  at  $p_i(\mu)$  are given by

$$S_i^\mu : y_{i,2} = \Psi_{i,2}(y_{i,1}, \mu) \text{ and } U_i^\mu : y_{i,1} = \Psi_{i,1}(y_{i,2}, \mu),$$

where  $\Psi_{i,1}$  and  $\Psi_{i,2}$  are  $C^\infty$  functions,  $i \in \{1, 2\}$ . Restricting  $\Lambda$  if necessary, it follows that there is  $\delta > 0$  such that

$$y_i^s(\mu) = (\delta, \Psi_{i,2}(\delta, \mu)) \in S_i^\mu \text{ and } y_i^u(\mu) = (\Psi_{i,1}(\delta, \mu), \delta) \in U_i^\mu,$$

$i \in \{1, 2\}$ . If  $C_i(\mu)$  is the diagonalization of  $DX_i(p_i(\mu), \mu)$ , then at the original coordinate system  $(x_1, x_2)$  we obtain

$$x_i^s(\mu) = p_i(\mu) + C_i(\mu)y_i^s(\mu) \in S_i^\mu \text{ and } x_i^u(\mu) = p_i(\mu) + C_i(\mu)y_i^u(\mu) \in U_i^\mu,$$

$i \in \{1, 2\}$ . Furthermore,  $x_i^s(\mu)$  and  $x_i^u(\mu)$  are also  $C^\infty$  at  $\Lambda$ . Let  $\phi_i(t, \xi, \mu)$  be the flow of  $X_i(\cdot, \mu)$  such that  $\phi_i(0, \xi, \mu) = \xi$  and  $L_0^s = L_0^s(\mu)$ ,  $L_0^u = L_0^u(\mu)$  be the perturbations of  $L_0$  such that  $\omega(L_0^s(\mu)) = p_1(\mu)$  and  $\alpha(L_0^u(\mu)) = p_2(\mu)$ . Then it follows that

$$x^s(t, \mu) = \phi_1(t, x_1^s(\mu), \mu) \text{ and } x^u(t, \mu) = \phi_2(t, x_2^u(\mu), \mu)$$

are parametrizations of  $L_0^s(\mu)$  and  $L_0^u(\mu)$ , respectively. Since  $L_0$  intersects  $\Sigma$  it follows that there are  $t_0^s < 0$  and  $t_0^u > 0$  such that  $x^s(t_0^s, \mu_0) = x_0 = x^u(t_0^u, \mu_0)$  and thus by the uniqueness of solutions we have

$$x^s(t + t_0^s, \mu_0) = \gamma_0(t) = x^u(t + t_0^u, \mu_0),$$

for  $t \in [0, +\infty)$  and  $t \in (-\infty, 0]$ , respectively.

**Lemma 6.10.** *Restricting  $\Lambda$  if necessary, there exists unique  $C^\infty$  functions  $\tau^s(\mu)$  and  $\tau^u(\mu)$  such that  $\tau^s(\mu) \rightarrow t_0^s$  and  $\tau^u(\mu) \rightarrow t_0^u$ , as  $\mu \rightarrow \mu_0$ , and  $x_0^s(\mu) = x^s(\tau^s(\mu), \mu) \in \Sigma$  and  $x_0^u(\mu) = x^u(\tau^u(\mu), \mu) \in \Sigma$  for  $\mu \in \Lambda$ . See Figure 6.10.*

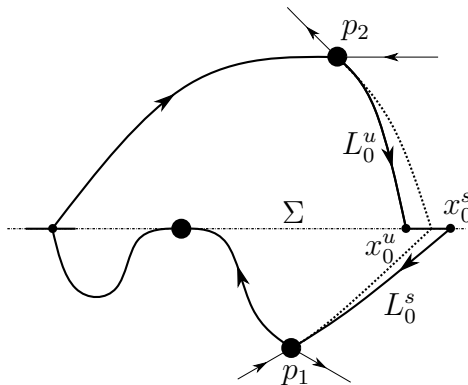


Figure 6.10: Illustration of  $x_0^s(\mu)$  and  $x_0^u(\mu)$ . Figure source: made by the author.

*Proof.* Let  $X_1$  denote a  $C^\infty$  extension of  $X_1$  to a neighborhood of  $\overline{A_1}$  and observe that now  $x^s(t, \mu_0)$  is well defined for  $|t - t_0^s|$  small enough. Define  $S(t, \mu) = h(x^s(t, \mu))$  and observe that  $S(t_0^s, \mu_0) = h(x_0) = 0$  and

$$\frac{\partial S}{\partial t}(t_0^s, \mu_0) = \langle \nabla h(x_0), X_1(x_0) \rangle \neq 0.$$

It then follows from the Implicit Function Theorem that there exist a  $C^\infty$  function  $\tau^s(\mu)$  such that  $\tau^s(\mu_0) = t_0^s$  and  $S(\tau^s(\mu), \mu) = 0$  and thus  $x_0^s(\mu) = x^s(\tau^s(\mu), \mu) \in \Sigma$ . In the same way one can prove the existence of  $\tau^u$ .  $\square$

**Definition 6.11.** It follows from Lemma 6.10 that the displacement function

$$d(\mu) = \omega_0[x_0^u(\mu) - x_0^s(\mu)] \wedge u_0,$$

where  $(x_1, x_2) \wedge (y_1, y_2) = x_1y_2 - y_1x_2$ , is well defined near  $\mu_0$  and it is of class  $C^\infty$ . See Figure 6.11.

**Remark 6.12.** We observe that  $L_0$  can intersect  $\Sigma$  multiple times. In this case, following Section 6.2 we would have  $L_0 \cap \Sigma = \{x_0, x_1, \dots, x_n\}$  and  $\gamma_0(t)$  a parametrization of  $L_0$  such that  $\gamma_0(t_i) = x_i$ , with  $0 = t_0 > t_1 > \dots > t_n$ . Therefore, applying Lemma 6.10 one shall obtain  $x_n^u(\mu)$  and then applying the Implicit Function Theorem multiple times one shall obtain  $x_i^u(\mu)$  as a function of  $x_{i+1}^u(\mu)$ ,  $i \in \{0, \dots, n-1\}$ , and thus the displacement function would still be defined at  $x_0$ .

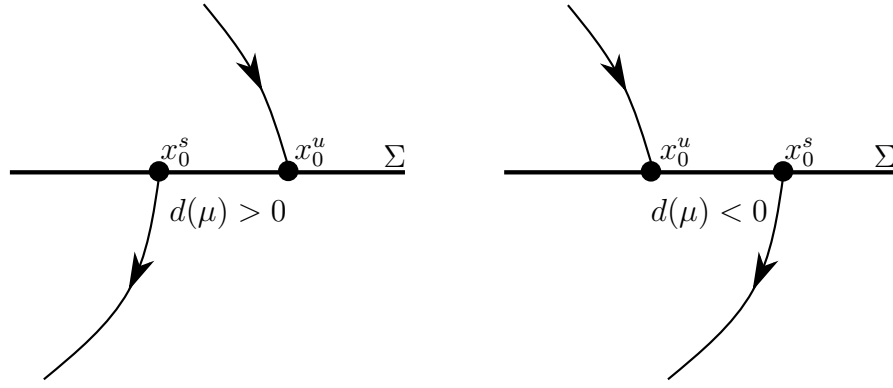


Figure 6.11: Illustration of  $d(\mu) > 0$  and  $d(\mu) < 0$ . Figure source: made by the author.

Let us define

$$\begin{aligned} x_\mu^s(t) &= \phi_1(t, x_0^s(\mu), \mu) \text{ for } t \geq 0 \text{ and} \\ x_\mu^u(t) &= \phi_2(t, x_0^u(\mu), \mu) \text{ for } t \leq 0, \end{aligned}$$

new parametrizations of  $L_0^s(\mu)$  and  $L_0^u(\mu)$ , respectively. In the following Lemma we will denote by  $X_i$  some  $C^\infty$  extension of  $X_i$  at some neighborhood of  $\bar{A}_i$ ,  $i \in \{1, 2\}$ , and thus  $x_\mu^s(t)$  and  $x_\mu^u(t)$  are well defined for  $|t|$  small enough. The following Lemma is an adaptation of [33].

**Lemma 6.13.** *For any  $\mu_* \in \Lambda$  and any  $i \in \{1, \dots, n\}$  the maps*

$$\frac{\partial x_{\mu_*}^s}{\partial \mu_i}(t) \text{ and } \frac{\partial x_{\mu_*}^u}{\partial \mu_i}(t)$$

are bounded as  $t \rightarrow +\infty$  and  $t \rightarrow -\infty$ , respectively.

*Proof.* Let us consider a small perturbation of the parameter in the form

$$\mu = \mu_* + \varepsilon e_i, \tag{6.2}$$

where  $e_i$  is the  $i$ th vector of the canonical base of  $\mathbb{R}^r$ . The corresponding perturbation of the singularity  $p_2(\mu_*)$  takes the form

$$p_2(\mu) = p_2(\mu_*) + \varepsilon y_0 + o(\varepsilon).$$

Knowing that  $X_2(p_2(\mu), \mu) = 0$  for any  $\varepsilon$  it follows that

$$0 = \frac{\partial X_2}{\partial \varepsilon}(p_2(\mu), \mu) = DX_2(p_2(\mu), \mu)[y_0 + o(\varepsilon)] + \frac{\partial X_2}{\partial \mu}(p_2(\mu), \mu)e_i$$

and thus applying  $\varepsilon \rightarrow 0$  we obtain

$$y_0 = -F_0^{-1}G_0e_i,$$

where  $F_0 = DX_2(p_2(\mu_*), \mu_*)$  and  $G_0 = \frac{\partial X_2}{\partial \mu}(p_2(\mu_*), \mu_*)$ . Hence,

$$\frac{\partial p_2}{\partial \mu_i}(\mu_*) = -F_0^{-1}G_0e_i.$$

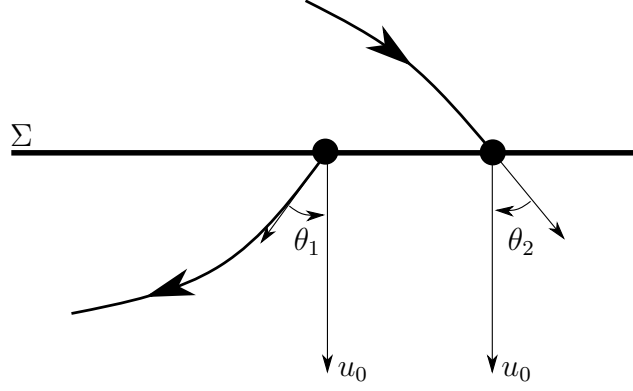


Figure 6.12: Illustration of  $\theta_s > 0$  and  $\theta_u < 0$ . Figure source: made by the author.

Therefore, it follows from the  $C^\infty$ -differentiability of the flow near  $p_2(\mu)$  that

$$\lim_{t \rightarrow -\infty} \frac{\partial x_{\mu^*}^u(t)}{\partial \mu_i} = \frac{\partial p(\mu^*)}{\partial \mu_i} = -F_0^{-1} G_0 e_i$$

and thus we have the proof for  $x_{\mu^*}^u$ . The proof for  $x_{\mu^*}^s$  is similar.  $\square$

Let  $\theta_i \in (-\pi, \pi)$  be the angle between  $X_i(x_0)$  and  $u_0$ ,  $i \in \{1, 2\}$ . See Figure 6.12. For  $i \in \{1, 2\}$  we denote by  $M_i$  the rotation matrix of angle  $\theta_i$ , i.e.

$$M_i = \begin{pmatrix} \cos \theta_i & -\sin \theta_i \\ \sin \theta_i & \cos \theta_i \end{pmatrix}.$$

Defining

$$n^u(t, \mu) = \omega_0[x_\mu^u(t) - x_0] \wedge u_0 \text{ and } n^s(t, \mu) = \omega_0[x_\mu^s(t) - x_0] \wedge u_0$$

it follows from Definition 6.11 that

$$d(\mu) = n^u(0, \mu) - n^s(0, \mu)$$

and thus

$$\frac{\partial d}{\partial \mu_j}(\mu_0) = \frac{\partial n^u}{\partial \mu_j}(0, \mu_0) - \frac{\partial n^s}{\partial \mu_j}(0, \mu_0). \quad (6.3)$$

Therefore, to understand the behavior of the displacement function  $d(\mu)$  it is enough to understand the behavior of  $x_\mu^s(t)$  and  $x_\mu^u(t)$  relatively to  $x_0$ . Let  $X_i = (P_i, Q_i)$ ,  $i \in \{1, 2\}$ . Knowing that  $\gamma_0$  is a parametrization of  $L_0$  such that  $\gamma_0(0) = x_0$  let  $L_0^+ = \{\gamma_0(t) : t > 0\} \subset A_1$  and

$$I_j^+ = \int_{L_0^+} e^{D_1(t)} \left[ (M_1 X_1) \wedge \frac{\partial X_1}{\partial \mu_j}(\gamma_0(t), \mu_0) - \sin \theta_1 R_{1,j}(\gamma_0(t), \mu_0) \right] dt,$$

where

$$D_i(t) = - \int_0^t \text{Div} X_i(\gamma_0(s), \mu_0) ds,$$

and

$$R_{i,j} = \frac{\partial P_i}{\partial \mu_j} \left[ \left( \frac{\partial Q_i}{\partial x_1} + \frac{\partial P_i}{\partial x_2} \right) Q_i + \left( \frac{\partial P_i}{\partial x_1} - \frac{\partial Q_i}{\partial x_2} \right) P_i \right] \\ + \frac{\partial Q_i}{\partial \mu_j} \left[ \left( \frac{\partial P_i}{\partial x_2} + \frac{\partial Q_i}{\partial x_1} \right) P_i + \left( \frac{\partial Q_i}{\partial x_2} - \frac{\partial P_i}{\partial x_1} \right) Q_i \right],$$

$i \in \{1, 2\}$ ,  $j \in \{1, \dots, r\}$ . The following Proposition is an adaptation of [49].

**Proposition 6.14.** For any  $j \in \{1, \dots, r\}$  it follows that

$$\frac{\partial n^s}{\partial \mu_j}(0, \mu_0) = \frac{\omega_0}{\|X_1(x_0, \mu_0)\|} I_j^+.$$

*Proof.* From now on in this proof we will denote  $X_1$  some  $C^\infty$  extension of  $X_1$  at some neighborhood of  $\overline{A_1}$  and thus  $x_\mu^s(t)$  is well define for  $|t|$  small enough. Let  $j \in \{1, \dots, r\}$ . Defining

$$\xi(t, \mu) = \frac{\partial x_\mu^s}{\partial \mu_j}(t)$$

it then follows that

$$\begin{aligned} \dot{\xi}(t, \mu) &= \frac{\partial \dot{x}_\mu^s}{\partial \mu_j}(t) \\ &= \frac{\partial X_1}{\partial \mu_j}(x_\mu^s(t), \mu) \\ &= DX_1(x_\mu^s(t), \mu)\xi(t, \mu) + \frac{\partial X_1}{\partial \mu_j}(x_\mu^s(t), \mu). \end{aligned}$$

Let  $(s, n) = (s(t, \mu), n(t, \mu))$  be the coordinate system with origin at  $x_\mu^s(t)$  such that the angle between  $X_1(x_\mu^s(t), \mu)$  and  $s$  equals  $\theta_1$  and  $n$  is orthogonal to  $s$ , pointing outwards in relation to  $G$ . See Figure 6.13. Observe that the component of  $\xi$  in the direction of  $n$

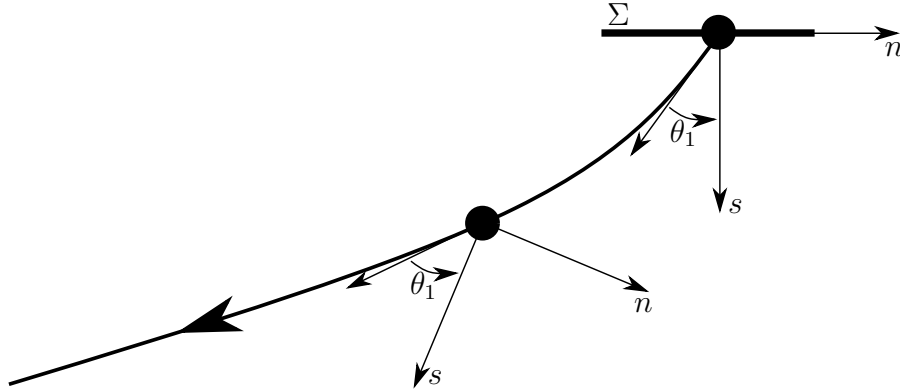


Figure 6.13: Illustration of  $(s, n)$  along  $x_\mu^s(t)$ . Figure source: made by the author.

is precisely equals to  $\frac{\partial n^s}{\partial \mu_j}(t, \mu)$  and thus we conclude

$$\frac{\partial n^s}{\partial \mu_j}(t, \mu) = \omega_0 \frac{\xi \wedge M_1 X_1(x_\mu^s(t), \mu)}{\|X_1(x_\mu^s(t), \mu)\|}. \quad (6.4)$$

Denoting  $M_1 X_1 = (P_0, Q_0)$ ,  $\xi = (\xi_1, \xi_2)$  and

$$\rho(t, \mu) = \xi \wedge M_1 X_1(x_\mu^s(t), \mu) \quad (6.5)$$

we conclude that

$$\rho = \xi_1 Q_0 - P_0 \xi_2,$$

where

$$P_0 = P_1 \cos \theta_1 - Q_1 \sin \theta_1,$$

$$Q_0 = Q_1 \cos \theta_1 + P_1 \sin \theta_1.$$

Hence,

$$\dot{\rho} = \dot{\xi}_1 Q_0 - \dot{\xi}_2 P_0 + \xi_1 \dot{Q}_0 - \xi_2 \dot{P}_0. \quad (6.6)$$

Knowing that

$$\begin{aligned} \dot{P}_1 &= \ddot{x}_1 = \frac{\partial P_1}{\partial x_1} P_1 + \frac{\partial P_1}{\partial x_2} Q_1, \\ \dot{Q}_1 &= \ddot{x}_2 = \frac{\partial Q_1}{\partial x_1} P_1 + \frac{\partial Q_1}{\partial x_2} Q_1, \end{aligned}$$

we conclude,

$$\begin{aligned} \dot{P}_0 &= \frac{\partial P_1}{\partial x_1} P_1 \cos \theta_1 + \frac{\partial P_1}{\partial x_2} Q_1 \cos \theta_1 - \frac{\partial Q_1}{\partial x_1} P_1 \sin \theta_1 - \frac{\partial Q_1}{\partial x_2} Q_1 \sin \theta_1, \\ \dot{Q}_0 &= \frac{\partial Q_1}{\partial x_1} P_1 \cos \theta_1 + \frac{\partial Q_1}{\partial x_2} Q_1 \cos \theta_1 + \frac{\partial P_1}{\partial x_1} P_1 \sin \theta_1 + \frac{\partial P_1}{\partial x_2} Q_1 \sin \theta_1. \end{aligned} \quad (6.7)$$

Replacing (6.7) in (6.6) one can conclude

$$\dot{\rho} = \text{Div} X_1 \rho - M_1 X_1 \wedge \frac{\partial X_1}{\partial \mu_j} + \sin \theta_1 R_{1,j}. \quad (6.8)$$

Solving (6.8) we obtain

$$\rho(t, \mu) e^{D_1(t)} \Big|_{t_0}^{t_1} = \int_{t_0}^{t_1} e^{D_1(t)} \left[ \sin \theta_1 R_{1,j}(x_\mu^s, \mu) - M_1 X_1 \wedge \frac{\partial X_1}{\partial \mu_j}(x_\mu^s(t), \mu) \right] dt. \quad (6.9)$$

Observe that  $X_1(x_\mu^s(t), \mu) \rightarrow 0$  as  $t \rightarrow +\infty$ . Therefore, it follows from (6.4) and (6.5) that  $\rho(t, \mu) \rightarrow 0$  as  $t \rightarrow +\infty$  (since from Lemma 6.13 we know that  $\frac{\partial n^s}{\partial \mu_j}$  is bounded). Thus, if we take  $t_0 = 0$  and let  $t_1 \rightarrow +\infty$  in (6.9) it follows that

$$\rho(0, \mu) = \int_0^{+\infty} e^{D_1(t)} \left[ M_1 X_1 \wedge \frac{\partial X_1}{\partial \mu_j}(x_\mu^s(t), \mu) - \sin \theta_1 R_{1,j}(t, \mu) \right] dt$$

and thus it follows from (6.4) and (6.5) we have that

$$\frac{\partial n^s}{\partial \mu_j}(0, \mu_0) = \frac{\omega_0}{\|X_1(x_0, \mu_0)\|} I_j^+.$$

□

**Remark 6.15.** Observe that  $L_0^+$  was defined in such a way that there is no discontinuities on it. Therefore, if  $L_0 \cap \Sigma = \{x_0\}$ , then  $L_0^- = \{\gamma_0(t) : t < 0\}$  also has no discontinuities and thus as in Proposition 6.14 one can prove that

$$\frac{\partial n^u}{\partial \mu_j}(t, \mu) = \omega_0 \frac{\bar{\rho}(t, \mu)}{\|X_2(x_\mu^u(t), \mu)\|}$$

with  $\bar{\rho}$  satisfying (6.8) but with  $x_\mu^u$  instead of  $x_\mu^s$  and  $X_2$  instead of  $X_1$ . Furthermore we have  $\bar{\rho}(t, \mu) \rightarrow 0$  as  $t \rightarrow -\infty$  and thus by setting  $t_1 = 0$  and letting  $t_0 \rightarrow -\infty$  we obtain

$$\bar{\rho}(0, \mu) = - \int_0^{+\infty} e^{D_2(t)} \left[ M_2 X_2 \wedge \frac{\partial X_2}{\partial \mu_j}(x_\mu^u(t), \mu) - \sin \theta_2 R_{2,j}(t, \mu) \right] dt.$$

Hence, in the simply case where  $L_0$  intersects  $\Sigma$  in a unique point  $x_0$  it follows from (6.3) and from Proposition 6.14 that

$$\frac{\partial d}{\partial \mu_j}(\mu_0) = -\omega_0 \left( \frac{1}{\|X_2(x_0, \mu_0)\|} I_j^- + \frac{1}{\|X_1(x_0, \mu_0)\|} I_j^+ \right),$$

with

$$\begin{aligned} I_j^+ &= \int_{L_0^+} e^{D_1(t)} \left[ (M_1 X_1) \wedge \frac{\partial X_1}{\partial \mu_j}(\gamma_0(t), \mu_0) - \sin \theta_1 R_{1,j}(\gamma_0(t), \mu_0) \right] dt, \\ I_j^- &= \int_{L_0^-} e^{D_2(t)} \left[ (M_2 X_2) \wedge \frac{\partial X_2}{\partial \mu_j}(\gamma_0(t), \mu_0) - \sin \theta_2 R_{2,j}(\gamma_0(t), \mu_0) \right] dt. \end{aligned}$$

**Remark 6.16.** If we drop the hypothesis of non-smooth vector field and suppose  $Z = X$  a planar  $C^\infty$  vector field defined in the entire  $\mathbb{R}^2$ , then all this section holds and thus we can just assume  $X_1 = X_2$  and take  $u_0 = \frac{X(x_0, \mu_0)}{\|X(x_0, \mu_0)\|}$ . In this case  $\theta_1 = \theta_2 = 0$  and therefore we conclude

$$\frac{\partial d}{\partial \mu_j}(\mu_0) = \frac{-\omega_0}{\|X(x_0, \mu_0)\|} \int_{-\infty}^{+\infty} e^{-\int_0^t \text{Div} X(\gamma_0(s), \mu_0) ds} \left[ X \wedge \frac{\partial X}{\partial \mu_j}(\gamma_0(t), \mu_0) \right] dt,$$

as in [49, 26, 22].

**Remark 6.17.** The hypothesis of a polycycle is not necessary. In fact if we drop this and suppose only a heteroclinic connection between saddles, then again all this section holds and thus we can define the displacement function as

$$d(\mu) = [x_0^u(\mu) - x_0^s(\mu)] \wedge u_0,$$

and therefore,

$$\frac{\partial d}{\partial \mu_j}(\mu_0) = - \left( \frac{1}{\|X_2(x_0, \mu_0)\|} I_j^- + \frac{1}{\|X_1(x_0, \mu_0)\|} I_j^+ \right).$$

It is only necessary to pay attention at which direction we have  $d(\mu) > 0$  or  $d(\mu) < 0$ . The inclusion of  $\omega_0$  was only to follow [49, 17] in a standardization of the external direction of the polycycle as the positive direction of the displacement function.

**Remark 6.18.** If we suppose that  $p_i$  is a tangential singularity instead of a hyperbolic saddle such that the perturbation  $Z_\mu$  of  $Z_{\mu_0}$  is such that there is a neighborhood  $B$  of  $p_i$  such that for  $\mu \in \Lambda$  we have a  $C^\infty$  map  $p_i(\mu)$  such that  $p_i(\mu)$  is  $C^\infty$ -equivalent to  $p_i$ ,  $p_i(\mu) \rightarrow p_i$  as  $\mu \rightarrow \mu_0$  and  $B$  is free of any other singularity and tangential singularity other than  $p_i(\mu)$ , then one can apply the Implicit Function Theorem at the orbit  $x^s(t, \mu)$  through the point  $p_i(\mu)$  and obtain once again Lemma 6.10. Therefore, the displacement map

$$d(\mu) = \omega_0 [x_0^u(\mu) - x_0^s(\mu)] \wedge u_0$$

is well defined and of class  $C^\infty$  whether  $p_i$  is a hyperbolic saddle or a tangential singularity satisfying the above conditions.

**Proposition 6.19.** *Let  $p_1$  be a tangential singularity satisfying the above hypothesis. Then for any  $j \in \{1, \dots, r\}$  it follows that*

$$\frac{\partial n^s}{\partial \mu_j}(0, \mu_0) = \frac{\omega_0}{\|X_1(x_0, \mu_0)\|} (I_j^+ + H_j^+),$$

where

$$H_j^+ = e^{D_1(t_1)} \frac{\partial \gamma_0}{\partial \mu_j}(t_1) \wedge M_1 X_1(p_1, \mu_0),$$

with  $\gamma_0$  a parametrization of  $L_0$  such that  $\gamma_0(0) = x_0$  and  $\gamma_0(t_1) = p_1$ .

*Proof.* It follows from Proposition 6.14 that

$$\frac{\partial n^s}{\partial \mu_j}(t, \mu) = \omega_0 \frac{\rho(t, \mu)}{\|X_1(x_\mu^s(t), \mu)\|},$$

with

$$\rho(t, \mu) = \xi \wedge M_1 X_1(x_\mu^s(t), \mu)$$

satisfying

$$\rho(t, \mu) e^{D_1(t)} \Big|_{t_0}^{t_1} = \int_{t_0}^{t_1} e^{D_1(t)} \left[ \sin \theta_1 R_{1,j}(x_\mu^s, \mu) - M_1 X_1 \wedge \frac{\partial X_1}{\partial \mu_j}(x_\mu^s(t), \mu) \right] dt. \quad (6.10)$$

Let  $t_0 = 0$ ,  $t_1$  be such that  $\gamma_0(t_1) = p_1$  and  $L_0^+ = \{\gamma_0(t) : 0 < t < t_1\}$ . Then it follows from (6.10) that

$$\rho(0, \mu_0) = I_j^+ + e^{D_1(t_1)} \rho(t_1, \mu_0).$$

Thus, the result follows from the fact that  $H_j^+ = e^{D_1(t_1)} \rho(t_1, \mu_0)$ .  $\square$

The hypothesis over the perturbation ensuring the existence of a  $C^\infty$  function  $p_i(\mu)$  for  $\mu \in \Lambda$  such that  $p_i(\mu)$  and  $p_i$  are  $C^\infty$ -equivalent seems to be too strong and, in fact it, is. But as we shall see in further sections, this hypothesis will not be a problem here because we will take perturbations that are suitable for our goals. In fact, we will construct perturbations that play no role near any tangential singularity. Nevertheless, we point out the fact that *regular-quadratic* tangential singularities, i.e. a tangential singularities such that  $n_u = 2$  and  $n_s = 1$  or vice-versa, satisfies this hypothesis for any small enough perturbation. The following Proposition is an adaptation of [49].

**Proposition 6.20.** *Under the hypotheses of this section, suppose that  $\frac{\partial d}{\partial \mu_1}(\mu_0) \neq 0$ , with  $\mu_0 = (\bar{\mu}_1, \dots, \bar{\mu}_r)$ . Then given  $\varepsilon > 0$  there exists  $\delta > 0$  and a unique  $C^\infty$  function  $h(\mu_2, \dots, \mu_r)$  for  $|\mu_j - \bar{\mu}_j| < \delta$ ,  $j \in \{2, \dots, r\}$ , with  $h(\bar{\mu}_2, \dots, \bar{\mu}_r) = \bar{\mu}_1$ , such that system  $Z$  with  $\mu_1 = h(\mu_2, \dots, \mu_r)$  has a unique heteroclinic connection in an  $\varepsilon$ -neighborhood of  $L_0$ ; i.e.  $Z$  has a unique, local,  $(r - 1)$ -dimensional heteroclinic connection bifurcation surface  $S : \mu_1 = h(\mu_2, \dots, \mu_r)$  through the point  $\mu_0 \in \mathbb{R}^r$ .*

*Proof.* Applying the Implicit Function Theorem at  $d$  we have the existence of  $h(\mu_2, \dots, \mu_r)$  of class  $C^\infty$  in a neighborhood of  $(\bar{\mu}_2, \dots, \bar{\mu}_r)$  such that  $d(h(\mu_2, \dots, \mu_r), \mu_2, \dots, \mu_r) = 0$ . Therefore, if  $\mu_1 = h(\mu_2, \dots, \mu_r)$ , then  $x_0^s(\mu) = x_0^u(\mu)$  and thus the heteroclinic connection  $L_0(\mu)$  can be parametrized by  $x_\mu^u$  for  $t \leq 0$  and by  $x_\mu^s$  for  $t \geq 0$ . Inside of each  $\bar{A}_i$  we can apply the continuity of solutions with respect to the initial conditions and thus

$$\lim_{\mu \rightarrow \mu_0} x_\mu^s(t) = \gamma_0(t), \text{ for } t \geq 0,$$

$$\lim_{\mu \rightarrow \mu_0} x_\mu^u(t) = \gamma_0(t), \text{ for } t \leq 0,$$

with the convergence being uniform on any compact time interval  $-a \leq t \leq 0$  (or  $0 \leq t \leq a$ ). And according to the Stable Manifold Theorem, in the case where  $p_i$  is a hyperbolic

saddle, for sufficiently large  $a > 0$  the limits above are uniform for all  $t$ . Thus, given  $\varepsilon > 0$  there exist a  $\delta > 0$  such that for  $t \in \mathbb{R}$  and  $\|\mu - \mu_0\| < \delta$ ,  $\mu = (h(\mu_2, \dots, \mu_r), \mu_2, \dots, \mu_r)$ , we have both  $\|x_\mu^s(t) - \gamma_0(t)\| < \varepsilon$  and  $\|x_\mu^u(t) - \gamma_0(t)\| < \varepsilon$ , i.e. the heteroclinic connection  $L_0(\mu)$  is in a  $\varepsilon$ -neighborhood of  $\Gamma_0$ . The uniqueness of  $L_0(\mu)$  follows from the uniqueness of  $h$ .  $\square$

**Remark 6.21.** Observe that in the former proposition we could have supposed  $\frac{\partial d}{\partial \mu_j}(\mu_0) \neq 0$  for any  $j \in \{1, \dots, r\}$ . In fact, we supposed  $\frac{\partial d}{\partial \mu_1}(\mu_0) \neq 0$  only to simplify the notation.

**Proposition 6.22.** *Let  $Z$  and  $\Gamma^n$  be as in Section 6.2 and  $d_i : \Lambda \rightarrow \mathbb{R}$ ,  $i \in \{1, \dots, n\}$ , be the displacement maps defined at the heteroclinic connections of  $\Gamma^n$ . Let  $\sigma_0 \in \{-1, 1\}$  be a constant such that  $\sigma_0 = 1$  (resp.  $\sigma_0 = -1$ ) if the Poincaré map is defined in the bounded (resp. unbounded) region delimited by  $\Gamma^n$ . Then following statements holds.*

- (a) *If  $p(\Gamma^n) > 1$  and  $\mu \in \Lambda$  is such that  $\sigma_0 d_1(\mu) \leq 0, \dots, \sigma_0 d_n(\mu) \leq 0$  with  $\sigma_0 d_i(\mu) < 0$  for some  $i \in \{1, \dots, n\}$ , then at least one stable limit cycle  $\Gamma$  bifurcates from  $\Gamma^n$ .*
- (b) *If  $p(\Gamma^n) < 1$  and  $\mu \in \Lambda$  is such that  $\sigma_0 d_1(\mu) \geq 0, \dots, \sigma_0 d_n(\mu) \geq 0$  with  $\sigma_0 d_i(\mu) > 0$  for some  $i \in \{1, \dots, n\}$ , then at least one unstable limit cycle  $\Gamma$  bifurcates from  $\Gamma^n$ .*

*Proof.* For the simplicity we will use the same polycycle  $\Gamma^3$  used in the proof of Theorem 6.4. Let  $x_{i,0} \in L_i$  be as in Section 6.2 and  $l_i$  be transversal sections of  $L_i$  through  $x_{i,0}$ ,  $i \in \{1, 2, 3\}$ . Let  $R_i : l_i \times \Lambda \rightarrow l_{i-1}$  be functions given by the compositions of the functions used in the demonstration of Theorem 6.4,  $i \in \{1, 2, 3\}$ . See Figure 6.14(a). Hence, if  $d_i(\mu) \leq 0$ ,  $i \in \{1, 2, 3\}$ , then a new Poincaré map  $P : l_1 \times \Lambda \rightarrow l_1$  can be written as

$$P(x, \mu) = R_3(R_2(R_1(x, \mu), \mu), \mu).$$

We observe that  $P$  is  $C^\infty$  in  $x$ , continuous in  $\mu$ , and it follows from the proof of Theorem 6.4 that  $P(\cdot, \mu_0)$  is non-flat. It follows from Theorem 6.4 that there is an open ring  $A_0$  in

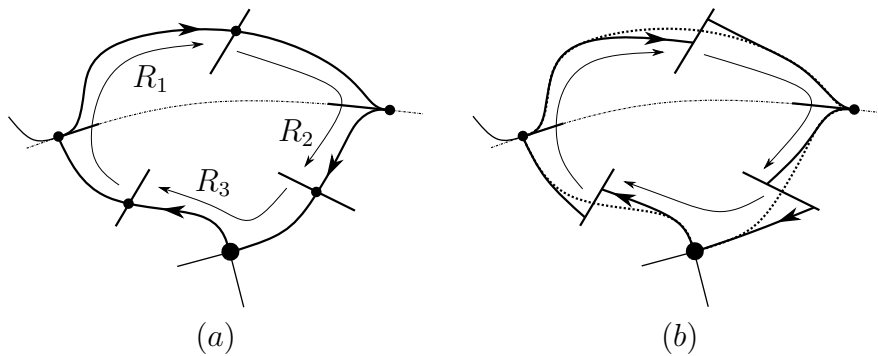


Figure 6.14: Illustration of  $R_1$ ,  $R_2$  and  $R_3$  with  $d_i(\mu) = 0$  in (a), and  $d_i(\mu) < 0$  in (b). Observe that if  $d_i(\mu) > 0$ , then the composition may not be well defined. Figure source: made by the author.

the bounded region limited by  $\Gamma^3$ , with  $\Gamma^3$  as the connect external boundary of  $A_0$ , such that the orbit  $\Gamma$  through any point  $q \in A_0$  spiral towards  $\Gamma^3$  as  $t \rightarrow +\infty$ . Let  $p$  be the interception of  $\Gamma^3$  and  $l_1$ ,  $q_0 \in A_0 \cap l_1$ ,  $\xi$  a coordinate system along  $l_1$  such that  $\xi = 0$  at  $p$  and  $\xi > 0$  at  $q_0$  and let we identify this coordinate system with  $\mathbb{R}_+$ . Observe that  $P(q_0, \mu_0) < q_0$  and thus by continuity  $P(q_0, \mu) < q_0$  for any  $\mu \in \Lambda$ . See Figure 6.15.

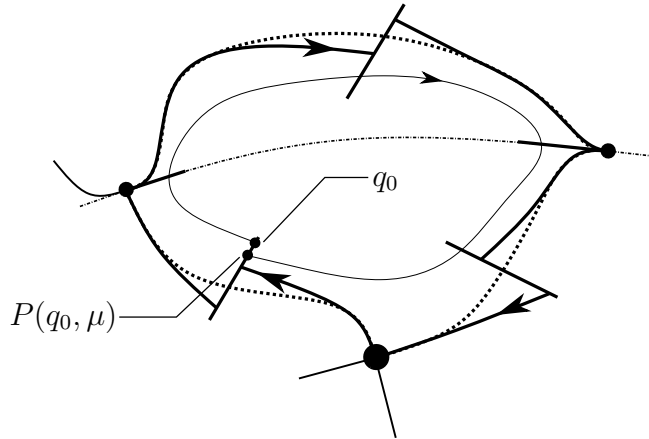


Figure 6.15: Observe that the arc of orbit between  $q_0$  and  $P(q_0, \mu)$  together with the perturbation of  $\Gamma^3$  creates a positive invariant set in which we can apply the Poincaré-Bendixson theory. Figure source: made by the author.

Therefore, it follows from the Poincaré-Bendixson theory for non-smooth vector field (see [10]) and from the non-flatness of  $P$  that at least one stable limit cycle  $\Gamma_0$  bifurcates from  $\Gamma^3$ . Statement (b) can be prove by time reversing.  $\square$

### 6.6 The further displacement map

Let  $Z$  and  $\Gamma^n$  be as in Section 6.2. Let  $L_i^u(\mu)$  and  $L_i^s(\mu)$  be the perturbations of  $L_i$  such that  $\alpha(L_i^u) = p_{i+1}$  and  $\omega(L_i^s) = p_i$ ,  $i \in \{1, \dots, n\}$ , with each index being modulo  $n$ . Following [23], let  $C_i = x_{i,0}$ . If  $C_i \notin \Sigma$ , then let  $v_i$  be the unique unitarian vector orthogonal to  $Z(C_i, \mu_0)$  and pointing outwards in relation to  $\Gamma^n$ . Now, if  $C_i \in \Sigma$ , then let  $v_i$  be the unique unitarian vector tangent to  $T_{C_i}\Sigma$  and pointing outwards in relation to  $\Gamma^n$ . In both cases, let  $l_i$  be the transversal section normal to  $L_i$  at  $C_i$ . It is clear that any point  $B \in l_i$  can be written as  $B = C_i + \lambda v_i$ , with  $\lambda \in \mathbb{R}$ . See Figure 6.16.

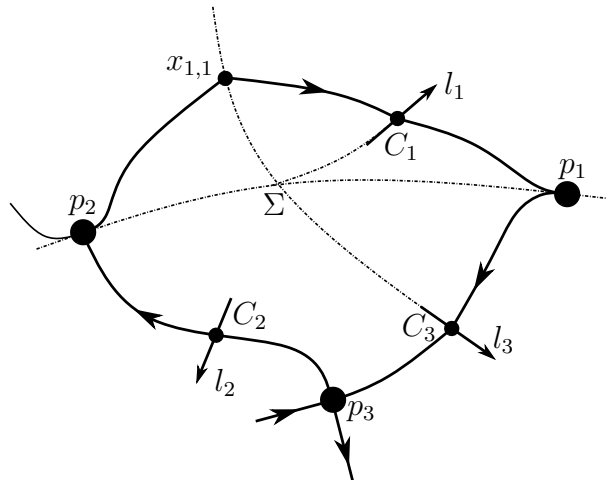


Figure 6.16: An example of the construction of the points  $C_i$  and the lines  $l_i$ . Figure source: made by the author.

Now, if  $C_i \in \Sigma$ , then let  $N_i$  be a small enough neighborhood of  $C_i$  and  $J_i = N_i \cap \Sigma$ . It then follows that any point  $B \in J_i$  can be orthogonally projected on the line  $l_i : C_i + \lambda v_i$ ,  $\lambda \in \mathbb{R}$ , and thus it can be uniquely, and smoothly, identified with  $C_i + \lambda_B v_i$ , for some  $\lambda_B \in \mathbb{R}$ . Either  $C_i \in \Sigma$  or  $C_i \notin \Sigma$ , observe that if  $\lambda > 0$ , then  $B$  is outside  $\Gamma^n$  and if  $\lambda < 0$ , then  $B$  is inside  $\Gamma^n$ . For each  $i \in \{1, \dots, n\}$  we define

$$B_i^u = L_i^u \cap l_i = C_i + b_i^u(\mu)v_i, \quad B_i^s = L_i^s \cap l_i = C_i + b_i^s(\mu)v_i. \quad (6.11)$$

Therefore, it follows from Section 6.5 that

$$d_i(\mu) = b_i^u(\mu) - b_i^s(\mu),$$

$i \in \{1, \dots, n\}$ . Also, define  $r_i = \frac{|\nu_i(\mu_0)|}{\lambda_i(\mu_0)}$  if  $p_i$  is a hyperbolic saddle, and  $r_i = \frac{n_{i,u}}{n_{i,s}}$  if  $p_i$  is a tangential singularity,  $i \in \{1, \dots, n\}$ . If  $r_i > 1$  and  $d_i(\mu) < 0$ , then following [23], we observe that

$$B_{i-1}^* = L_i^u \cap l_{i-1} = C_{i-1} + b_{i-1}^*(\mu)v_{i-1}$$

is well defined and thus we define the *further displacement map* as

$$d_{i-1}^*(\mu) = b_{i-1}^*(\mu) - b_{i-1}^s(\mu).$$

See Figure 6.17. On the other hand, if  $r_i < 1$  and  $d_{i-1}(\mu) > 0$ , then

$$B_i^* = L_{i-1}^s \cap l_i = C_i + b_i^*(\mu)v_i$$

is well defined and thus we define the *further displacement map* as

$$d_{i-1}^*(\mu) = b_i^u(\mu) - b_i^*(\mu).$$

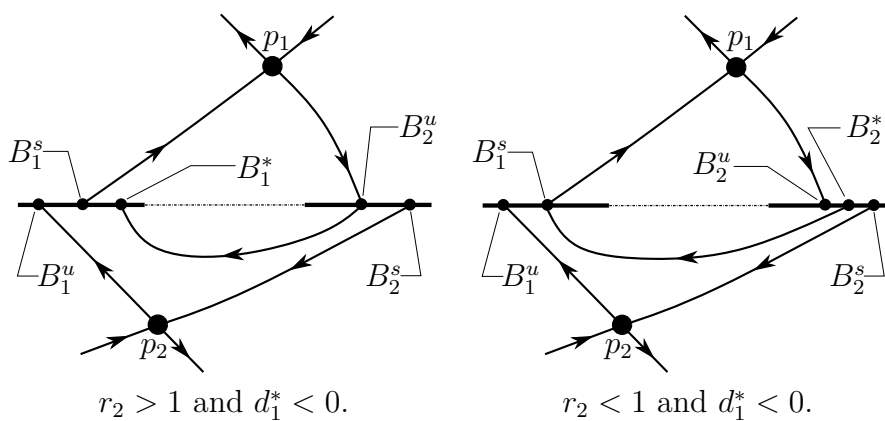


Figure 6.17: Illustration of  $d_1^* < 0$  for both  $r_2 > 1$  and  $r_2 < 1$ . Figure source: made by the author.

**Remark 6.23.** We observe that in both cases  $r_i < 1$  and  $r_i > 1$  we have that  $d_{i-1}(\mu) > 0$  and  $d_i(\mu) < 0$  are necessary conditions for  $d_{i-1}^*(\mu) = 0$ . Furthermore, observe that the signal of  $d_{i-1}^*$  has the same topological meaning whether  $r_i < 1$  or  $r_i > 1$ .

The following Proposition is an adaptation of [23].

**Proposition 6.24.** For  $i \in \{1, \dots, n\}$  and  $\Lambda \subset \mathbb{R}^r$  small enough we have

$$d_{i-1}^*(\mu) = \begin{cases} d_{i-1}(\mu) + O(\|\mu - \mu_0\|^{r_i}) & \text{if } r_i > 1, \\ d_i(\mu) + O(\|\mu - \mu_0\|^{\frac{1}{r_i}}) & \text{if } r_i < 1. \end{cases}$$

*Proof.* For simplicity let us assume  $i = n$  and  $r_n > 1$ . Following [23], it follows from the definition of  $d_{n-1}^*$  and  $d_{n-1}$  that

$$d_{n-1}^* = (b_{n-1}^* - b_{n-1}^u) + d_{n-1}. \quad (6.12)$$

Let  $B = B_n^s + \lambda v_n \in l_n$ ,  $\lambda < 0$ , with  $|\lambda|$  small enough and observe that the orbit through  $B$  will intersect  $l_{n-1}$  in a point  $C$  which can be written as

$$C = B_{n-1}^u + F(\lambda, \mu)v_{n-1}.$$

Therefore, we have a function  $F : l_n \rightarrow l_{n-1}$  with  $F(\lambda, \mu) < 0$  for  $\lambda < 0$ ,  $|\lambda|$  small enough, such that  $F(\lambda, \mu) \rightarrow 0$  as  $\lambda \rightarrow 0$ . From (6.11) we have

$$\begin{aligned} B_n^u &= (C_n + b_n^s v_n) + (b_n^u - b_n^s)v_n = B_n^s + d_n v_n \\ B_{n-1}^* &= (C_{n-1} + b_{n-1}^u v_{n-1}) + (b_n^* - b_{n-1}^u)v_{n-1} = B_{n-1}^u + (b_n^* - b_{n-1}^u)v_{n-1}. \end{aligned} \quad (6.13)$$

Since  $B_{n-1}^*$  is the intersection of the positive orbit through  $B_n^u$  with  $l_{n-1}$ , it follows from (6.13) that

$$b_n^* - b_{n-1}^u = F(d_n, \mu).$$

Therefore, it follows from (6.12) that

$$d_{n-1}^* = F(d_n, \mu) + d_{n-1}. \quad (6.14)$$

If  $p_i$  is a hyperbolic saddle, then  $F$  is, up to the composition of some diffeomorphisms given by the flow of the components of  $Z$ , the Dulac map  $D_i$  defined at Section 2.8. If  $p_i$  is a tangential singularity (we remember that we are under the hypothesis of Remark 6.18), then  $F$  is, up to the composition of some diffeomorphisms given by the flow of the components of  $Z$ , the composition  $T_i^u \circ (T_i^s)^{-1}$  defined at Section 6.3. In either case it follows that

$$-F(\lambda, \mu) = |\lambda|^{r_n} (A(\mu) + O(1)), \quad (6.15)$$

with  $A(\mu_0) \neq 0$ . Since  $d_n = O(\|\mu\|)$  it follows from (6.15) that

$$F(d_n, \mu) = O(\|\mu\|^{r_n})$$

and thus from (6.14) we have the result. The case  $r_n < 1$  follows similarly from the fact that the inverse  $F^{-1}$  has order  $r_n^{-1}$  in  $\lambda$ .  $\square$

**Corollary 6.25.** For each  $i \in \{1, \dots, n\}$  the further displacement map  $d_i^*$  is continuous differentiable with the  $j$ -partial derivative given either by the  $j$ -partial derivative of  $d_i$  or  $d_{i+1}$ . Furthermore, a connection between  $p_i$  and  $p_{i-2}$  exists if and only if  $d_{i-2}^*(\mu) = 0$  and  $d_{i-1}(\mu) \neq 0$ .

### 6.7 Proof of theorem 6.8

*Proof of Theorem 6.8.* Let  $Z = (X_1, \dots, X_M)$  and denote  $X_i = (P_i, Q_i)$ ,  $i \in \{1, \dots, M\}$ . Let  $\{p_1, \dots, p_n\}$  be the singularities of  $\Gamma^n$  and  $L_i$  the heteroclinic connections between them such that  $\omega(L_i) = p_i$  and  $\alpha(L_i) = p_{i+1}$ . If  $L_i \cap \Sigma = \emptyset$ , then take  $x_{i,0} \in L_i$  and  $\gamma_i(t)$  a parametrization of  $L_i$  such that  $\gamma_i(0) = x_{i,0}$ . If  $L_i \cap \Sigma \neq \emptyset$ , then let  $L_i \cap \Sigma = \{x_{i,0}, \dots, x_{i,n(i)}\}$  and take  $\gamma_i(t)$  a parametrization of  $L_i$  such that  $\gamma_i(t_{i,j}) = x_{i,j}$  with  $0 = t_{i,0} > t_{i,1} > \dots > t_{i,n(i)}$ . In either case denote  $L_i^+ = \{\gamma_i(t) : t > 0\}$  if  $p_i$  is a hyperbolic saddle or  $L_i^+ = \{\gamma_i(t) : 0 < t < t_i\}$ , where  $t_i$  is such that  $\gamma_i(t_i) = p_i$ , if  $p_i$  is a  $\Sigma$ -singularity. Following [23], for each  $i \in \{1, \dots, n\}$  let  $G_{i,j}$ ,  $j \in \{1, 2\}$ , be two compact disks small enough such that

- 1)  $\Gamma^n \cap G_{i,j} = L_i^+ \cap G_{i,j} \neq \emptyset$ ,  $j \in \{1, 2\}$ ;
- 2)  $G_{i,1} \subset \text{Int}G_{i,2}$ ;
- 3)  $G_{i,2} \cap G_{s,2} = \emptyset$  for any  $i \neq s$ ;
- 4)  $G_{i,j} \cap \Sigma = \emptyset$ .

Let  $k_i : \mathbb{R}^2 \rightarrow [0, 1]$  be a  $C^\infty$ -bump function such that

$$k_i(x) = \begin{cases} 0, & x \notin G_{i,2}, \\ 1, & x \in G_{i,1}. \end{cases}$$

See Figure 6.18. Let  $\mu \in \mathbb{R}^n$  and  $g_i : \mathbb{R}^2 \rightarrow \mathbb{R}^2$ ,  $i \in \{1, \dots, n\}$ , be maps that we yet have

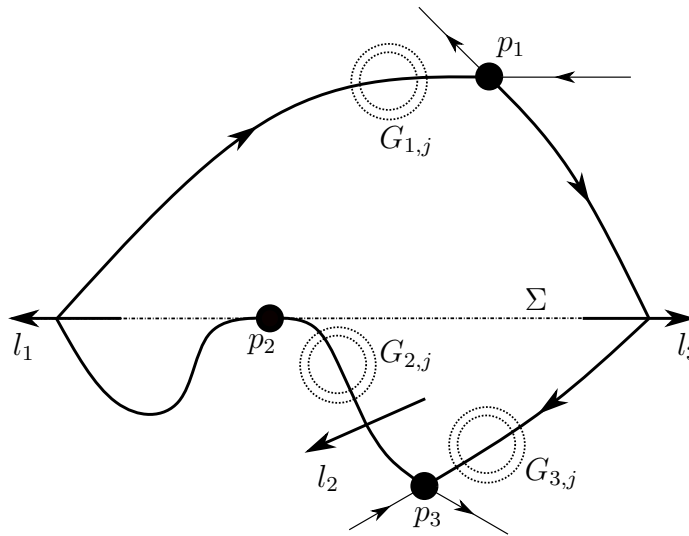


Figure 6.18: Illustration of the sets  $G_{i,j}$ . Figure source: made by the author.

to define. Let also

$$g(x, \mu) = \sum_{i=1}^n \mu_i k_i(x) g_i(x),$$

and for now one let us denote  $X_i = X_i + g$ . Let  $\Lambda$  be a small enough neighborhood of the origin of  $\mathbb{R}^n$ . It follows from Section 6.5 that each displacement map  $d_i : \Lambda \rightarrow \mathbb{R}$  controls the bifurcations of  $L_i$  near  $x_{i,0}$ . It follows from Definition 6.11 that

$$d_i(\mu) = \omega_0[x_{i,0}^u(\mu) - x_{i,0}^s(\mu)] \wedge \eta_i,$$

where  $\eta_i$  is the analogous of  $u_0$  in Figure 6.9. But from the definition of  $g$  we have that each  $x_{i,0}^u(\mu)$  does not depend on  $\mu$  and thus  $x_{i,0}^u \equiv x_{i,0}$ . Furthermore it follows from the definition of  $k_i$  that each singularity  $p_i$  of  $\Gamma^n$  also does not depend on  $\mu$  and thus  $\frac{\partial \gamma_i}{\partial \mu_j}(t_i) = 0$  for every tangential singularity  $p_i$ . Therefore, it follows from Propositions 6.14 and 6.19 that

$$\frac{\partial d_i}{\partial \mu_j}(0) = -\frac{\omega_0}{\|X_i(x_0, \mu_0)\|} \int_{L_i^+} e^{D_i(t)} \left[ (M_i X_i) \wedge \frac{\partial X_i}{\partial \mu_j}(\gamma_i(t), 0) - \sin \theta_i R_{i,j}(\gamma_i(t), 0) \right] dt,$$

with

$$D_i(t) = -\int_0^t \text{Div} X_i(\gamma_0(s), \mu_0) ds,$$

and

$$\begin{aligned} R_{i,j} &= \frac{\partial P_i}{\partial \mu_j} \left[ \left( \frac{\partial Q_i}{\partial x_1} + \frac{\partial P_i}{\partial x_2} \right) Q_i + \left( \frac{\partial P_i}{\partial x_1} - \frac{\partial Q_i}{\partial x_2} \right) P_i \right] \\ &+ \frac{\partial Q_i}{\partial \mu_j} \left[ \left( \frac{\partial P_i}{\partial x_2} + \frac{\partial Q_i}{\partial x_1} \right) P_i + \left( \frac{\partial Q_i}{\partial x_2} - \frac{\partial P_i}{\partial x_1} \right) Q_i \right], \end{aligned}$$

$i, j \in \{1, \dots, n\}$ . We observe that if  $L_i \cap \Sigma = \emptyset$ , then  $\theta_i = 0$ . It follows from the definition of the sets  $G_{i,j}$  that  $\frac{\partial d_i}{\partial \mu_j}(0) = 0$  if  $i \neq j$ . Let  $M_i X_i = (\bar{P}_i, \bar{Q}_i)$  and  $R_{i,i} = \frac{\partial P_i}{\partial \mu_i} F_{i,1} + \frac{\partial Q_i}{\partial \mu_i} F_{i,2}$ , where

$$\begin{aligned} F_{i,1} &= \left( \frac{\partial Q_i}{\partial x_1} + \frac{\partial P_i}{\partial x_2} \right) Q_i + \left( \frac{\partial P_i}{\partial x_1} - \frac{\partial Q_i}{\partial x_2} \right) P_i, \\ F_{i,2} &= \left( \frac{\partial P_i}{\partial x_2} + \frac{\partial Q_i}{\partial x_1} \right) P_i + \left( \frac{\partial Q_i}{\partial x_2} - \frac{\partial P_i}{\partial x_1} \right) Q_i. \end{aligned}$$

Let  $g_i = (g_{i,1}, g_{i,2})$  and observe that

$$(M_i X_i) \wedge \frac{\partial X_i}{\partial \mu_i} - \sin \theta_i R_{i,i} = k_i [g_{i,2}(\bar{P}_i - \sin \theta_i F_{i,2}) - g_{i,1}(\bar{Q}_i + \sin \theta_i F_{i,1})].$$

Therefore, if we take  $g_i = -\omega_0(-\bar{Q}_i - \sin \theta_i F_{i,1}, \bar{P}_i - \sin \theta_i F_{i,2})$ , then we can conclude that

$$d_i(\mu) = a_i \mu_i + O(\|\mu\|^2), \quad (6.16)$$

with  $a_i = \frac{\partial d_i}{\partial \mu_i}(0) > 0$ ,  $i \in \{1, \dots, n\}$ . If  $n = 1$ , then it follows from Proposition 6.22 that any  $\mu \in \mathbb{R}$  arbitrarily small such that  $(R_1 - 1)\sigma_0 \mu < 0$  result in the bifurcation of at least one limit cycle. Suppose  $n \geq 2$  and that the result had been proved in the case  $n - 1$ . We will now prove by induction in  $n$ . For definiteness we can assume  $R_n > 1$  and therefore  $R_{n-1} < 1$  and thus  $r_n > 1$ . Moreover it follows from Theorem 6.4 that  $\Gamma^n$  is stable. Define

$$D = (d_1, \dots, d_{n-2}, d_{n-1}^*).$$

It follows from Proposition 6.24 and from (6.16) that we can apply the Implicit Function Theorem on  $D$  and thus obtain unique  $C^\infty$  functions  $\mu_i = \mu_i(\mu_n)$ ,  $\mu_i(0) = 0$ ,  $i \in \{1, \dots, n-1\}$ , such that

$$D(\mu_1(\mu_n), \dots, \mu_{n-1}(\mu_n), \mu_n) = 0$$

for  $|\mu_n|$  small enough. It also follows from (6.16) that  $d_n \neq 0$  if  $\mu_n \neq 0$ , with  $|\mu_n|$  small enough. Therefore, if  $\mu_i = \mu_i(\mu_n)$  and  $\mu_n \neq 0$ , then it follows from the definition of  $D = 0$  that there exist a  $\Gamma^{n-1} = \Gamma^{n-1}(\mu_n)$  polycycle formed by  $n - 1$  singularities and  $n - 1$  heteroclinic connections  $L_i^* = L_i^*(\mu_n)$  such that

- 1)  $\Gamma^{n-1} \rightarrow \Gamma^n$ ,
- 2)  $L_{n-1}^* \rightarrow L_n \cup L_{n-1}$  and
- 3)  $L_i^* \rightarrow L_i, i \in \{1, \dots, n-2\}$ ,

as  $\mu_n \rightarrow 0$ . See Figure 6.19.

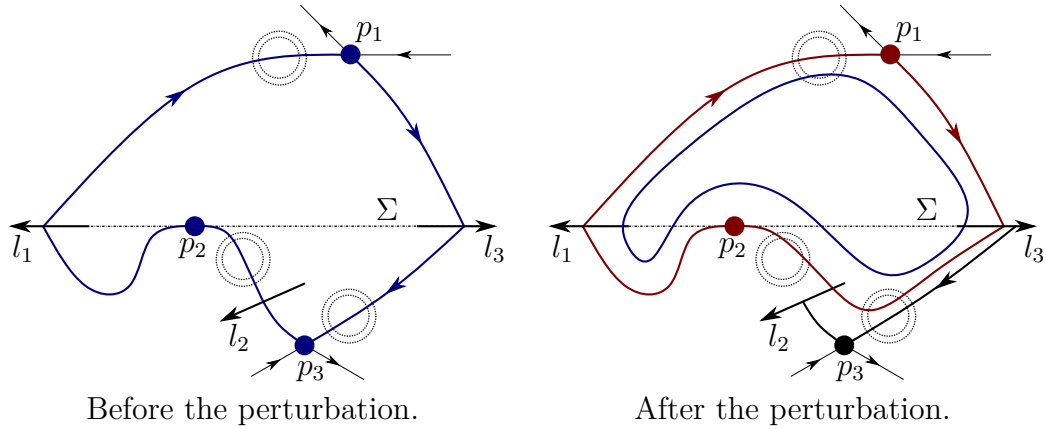


Figure 6.19: Illustration of the induction process with  $R_3 > 1$  and  $R_2 < 1$ . Blue (resp. red) means a stable (resp. unstable) polycycle or limite cycle. Figure source: made by the author.

Let

$$R_j^* = r_1 \dots r_j \Big|_{\mu_i = \mu_i(\mu_n), i \in \{1, \dots, n-1\}}$$

$j \in \{1, \dots, n-1\}$ . Then it follows from the hypothesis

$$(R_i - 1)(R_{i+1} - 1) < 0$$

for  $i \in \{1, \dots, n-1\}$  and from the hypothesis  $R_{n-1} < 1$ , that

$$(R_i^* - 1)(R_{i+1}^* - 1) < 0$$

for  $i \in \{1, \dots, n-2\}$  and  $R_{n-1}^* < 1$  for  $\mu_n \neq 0$  small enough. Thus, it follows from Theorem 6.4 that  $\Gamma^{n-1}$  is unstable while  $\Gamma^n$  is stable. It then follows from the Poincaré-Bendixson theory (see [10]) and from the non-flats of the Poincaré map that at least one stable limit cycle  $\bar{\gamma}_n(\mu_n)$  exists near  $\Gamma^{n-1}$ . In fact both the limit cycle and  $\Gamma^{n-1}$  bifurcates from  $\Gamma^n$ . Now fix  $\mu_n \neq 0$ ,  $|\mu_n|$  arbitrarily small, and define the non-smooth system

$$Z_0^* = Z^*(x) + g^*(x, \bar{\mu}),$$

where  $Z^*(x) = Z(x) + g(x, \mu_1(\mu_n), \dots, \mu_{n-1}(\mu_n), \mu_n)$  and

$$g^*(x, \bar{\mu}) = \sum_{i=1}^{n-1} \bar{\mu}_i k_i(x) g_i(x),$$

with  $\bar{\mu}_i = \mu_i - \mu_i(\mu_n)$ . It then follows by the definitions of  $G_{i,j}$  and  $L_i^*$  that

$$\Gamma^{n-1} \cap G_{i,j} = (L_i^*)^+ \cap G_{i,j} \neq \emptyset,$$

$i \in \{1, \dots, n - 1\}$  and  $j \in \{1, 2\}$ . In this new parameter coordinate system the bump functions  $k_i$  still ensures that  $\frac{\partial d_i}{\partial \mu_j}(\mu) = 0$  if  $i \neq j$ . Since  $a_i > 0$  it also follows that at the origin of this new coordinate system we still have  $\frac{\partial d_i}{\partial \mu_i}(0) > 0$ . Therefore, it follows by induction that at least  $n - 1$  crossing limit cycles  $\bar{\gamma}_j(\bar{\mu})$ ,  $j \in \{1, \dots, n - 1\}$ , bifurcates near  $\Gamma^{n-1}$  for arbitrarily small  $|\bar{\mu}|$ . We observe that  $\bar{\gamma}_n(\mu_n)$  persists for  $\bar{\mu}$  small enough.  $\square$

### 6.8 Proof of theorem 6.9

Let  $Z_0 = (X_1, X_2)$  be a planar non-smooth vector field with a discontinuity  $\Sigma = h^{-1}(0)$  and  $\Gamma = \Gamma^2$  be a polycycle composed by a hyperbolic saddle  $p_1 \in A_1$  and a regular-quadratic tangential singularity  $p_2 \in \Sigma$  such that  $n_u = 2$  and  $n_s = 1$ . Let also  $L_1$  and  $L_2$  be the heteroclinic connections such that  $\omega(L_i) = p_i$ ,  $i \in \{1, 2\}$ , and without loss of generality let us suppose  $L_1 \cap \Sigma = \{x_{1,0}\}$  and  $L_2 \cap \Sigma = \emptyset$ . See Figure 6.20(a). Following Section 6.5 we take any point  $x_{2,0} \in L_2$  and any small enough neighborhood  $U$  of  $Z_0$  and define the displacement maps  $d_i : U \rightarrow \mathbb{R}$  near the point  $x_{i,0}$ ,  $i \in \{1, 2\}$ . Since  $p_1$  and  $p_2$  are both structural stable it follows from the previous sections that to describe any small enough bifurcation of  $\Gamma$  it is enough to look at the two parameters  $\beta = (\beta_1, \beta_2) \in \mathbb{R}^2, 0$  given by  $\beta_i = d_i(Z)$ ,  $i \in \{1, 2\}$ . See Figure 6.20(b). Let  $\nu < 0 < \lambda$  be the eigenvalues of  $p_1 = p_1(Z_0)$  and  $r_1 = \frac{|\nu|}{\lambda}$  the hyperbolicity ratio of  $p_1$ .

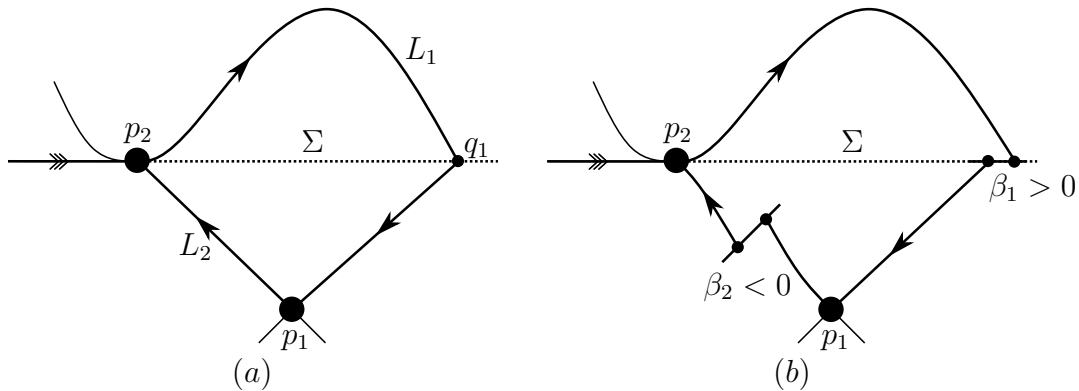


Figure 6.20: Illustration of  $\Gamma$  unperturbed (a) and perturbed (b). Figure source: made by the author.

**Lemma 6.26.** *If  $(\beta_1, \beta_2) \in \mathbb{R}^2$  is close enough to the origin, then following statements holds.*

- (a) *If  $r_1 > 1$ , then the cyclicity of  $\Gamma$  is one and when a limit cycle bifurcate from  $\Gamma$  it is hyperbolic and stable;*
- (b) *If  $\frac{1}{2} < r_1 < 1$ , then the following statements holds:*
  - (i) *The cyclicity of  $\Gamma$  is two and when two limit cycles bifurcates from  $\Gamma$ , then both are hyperbolic and the inner one is stable while the outer one is unstable;*
  - (ii) *Let  $\beta^* = (\beta_1^*, \beta_2^*)$ ,  $\beta_1^* > 0$ , be such that two limit cycles exists. Then  $\beta_2^* < 0$  and there exists at least one  $\bar{\beta}_2 \in (\beta_2^*, 0)$  such that a saddle-node bifurcation happens between these two limit cycles at  $\beta = (\beta_1^*, \bar{\beta}_2)$ ;*

(c) If  $r_1 < \frac{1}{2}$ , then the following statement holds:

- (i) The cyclicity of  $\Gamma$  is two and when two limit cycles bifurcate from  $\Gamma$ , then both are hyperbolic and the inner one is unstable while the outer one is stable;
- (ii) Let  $\beta^* = (\beta_1^*, \beta_2^*)$ ,  $\beta_1^* < 0$ , be such that two limit cycles exist. Then  $\beta_2^* > 0$  and there exists at least one  $\bar{\beta}_2 \in (0, \beta_2^*)$  such that a saddle-node bifurcation happens between these two limit cycles at  $\beta = (\beta_1^*, \bar{\beta}_2)$ .

*Proof.* First observe that statement (a) follows directly from Theorem 6.7. Let  $L_i^s = L_i^s(\beta_i)$  and  $L_i^u = L_i^u(\beta_i)$  be the perturbations of  $L_i$  such that  $\omega(L_i^s) = p_i$ ,  $i \in \{1, 2\}$ ,  $\alpha(L_1^u) = p_2$  and  $\alpha(L_2^u) = p_1$ . Let  $\tau_i$  be a transversal section through  $L_i$  at  $x_{i,0}$ ,  $\sigma_1$  be a transversal section through  $L_1$  close enough to  $p_1$  and  $\sigma_2 = \Sigma \cap \bar{A}$ . See Figure 6.21. Let

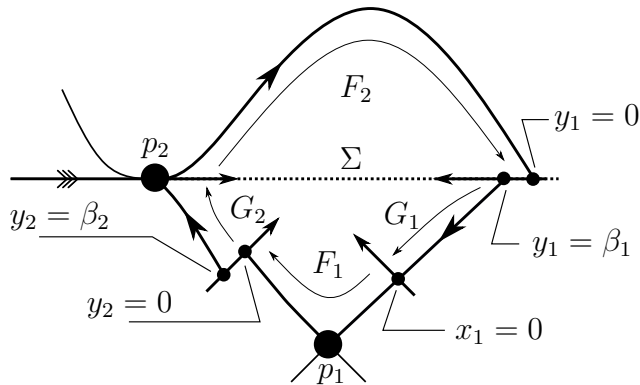


Figure 6.21: Illustration of the maps  $F_i$  and  $G_i$ ,  $i \in \{1, 2\}$ , with  $\beta_1 > 0$  and  $\beta_2 < 0$ . Observe that the point  $p_2$  is equivalent to  $x_2 = 0$ . Figure source: made by the author.

$G_i : \tau_i \rightarrow \sigma_i$  and  $F_i : \sigma_i \rightarrow \tau_{i-1}$  be given by the flow of  $Z$ . It follows from Sections 2.8 and 2.9 that we can assume

$$G_i(y_i) = y_i - \beta_i, \quad F_1^{-1}(y_2) = x^{s_1}(A(\beta) + \varphi(y_2, \beta)), \quad F_2(x_2) = kx_2^2 + O(x_2^3),$$

with  $k > 0$ ,  $A_1(\beta) > 0$  and  $s_1 = \frac{1}{r_1}$ . See Figure 6.21. Following [20] we define

$$\begin{aligned} H(x_2) &= G_1 \circ F_2(x_2) - F_1^{-1} \circ G_2^{-1}(x_2) \\ &= kx_2^2 + O(x_2^3) - \beta_1 - (x_2 + \beta_2)^{s_1}(A(\beta) + \varphi(x_2 + \beta_2, \beta)), \end{aligned} \quad (6.17)$$

and observe that

$$\begin{aligned} H'(x_2) &= 2kx_2 + O(x_2^2) - s_1(x_2 + \beta_2)^{s_1-1}(A(\beta) + \psi(x_2 + \beta_2, \beta)), \\ H''(x_2) &= 2k + O(x_2) - s_1(s_1 - 1)(x_2 + \beta_2)^{s_1-2}(A(\beta) + \xi(x_2 + \beta_2, \beta)). \end{aligned} \quad (6.18)$$

Therefore, if  $\frac{1}{2} < r_1 < 1$ , then  $s_1 - 2 < 0$  and thus it follows from (6.18) that

$$\lim_{(x_2, \beta) \rightarrow 0} H''(x_2) = -\infty$$

and hence at most two limit cycles can bifurcate from  $\Gamma$ , i.e. the cyclicity of  $\Gamma$  is at most two. From Theorem 6.8 we have that there is some bifurcation which two limit cycles bifurcate and thus the cyclicity of  $\Gamma$  is two. Moreover, since  $H''(x_2) < 0$  for  $\|(x_2, \beta)\|$

small enough it follows that when we have two limit cycles, then the inner one is stable and the outer one is unstable and thus we have statement (b)(i).

Statement (b)(ii) follows from an analysis of the degrees of  $G_1 \circ F_2$  and  $F_1^{-1} \circ G_2^{-1}$ . Let  $\beta^* = (\beta_1^*, \beta_2^*)$ ,  $\beta_1^* > 0$ , be such that we have two limit cycles near  $\Gamma$ . Let  $0 < x_{2,1}(\beta) < x_{2,2}(\beta)$  be the respective zeros of  $H$  which gives those limit cycles and observe that  $H'(x_{2,1}) > 0$  and  $H'(x_{2,2}) < 0$ . Observe also that  $x_2 + \beta_2 \geq 0$  is a necessary condition for the well definition of  $H$ . Therefore, since  $H'(x_{2,1}) > 0$  and  $0 < s_1 - 1 < 1$  it follows that  $\beta_2^* < 0$ . Moreover, since  $1 < s_1 < 2$  it follows from (6.17) and (6.18) that  $H(x_2) < 0$  and  $H'(x_2) < 0$  if  $|\beta_2|$  is small enough. Then if we fix  $\beta_1 = \beta_1^*$  and make  $\beta_2 \rightarrow 0$  we will have the collapse of  $x_{2,1}$  and  $x_{2,2}$  and thus the birth of a semi-stable limit cycle at some  $\bar{\beta}_2 \in (\beta_2^*, 0)$ .

Statement (c) is similar, just observe that  $r_1 < \frac{1}{2}$  implies  $s_1 > 2$ .  $\square$

**Lemma 6.27.** *The tangencies of the curves  $d_1^* = 0$ ,  $d_2^* = 0$  and  $\gamma$  at  $\beta = 0$  are those given by Figures 6.2, 6.3 and 6.4.*

*Proof.* Since the tangential singularity  $p_2$  is structural stable it follows from Section 6.6 and Proposition 6.24 that  $d_1^*(\beta) = \beta_1 + f(\beta)$ , with  $f(0) = \frac{\partial f}{\partial \beta_i}(0) = 0$ ,  $i \in \{1, 2\}$ , and

$$d_2^*(\beta) = \begin{cases} \beta_2 + g(\beta), & \text{if } r_1 > 1, \\ \beta_1 + g(\beta), & \text{if } r_1 < 1, \end{cases}$$

with  $g(0) = \frac{\partial g}{\partial \beta_i}(0) = 0$ ,  $i \in \{1, 2\}$ . Therefore,  $\nabla d_1^*(0) = (1, 0)$  and

$$\nabla d_2^*(0) = \begin{cases} (0, 1), & \text{if } r_1 > 1, \\ (1, 0), & \text{if } r_1 < 1. \end{cases}$$

Hence, the tangencies of the curves  $d_1^* = 0$  and  $d_2^* = 0$  at  $\beta = 0$  are those given by figures 6.2, 6.3 and 6.4. Let  $F = (F_1, F_2)$  be given by

$$F_1(x, \beta_1, \beta_2) = H(x, \beta_1, \beta_2), \quad F_2(x, \beta_1, \beta_2) = \frac{\partial H}{\partial x}(x, \beta_1, \beta_2).$$

It follows from (6.17), (6.18) and from Section 2.8 that

$$\lim_{(x,\beta) \rightarrow 0} \frac{\partial F_1}{\partial \beta_1} = -1, \quad \lim_{(x,\beta) \rightarrow 0} \frac{\partial F_1}{\partial \beta_2} = 0, \quad \lim_{(x,\beta) \rightarrow 0} \frac{\partial F_2}{\partial \beta_2} = -\infty,$$

and that  $\lim_{(x,\beta) \rightarrow 0} \frac{\partial F_1}{\partial \beta_1}$  is bounded for  $(x, \beta)$  near the origin. Therefore,

$$\frac{\partial F}{\partial \beta_1 \partial \beta_2} = \begin{pmatrix} \frac{\partial F_1}{\partial \beta_1} & \frac{\partial F_1}{\partial \beta_2} \\ \frac{\partial F_2}{\partial \beta_1} & \frac{\partial F_2}{\partial \beta_2} \end{pmatrix}$$

is invertible for *all*  $(x, \beta)$  near the origin. Let  $(x^*, \beta_1^*, \beta_2^*)$  small enough be such that  $F(x^*, \beta_1^*, \beta_2^*) = 0$ . In fact, it follows from Theorem 6.8 that we can take  $\beta^*$  arbitrarily near to the origin. It follows from the Implicit Function Theorem that there exist two unique

functions  $\beta_1 = \beta_1(x)$  and  $\beta_2 = \beta_2(x)$ , at least of class  $C^1$ , such that  $F(x, \beta_1(x), \beta_2(x)) \equiv 0$ , with  $\beta_i(x^*) = \beta_i^*$ ,  $i \in \{1, 2\}$ . It also follows from the Implicit Function Theorem that

$$\begin{pmatrix} \beta_1'(x^*) \\ \beta_2'(x^*) \end{pmatrix} = - \left[ \frac{\partial F}{\partial \beta_1 \partial \beta_2} \right]^{-1} \cdot \begin{pmatrix} \frac{\partial F_1}{\partial x} \\ \frac{\partial F_2}{\partial x} \end{pmatrix}. \quad (6.19)$$

Since  $\frac{\partial F_1}{\partial x} = F_2$  it follows from (6.19) that

$$\frac{d\beta_1}{d\beta_2} = - \frac{\partial F_1}{\partial \beta_2} \cdot \left( \frac{\partial F_1}{\partial \beta_1} \right)^{-1}. \quad (6.20)$$

It follows from (6.17) that  $\beta_2^* \rightarrow 0$  implies  $(x^*, \beta^*) \rightarrow 0$  and thus from (6.20) we have that

$$\lim_{\beta_2^* \rightarrow 0} \frac{d\beta_1}{d\beta_2} = 0.$$

Hence, the tangency of the curve  $\gamma$  is the one given at Figures 6.3 and 6.4. □

**Remark 6.28.** It follows from the uniqueness of the functions  $\beta_i(x)$  of Lemma 6.27 that  $\bar{\beta}_i$ , from statements (b)(ii) and (c)(ii) of Lemma 6.26, are also unique. Furthermore, as we shall see, the restrictions  $\beta_1^* > 0$  and  $\beta_1^* < 0$  of statements (b) and (c) of Lemma 6.26 are in fact no restrictions at all since these conditions are necessary for the existence of two limit cycles.

*Proof of Theorem 6.9.* First let us suppose  $r_1 > 1$ . Then from Theorem 6.4 we know that  $\Gamma$  is stable and it follows from Theorem 6.7 that if a limit cycle bifurcates from  $\Gamma$ , then it is unique, hyperbolic and stable. Therefore, it follows from Theorem 6.7 that if  $\beta_1 \leq 0$ ,  $\beta_2 \leq 0$  and  $\beta_1^2 + \beta_2^2 > 0$ , then a unique stable and hyperbolic limit cycle bifurcates from  $\Gamma$  and thus we have phase portraits 8, 9 and 10. It also follows from the Poincaré-Bendixson theory for non-smooth vector fields (see [10]) that if  $d_1^* < 0$  or  $d_2^* < 0$ , then again a unique stable and hyperbolic limit cycle bifurcates from  $\Gamma$  and thus we have phase portraits 7 and 11. By definition of  $d_i^* = 0$  it follows that if  $d_1^* = 0$  or  $d_2^* = 0$ , then a new polycycle  $\Gamma^*$  composed either by  $p_1$  or  $p_2$ , respectively. Since  $\Gamma^*$  is stable in both cases we can ensure from Theorem 6.7 that no limit cycle bifurcates from it and hence we have phase portraits 6 and 12. Clearly if  $\beta_2 > 0$  and  $d_2^* \geq 0$ , then a sliding polycycle  $\Gamma^s$  composed by  $p_1$  and  $p_2$  bifurcates from  $\Gamma$ , giving us phase portraits 2 and 13. The other phase portraits are obtained in a similar way.

Let us now suppose  $\frac{1}{2} < r_1 < 1$ . In this case it follows from statement (b) of Lemma 6.26 that at most two limit cycles can bifurcate from  $\Gamma$  and in this case the outer one is necessary unstable. Therefore, the phase portraits of the first, the second and the third quadrant follows in a similar way to the previous case. Hence, we will focus on the fourth quadrant. Phase portrait 9 follows from the Poincaré-Bendixson Theory for non-smooth vector fields (see [10]) and from Statement (b) of Lemma 6.26. If  $d_1^* = 0$ , then the polycycle  $\Gamma^*$  composed by  $p_1$  is unstable and thus we have phase portrait 8. From Theorem 6.7 a unique hyperbolic unstable limit cycle bifurcate from  $\Gamma^*$  if  $d_1^* > 0$  and thus we have phase portrait 7. Phases portrait 5 and 6 follows from statement (b)(ii) of Lemma 6.26. The case  $r_1 < \frac{1}{2}$  is similar to the previous two cases. □



## 7 CONCLUSION

We would like to point out that we are very impressed on how the systematic chasing for convenient curves such that the flow crosses it in a convenient way proved to be a very fruitful tool in the classification of the phase portraits of the planar reversible vector fields. We also point out the qualitative simplification done in the Friedmann-Robertson-Walker system, shrinking the dimensional from four to two and hence recovering all the theory of planar vector fields. Finally, we point out the fact that polycycles in non-smooth vector fields, at least when generic, behaves in a very similar way from its siblings in the smooth realm.



## REFERENCES

- [1] ABRAHAM, R., MARSDEN, J., AND RATIU, T. *Manifolds, tensor analysis, and applications*, second ed., vol. 75 of *Applied Mathematical Sciences*. Springer-Verlag, New York, 1988.
- [2] ANDRADE, K., GOMIDE, O., AND NOVAES, D. Qualitative analysis of polycycles in filippov systems. *arXiv 1905.11950v2* (2019).
- [3] ANDRONOV, A., VITT, A., AND KHAIKIN, S. *Theory of oscillators*. Pergamon Press, Oxford-New York-Toronto, Ont., 1966. Translated from the Russian by F. Immirzi; translation edited and abridged by W. Fishwick.
- [4] BELMONTE, C., BOCCALETTI, D., AND PUCACCO, G. On the orbit structure of the logarithmic potential. *The Astrophysical Journal* 669, 1 (2007), 202–217.
- [5] BROWDER, F. Fixed point theory and nonlinear problems. *Bull. Amer. Math. Soc. (N.S.)* 9, 1 (1983), 1–39.
- [6] BUENDÍA, J., AND LÓPEZ, V. On the Markus-Neumann theorem. *J. Differential Equations* 265, 11 (2018), 6036–6047.
- [7] BUICA, A., GINÉ, J., AND LLIBRE, J. A second order analysis of the periodic solutions for nonlinear periodic differential systems with a small parameter. *Phys. D* 241, 5 (2012), 528–533.
- [8] BUICA, A., AND LLIBRE, J. Averaging methods for finding periodic orbits via Brouwer degree. *Bull. Sci. Math.* 128, 1 (2004), 7–22.
- [9] BUZZI, C. Generic one-parameter families of reversible vector fields. In *Real and complex singularities (São Carlos, 1998)*, vol. 412 of *Chapman & Hall/CRC Res. Notes Math.* Chapman & Hall/CRC, Boca Raton, FL, 2000, pp. 202–214.
- [10] BUZZI, C., CARVALHO, T., AND EUZÉBIO, R. On Poincaré-Bendixson theorem and non-trivial minimal sets in planar nonsmooth vector fields. *Publ. Mat.* 62, 1 (2018), 113–131.
- [11] BUZZI, C., LLIBRE, J., AND SANTANA, P. Phase portraits of (2;1) reversible vector fields of low codimension. *Submitted for publication*.
- [12] BUZZI, C., LLIBRE, J., AND SANTANA, P. Periodic orbits of a Hamiltonian system related with the Friedmann-Robertson-Walker system in rotating coordinates. *Phys. D* 413 (2020), 132673.
- [13] BUZZI, C., LLIBRE, J., AND SANTANA, P. Phase portraits of (2;0) reversible vector fields with symmetrical singularities. *Journal of Mathematical Analysis and Applications* 503 (2021), 125324.
- [14] BUZZI, C., ROBERTO, L., AND TEIXEIRA, M. Branching of periodic orbits in reversible hamiltonian systems. In *Real and complex singularities*, London Mathematical Society Lecture Note Series. Cambridge University Press, 2010, p. 46–70.

- 
- [15] CALZETTA, E., AND EL HASI, C. Chaotic Friedmann–Robertson–Walker cosmology. *Classical Quantum Gravity* 10, 9 (1993), 1825–1841.
- [16] CHERKAS, L. The stability of singular cycles. *Differencial'nye Uravnenija* 4 (1968), 1012–1017.
- [17] DUFF, G. Limit-cycles and rotated vector fields. *Ann. of Math. (2)* 57 (1953), 15–31.
- [18] DULAC, H. Sur les cycles limites. *Bull. Soc. Math. France* 51 (1923), 45–188.
- [19] DUMORTIER, F., LLIBRE, J., AND ARTÉS, C. *Qualitative theory of planar differential systems*. Universitext. Springer-Verlag, Berlin, 2006.
- [20] DUMORTIER, F., ROUSSARIE, R., AND ROUSSEAU, C. Elementary graphics of cyclicity 1 and 2. *Nonlinearity* 7, 3 (1994), 1001–1043.
- [21] FILIPPOV, A. *Differential Equations with Discontinuous Righthand Sides*. Springer, Dordrecht, 1988. Translated from the Russian.
- [22] GUCKENHEIMER, J., AND HOLMES, P. *Nonlinear oscillations, dynamical systems, and bifurcations of vector fields*, vol. 42 of *Applied Mathematical Sciences*. Springer-Verlag, New York, 1983.
- [23] HAN, M., AND WU, Y. AND, B. P. Bifurcation of limit cycles near polycycles with  $n$  vertices. *Chaos Solitons Fractals* 22, 2 (2004), 383–394.
- [24] HAWKING, S. Arrow of time in cosmology. *Phys. Rev. D (3)* 32, 10 (1985), 2489–2495.
- [25] HIRSCH, M., SMALE, S., AND DEVANEY, R. *Differential equations, dynamical systems, and an introduction to chaos*, second ed., vol. 60 of *Pure and Applied Mathematics (Amsterdam)*. Elsevier/Academic Press, Amsterdam, 2004.
- [26] HOLMES, P. Averaging and chaotic motions in forced oscillations. *SIAM J. Appl. Math.* 38, 1 (1980), 65–80.
- [27] KUZNETSOV, Y. *Elements of applied bifurcation theory*, third ed., vol. 112 of *Applied Mathematical Sciences*. Springer-Verlag, New York, 2004.
- [28] LAMB, J., AND ROBERTS, J. Time-reversal symmetry in dynamical systems: a survey. vol. 112. 1998, pp. 1–39. Time-reversal symmetry in dynamical systems (Coventry, 1996).
- [29] LLIBRE, J., AND MAKHLOUF, A. Periodic orbits of the generalized friedmann–robertson–walker hamiltonian systems. *Astrophysics and Space Science* 344, 1 (2013), 45–50.
- [30] LLIBRE, J., AND MEDRADO, J. Darboux integrability and reversible quadratic vector fields. *Rocky Mountain Journal of Mathematics* 35, 6 (2005), 1999 – 2057.
- [31] LLIBRE, J., NOVAES, D., AND TEIXEIRA, M. Higher order averaging theory for finding periodic solutions via Brouwer degree. *Nonlinearity* 27, 3 (2014), 563–583.

- 
- [32] LLOYD, N. *Degree theory*. Cambridge University Press, Cambridge-New York-Melbourne, 1978. Cambridge Tracts in Mathematics, No. 73.
- [33] MAILYBAEV, A., MARCHESIN, D., AND DE SÁ VERA, M. Sensitivity analysis of stable and unstable manifolds: Theory and application. *IMPA* (2001).
- [34] MARKUS, L. Global structure of ordinary differential equations in the plane. *Trans. Amer. Math. Soc.* 76 (1954), 127–148.
- [35] MEDRADO, J., AND TEIXEIRA, M. Symmetric singularities of reversible vector fields in dimension three. *Physica D: Nonlinear Phenomena* 112, 1 (1998), 122–131.
- [36] MEDRADO, J., AND TEIXEIRA, M. Codimension-two singularities of reversible vector fields in 3D. *Qual. Theory Dyn. Syst.* 2, 2 (2001), 399–428.
- [37] MERRITT, D., AND VALLURI, M. Chaos and mixing in triaxial stellar systems. *Astrophysical Journal* 471 (1996), 82–105.
- [38] MOURTADA, A. Cyclicité finie des polycycles hyperboliques de champs de vecteurs du plan: mise sous forme normale. In *Bifurcations of planar vector fields (Luminy, 1989)*, vol. 1455 of *Lecture Notes in Math*. Springer, Berlin, 1990, pp. 272–314.
- [39] NEUMANN, D. Classification of continuous flows on 2-manifolds. *Proc. Amer. Math. Soc.* 48 (1975), 73–81.
- [40] NOVAES, D., TEIXEIRA, M., AND ZELI, I. The generic unfolding of a codimension-two connection to a two-fold singularity of planar Filippov systems. *Nonlinearity* 31, 5 (2018), 2083–2104.
- [41] PAGE, D. Will entropy decrease if the Universe recollapses? *Phys. Rev. D* (3) 32, 10 (1985), 2496–2499.
- [42] PAPAPHILIPPOU, Y., AND LASKAR, J. Frequency map analysis and global dynamics in a galactic potential with two degrees of freedom. *Astronomy and Astrophysics* 307 (1996), 427–449.
- [43] PAPAPHILIPPOU, Y., AND LASKAR, J. Global dynamics of triaxial galactic models through frequency map analysis. *Astronomy and Astrophysics* 329 (12 1997), 451–481.
- [44] PEIXOTO, M. Structural stability on two-dimensional manifolds. *Topology* 1 (1962), 101–120.
- [45] PEIXOTO, M. On the classification of flows on 2-manifolds. *Dynamical systems (Proc. Sympos., Univ. Bahia, Salvador, 1971)* (1973), 389–419.
- [46] PEREIRA, W., AND PESSOA, C. A class of reversible quadratic polynomial vector fields on  $S^2$ . *Journal of Mathematical Analysis and Applications* 371, 1 (2010), 203–209.
- [47] PEREIRA, W., AND PESSOA, C. On the reversible quadratic polynomial vector fields on  $S^2$ . *Journal of Mathematical Analysis and Applications* 396, 2 (2012), 455–465.

- [48] PERKO, L. Global families of limit cycles of planar analytic systems. *Trans. Amer. Math. Soc.* 322, 2 (1990), 627–656.
- [49] PERKO, L. Homoclinic loop and multiple limit cycle bifurcation surfaces. *Trans. Amer. Math. Soc.* 344, 1 (1994), 101–130.
- [50] PERKO, L. *Differential equations and dynamical systems*, third ed., vol. 7 of *Texts in Applied Mathematics*. Springer-Verlag, New York, 2001.
- [51] PUCACCO, G., BOCCALETTI, D., AND BELMONTE, C. Quantitative predictions with detuned normal forms. *Celestial Mech. Dynam. Astronom.* 102, 1-3 (2008), 163–176.
- [52] REES, E. Graphical Discussion of the Roots of a Quartic Equation. *Amer. Math. Monthly* 29, 2 (1922), 51–55.
- [53] SANDERS, J., VERHULST, F., AND MURDOCK, J. *Averaging methods in nonlinear dynamical systems*, second ed., vol. 59 of *Applied Mathematical Sciences*. Springer, New York, 2007.
- [54] SOTOMAYOR, J. Generic one-parameter families of vector fields on two-dimensional manifolds. *Inst. Hautes Études Sci. Publ. Math.*, 43 (1974), 5–46.
- [55] SOTOMAYOR, J. *Curvas definidas por equações diferenciais no plano*. Décimo terceiro Colóquio Brasileiro de Matemática. [13th Brazilian Mathematics Colloquium]. Instituto de Matemática Pura e Aplicada, Conselho Nacional de Desenvolvimento Científico e Tecnológico, Rio de Janeiro, 1981.
- [56] TEIXEIRA, M. Singularities of reversible vector fields. *Phys. D* 100, 1-2 (1997), 101–118.
- [57] VERHULST, F. *Nonlinear differential equations and dynamical systems*, second ed. Universitext. Springer-Verlag, Berlin, 1996. Translated from the 1985 Dutch original.
- [58] ZHAO, H., CAROLLO, C., AND DE ZEEUW, P. Can galactic nuclei be non-axisymmetric? the parameter space of power-law discs. *Monthly Notices of the Royal Astronomical Society*.